



**Development of non-esterified
fatty acid (NEFA) Electrochemical
Biosensor for Energy Metabolism
Studies**

A Thesis submitted by

Anisah Tariq Hussain

For the Degree of Doctor of Philosophy

School of Chemical Engineering and Advanced Materials

University of Newcastle-Upon-Tyne

June 2014

Abstract

There are many energy metabolism studies ongoing, including those for cardiovascular diseases and type-2-diabetes. With an increase in people being diagnosed with type-2-diabetes, there should be more ways to monitor not only the blood glucose levels but also the other biomarkers associated with type-2-diabetes. The metabolism biomarkers are essential in understanding the cause of diabetes early on. These biomarkers include: glucose, non-esterified fatty acid, lactate, urea, creatinine, glycosylated haemoglobin and cholesterol. Whilst glucose measurement has a clear role in type-2-diabetes management, the potential value of non-esterified fatty acid has not been explored or highlighted yet.

The aim of this project is to develop an electrochemical biosensor for the non-esterified fatty acid in human blood, as non-esterified fatty acid can cause β -cell loss in type-2-diabetes. Exploration of this biomarker would be a step forward in increasing research and patient understanding of the dynamic processes involved in establishing good metabolism control.

The project uses the enzymes in commercial optical methods for non-esterified fatty acid detection. Oleic acid was used as the standard non-esterified fatty acid in this work. The electrochemical techniques employed are cyclic voltammetry, linear sweep voltammetry, chronoamperometry and electrochemical impedance spectroscopy.

Enzyme electrodes were fabricated using the layer-by-layer immobilization of alternating polymer and enzyme combinations on carbon, cobalt phthalocyanine and single wall carbon nanotube screen printed electrodes. A chronoamperometric non-esterified fatty acid sensor was developed with the linear detection range of 0.10 mM to 0.90 mM oleic acid and with a sensitivity of 0.6562 $\mu\text{A}/\text{mM}$ oleic acid. This sensor was then further fabricated to detect non-esterified fatty acid concentrations in human plasma and serum samples. Commercial UV optical methods were used as method of validation of the blood sample concentrations. This work produced a platform for further non-esterified fatty acid detection studies.

Keywords

Biosensors; non-esterified fatty acid; electrochemical; diabetes; biomarkers; immobilisation

Acknowledgements

I would like to thank the following;

- EPSRC for funding.
- My supervisors, Dr. Eileen Yu and Professor Mike Catt for their guidance throughout the project. I am grateful that I was hired for my project.
- My research group (based in C318 and the Coulson Lab), especially Orlando and James for their kind support.
- Richard (Dr. Burkitt) for many things (including showing me how to use the potentiostat!).
- All the past and present members of my office C500.
- Newcastle Medical School for providing the blood samples.
- Dr. Kang for initial LbL experiment.

I was inspired to do a PhD from my undergraduate lecturers at Sunderland University. I thank them for always being my inspiration.

I would not be at this stage in my life if it was not for my loving parents, sisters (Zareen, Farah and Mahreen) and brother (Asad).

This thesis is dedicated to my family who are unfortunately genetically pre-disposed to type-2-diabetes.

Table of Contents

Abstract	i
List of figures	vii
List of tables.....	xviii
Nomenclature	xx
Abbreviations	xxi
1 Background and literature review part 1	1
1.1 Background	1
1.2 NEFA - Literature review part 1	3
1.2.1 NEFA and its role	3
1.2.2 NEFA in human blood	8
1.2.3 NEFA, obesity and prevention of T2D	13
1.2.4 Current methods of NEFA detection	15
1.2.5 The role of NEFA in other disease states.....	21
1.2.6 Conclusion	24
2 Biomarkers and Biosensors – Literature review part 2.....	25
2.1.1 Biomarkers for energy metabolism.....	25
2.1.2 Biosensor Development	27
2.1.3 Glucose biosensors.....	27
2.1.4 Advantages of electrochemical biosensors	31

2.1.5	Electrochemistry	32
2.1.6	H ₂ O ₂ produced as a by-product.....	34
2.1.7	H ₂ O ₂ oxidation and reduction	35
2.1.8	Conclusion	37
2.2	Aims and objectives	38
3	NEFA detection in solution using screen printed electrodes (SPE's).....	39
3.1	Introduction	39
3.2	Experimental	41
3.2.1	Materials	41
3.2.2	Electrochemical measurements.....	43
3.3	PA-CoA/OA-CoA detection electrochemically in solution	45
3.3.1	Detection using carbon screen printed electrode	45
3.3.2	Detection using single wall carbon nanotube screen printed electrode	56
3.3.3	Detection using cobalt phthalocyanine screen printed electrode	60
3.3.4	Screen printed electrode comparison	67
3.3.5	Interferences.....	68
3.4	Conclusions	74
4	Enzyme electrode for NEFA detection	75
4.1	Introduction	75
4.1.1	Layer-by-layer immobilization	76

4.1.2	H ₂ O ₂ detection via layer-by-layer.....	78
4.1.3	Experimental.....	79
4.2	Enzyme fabricated electrodes for PA-CoA/OA-CoA detection	83
4.3	Enzyme fabricated electrodes for OA detection	88
4.3.1	Determination of OA using (PDA-MWCNT/ACOD/PDA-MWCNT/ACS) fabricated electrode.....	88
4.3.2	Comparison of different SPE's performance using molar ratios	97
4.3.3	Multiple Layer comparison of (PDA-MWCNT/ACOD/PDA-MWCNT/ACS) electrode.....	100
4.3.4	Confirmation of multiple layer configuration.....	102
4.3.5	Use of N-ethyl-maleinimide and effect of excess CoA	106
4.3.6	Stability.....	109
4.3.7	Reproducibility	110
4.3.8	Determination of OA using (PDA/ACOD/PDA/ACS) fabricated electrode	111
4.3.9	Interferences.....	113
4.4	Conclusions	120
5	Enzyme fabricated electrodes for blood NEFA detection	121
5.1.1	Introduction.....	121
5.1.2	Experimental.....	123
5.1.3	Serum vs. plasma	127

5.2	Detection of plasma samples.....	127
5.3	Detection of serum samples	128
5.4	Comparison of different fabricated electrodes performance using human blood	130
5.4.1	Problems with working in blood.....	135
5.4.2	Why does NEFA concentration increase over time?	138
5.5	Conclusions	142
6	Conclusions and recommendations for future work	143
6.1	Conclusions	143
6.2	Recommendations for future work.....	144
7	Appendix.....	149
	PDA based electrode for blood detection	155
	PMBN based electrode for blood detection	156
	BSA based electrode for blood detection.....	160
	PSS based electrode for blood detection.....	161
	PMAA based electrode for blood detection.....	163
8	References.....	165

List of figures

Figure 1-1: NEFA publications over the last 5 years.....	3
Figure 1-2: Pie charts showing the percentage distribution of the topics of publications regarding NEFA over the last 5 years.	4
Figure 1-3: Palmitoyl-CoA oxidation.	10
Figure 1-4: Oleoyl-CoA oxidation.....	11
Figure 1-5: Citric acid cycle [97, 98].....	12
Figure 1-6: Full Structure of FAD and FAD oxidation and reduction reactions [97].	12
Figure 1-7: Model for the effects of adipocytes on pancreatic β -cell function/mass and insulin sensitivity in the pathogenesis of T2D [4]. IR = insulin resistance.	14
Figure 1-8: Reaction scheme of the enzymatic determination of NEFA [133].	16
Figure 1-9: Sensor based on 5 sequential enzyme reactions [135].....	17
Figure 1-10: Different assay schemes used for NEFA detection (colorimetric methods are shown in red, fluorometric in green) [136-146].	18
Figure 1-11: Chemical structure of Phytanic acid.	21
Figure 2-1: Clarke-type O ₂ electrode illustration [204].....	28
Figure 2-2: Schematic diagram of the second generation enzyme glucose sensors [228].....	29
Figure 2-3: Advantages and disadvantages of home based glucose sensors from the patients perspective [246].....	31
Figure 2-4: Typical electrochemical cell, with standard three-electrode set-up comprising of working, counter and reference electrodes [204].....	32
Figure 2-5: Clinically important reactions producing H ₂ O ₂ as a by-product.....	35
Figure 2-6: General scheme of oxygen reduction [266].	36

Figure 3-1: ACOD catalysed reaction of acylated NEFAs [272, 275].	40
Figure 3-2: Sheet of 16 screen printed carbon electrodes.	41
Figure 3-3: Experimental set-up for electrochemical experiments.	44
Figure 3-4: LSV for various concentrations of H ₂ O ₂ measured at a C-SPE in 0.1 M phosphate buffer pH 7.4, scan rate 1 mV s ⁻¹ .	45
Figure 3-5: Calibration graph at 500 mV.	46
Figure 3-6: The relationship between log <i>j</i> and log H ₂ O ₂ concentration on the C-SPE at various electrode potentials in 0.1 M phosphate buffer pH 7.4.	47
Figure 3-7: LSV for various concentrations of PA-CoA measured at a C-SPE with ACOD in 0.1 M phosphate buffer pH 7.4 , scan rate 1 mV s ⁻¹ . Inset: calibration graph at a potential of 500 mV.	49
Figure 3-8: The relationship between log <i>j</i> and log PA-CoA concentration at various electrode potentials in 0.1 M phosphate buffer pH 7.4.	50
Figure 3-9: Chronoamperometry at 500 mV of various PA-CoA concentrations on C-SPE in 0.1 M phosphate buffer pH 7.4 with ACOD in solution.	51
Figure 3-10: Calibration graph of current against PA-CoA concentration at 500 s.	51
Figure 3-11: Chronoamperometry at 500 mV of various OA-CoA concentrations on C-SPE in 0.1 M phosphate buffer pH 7.4 with ACOD in solution.	52
Figure 3-12: Calibration graph of current against OA-CoA concentration at 500 s.	53
Figure 3-13: Bar chart comparing the current produced from the two different acylated NEFAs on SWCNT SPE. CA at 500 mV, current taken at 500 s.	53
Figure 3-14: CV of 0.50 mM PA-CoA and ACOD at scan rate of 100 mV s ⁻¹ using a C-SPE with increasing upper limit potential varying from 0.6 V to 1.6 V.	55

Figure 3-15: CA at 500 mV of various PA-CoA concentrations on SWCNT SPE in 0.1 M phosphate buffer pH 7.4 with ACOD in solution.	57
Figure 3-16: Calibration graph at 500 s.	57
Figure 3-17: CA at 500 mV of various OA-CoA concentrations on SWCNT SPE in 0.1 M phosphate buffer pH 7.4 with ACOD in solution.	58
Figure 3-18: Calibration graph at 500 s.	58
Figure 3-19: LSV for various concentrations of PA-CoA measured at a SWCNT SPE with ACOD in 0.1 M phosphate buffer pH 7.4 , scan rate 1 mV s ⁻¹	59
Figure 3-20: Calibration graph at 500 mV.	59
Figure 3-21: CA at 500 mV of various PA-CoA concentrations on CoPc SPE in 0.1 M phosphate buffer pH 7.4 with ACOD in solution.	60
Figure 3-22: Calibration graph at 500 s.	61
Figure 3-23: Chemical structure of CoPc.	62
Figure 3-24: Schematic showing the principle of NEFA biosensor for H ₂ O ₂ detection using CoPc SPE.	62
Figure 3-25: CA at 500 mV of various OA-CoA concentrations on CoPc SPE in 0.1 M phosphate buffer pH 7.4 with ACOD in solution.	63
Figure 3-26: Calibration graph at 500 s.	63
Figure 3-27: Bar chart comparing the current produced from the two different acylated NEFAs on CoPc SPE. CA at 500 mV, current taken at 500 s.	64
Figure 3-28: CV of 75 scans of 0.00 mM (black) and 0.50 mM (blue) PA-CoA with ACOD in solution, at scan rate of 50 mV s ⁻¹ using a CoPc SPE.	65

Figure 3-29: CV of 0.50 mM PA-CoA with ACOD in solution, at scan rate of 100 mV s ⁻¹ using a CoPc SPE with increasing upper limit potential varying from 0.6 V to 1.6 V.....	66
Figure 3-30: CA at 500 mV for 0.20 mM PA-CoA with ACOD, spiked with various interferences on C-SPE, in 0.1 M phosphate buffer pH 7.4. The concentration of each interference is that listed in Table 3-5.....	71
Figure 4-1: Schematic representation of various immobilization techniques: (A) covalent binding, (B) adsorption, (C) gel entrapment, (D) cross-linking, (E) microencapsulation and (F) adsorption-cross-linking [204].....	76
Figure 4-2: Schematic display of the LbL fabrication of (PDA/ACOD) ₂ on C-SPE WE.	81
Figure 4-3: Schematic display of the LbL fabrication of (PDA-MWCNT/ACOD/PDA-MWCNT/ACS) ₁ on C-SPE WE.....	82
Figure 4-4: LSV for various concentrations of OA-CoA measured at a C-SPE modified with (PDA-MWCNT/ACOD) ₂ in 0.1 M phosphate buffer pH 7.4, scan rate 1 mV s ⁻¹ . Inset: calibration graph at $E = 500$ mV.....	83
Figure 4-5: The relationship between $\log j$ and \log OA-CoA concentration on the (PDA-MWCNT/ACOD) ₂ electrode at various electrode potentials in 0.1 M phosphate buffer pH 7.4.	84
Figure 4-6: LSV for various concentrations of PA-CoA measured at a C-SPE modified with (PDA-MWCNT/ACOD) ₂ in 0.1 M phosphate buffer pH 7.4, scan rate 1 mV s ⁻¹ . Inset: calibration graph at $E = 500$ mV.....	85
Figure 4-7: The relationship between $\log j$ and \log PA-CoA concentration on the (PDA-MWCNT/ACOD) ₂ electrode at various electrode potentials in 0.1 M phosphate buffer pH 7.4.	86

Figure 4-8: Bar chart comparing the current produced from the two different acylated NEFAs on (PDA-MWCNT/ACOD) ₂ electrode. LSV at 1 mV s ⁻¹ , current taken at 500 mV.	87
Figure 4-9: LSV of various concentrations of OA measured at a C-SPE modified with (PDA-MWCNT/ACOD/PDA-MWCNT/ACS) ₁ in 0.1 M phosphate buffer pH 7.4 and 1 mM ATP and CoA, scan rate 1 mV s ⁻¹	89
Figure 4-10: Calibration graph at 500 mV.	89
Figure 4-11: The relationship between log <i>j</i> and log OA concentration on the (PDA-MWCNT/ACOD/PDA-MWCNT/ACS) ₁ electrode at various electrode potentials in 0.1 M phosphate buffer pH 7.4.	90
Figure 4-12: LSV at 1 mV s ⁻¹ on C-SPE with 100 μL PBS only and with 100 μL of ACS solution A from Wako kit.	90
Figure 4-13: Calibration graph obtained by electrochemical measurement of various concentrations of OA at <i>E</i> = 500 mV (as shown in Figure 4-9). 0.30 mM and 0.60 mM were measured independently on a different electrode (shown in green).	91
Figure 4-14: CA at 500 mV for various concentrations of OA measured at a C-SPE modified with (PDA-MWCNT/ACOD/PDA-MWCNT/ACS) ₁ , in 0.1 M phosphate buffer pH 7.4 with 1 mM ATP and CoA.	92
Figure 4-15: Calibration at 500 s.	92
Figure 4-16: Current comparison with and without ATP and CoA on (PDA-MWCNT/ACOD/PDA-MWCNT/ACS) ₁ electrode, CA at 500 mV, current taken at 500 s.	93
Figure 4-17: CA at 500 mV for various concentrations of OA measured at a C-SPE modified with (PDA-MWCNT/ACS/PDA-MWCNT/ACOD) ₁ in 0.1 M phosphate buffer pH 7.4 with 1 mM ATP and CoA.	94

Figure 4-18: Calibration graph at 500 s.	94
Figure 4-19: CA at 500 mV for various concentrations of OA measured at a C-SPE modified with (PDA-MWCNT/ACOD+ACS)1 in 0.1 M phosphate buffer pH 7.4 with 1 mM ATP and CoA.	95
Figure 4-20: Calibration graph at 500 s.	95
Figure 4-21: Calibration graph obtained by LSV of various concentrations of OA on a CoPc-SPE modified with (PDA-MWCNT/ACOD/PDA-MWCNT/ACS)1 in 0.1 M phosphate buffer pH 7.4 and 1 mM ATP and CoA, scan rate 1 mV s ⁻¹	99
Figure 4-22: Calibration graph obtained by LSV of various concentrations of OA on a SWCNT SPE modified with (PDA-MWCNT/ACOD/PDA-MWCNT/ACS)1 in 0.1 M phosphate buffer pH 7.4 and 2 mM ATP and CoA, scan rate 1 mV s ⁻¹	99
Figure 4-23: CA ($E = 500$ mV) of OA spiking on (PDA-MWCNT/ACOD/PDA-MWCNT/ACS)1 as black line and (PDA-MWCNT/ACOD/PDA-MWCNT/ACS)4 as blue line, in 0.1 M phosphate buffer pH 7.4 and 1 mM ATP and CoA. The concentration of OA before and after the spike is 0 mM and 0.25 mM, respectively.	101
Figure 4-24: The Nyquist plots of C-SPE modified for: bare C-SPE; (PDA-MWCNT/ACOD/PDA-MWCNT/ACS)1; (PDA-MWCNT/ACOD/PDA-MWCNT/ACS)2 and (PDA-MWCNT/ACOD/PDA-MWCNT/ACS)4, all in 5 mM 1:1 mixture of K ₃ [Fe(CN) ₆] : K ₄ [Fe(CN) ₆] at an applied voltage of 0.17 V.	103
Figure 4-25: LSV at 1 mV s ⁻¹ showing (PDA-MWCNT/ACOD/PDA-MWCNT/ACS)1 as black line and (PDA-MWCNT/ACOD/PDA-MWCNT/ACS)4 as purple line, in 0.1 M phosphate buffer pH 7.4 and 1 mM ATP and CoA. The same electrode with 0.25 mM OA is then shown as the dashed line respectively.	105

Figure 4-26: LSV for 0.10 mM OA measured on two C-SPE's modified with (PDA-MWCNT/ACOD/PDA-MWCNT/ACS)1 (one electrode shown in green and one electrode shown in red) in 0.1 M phosphate buffer pH 7.4, scan rate 1 mV s⁻¹ 107

Figure 4-27: CA ($E = 500$ mV) of OA with and without NEM on (PDA-MWCNT/ACOD/PDA-MWCNT/ACS)1 at different molar ratios of CoA and ATP. All background subtracted. 108

Figure 4-28: Set-up for 4 C-SPE's immobilized at the same time. 109

Figure 4-29: CA ($E = 500$ mV) of 0.75 mM OA (PDA-MWCNT/ACOD/PDA-MWCNT/ACS)1 electrode in 0.1 M phosphate buffer pH 7.4 with 1 mM ATP and CoA. 0.00 mM OA consisted of 0.1 M phosphate buffer pH 7.4 with 1 mM ATP and CoA only. 110

Figure 4-30: LSV of various concentrations of OA measured at a C-SPE modified with (PDA/ACOD/PDA/ACS)1 in 0.1 M phosphate buffer pH 7.4 and 1 mM ATP and CoA, scan rate 1 mV s⁻¹ 111

Figure 4-31: Comparison of calibration graphs at 500 mV of LSV's obtained from (PDA/ACOD/PDA/ACS)1 in black and (PDA-MWCNT/ACOD/PDA-MWCNT/ACS)1 in blue on C-SPE..... 112

Figure 4-32: CA at 500 mV for various concentrations of Uric acid measured at a C-SPE modified with (PDA-MWCNT/ACOD/PDA-MWCNT/ACS)1 in 0.1 M phosphate buffer pH 7.4. Inset: Calibration graph at 500 s. 114

Figure 4-33: CV of various concentration of uric acid at scan rate of 5 mV s⁻¹ using a C-SPE modified with (PDA-MWCNT/ACOD/PDA-MWCNT/ACS)1 in 0.1 M phosphate buffer pH 7.4. 115

Figure 4-34: CA at 500 mV for various concentrations of Ascorbic acid measured at a C-SPE modified with (PDA-MWCNT/ACOD/PDA-MWCNT/ACS)1 in 0.1 M phosphate buffer pH 7.4. Inset: Calibration graph at 500 s.	116
Figure 4-35: Barchart of current obtained at 500 s of CA at 500 mV for 1 mM ascorbic acid added in as interference measured at a C-SPE modified with (PDA-MWCNT/ACOD/PDA-MWCNT/ACS)1 in 0.1 M phosphate buffer pH 7.4, 1 mM ATP and CoA with varying concentrations of OA.	117
Figure 4-36: CA at 500 mV for various concentrations of Acetaminophen measured at a C-SPE modified with (PDA-MWCNT/ACOD/PDA-MWCNT/ACS)1 in 0.1 M phosphate buffer pH 7.4. Inset: Calibration graph at 500 s.	118
Figure 4-37: LSV of various concentrations of acetaminophen measured at a C-SPE modified with (PDA-MWCNT/ACOD/PDA-MWCNT/ACS)1 in 0.1 M phosphate buffer pH 7.4, scan rate 1 mV s ⁻¹	118
Figure 4-38: Barchart of current obtained at 500 s of Chronoamperometry at 500 mV for 5 mM glucose added in as interference, measured at a C-SPE modified with (PDA-MWCNT/ACOD/PDA-MWCNT/ACS)1 in 0.1 M phosphate buffer pH 7.4, 1 mM ATP and CoA with varying concentrations of OA.	119
Figure 5-1: Various chemical, electrochemical and diffusion processes on the LbL electrode of the current NEFA sensor. Adapted from [338].	121
Figure 5-2: Chemical structure of commonly used polyelectrolytes.	122
Figure 5-3: Samples of serum and plasma (some haemolysed).	123
Figure 5-4: Optical validation. Concentrations 0.00 mM to 0.90 mM OA from left to right respectively. Far right concentrations 0.30 mM and 0.60 mM OA.	124

Figure 5-5: Calibration graph obtained by measurement of various concentrations of OA by the Roche colorimetric method. The fitting is based on average values obtained from three measurements ($\lambda=546$ nm). 0.30 mM and 0.60 mM were measured independently (shown in green). 125

Figure 5-6: Electrode with PMBN layer..... 126

Figure 5-7: CA at 500 mV for various concentrations of OA measured at a C-SPE modified with (PDA-MWCNT/ACOD/PDA-MWCNT/ACS)1 in 0.1 M phosphate buffer pH 7.4, with 1 mM ATP and CoA (in black) along with 6 plasma concentrations measured independently in duplicates (in red). 128

Figure 5-8: CA at 500 mV for various concentrations of serum NEFA (from 2 patients) measured at a C-SPE modified with (PDA-MWCNT/ACOD/PDA-MWCNT/ACS)1 in 1 mM ATP and CoA and 0.1 M phosphate buffer pH 7.4..... 129

Figure 5-9: CA at 500 mV for various concentrations of OA measured at a C-SPE modified with (PDA-MWCNT/ACOD/PDA-MWCNT/ACS)1 in 0.1 M phosphate buffer pH 7.4, with 1 mM ATP and CoA (in black) along with 5 serum concentrations (in red). 129

Figure 5-10: Chemical structure of water-soluble PMBN polymer [343, 344]..... 131

Figure 5-11: Structure of tetrahydrolipstatin [371]..... 138

Figure 6-1: Structure of Ferrocene (its derivatives have different functional groups on X/Y). . 145

Figure 6-2: CA at 300 mV for various concentrations of OA measured at a C-SPE modified with (PDA-MWCNT/ACOD/PDA-MWCNT/ACS)1 in 1 mM ATP and CoA and 0.1 M phosphate buffer pH 7.4..... 146

Figure 6-3: Calibration graph at 500 s. 146

Figure 7-1: The factors that contribute towards cardiovascular disease in obesity [385]. 150

Figure 7-2: CA at 500 mV for various concentrations of Uric acid measured at a C-SPE in 0.1 M phosphate buffer pH 7.4. Inset: Calibration graph at 500 s.	151
Figure 7-3: Series of reactions that occur with uric acid oxidation [389].	152
Figure 7-4: CA at 500 mV for various concentrations of Ascorbic acid measured at a C-SPE in 0.1 M phosphate buffer pH 7.4. Inset: Calibration graph at 500 s.....	153
Figure 7-5: CA at 500 mV for various concentrations of Acetaminophen measured at a C-SPE in 0.1 M phosphate buffer pH 7.4. Inset: Calibration graph at 500 s.....	154
Figure 7-6: CA at 500 mV for various concentrations of OA measured at a C-SPE modified with (PDA/ACOD/ PDA/ACS)1 in 1 mM ATP and CoA and 0.1 M phosphate buffer pH 7.4.	155
Figure 7-7: Calibration graph at 500 s. 4 serum samples from the same patient in red.	156
Figure 7-8: CA at 500 mV for various concentrations of OA measured at a C-SPE modified with (PDA-MWCNT/ACOD/PDA-MWCNT/ACS/PMBN)1 in 1 mM ATP and CoA and 0.1 M phosphate buffer pH 7.4.....	157
Figure 7-9: Calibration graph at 500 s. 5 plasma samples from the same patient in red.....	157
Figure 7-10: CA at 500 mV for various concentrations of OA measured at a C-SPE modified with (PDA-MWCNT/ACOD/PDA-MWCNT/ACS/PMBN)1 in 0.1 M phosphate buffer pH 7.4 (1 mM ATP and CoA in the PMBN layer).	159
Figure 7-11: Calibration graph at 500 s. 5 plasma samples from the same patient in red.....	159
Figure 7-12: CA at 500 mV for various concentrations of OA measured at a C-SPE modified with (PDA-MWCNT/ACOD/PDA-MWCNT/ACS/BSA)1 in 1 mM ATP and CoA and 0.1 M phosphate buffer pH 7.4.....	160
Figure 7-13: Calibration graph at 500 s. 5 different patient's plasma samples in red.	161

Figure 7-14: CA at 500 mV for various concentrations of OA measured at a C-SPE modified with (PDA-MWCNT/ACOD/PDA-MWCNT/ACS/PDA-MWCNT/PSS)1 in 1 mM ATP and CoA and 0.1 M phosphate buffer pH 7.4..... 162

Figure 7-15: Calibration graph at 500 s. 4 serum samples from the same patient in red. 162

Figure 7-16: CA at 500 mV for various concentrations of OA measured at a C-SPE modified with (PDA-MWCNT/ACOD/PDA-MWCNT/ACS/PDA-MWCNT/PMAA)1 in 1 mM ATP and CoA and 0.1 M phosphate buffer pH 7.4..... 164

Figure 7-17: Calibration graph at 500 s. 4 serum samples from the same patient in red. 164

List of tables

Table 1-1: Common NEFAs and their structures [67, 83-85]	7
Table 1-2: Fuel reserves in a typical 70 kg man [88].	8
Table 1-3: The companies/methods for NEFA detection on the market currently.....	19
Table 2-1: The normal and abnormal blood concentrations of each energy metabolism biomarker studied.....	27
Table 2-2: Leaders in glucose home sensing kits.	29
Table 3-1: The current obtained for each scan rate for each upper potential for 0.50 mM PA-CoA. All data is background subtracted. Data given in 6 significant figures.....	55
Table 3-2: The current obtained for each scan rate for each upper potential for 0.50 mM PA-CoA. All data is background subtracted. Data given in 6 significant figures.....	66
Table 3-3: Comparison of 3 different electrodes for CA at 500 mV at 500 s, current for 0.75 mM PA-CoA/OA-CoA/H ₂ O ₂	67
Table 3-4: Suggested reasons why each interference may cause incorrect NEFA readings.	68
Table 3-5: General information on the chosen interferences.....	70
Table 3-6: Each interference at 500 s CA at 500 mV.....	72
Table 4-1: Electrochemical biosensors based on LbL assembly methods for H ₂ O ₂ detection.....	78
Table 4-2: Comparison of CA at 500 mV at 500 s for OA on 3 different fabricated electrodes..	96
Table 4-3: Comparison of 3 different electrodes for CA at 500 mV at 500 s, current for 0.75 mM OA.....	98
Table 4-4: Comparison of 3 different electrodes for LSV at 1 mV s ⁻¹ at 500 mV, current for 0.75 mM OA.	98

Table 4-5: Comparison between (PDA-MWCNT/ACOD/PDA-MWCNT/ACS)1 and (PDA-MWCNT/ACOD/PDA-MWCNT/ACS)4 electrodes with OA spiking.....	102
Table 4-6: Properties determined by EIS of different enzyme layers.....	104
Table 4-7: Chronoamperometry at 500 mV, readings taken at 500 s.	109
Table 4-8: Each interference at 500 s CA at 500 mV.	113
Table 5-1: Advantages and disadvantages of plasma over serum [341].....	127
Table 5-2: Comparison of the NEFA values obtained in 6 plasma samples from the two different detection methods.	128
Table 5-3: Electrode comparison for CA at 500 mV, current taken at 500 s.	133
Table 5-4: Electrode comparison for LSV at 1 mV s^{-1} , current taken at 500 mV.	134
Table 5-5: Different methods of NEFA detection and concentration difference during storage.	136

Nomenclature

β -cells	beta cells
Cl^-	chloride ion
CO_2	carbon dioxide
E	potential (mV)
e^-	electron
H_2O_2	hydrogen peroxide
i	current (μA)
j	flux ($\mu\text{A cm}^{-2}$)
Na^+	sodium ion
O_2	oxygen
mEq/L	milliequivalent per litre, dependent on specific chemical species
R^2	correlation coefficient
s	time (seconds)

Abbreviations

ACOD	acyl-Coenzyme A oxidase
ACS	acyl-Coenzyme A synthetase
ATP	adenosine triphosphate
BSA	bovine serum albumin
C-SPE	carbon screen printed electrode
CNT	carbon nano-tubes
CoA	coenzyme A
CoPc	cobalt phthalocyanine
CV	cyclic voltammetry
EIS	electrochemical impedance spectroscopy
FAD	flavin adenine dinucleotide
FADH ₂	reduced flavin adenine dinucleotide
GOx	glucose oxidase
HbA1c	glycosylated haemoglobin
LbL	layer-by-layer
LSV	linear sweep voltammetry
MWCNT	multi-wall carbon nano-tubes
NAD ⁺	nicotinamide adenine dinucleotide
NADH	reduced nicotinamide adenine dinucleotide
NEB	negative energy balance
NEFA	non-esterified fatty acid
NEM	N-ethyl-maleinimide
OA	oleic acid
OA-CoA	oleoyl coenzyme A
PA-CoA	palmitoyl coenzyme A
PBS	phosphate buffer solution
PDA	poly(dimethyldiallylammonium chloride)
PMAA	poly(methacrylic acid)
PMBN	poly [2-methacryloyloxyethyl phosphorylcholine – co-n-butyl methacrylate – co-p-nitrophenyloxycarbonyl poly(ethylene glycol) methacrylate]
POD	peroxidase
PSS	poly(styrenesulfonate)
RBP4	Retinol binding protein 4
R _{CT}	charge transfer resistance
SPE	screen printed electrode
SD	standard deviation
SWCNT	single-wall carbon nano-tubes
T2D	Type-2-diabetes

1 Background and literature review part 1

1.1 Background

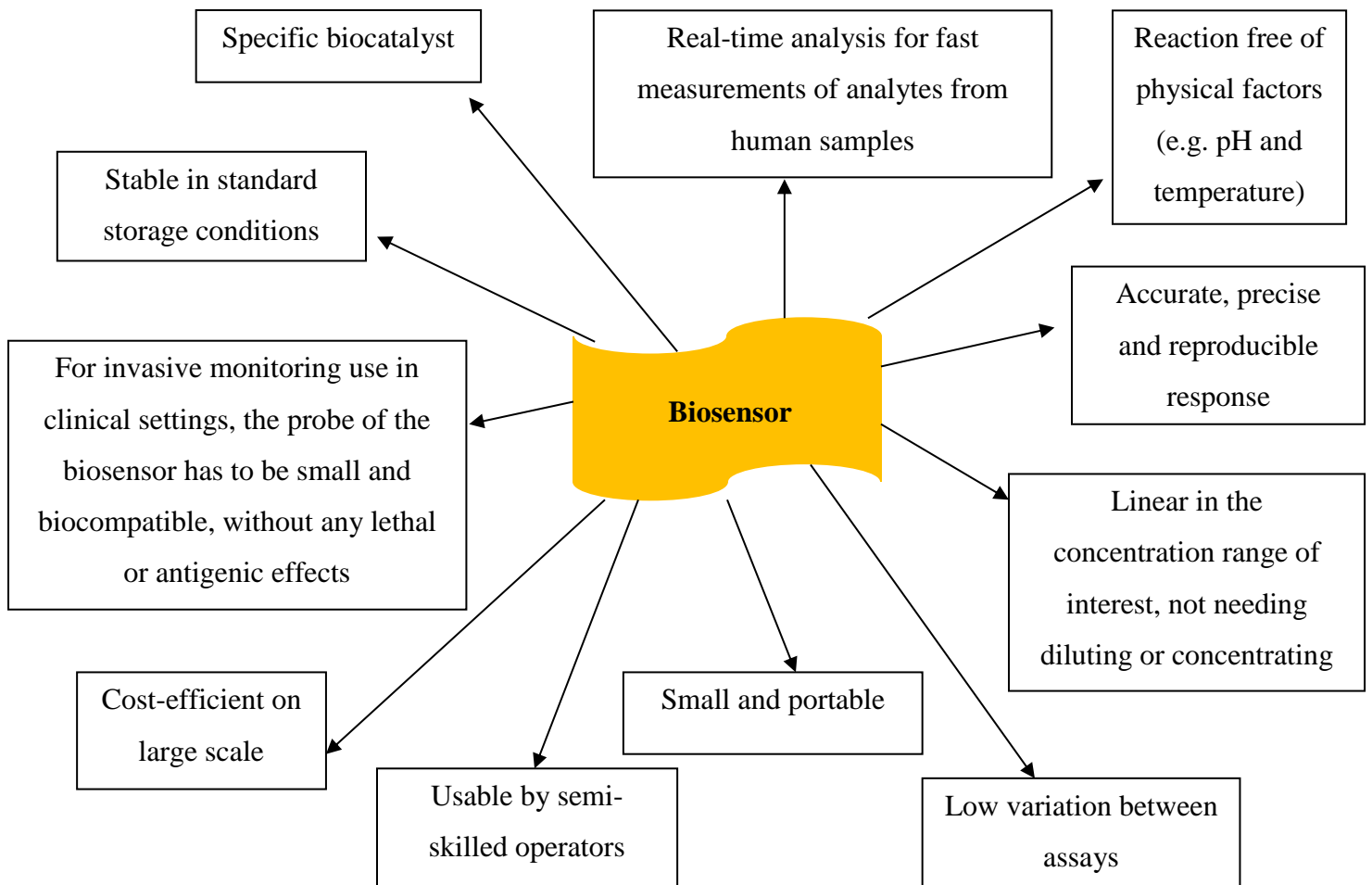
Diabetes mellitus is a typical disease of metabolism disorder [1]. Approximately 10 % of the annual NHS budget (~£9 billion), is spent on treating diabetes and its subsequent complications. It is the leading single expenditure for the NHS. According to Diabetes UK approximately over 4 million people are predicted to have diabetes by the year 2025 [2]. Mostly being type-2-diabetes (T2D), this is caused by the ageing population and large increase in overweight and obese people. These people are in danger of short and long term illnesses, such as cardiovascular events and renal malfunction [3]. Diabetes poses a major and growing health and socio-economic burden on society [4].

T2D is a chronic metabolic disorder, characterised by insulin resistance, hyperglycemia, hyperinsulinemia and elevated plasma non-esterified fatty acid (NEFA) and glucose concentrations, with poor glycemic control associated with an increased risk of heart failure [5]. With obesity having reached epidemic proportions in many countries and due to the close relationship between obesity and T2D, an epidemic of diabetes is expected to follow [6]. The vast majority diagnosed with T2D are obese. Obesity arises from an energy imbalance where energy intake exceeds energy expenditure. Dealing with obesity requires modification of one or both components of energy balance. A key drawback is the lack of suitable biomarkers to assess the power/use of different treatments on components of energy balance.

Assessment of NEFA may be a useful addition to routine diabetes management. NEFA, like glucose can reflect acute change of an individual's energy status. Glucose and NEFA are biomarkers of immediate energy metabolism. There are many glucose biosensors, but there is a need to develop a biosensor for NEFA measurements. Conventional glucose measurements provide patients with some information, but combining that with NEFA will give the patient a fuller picture on what is going on in their body with regards to their insulin resistance and insulin sensitivity.

The ideal NEFA sensor is required to be selective for NEFA with a fast, predictable response to shifting NEFA concentrations [7]. This must rely on a signal that is reversible and reproducible. The fabrication of the sensor ought to be cost efficient when applied to a large scale. It is crucial to have a lengthy operational lifetime under physiological conditions, yet most importantly it has to be tolerable for the patient. For that reason, the biosensor should not require user calibration and preferably offer real-time continuous information concerning NEFA. Fast diagnosis along with early prevention are critical in controlling T2D [8].

Conditions for a successful biosensor [9]:



1.2 NEFA - Literature review part 1

1.2.1 NEFA and its role

Over the last 5 years there have been ~150 papers published per year on NEFA as shown in Figure 1-1. This search was carried out using the database web of knowledge. The topic searched was ‘non-esterified fatty acid’ for the years 2009-2013. Only articles in English were included and studies that had repeat publications were counted as one.

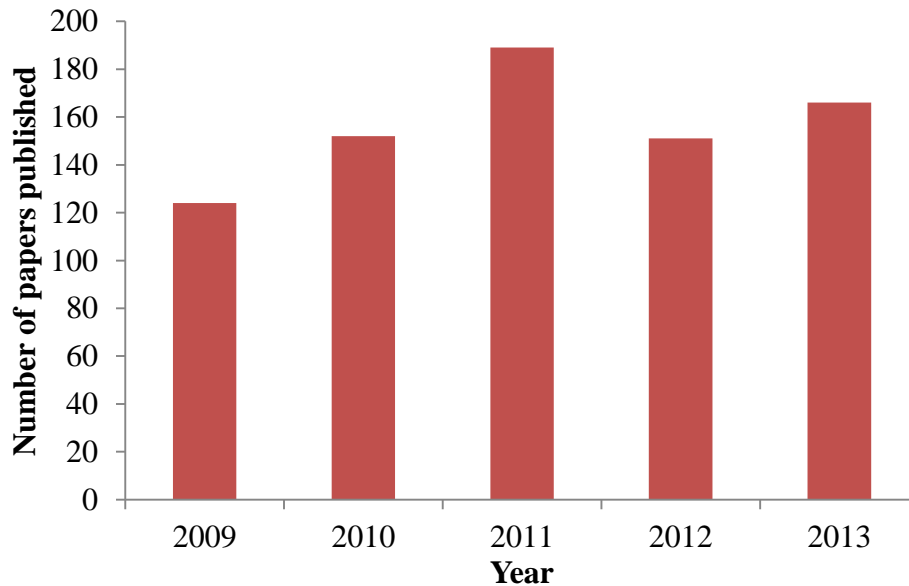


Figure 1-1: NEFA publications over the last 5 years.

Most frequently NEFA is measured in animals (especially mammals) rather than humans, 61-72 % vs. 17-29 % respectively (over the last 5 years). As NEFA is also a metabolism biomarker for lactating cows, this is another big market for NEFA biosensor development. In literature the other animals that NEFA is detected in are; rat, mice, sheep, water buffalo, bull, camel, cats, chicken, dogs, goat, hamsters, horses, pig, rabbit, elephant seal, squirrel and birds. Animal models in rats and mice have been used extensively as they relate to human energy metabolism states, plus certain things/studies that can be done in using animal models cannot be done with humans. An example of this would be fasting for 6 days, which can be ethically approved for animal studies only [10]. The breakdown of the topics of published papers per year is given in the pie charts in Figure 1-2. The papers published came under 8 sections. The section titled ‘General literature’ was created as there were some papers published on general information on

NEFA (including its use in biodiesel applications) which does not fall under any of the main categories for NEFA detection. This was the smallest section, only accounting for 2-4 % of the total.

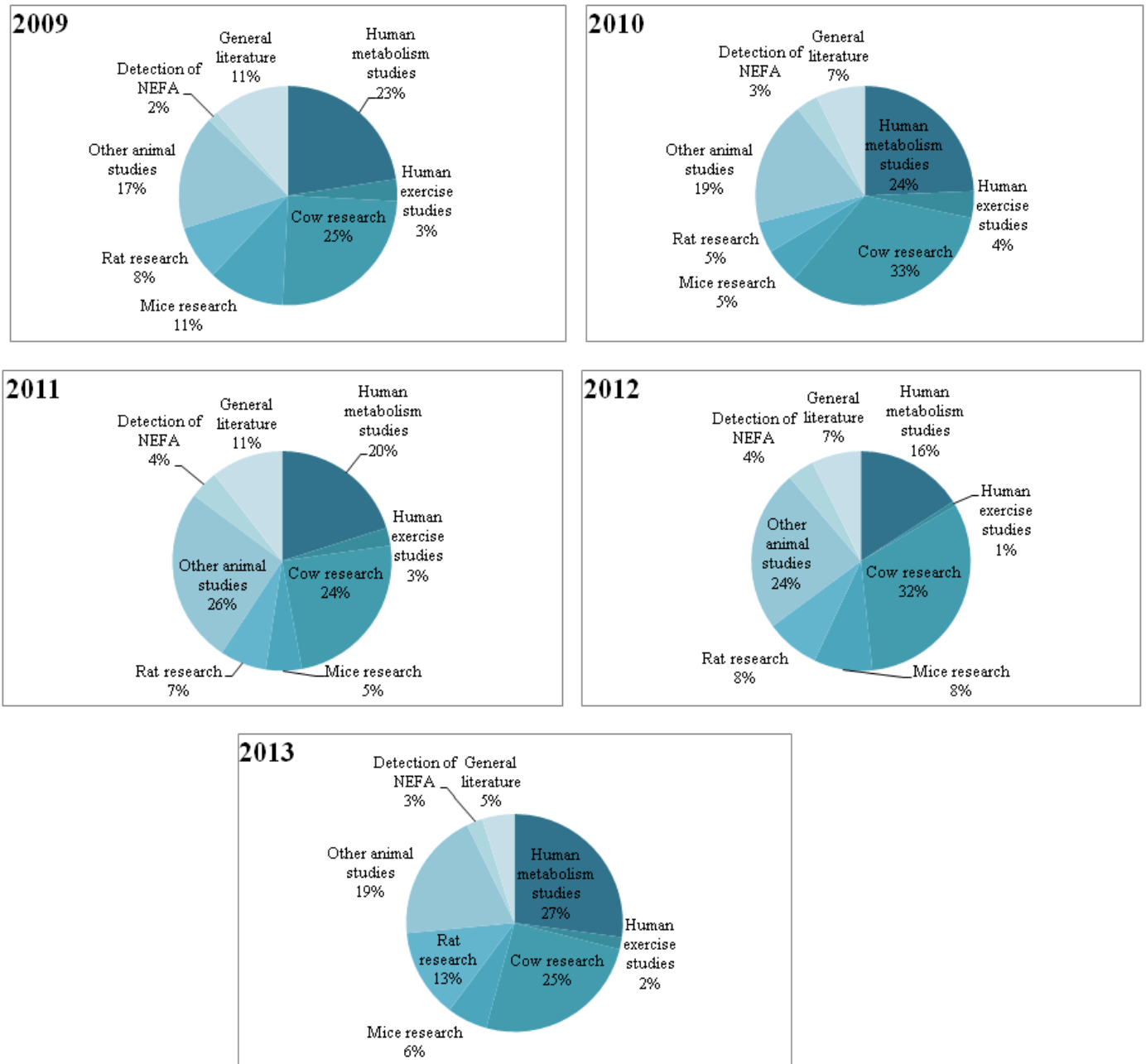


Figure 1-2: Pie charts showing the percentage distribution of the topics of publications regarding NEFA over the last 5 years.

NEFA in humans has been detected in plasma/serum for two main reasons:

1. Energy metabolism studies – such as metabolic syndrome [11, 12], obesity [13, 14], T2D [15-19], insulin resistance [20, 21], atherosclerosis [22-24], cardiovascular studies [25-27] and non-alcoholic fatty liver disease [28-30]. Other diseases include; cystic fibrosis [31], thyroid [32, 33], Alzheimer's [34, 35], multiple sclerosis [36, 37], schizophrenia [38], Rett syndrome [39], kidney function [40] and gallstone formation [41].
2. Exercise studies – in which NEFA is used as a substrate to provide energy during exercise [42-46].

NEFA levels have also been measured in pregnant women because the development and growth of the foetus depends on transport of fatty acids from the circulation of the mother's blood [47, 48]. Increase in NEFA levels are linked to maternal obesity which gives an exaggerated lipid response and higher insulin resistance, indicating a risk of future obesity in the unborn offspring [48]. Women generally have higher NEFA levels compared to men but are more insulin sensitive with better lipid profiles in comparison [49].

There have also been some publications on using Chinese herbal medications for treatment in metabolic syndrome, in which NEFA is a biomarker that is assessed routinely [50, 51]. These papers came under 'Human metabolism studies' too. Giving a total of 16-27 % share of the published literature in that section over the last 5 years.

There have been a few ways of detection and quantification of NEFA levels, including techniques such as NMR [52-54], flow cytometry [55], GC-MS [56-58], LC [59, 60], HPLC [61], fluoroimmunoassay [62], supercritical fluid extraction [63], GC-MS and GC-FTIR [64]. Obviously these came under the 'Detection of NEFA' section, with a minor 5-11 % of the overall papers published.




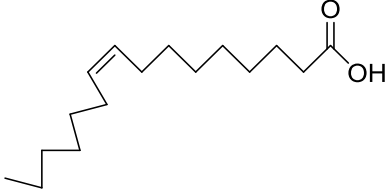
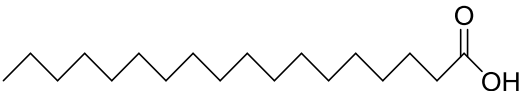
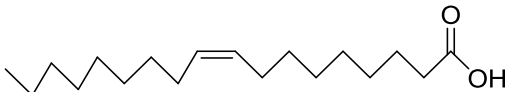
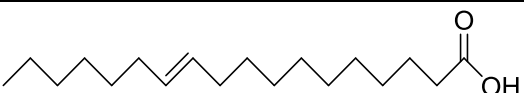
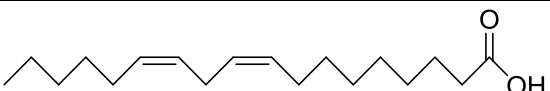

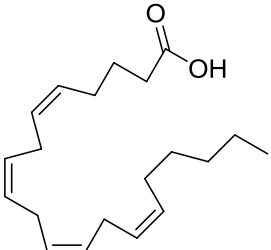
NEFA are highly hydrophobic, shunning the aqueous medium of body fluids [65]. They are generally toxic to cells and are metabolically kept at low nanomolar or micromolar concentrations in plasma. When NEFA are not attached to other molecules they are known as free fatty acids (FFA's) [66]. They are transported while being bound to plasma protein albumin

[67]. The levels of NEFA in the blood are restricted by the availability of albumin binding sites. Specific dietary fatty acids may raise total serum cholesterol levels and low-density lipoprotein (LDL) cholesterol levels [68]. Fatty acids are metabolic substrates for producing energy, precursors for many lipid species and substrates for the acylation of proteins [22].

The pattern of NEFA concentrations in blood is interesting for a variety of biochemical and clinical investigations both in animals and humans. NEFA make up approximately 10 % of the total blood fatty acids, usually 0.5 - 2.0 mmol/L [69]. The plasma concentration increases during periods of fasting as fatty acids are released from adipose tissue for use as metabolic fuel. The oxidation of fatty acid is increased 2.5 times during fasting [70]. In fasting NEFA is the energy source for most tissues (peripheral – heart, skeletal muscle and liver) except the brain and red blood cells [71]. Typical plasma NEFA levels are ~ 0.3 – 0.6 mmol/L after overnight fasting, and up to 1.3 mmol/L after 72 hours of fasting [49]. In other literature plasma NEFA concentration is stated to be between the range of 0.1 – 1.0 mmol/L [72]. Parallel to this, there have been significant increases in NEFA blood levels reported (up to 1.143 mmol/L higher than at rest) during stressful periods (that is mental and emotional stress) in humans [73, 74]. Palmitic acid accounts for ~ 30 % of the total NEFA pool independently of the plasma NEFA concentration [75].

Elevated plasma NEFA levels are predictive/indicative of obesity, T2D, hypertension, dyslipidemia, atherosclerotic vascular disease, non-alcoholic fatty liver disease, sudden death and cancer mortality [49, 72, 76-81]. The elevation increases as adipose tissue accumulates, particularly with abdominal obesity [72]. The type of fat consumed may alter the NEFA pool in plasma [82]. This affects both short and long term NEFA composition of the human diet. The common NEFAs that have been investigated in NEFA studies are listed in Table 1-1.

Table 1-1: Common NEFAs and their structures [67, 83-85]

NEFA	Chain formula	Chemical formula	Structure
Lauric acid	C12:0	C ₁₂ H ₂₄ O ₂	
Myristic acid	C14:0	C ₁₄ H ₂₈ O ₂	
Palmitic acid	C16:0	C ₁₆ H ₃₂ O ₂	
Palmitoleic acid	C16:1 cis	C ₁₆ H ₃₀ O ₂	
Stearic acid	C18:0	C ₁₈ H ₃₆ O ₂	
Oleic acid	C18:1 cis	C ₁₈ H ₃₄ O ₂	
Vaccenic acid	C18:1 trans	C ₁₈ H ₃₄ O ₂	
Linoleic acid	C18:2 cis	C ₁₈ H ₃₂ O ₂	
Arachidic acid	C20:0	C ₂₀ H ₄₀ O ₂	
Arachidonic acid	C20:4 cis	C ₂₀ H ₃₂ O ₂	

1.2.2 NEFA in human blood

The blood plasma of an average 70 kg man contains 50 milliequivalent per litre (mEq/L) of fatty acids (25 mEq/L in phospholipids, 12 mEq/L in cholesterol esters, 10 mEq/L in triglycerides and 3 mEq/L in NEFA) [86]. Fatty acids are stored as triacylglycerols, which are our principle energy reserves [87]. As can be seen from Table 1-2 the potential energy stored in triacylglycerols in the average person exceeds that which is stored anywhere else. Stored fuels serve to meet caloric needs during starvation for 1 to 3 months, whereas carbohydrate reserves are exhausted in 1 day [88]. NEFA is the major fuel during long periods between meals [89]. NEFA are also a major fuel for muscle contraction in light to moderate exercise and for longer periods of exercise [90]. Whilst exercising the NEFA concentration is 2 to 3 times higher than it is at rest [91-93]. The triacylglycerol/fatty acid substrate cycle regulates lipid metabolism [70].

Table 1-2: Fuel reserves in a typical 70 kg man [88].

Organ	Available energy in kcal (kJ)		
	Glucose or glycogen	Triacylglycerols	Mobilizable proteins
Blood	60 (250)	45 (200)	0 (0)
Liver	400 (1,700)	450 (2,000)	400 (1,700)
Brain	8 (30)	0 (0)	0 (0)
Muscle	1,200 (5,000)	450 (2,000)	24,000 (100,000)
Adipose tissue	80 (330)	135,000 (560,000)	40 (170)

There is an early rise in blood triglyceride concentrations minutes after having a meal that contains fat [94]. Diets high in fat are associated with obesity, T2D and atherosclerosis. Another side effect of obesity is non-alcoholic fatty liver disease. In obesity-related insulin resistance, the oxidation of fatty acid is reduced.

There are 3 stages of mitochondrial oxidation of fatty acids [95]:

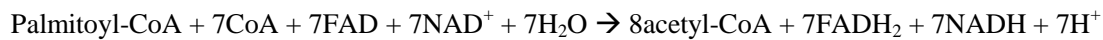
1. β -oxidation of the fatty acids - the oxidative removal of two-carbon units successively as acetyl-Coenzyme A (acetyl-CoA).

2. Acetyl-CoA's acetyl residues are oxidized to CO₂ in the citric acid cycle (also known as the tricarboxylic acid or Krebs's cycle) in the mitochondrial matrix.
3. Electrons derived from the 1st two stages are passed to O₂ in the mitochondrial respiratory chain; this provides energy for ATP synthesis by oxidative phosphorylation.

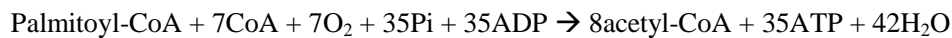
In the 1st stage for palmitic acid (carbon-16, typical saturated fatty acid as an example), seven passes are undergone through this oxidative sequence using 4 enzyme-catalysed reactions (shown in Figure 1-3), losing 2-carbons as acetyl-CoA each time. The equation for the 1st pass is:



7 more passes through this sequence oxidizes one molecule of palmitoyl-CoA to 8 molecules of acetyl-CoA. The overall equation:



Including the electron transfers and oxidative phosphorylation:



The 2nd stage, together with the coupled phosphorylations of the 3rd stage gives:



Overall equation for palmitoyl-CoA's complete oxidation to CO₂ and H₂O:



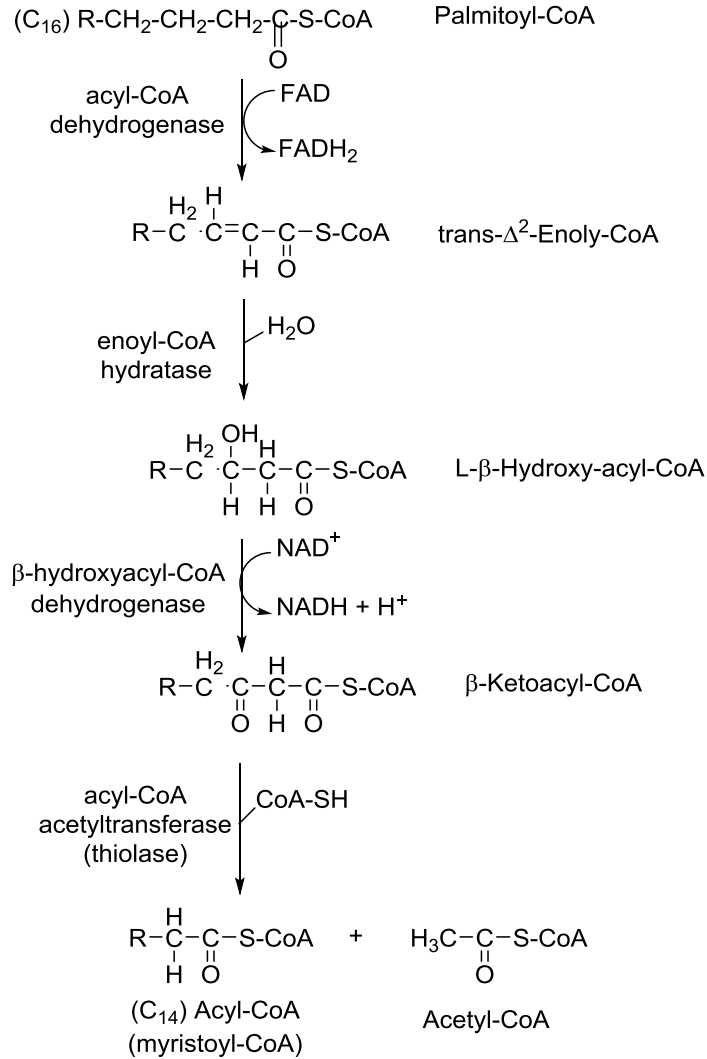


Figure 1-3: Palmitoyl-CoA oxidation.

The oxidation of monounsaturated fatty acyl-CoA's (e.g. oleoyl-CoA) require an additional enzyme, enoyl-CoA isomerase (Figure 1-4). This enzyme converts the cis isomer to trans isomer.

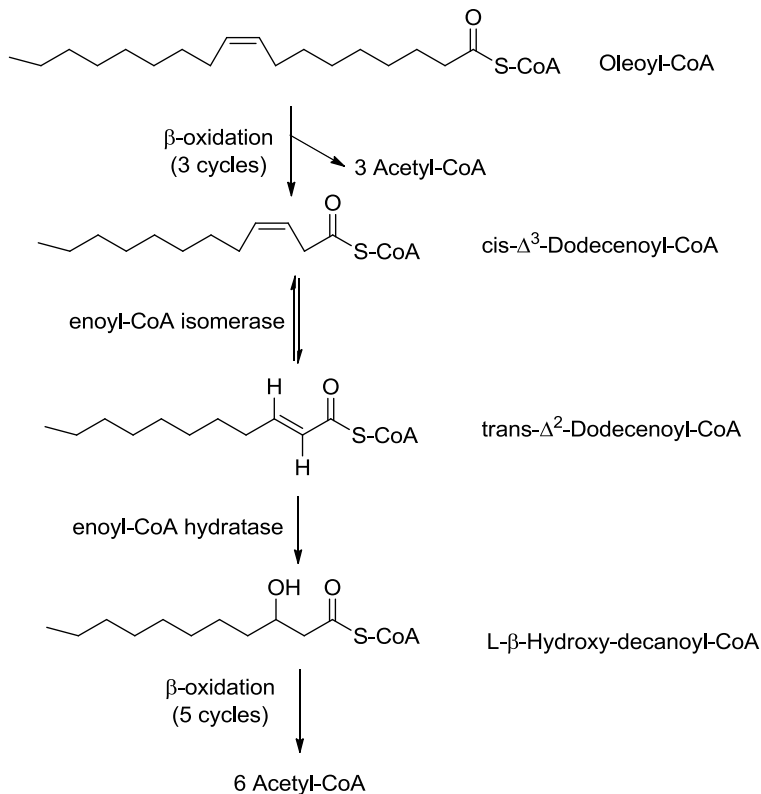


Figure 1-4: Oleoyl-CoA oxidation.

The acetyl-CoA generated from the oxidation of glucose and NEFA is then further metabolized by the citric acid cycle [96]. In the cycle two things happen, phase 1 (reactions 1-4) oxidize two carbons to CO₂, phase 2 (reactions 5-8) regenerates oxaloacetate [97]. This is illustrated in Figure 1-5. Four oxidation reactions occur. The coenzyme for 3 of the reactions was nicotinamide adenine dinucleotide (NAD⁺) and for 1 was flavin adenine dinucleotide (FAD). The structure of FAD is shown in Figure 1-6. FAD undergoes two electron oxidation and reduction reactions (Figure 1-6). Having an intermediate of semiquinone free radical results in these reactions occurring one electron at a time. Reduced flavin adenine dinucleotide (FADH₂) and reduced nicotinamide adenine dinucleotide (NADH) then transport energy to the mitochondrial electron transport chain (ETC) [96]. This is where oxidative phosphorylation happens.

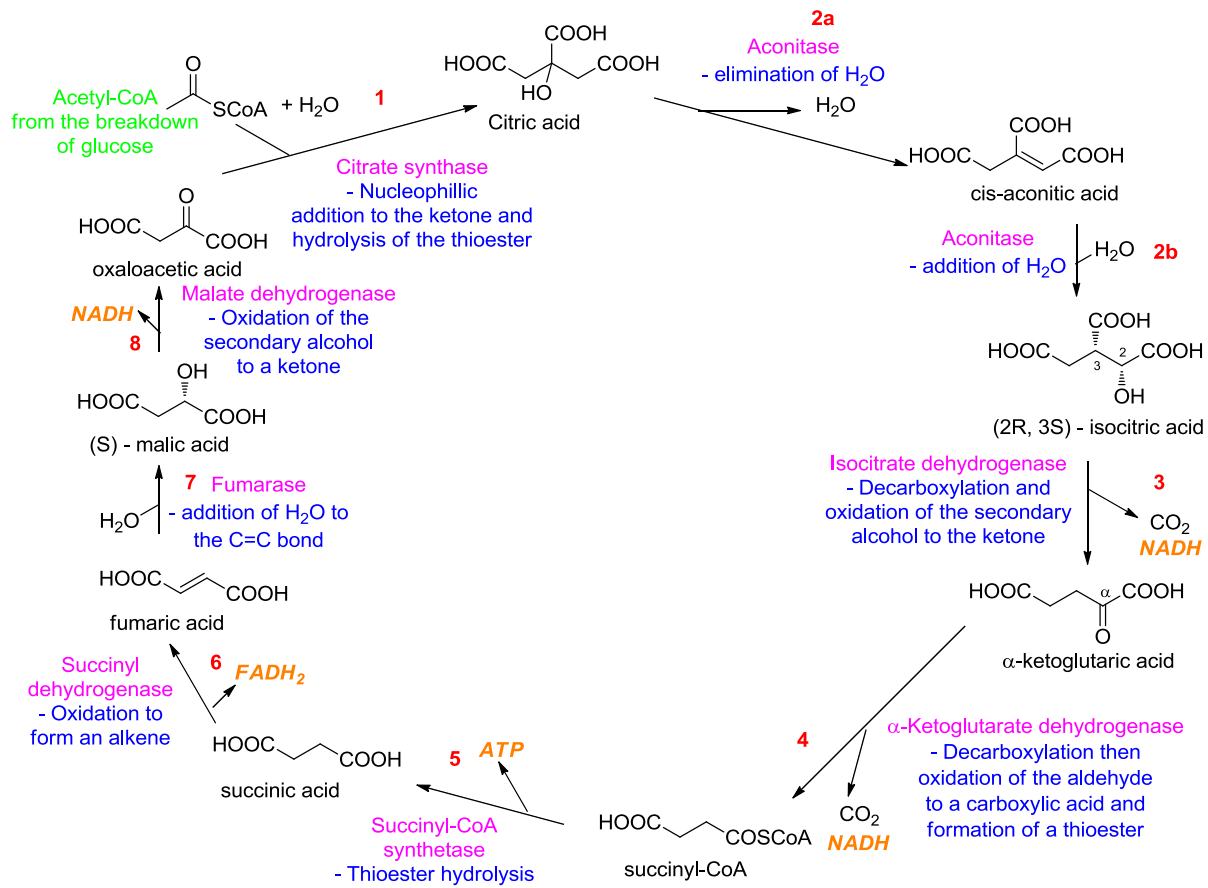


Figure 1-5: Citric acid cycle [97, 98].

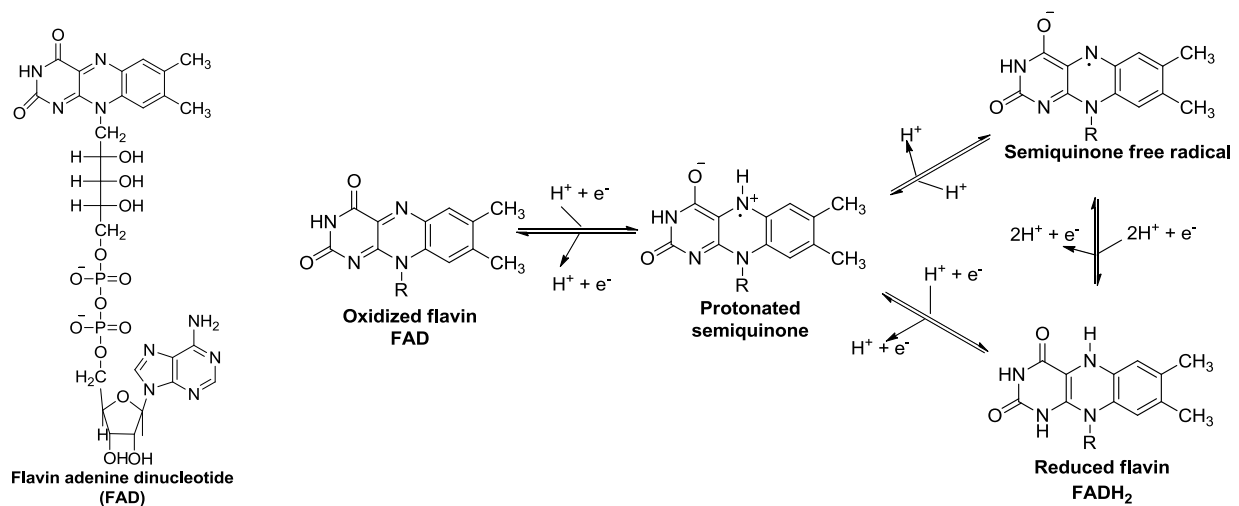


Figure 1-6: Full Structure of FAD and FAD oxidation and reduction reactions [97].

Once the acetyl-CoA formed (β -oxidation in the liver), exceeds the capacity of the citric acid cycle, that excess forms ketone bodies, as in acetone, acetoacetate and D- β -hydroxybutyrate [99]. This happens in severe, uncontrolled diabetes. Diabetics oxidize large amounts of fatty acid instead as glucose is not used efficiently. The activity of the citric acid cycle is therefore reduced and acetyl-CoA accumulates.

1.2.3 NEFA, obesity and prevention of T2D

Diets containing high levels of saturated fats lead to obesity and insulin resistance, and increase levels of circulating NEFAs [4, 79]. In addition, they contribute to pancreatic β -cell failure in genetically predisposed individuals. NEFAs cause β -cell apoptosis and may thus contribute to progressive β -cell loss/damage in T2D (Figure 1-7) [4]. NEFA concentration in blood is a biomarker for diabetes. Once diabetic, the plasma NEFA levels show linear correlation with blood glucose and hepatic glucose production (in both lean and obese individuals) [100]. Cross-talk between adipocytes and β -cells is mediated by NEFA and adipocyte secreted adipokines [4]. High concentrations of circulating NEFAs (especially saturated NEFAs) and low adiponectin levels are predictive of developing diabetes. NEFA and adipokines play a direct role in pancreatic β -cell failure in T2D.

Prolonged increase of circulating NEFAs by lipid infusion damages the task of pancreatic β -cells *in vivo*, especially in people with a genetic predisposition to T2D. People with T2D in the family are 2-6 times more susceptible to developing it than people without [101, 102]. After myocardial infarction, NEFA has been stated responsible for ventricular arrhythmias and is strongly correlated with heart rate and blood pressure [103]. Lipotoxicity has damaging effects of regularly elevated NEFA by reducing the secretion of insulin, diminishing insulin synthesis and β -cell apoptosis [16]. Preventing β -cells from exposure to high serum levels could delay the progression of T2D. During morning hours, high levels of NEFA and very low density lipoproteins relate to prevalence of heart attacks being most frequent [74].

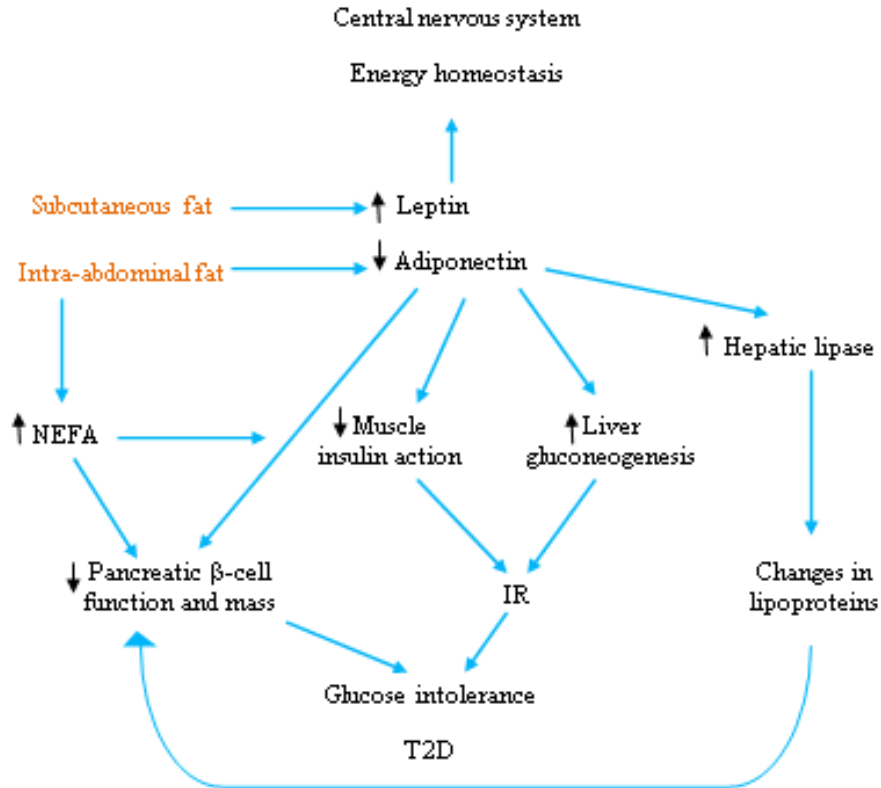


Figure 1-7: Model for the effects of adipocytes on pancreatic β -cell function/mass and insulin sensitivity in the pathogenesis of T2D [4]. IR = insulin resistance.

NEFA is considered to link obesity with insulin resistance and T2D [104, 105]. Weight loss of ~5 % in people at risk of developing T2D cuts the risk in half [6]. The factors that contribute to cardiovascular disease are shown in the appendix in Figure 7-1. National Institute of Health (1998) issued obesity treatment guidelines proposing a 10 % weight loss. Currently there are two ways to reverse T2D, that is either by surgery (bariatric gastric band) or by lifestyle interventions (diet – calorie restriction and exercise) [106, 107]. Studies have been done to explore the lifestyle intervention option by many including the Finnish Diabetes Prevention Study Group, groups also in China, Sweden and in UK by Professor Roy Taylor’s Group based at Newcastle University [108-111]. In the latter study, 11 patients who had T2D (for a period < 4 years) were put on a 600 kcal/day diet for 8 weeks [111]. Multiple variables (such as weight, BMI and waist circumference) and metabolism biomarkers (including glucose, NEFA and cholesterol) were monitored, after weeks 1, 4 and 8. At the end of the study, following the diet, normal β -cell

function and glucose levels were restored. The NEFA levels were reduced from 0.93 mM at week 1 to 0.81 mM at week 4 to 0.72 mM at week 8, compared to the controls (0.57 mM).

Commercial UV NEFA detection method was used in the study. Having a NEFA electrochemical sensor would be useful for research in lifestyle interventions such as this. This research encouraged the public to share their weight loss and T2D reversal experience [112]. 61 % of this population studied was successful, with minimal/no support from healthcare practitioners. As there is no commercial NEFA sensor at the moment, these self-monitoring home patients used fasting capillary blood glucose and glycosylated haemoglobin (HbA1c) as methods of measurement for their T2D. Glucose meters and glycohaemoglobin test-kits are used as they are the two foremost indicators in diabetes diagnosis and long-term management [8].

More long-term studies have been done by the Look AHEAD Research group, in which the NEFA concentrations have significantly decreased with weight loss over a longer time [113, 114].

1.2.4 Current methods of NEFA detection

1.2.4.1 Initial methods

For NEFA detection most investigators have employed palmitate and/or oleate as their fatty acids of choice, probably because these two fatty acids represent the major species present in human serum and therefore, they are the principal molecules to which β -cells might be exposed to *in vivo* [115].

NEFA detection in blood can be dated back to the late 1950s [116-120]. The methods developed during this time can be classified into four groups [121]:

- (a) colorimetric titration of NEFA in the presence of a pH indicator [122-124]
- (b) spectrophotometric or radiochemical measurements of complexes of NEFA with divalent metal ions such as Cu^{2+} , Ni^{2+} or Co^{2+} [125]
- (c) colorimetric assays based on a reaction between NEFAs [126]
- (d) radiochemical assay of NEFA [127, 128]

These methods, however, were either laborious, time-consuming or showed a lack of good sensitivity. Of these methods only colorimetric and radioassay methods met the requirements for a small sample volume with radioassay requiring specialised equipment and radioisotope handling [129].

Several molecules were found to cause interference with NEFA level determination, namely, phospholipids, bilirubin, albumin, haemoglobin, lecithin, lactic acid, acetic acid, ascorbic acid, β -hydroxybutyric acids, triglycerides, glutathione, cysteine and unreacted CoA [118, 121, 125, 127, 129-132]. These will be discussed in detail later.

1.2.4.2 NEFA multiple enzyme biosensor development

In 1989, Sode *et al* developed two NEFA sensors. The first biosensor was developed following the reaction in Figure 1-8 [133]. The measurement was based on monitoring dissolved O_2 consumed by the two sequential reactions catalysed by the enzymes immobilized in photo-cross-linked polyvinyl alcohol. They were entrapped on a cellulose nitrate membrane, which was then placed over a Teflon membrane of a Clark-type membrane O_2 sensor [134]. The two enzymes used were acyl-Coenzyme A synthetase (ACS) and acyl-Coenzyme A oxidase (ACOD).

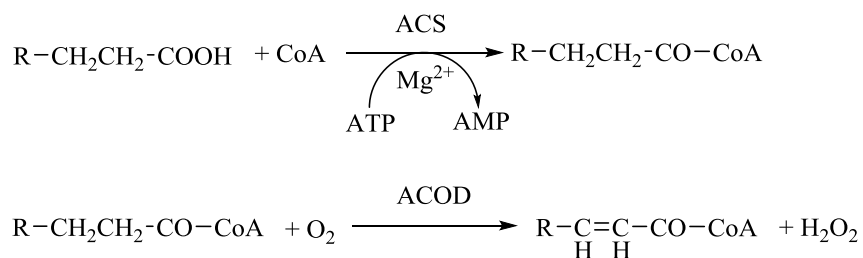


Figure 1-8: Reaction scheme of the enzymatic determination of NEFA [133].

Aqueous emulsions of oleic and palmitic acid were tested. The biosensor was linear from 0.38 to 2.0 mM for oleic acid and to 2.6 mM for palmitic acid and was stable and usable for three days.

The second amperometric sensor was developed using 5 sequential enzyme reactions (Figure 1-9) for the measurement of NEFA in oily foods [135]. The sensitivity of the sensor towards oleic acid was 0.046 $\mu\text{A}/\text{mM}$ and for palmitic acid was 0.039 $\mu\text{A}/\text{mM}$. Further improvement of the sensor was essential for its use in clinical analysis.

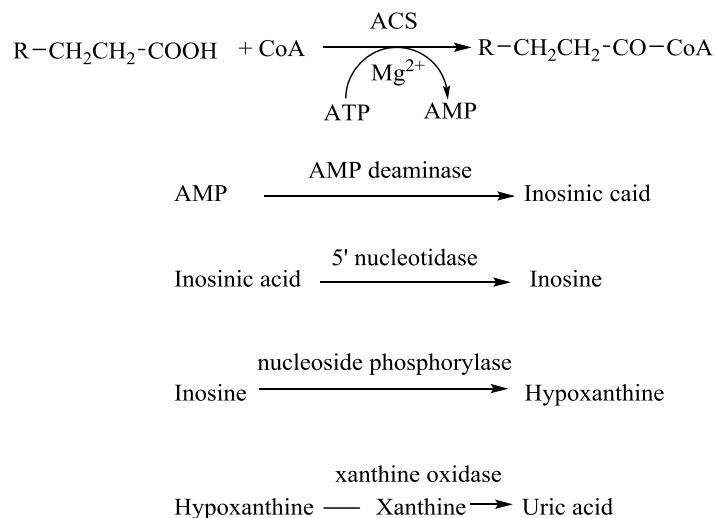


Figure 1-9: Sensor based on 5 sequential enzyme reactions [135].

1.2.4.3 Current clinical NEFA detection

Many companies worldwide (including; Wako Diagnostics, Roche Applied Science, Zen-Bio Inc. and Randox) have developed an enzymatic method to detect the amount of NEFA in a given sample of blood. All enzymatic methods rely upon the acylation of coenzyme A (CoA) by the NEFA in the presence of added enzyme ACS. The acylated CoA (acyl-CoA) is then oxidized by added enzyme ACOD with the generation of hydrogen peroxide (H₂O₂). In the presence of peroxidase (POD) this H₂O₂ allows the oxidative condensation of another compound to form a coloured dye which is then measured colorimetrically at a particular wavelength. There are different coloured dyes produced depending on which compounds as dye the companies use, and their respective absorbance is measured at wavelengths accordingly.

Figure 1-10 shows the enzymatic reactions used in the different assays for NEFA detection. Table 1-3 summarizes the information provided commercially by the same companies. These kits are explicitly for research use only and are not to be used for diagnostic procedures, as stated in the leaflet of instructions provided. The use of ascorbate oxidase and N-ethyl-maleinimide (NEM) in some kits is for elimination of interferences from ascorbic acid or excess CoA, respectively.

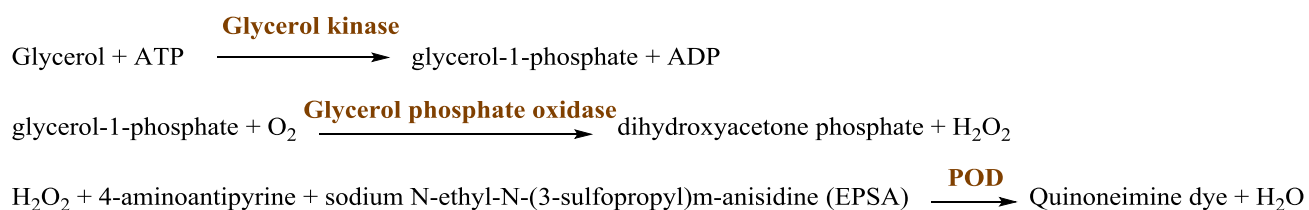


Figure 1-10: Different assay schemes used for NEFA detection (colorimetric methods are shown in red, fluorometric in green) [136-146].

Table 1-3: The companies/methods for NEFA detection on the market currently.

Company name	Method of detection	Serum/plasma	Used for?	Standard used	Detection range (mmol/L)	Ascorbate oxidase?	NEM ?	Measured wavelength (nm)	Reference
Roche Applied Science	Colorimetric	Both	Humans	Palmitic acid	Up to 1.5	Yes	Yes	546	[142]
Wako Diagnostics	Colorimetric	Serum	Humans	Oleic acid	0.01 to 4	No	No	550	[143]
Zen-Bio Inc.	Colorimetric	Both	Humans, mice, rats and other animals	Oleic acid	0.333 to 1	No	No	540	[144-147]
Randox Laboratories Ltd.	Colorimetric	Both	Humans, mice, rats and other animals	Palmitic acid	0.072 to 2.24	Yes	Yes	550	[148]
Cusabio	ELISA	Both	Bovine	Palmitic acid	1×10^{-8} to 4×10^{-7}	-	-	450	[149]
BioVision Inc.	Colorimetric	Both	Mammalian	Palmitic acid	2×10^{-3}	No	No	570	[150]
	Fluorometric	Both	Mammalian	Palmitic acid	2×10^{-3}	No	No	535/590	[150]
Shanghai Crystal Day Biotech Co. LTD	ELISA	Both	Bovine	Oleic/palmitic/stearic acids	2×10^{-3} to 0.6	-	-	450	[151]
Catachem Inc.	Colorimetric	Both	Humans, mice, rats and other animals	Synthetic fatty acids	0 to 2.5	Yes	No	550	[136]
Diagnostic systems	Colorimetric	Both	Humans	Oleic acid	0.01 to 3	No	No	546/600	[138]
Cell Biolabs Inc.	Colorimetric	Both	Humans	Palmitic acid	0 to 0.5	No	Yes	570	[140]
	Fluorometric	Both	Humans	Palmitic acid	0 to 0.5	No	Yes	530/590	[141]
Sigma-Aldrich	Colorimetric	Both	Humans	Palmitic acid	1	No	No	570	[152]
	Fluorometric	Both	Humans	Palmitic acid	1	No	No	535/587	[152]
Abcam	Colorimetric	Both	Humans	Palmitic acid	2×10^{-3}	No	No	570	[153]
	Fluorometric	Both	Humans	Palmitic acid	2×10^{-3}	No	No	535/590	[153]
Cayman Chemical Company	Fluorometric	Both	Humans	Oleic acid	0 to 0.25	Yes	Yes	530/590	[137]

A few 96-well NEFA detection kits have been developed by the company Zen-Bio Inc. (cat # SFA-1/SFA-10) for increased throughput analysis [144, 145]. This was produced for ease, to reduce the cost of labour and supplies [154]. Zen-Bio Inc. have also developed a 96-well NEFA and free glycerol detection kit (cat # GFA-1) and a cellulite treatment screening kit for NEFA and free glycerol detection (cat # LIP-12) [146, 147]. In these two kits the method for NEFA detection is the same as that shown in Figure 1-10. However the glycerol is detected via the following reaction scheme:



The increase in absorbance at 540 nm is directly proportional to the glycerol concentration of the given sample.

The first two reactions in Figure 1-10 are highly specific for NEFA, but there is interference with the third reaction due to the incomplete selectivity of the POD [155]. The known interferences in these methods were; haemoglobin, ascorbic acid, uric acid, hemolysis, bilirubin, lipids, heparin, citrate, oxalate, ethylenediaminetetraacetic acid (EDTA), sodium fluoride and drug metabolites [140, 141, 143, 155, 156]. CoA is also known to interfere with the POD reaction [139]. Interference of excess CoA and use of NEM can be avoided by use of special trinder reagent (for colour change test) such as p-sulfonyl-carbethoxy pyrazolone (p-SCEP), as the company Diagnostic Systems based in Germany had done. In the listed assays the limits of detection vary from 1.5 mM to 3.0 mM NEFA, and some assays state that they are usable for urine, saliva and other related biological tissue liquid too.

These commercial kits are not only expensive, but once the reagents are mixed they have to be used up within a month, as the enzymes have a limited lifetime. The assays do take a long time to complete if done individually. However for doing long term studies of NEFA concentrations in humans/animals, these kits are not ideal.

1.2.5 The role of NEFA in other disease states

1.2.5.1 Refsum's disease

Mitochondrial disorders affect metabolically active tissues right through the body [157]. The determination of percentage composition of individual NEFA in plasma is important when investigating metabolic disorders involving fatty acids, like in Refsum's disease [158]. Refsum's disease is a rare autosomal recessive disorder (prevalence is 1 in 10^6 people) [159]. Typical characteristics of this disease include retinitis pigmentosa, progressive deafness, anosmia, peripheral neuropathy, cerebellar ataxia, skin changes, cardiac complications (in later life) and skeletal abnormalities [159, 160].

Refsum's disease is a disorder of the metabolism of phytanic acid, which consists of 20 carbons, multibranched (3,7,11,15-tetramethylhexadecanoic acid), structure is shown in Figure 1-11 [160].

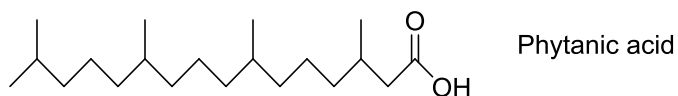


Figure 1-11: Chemical structure of Phytanic acid.

Phytanic acid is virtually undetectable in normal plasma ($< 10 \mu\text{mol/L}$), but in patients with the disease the plasma concentration of the fatty acid becomes $> 200 \mu\text{mol/L}$ [161]. Other peroxisomal diseases in which phytanic acid is increased are:

- α -methylacyl-CoA racemase (AMACR) deficiency
- peroxisomal biogenesis disorders
- rhizomelic chondrodysplasia punctata (RCDP) type 1

Patients who have Refsum's disease must cut phytanic acid from their diet (present in dairy products, ruminant animal fats and meats), reducing its concentration in plasma and some of its symptoms quite drastically [160]. Peroxisomal acyl-CoA oxidase deficiency like Refsum's disease is a recessive genetic disorder, which is detectable by the accumulation of very long-chain fatty acids (26 carbon atoms) in plasma [162].

1.2.5.2 NEFA measurements in saliva

Saliva glands are located in the oral cavity with saliva consisting of proteins, glycoproteins, lipids and inorganic ions, whose composition is affected by the diet of the individual [163, 164]. With neutral lipids (cholesterol, cholesterol esters, tri-, di- and mono-glycerides and NEFA) constituting 70-95 % of the total lipids, having NEFA (C₁₂ to C₂₂) as at least 10 % of that contribution [165, 166]. Recently using gas chromatography–mass spectrometry in resting saliva, the 4 main predominant NEFAs were identified as palmitic, oleic, linoleic and stearic acids with the concentrations ranging from 20 to 60 µM [167, 168]. At the pH of saliva, NEFA is in its undissociated form so it is perceived as an irritant [169]. Oleic acid is used in studies due to its resistance to oxidation, low cost and high concentration in the human diet [170].

Humans can detect short, medium and long chain NEFAs via oral chemosensory detection [167, 171]. NEFA can act as a signal for the presence of fat in the oral cavity and reflect the fatty acid composition in the diet, therefore the analysis of salivary NEFA may provide an objective and non-invasive method for the assessment of dietary fat intake in individuals [168]. Also in rodents, fat detection can be measured from the in-mouth release and detection of NEFA [172]. However the surface active properties of NEFA lead to desorption of interfacial properties and destabilization of emulsions, due to the favoured droplet coalescence [169].

In diseases such as cystic fibrosis and Sjögren's syndrome, there are also elevated NEFA levels in the patients saliva making NEFA an important biomarker for the disease diagnosis of these [163]. Cystic fibrosis is a hereditary disease in which the transmembrane regulator protein is affected, in this disease there are reduced levels of docosahexaenoic acid (C_{22:6}) and increased levels of oleic acid [31]. Increasing the amount of docosahexaenoic acid in the diet has shown to improve the condition in some work [173]. In patients with multiple sclerosis, fatty acid supplements are used for treatment of symptoms, detection of NEFA would help in formulation of fatty acid supplements [36]. Increase in NEFA levels has also been found in patients with schizophrenia, as there are changes in metabolism [38].

However, there are three different types of salivary glands (submandibular, sublingual and parotid), each differing in the amount of NEFA they produce, further work is needed in this area, if an oral sensor was to be developed.

1.2.5.3 NEFA detection in animals

Quantitation of NEFA in plasma and serum can be used to assess and monitor nutritional status in transitional cows (who are going through rapid foetal development, parturition and milk production) [174]. A negative energy balance (NEB) occurs in transitional dairy cows because of [175, 176]:

- increased energy demands at parturition
- decreased dry matter intake (DMI) shortly before parturition
- lagging DMI compared with energy demands due to production of milk

NEB causes increased circulation of NEFA and is positively associated with increased incidence of several postpartum diseases such as fatty liver, ketosis, hepatic lipidosis, metritis, retained placentas and displaced abomasums [175, 177-179].

Desirable NEFA concentrations in cow plasma are $\sim 325 \mu\text{M}$. Above $400 \mu\text{M}$ means there is a NEB along with subsequent intensive lipomobilization and NEFA serum concentrations above $700 \mu\text{M}$ are associated with ketosis [179-181]. In dairy cows, serum NEFA concentrations higher than $720 \mu\text{M}$ has a reduced risk of pregnancy and milk production because of the direct physiological relationship between NEFA concentration and NEB [177]. During late pregnancy, there is an increased demand of glucose which leads to mobilization of lipid reservoir and increasing NEFA levels, plus there is higher NEFA concentration found in the plasma of twin bearing animals than there is a single foetus [182].

Household pets, such as cats and dogs can develop either type 1 or T2D, NEFA levels could be monitored here. In insulin-resistant horses there are also increased NEFA levels [183]. Normal NEFA concentrations are $\sim 46 \mu\text{mol/L}$ in healthy adult horses and $\sim 100 \mu\text{mol/L}$ in obese ones [184]. Lately a study of NEFA levels have also been done in camels [185].

Representative animal models are used to help in diabetes research for humans. The chosen animals for these controlled conditions are rats, mice, transgenic mice, desert gerbils, guinea pigs, sheep and pigs, because of their similar embryology, anatomy, physiology and pharmacology to humans [186-189]. It is best to use more than 1 model as this shows the variety in human diabetic patients [187]. These animals do not exactly develop diabetes but develop

conditions that would equate to human diabetes by exploration [188]. The analysis of the NEFA levels of these animal models would give biochemical and molecular biological mechanisms of the pathophysiology of disease.

There are several blood variables (including glucose and NEFA) that are increased by transporting bulls from one area to another, due to stress [190, 191]. NEFA parameters have been measured in bulls that are going to slaughter houses and to genetic testing centres. Increase in NEFA concentrations were found in both types of transport. This is parallel to the increase in NEFA found in humans under stress discussed earlier [73, 74].

1.2.6 Conclusion

In conclusion to part 1 of the literature review regarding NEFA itself, multiple interesting points have been highlighted. Firstly there has been no electrochemical NEFA biosensor ever developed for NEFA detection in human blood or blood in mammals. The current way of detecting NEFA in humans and mammals relies on expensive assays, which are beneficial for mass throughput only. This would not be needed for individual patient NEFA values.

The importance of NEFA for T2D studies has been mentioned at length here and its evidence is also present in numerous literature regarding energy metabolism studies. The measurement of NEFA is useful in diseases/disorders other than T2D, such as Refsum's disease, cystic fibrosis and Sjögren's syndrome. The NEFA value in saliva has also been significant as a biomarker in some of these conditions, however due to the complexity of the secretions from the three salivary glands it has never been taken forward.

NEFA has been detected in many energy metabolism studies in animals. With most of the recent publications of NEFA being in this sector, it gives another incentive to develop a sensor for blood NEFA measurements.

2 Biomarkers and Biosensors – Literature review part 2

2.1.1 Biomarkers for energy metabolism

Biomarkers are induced variations within cellular or biochemical mechanisms, processes, structures, or functions, that are quantifiable in a biological system or sample [192]. The International Programme on Chemical Safety (IPSC) of the World Health Organisation (WHO) has recognized three types of biomarkers; exposure, effect or susceptibility. Biomarkers are subjectively analyzed and evaluated as an indicator of normal biological/pathogenic process, or pharmacological reaction to therapeutic intervention by drugs or therapy [193].

Glucose, glycosylated haemoglobin (HbA1c), lactate, cholesterol, creatinine, urea and retinol binding protein 4 (RBP4) are clinically important analytes and can be used as energy metabolism biomarkers. Each biomarkers relevance will be discussed in further detail below.

The sweet taste of a diabetic patients urine as a biomarker for diabetes was recorded in the first century B.C. by Indian physicians in the Ayurveda scriptures of ancient Indian medicine, reported in Sanskrit [194]. Since then it has been noted that the proper absorption of glucose is biologically essential; diabetes can be caused by the poor absorption of glucose [195]. Currently the detection of glucose in blood is medically central for the diagnosis and management of diabetes as T2D is characterized by elevated glucose levels [196]. For this reason there have been multiple biosensors developed for glucose, with enzyme based biosensors being the main focus of biosensor research [197].

HbA1c is well known as a key diabetes marker protein and is the gold standard procedure for monitoring long-term glycemic control clinically in diabetics [198-200]. HbA1c is the major form of all glycohaemoglobin species in human blood and is defined as the stable adduct of glucose and the N-terminal amino group of the β -chain of HbA₀ [N-(1-deoxyfructosyl)haemoglobin] [201]. It is haemoglobin that has been irreversibly modified by addition of glucose through a slow, non-enzymatic process and the rate of its formation is directly proportional to the ambient glucose concentrations [193, 202]. HbA1c gives the mean glycemia over the preceding 2-3 months [8, 203]. It is also used by quality assurance programs to

assess the quality of diabetes care. HbA1c can be measured at any time of the day regardless of the duration of fasting or the content of the previous meal.

The optimal therapy requires carefully validated, method-independent therapeutic target values for the glycohaemoglobin levels of patients with diabetes, lowering the long-term risk of late complications (e.g. retinopathy, nephropathy and neuropathy) and the short-term risk of life-threatening hypoglycaemia [200, 201].

The measurement of L-lactate is helpful in monitoring respiratory insufficiency, heart failure, metabolic syndrome, diabetes, tissue injuries and thrombosis [204]. The levels of lactate are also linked to status of anaerobic metabolism associated with muscle contraction and indicates oxygen supply [205].

Creatinine is used as a biomarker for renal and muscular dysfunctions [204]. It is a by-product of muscle metabolism and remains in a steady state by renal elimination [206].

High cholesterol build up in blood serum is strongly linked with many diseases, including coronary heart disease, arteriosclerosis, myocardial infarction, brain/cerebral thrombosis, lipid metabolism dysfunction, hypertension, hyperthyroidism and anaemia [207-210].

Indirect markers of mitochondrial function can also be abnormal in mitochondrial dysfunction [96]. Mitochondrial dysfunction can result in secondary urea cycle dysfunction and an elevation in ammonia levels, as the urea cycle is partially located in the mitochondria. Urea determination is used to study the proper functioning of the kidney, as progressive kidney function results in uraemia [211].

RBP4, a serum protein, facilitates the transport of retinol through the circulation to peripheral tissues [212]. It has been linked to obesity induced insulin resistance and T2D [213-215]. Its concentration in serum can be used to identify cardiovascular risk factors, including fatty liver disease.

Table 2-1 lists the biomarkers and their relevant concentration in blood. Of course these concentrations vary on age, gender, disease, diet, exercise and disease etc., so fluctuations are possible. But typical ranges are listed here.

Table 2-1: The normal and abnormal blood concentrations of each energy metabolism biomarker studied.

Biomarker	Normal concentration	Abnormal concentration	Reference
Glucose	5 mM	7 mM	[216, 217]
HbA1c	~ 5 %	≥ 6.5 %	[218-220]
Lactate	0.6 -2.0 mM	20 – 30 mM	[205, 216]
Cholesterol	11.1 mM	13.3 mM	[221]
Creatinine	53 – 115 μM	~ 700 μM	[222]
Urea	2.6 – 6.7 mM	~ 20 mM	[211, 222]
RBP4	~ 30 μM	~ 100 μM	[219, 222-224]

2.1.2 Biosensor Development

Biosensors are analytical devices which can convert a biological response into a measurable and processable signal [9]. Biosensors are selective biological systems (enzymes, antibodies, organelles, cells) combined with a transducer (thermistor, potentiometric and amperometric electrode, piezoelectric and optical receivers) which generate on-line information from the investigated environment [225].

The systematic depiction of a biosensor ought to have five features [226];

1. detecting/ measuring factor
2. working principle of the transducer
3. physical and chemical:biochemical representation
4. appliance
5. technology and materials for sensor fabrication.

2.1.3 Glucose biosensors

From all glucose biosensors, the enzyme-based electrochemical biosensors have been the major focus of biosensor research [197]. This can be due to their simplicity of use, moderately low cost and high sensitivity. Enzymes in enzyme electrodes catalyse redox reactions, during which they

give or take electrons (e^- 's) [7]. The transfer of e^- 's can produce current or voltage that is concentration-dependent; this can be quantified using electrodes.

The first generation of glucose biosensors (Figure 2-1) had glucose oxidase (GOx) as the enzyme in the biosensor (known as the 'enzyme electrode') in 1962 by Clark and Lyons [227]. In which the electrochemical reactions were:

GOx

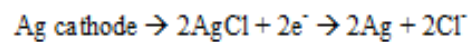
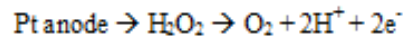
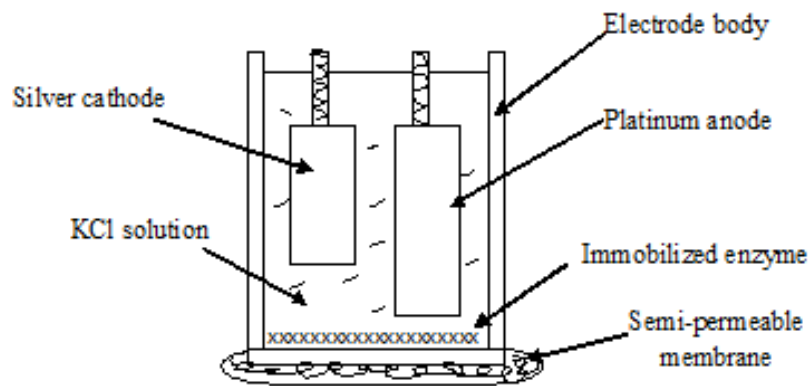
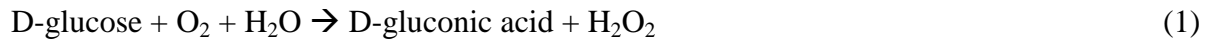


Figure 2-1: Clarke-type O_2 electrode illustration [204].

It made use of O_2 as an e^- mediator from GOx to the surface of electrode. GOx reduces O_2 into H_2O_2 with glucose present [228]. The concentration of glucose is proportional to the rate of O_2 reduced. This is detected by measuring the increase of H_2O_2 concentration or decrease of O_2 concentration. This generation of glucose sensors suffered from O_2 dependence and intervention by redox-active species.

Figure 2-2 illustrates the general construction of the second generation of glucose sensors. These use artificial mediators to overcome O_2 limitation under low O_2 pressure [228]. The e^- mediators facilitate the e^- transfer by fast shuttling of e^- 's between the enzyme and electrode. The most

popular e^- mediators are ferro/ferricyanide, hydroquinone, ferrocene and various redox organic dyes. Having other redox-active species (e.g. O_2) will compete with the mediators.

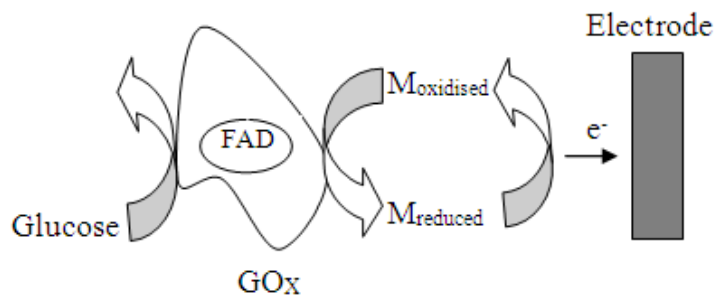


Figure 2-2: Schematic diagram of the second generation enzyme glucose sensors [228].

The third generation glucose sensors use direct e^- transfer [228]. Here the e^- 's are directly transferred between the enzyme and electrode. If the electrode and the active redox sites of the enzyme were electrically wired, the direct e^- transfer would convert the enzymatic recognition events of glucose to an amperometric signal, in effect not considering the concentration of co-substrates, for instance those of O_2 or redox mediators. The best plus point of this design is the successful elimination of potential interferences.

In the 1980s the development of self-monitoring of blood glucose with a single drop of blood became possible [229]. Over 90 % of the glucose sensor market is being shared by the companies LifeScan, Roche Diagnostics, Abbott and Bayer [230]. Table 2-2 lists the products and their relevant information. All these rely on the finger-prick method of glucose detection.

Table 2-2: Leaders in glucose home sensing kits.

Company	Trade name of product	Mediator used	Sample volume (μ L)	Reference
Abbott	Precision	Ferrocene	0.6	[231, 232]
	FreeStyle	Osmium "wire"	0.3	[233]
Bayer	Elite	Ferricyanide	2.0	[234]
LifeScan	SureStep	Ferricyanide	5.0	[235]
	One Touch Ultra		1.0	[236]
Roche Diagnostics	Accu-Check	Ferricyanide	1.5	[237]

American Diabetes Association, the FDA and the National Institutes of Health did issue a collaborated declaration in 1986, regarding the self-monitoring of blood glucose for [7]:

- diabetes causing pregnancy to be problematic;
- people having severe ketosis or hypoglycaemia;
- people prone to hypoglycaemia;
- people on intensive treatment programmes;
- people having abnormal renal glucose thresholds.

Nowadays self-monitoring of glucose is routine in patients of T2D, as this helps them manage their diabetes and improve their lifestyle. Self-monitoring of plasma glucose is recommended by the National Institute for Health and Care Excellence (NICE) for the following individuals [238]:

- on insulin treatment
- on oral glucose lowering medications (so information on hypoglycaemia can be obtained)
- who need to assess changes in glucose control subsequent to medications and lifestyle changes
- who monitor changes during illness
- who need to ensure safety during activities (such as driving)

There have been many review papers on the home blood glucose sensors [239, 240]. There are over 6000 peer reviewed articles on electrochemical glucose assays and sensors [241]. Along with many papers comparing the accuracy of one commercial meter to others [242-245]. This is a well established field in the biosensor market. The advantages and disadvantages of self-monitoring are illustrated in Figure 2-3 below. The same advantages and disadvantages would apply for NEFA finger-prick sensing too.

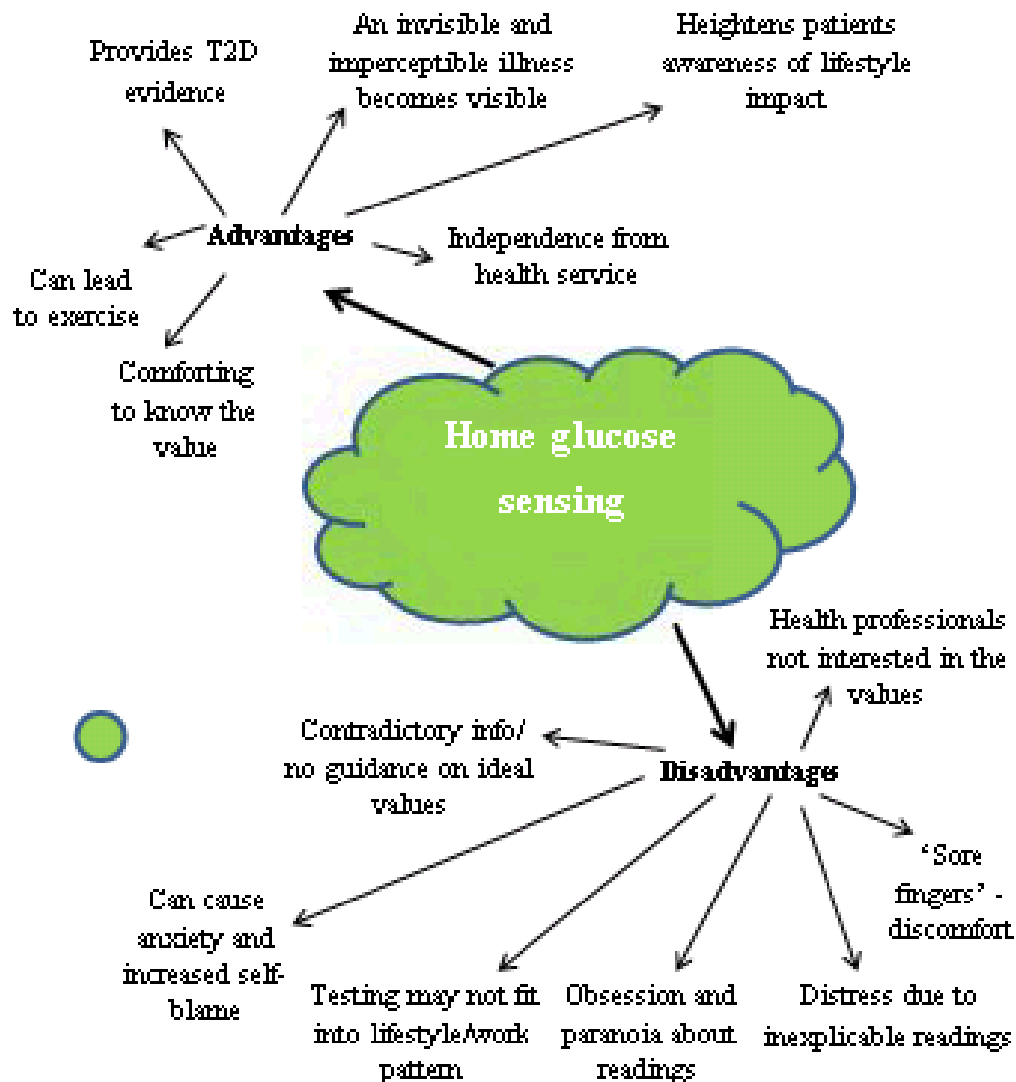


Figure 2-3: Advantages and disadvantages of home based glucose sensors from the patients perspective [246].

2.1.4 Advantages of electrochemical biosensors

Electrochemical biosensors are robust, easily miniaturized and have outstanding detection limits compared to optical biosensors. Electrochemical biosensors take low analyte volumes, and can work in turbid biofluids which have optically absorbing and fluorescing components [9]. They are greatly sensitive and selective, portable, giving a fast response, specific, and low cost. They can be used for a number clinical applications, from ‘alternative-site’ testing (e.g. physician’s office), emergency-room screening, bedside monitoring, or home self-testing [207, 247]. There

are some disadvantages of electrochemical sensors, including: the sample could have electrochemically active interferences, it could be weak in relation to long-term reliability and have complicated e^- transfer pathways.

2.1.5 Electrochemistry

Electrochemistry deals with nature and properties of substances containing charged particles (ions) and the relationship between chemical reactions and electrical currents [248].

Analytical applications of current-voltage relationships forms the foundation of the wide range of voltammetric methods [249]. In this study Cyclic Voltammetry (CV), Linear Sweep Voltammetry (LSV) and Chronoamperometry (CA) were selected. All are accomplished using a three-electrode arrangement. Electrochemical sensing usually requires a *reference* electrode, a *counter* or auxiliary electrode plus a *working* electrode, also known as the sensing or redox electrode [9]. The reference electrode is kept at a distance from the reaction site in order to maintain a known and stable potential with which the current produced on the working electrode is compared. The working electrode serves as the transduction element in the biochemical reaction, while the counter electrode (non-reactive high surface area) establishes a connection to the electrolytic solution so that a current can be applied on the working electrode (well defined area). The electrodes ought to be both conductive and chemically stable. A typical electrochemical cell can be seen in Figure 2-4. The electrodes would be connected to a potentiostat.

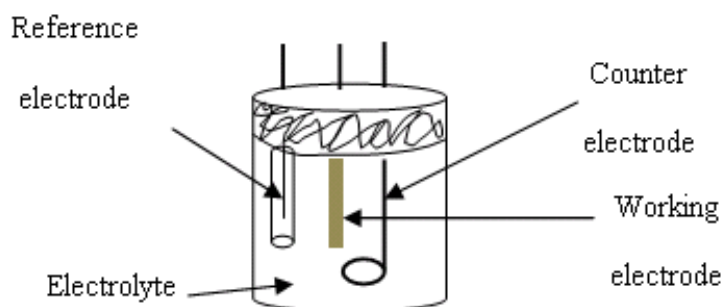


Figure 2-4: Typical electrochemical cell, with standard three-electrode set-up comprising of working, counter and reference electrodes [204].

2.1.5.1 Cyclic voltammetry (CV)

CV is an incredibly handy and resourceful electrochemical technique in the characterization of electroactive species [250]. It collects valuable information in relation to the stability of the oxidation states and the rate of e^- transfer from the electrode and the analyte. Current measurement as a function of the applied potential gives information about the analyte. The current response against a variety of potentials is measured, beginning at an initial value and changing the potential in a linear way up to a limiting value. At this limiting potential value the course of the potential scan is reversed and the same potential range is run in the reverse direction. The species that were oxidized in the forward scan can be reduced in the backward scan. CV is useful in the elucidation of reaction mechanism, especially with identification of intermediates [249].

2.1.5.2 Linear sweep voltammetry (LSV)

In LSV the potential scan is done in one direction only, and stopped at a chosen potential [251]. The direction of the scan can be either positive or negative. On reaching a potential where the electrode reaction begins, the current produced will rise. Nonetheless, a concentration gradient is created and consumption of electroactive species results in continuing to sweep the potential, from a certain value just before the maximum value of the current (peak current), the supply of electroactive species fall. Due to depletion the current decays.

2.1.5.3 Chronoamperometry (CA)

This is the study of variation of the current response with time. CA is a technique extensively engaged to establish kinetic rate constants in reactions which have e^- transfer of their surface-confined redox couples [252]. The Cottrell equation is what the results of the CA are derived from, this demonstrates the current-time dependence for linear diffusion control [253]:

$$i = nFACD^{1/2}\pi^{-1/2}t^{-1/2}$$

In which: i = current

n = number of e^- 's transferred/molecule

F = Faraday constant (96,500 C mol⁻¹)

A = area of the electrode (cm²)

D = diffusion coefficient (cm²s⁻¹)

C = concentration (mol cm⁻³)

t = time (seconds)

Subsequently this shows that following the conditions listed the relationship among the current and the 1/square root of time is a linear one.

2.1.6 H₂O₂ produced as a by-product

Just as the quantification of glucose, cholesterol and lactate can be achieved via the electrochemical detection of the enzymatically liberated H₂O₂ (Figure 2-5), in principle so can the quantification of NEFA [209, 254]. H₂O₂ as a by-product of enzymatic reactions catalysed by the oxidase enzymes renders it an important analyte in the biosensor field [255-257]. H₂O₂ serves as an electroactive reporter molecule in the indirect detection of non-electroactive biomolecules, e.g. glucose, glutamate and acetylcholine [258]. Other classical biochemical reactions which produce H₂O₂ as a side product are catalyzed by the enzymes alcohol oxidase (AlOx), urate oxidase (UOx), D-amino acid oxidase (DAAO), glutamate oxidase (GLOx), lysine oxidase (LyOx), oxalate oxidase (OxaOx), and so on [259].

The enzymatic detection of NEFA relies on the oxidation of acylated NEFA, e.g. palmitoyl coenzyme A (PA-CoA) or oleoyl coenzyme A (OA-CoA) by the enzyme acyl-Coenzyme A oxidase (ACOD), producing H₂O₂ which is then quantifiable.

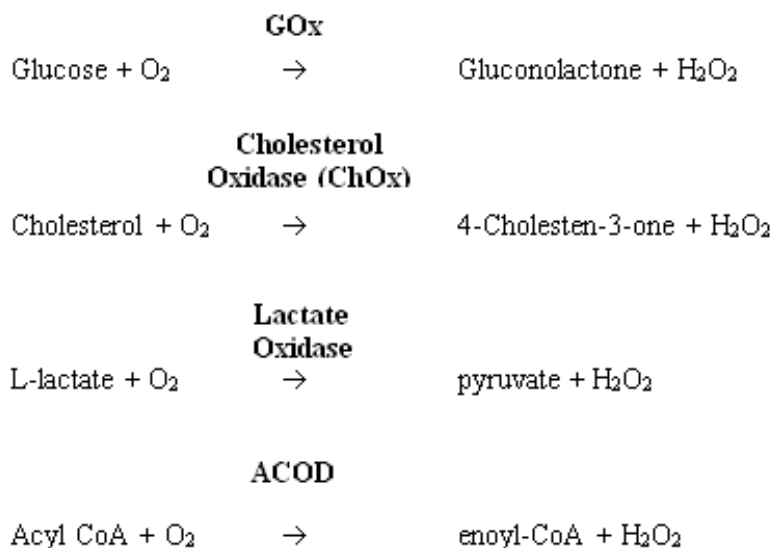


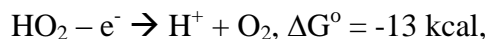
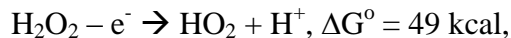
Figure 2-5: Clinically important reactions producing H₂O₂ as a by-product.

H₂O₂ is a simple compound. The dissociation energy of the O-O bond in H₂O₂ is 35 kcal mol⁻¹ [260]. The detection of H₂O₂ is important for pharmaceutical, clinical, environmental, mining, textile and food manufacturing applications [259, 261, 262]. Accurate and reliable detection of H₂O₂ has been thoroughly investigated using chromatography, titrimetry, chemiluminescence and electrochemistry [261, 262]. Over other detection methods of H₂O₂, electrochemical analysis offers improved sensitivity, an extended dynamic range and a rapid response time [257]. Amperometric H₂O₂ detection possesses good temporal resolution for rapid and real-time measurements, allowing continuous recording of the oxidation/reduction currents as a function of time without severe contamination by capacitive current [263].

2.1.7 H₂O₂ oxidation and reduction

Electrochemically H₂O₂ can be directly oxidized or reduced at ordinary solid electrodes [259]. Both these process can be electrocatalyzed by carbon nano-tubes (CNT).

The oxidation of H₂O₂ to O₂ occurs by HO₂ radicals and without chain reactions, the process is in two stages in aqueous solutions [264]:



i.e., for the complete reaction $\text{H}_2\text{O}_2 \rightarrow \text{O}_2 + 2\text{H}^+$, $\Delta G^\circ = 36 \text{ kcal}$.

H_2O_2 decomposition is presumed to be pseudo-first-order kinetics [265]:

$$- \frac{dC_{\text{H}_2\text{O}_2}}{dt} = k_d \times C_{\text{H}_2\text{O}_2}$$

k_d represents an apparent kinetic constant (including many parameters e.g. temperature, catalyst concentration and pH).

The general scheme of oxygen reduction is shown in Figure 2-6. The direct four electron reduction to water (or OH^-) is k_1 , k_2 is the two electron reduction to H_2O_2 (or OH_2^-), k_{-2} is the oxidation of H_2O_2 (or HO_2^-) to O_2 , k_3 is the electrochemical reduction to H_2O or (OH^-) of H_2O_2 , k_4 is the catalytic decomposition of H_2O_2 (or HO_2^-) to the reducible O_2 , k_5 is the desorption of the adsorbed H_2O_2 (or HO_2^-) and finally k_6 is the adsorption of H_2O_2 (or HO_2^-) [266]. The * term is the vicinity of the disc electrode, as the rotating ring disk assembly was not used in this work, therefore these species are not relevant here.

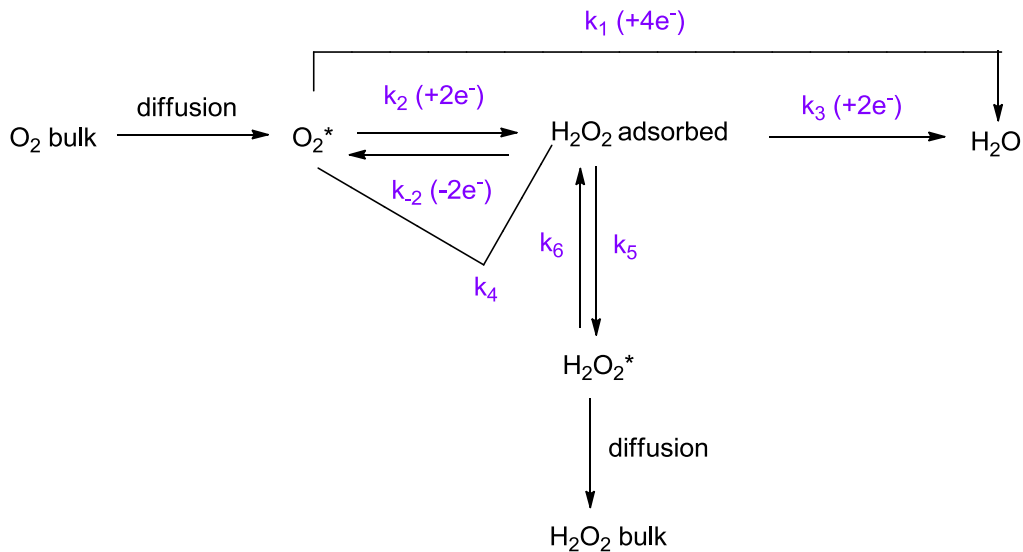


Figure 2-6: General scheme of oxygen reduction [266].

The adsorbed peroxides desorption depends on the electrolyte plus the impurities and on the electronic and morphological properties of the electrode too [267].

2.1.8 Conclusion

The second half of the literature review focussed on biomarkers of energy metabolism, biosensors, glucose biosensor development and electrochemistry involving H_2O_2 detection. There are multiple energy metabolism biomarkers (as discussed previously) and biosensors have been developed subsequently to analyse these concentrations in patients. The glucose biosensor is by far the largest market in energy metabolism biosensors. These sensors do involve the electrochemical detection of H_2O_2 from an enzymatic reaction. The same principle would be used for NEFA detection from the enzymes and then from in blood. An electrochemical biosensor for detecting NEFA levels would be useful in many energy metabolism fields. This draws on the conclusions found after the first part of the literature review.

2.2 Aims and objectives

Aim

- To develop an electrochemical based NEFA biosensor for patients with T2D or energy metabolism conditions. The biosensor will measure NEFA concentrations in blood and will be useful for the future development of personalised intervention programmes for the treatment and management of the disease.
- To collate useful information regarding NEFA in literature and see where else a NEFA sensor would be beneficial.

Objectives

- To use optical methods (such as those used by the companies, Wako Diagnostics and Roche Applied Science) for NEFA detection as feasibility study, and develop electrochemical methods for measuring NEFA concentrations in blood.
- To develop enzyme electrodes for NEFA sensors and improve its sensitivity and measurement limitation by enhancing signal generation and improving the electrode surface properties. The enzyme electrode will be fabricated by immobilizing enzymes to the screen printed carbon electrode using polymers. The interaction and electron transfer between the enzymes and the electrode will be studied. There will be optimization and modification of materials on the surface property of the electrode.
- To investigate the interference with multiple analytes on the electrode. This is needed to understand the interference of mixed analytes on the sensor, and whether this would affect the sensors sensitivity and selectivity.

The initial work in solution with the enzyme ACOD and the substrates OA-CoA/PA-CoA is shown in Chapter 3, followed by the work on enzyme electrode fabrication for NEFA (oleic acid) detection in Chapter 4. Both these chapters include sections on interference using these unfabricated and fabricated electrodes. Chapter 5 covers detection of NEFA in human blood using the fabricated enzyme electrodes. The overall conclusions and recommendations of future work are given in Chapter 6. The appendix (Chapter 7) contains data/explanations that support the work in the main body of the thesis. This section has been referred to whenever necessary.

3 NEFA detection in solution using screen printed electrodes (SPE's)

3.1 Introduction

The oxidation of NEFA requires an oxidase enzyme Acyl-Coenzyme A oxidase (ACOD). In literature there are over 200 dehydrogenases enzymes and 100 oxidases [268]. Many of which specifically catalyse the reactions of clinically important analytes (e.g. glucose, lactate, cholesterol, amino acids, urate, pyruvate, glutamate and alcohol hydroxybutyrate) to generate products that are electrochemically detectable (e.g. reduced nicotinamide adenine dinucleotide (NADH) and H_2O_2).

Glucose oxidase (GOx) is the most widely used of the class of oxidoreductases enzymes [269]. First generation glucose sensors monitored glucose concentrations by monitoring H_2O_2 evolution. This was from the reaction of GOx converting glucose to gluconolactone and oxygen to H_2O_2 . Applying this principle to the NEFA sensor would replace glucose with NEFA (as the substrate) and GOx with ACOD (as the enzyme) and then monitor the H_2O_2 evolution from this reaction. This would make a first generation NEFA sensor.

ACOD is a flavoprotein, that donates its electrons directly, catalysing the stoichiometric conversion of acyl-Coenzyme A and O_2 into enoyl-Coenzyme A and H_2O_2 [162, 270]. ACOD oxidises acyl-CoA's with 4 to 20 carbon atoms, it is an octamer with a molecular weight of ~600,000 approximately, with its isoelectric point being 5.5 [270]. ACOD catalyses the first and rate-determining step of fatty acid β -oxidation [271, 272]. The activity of ACOD is stimulated by flavin adenine dinucleotide (FAD), a redox active prosthetic group of flavoenzyme that catalyses important biological redox reactions [273, 274]. There are 8 mol of FAD per mol of ACOD [270, 272, 275]. ACOD has enoyl-CoA isomerase activity. Reduced flavin adenine dinucleotide ($FADH_2$) is reoxidised by molecular oxygen, as shown in Figure 3-1.

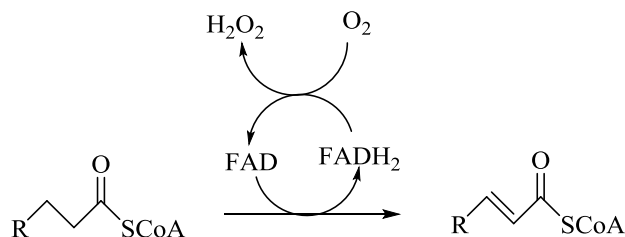
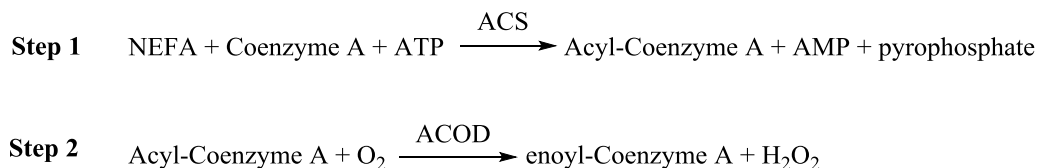


Figure 3-1: ACOD catalysed reaction of acylated NEFAs [272, 275].

The two step enzymatic reaction is shown in Scheme 1. In the first step NEFA reacts with Coenzyme A (CoA) and adenosine triphosphate (ATP) with the enzyme acyl-Coenzyme A synthetase (ACS) to produce Acyl-Coenzyme A, which then reacts with the enzyme ACOD to produce H_2O_2 , which is of interest in this work.



Scheme 1: Reaction scheme of the enzymatic method for H_2O_2 production from NEFA.

In step 1 of scheme 1, palmitoyl Coenzyme A (PA-CoA) would be the product if palmitic acid (saturated carbon 16 fatty acid chain) was the NEFA or oleoyl Coenzyme A (OA-CoA) would be the product if oleic acid (carbon 18 with 1 double bond) was used.

Palmitic acid and oleic acid represent the major species present in human serum and therefore are some of the principal molecules to which β -cells might be exposed to *in vivo* [115]. For this reason they are also used as standards for the commercial kits on the market. Therefore palmitic acid/oleic acid (or their acylated forms, PA-CoA/OA-CoA) would be good reference NEFAs for this investigation. The H_2O_2 produced after step 2 was to be detected electrochemically using different screen printed electrodes (SPE's).

Requirements for electrodes in electrochemistry are on the basis of having good electrode material with stability over a long-time, low residual current and use over a wide potential range [276]. Carbon electrodes have all these 3 requirements along with a rich surface chemistry. Carbon oxidation has slow kinetics resulting in a wide useful potential range, particularly in the

anodic direction. Carbon based electrodes have congruity for many applications in electroanalytical chemistry, so were chosen as the initial electrode in this work. Single use screen printed electrodes (SPE's) eliminate problems such as loss of response caused by electrode fouling and enzyme denaturization [276]. Their surface can be easily modified, they are easy to use and cost-effective [256].

Screen-printing can produce electrodes as those shown in Figure 3-2. These are produced by printing patterns using a stencil and building-up each layer onto the plastic or ceramic sheet substrate. Each strip consists of a working electrode coated with the necessary reagents such as the enzyme, mediator, linking and binding agents, the counter electrode and the reference electrode [230].

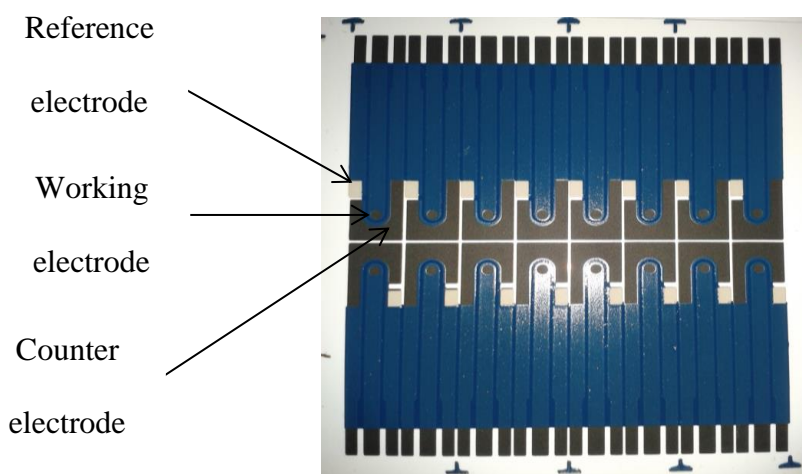


Figure 3-2: Sheet of 16 screen printed carbon electrodes.

3.2 Experimental

3.2.1 Materials

H₂O₂ 33 % ^w/_w in water was purchased from VWR (Leicestershire). Stock solutions were made using distilled water as the diluent.

Disodium hydrogen phosphate (Na₂HPO₄) and sodium dihydrogen phosphate dehydrate (NaH₂PO₄), was purchased from Sigma Aldrich (Dorset, UK). 0.1 M phosphate buffer (pH 7.4)

was prepared from stock solutions of 1 M Na_2HPO_4 and NaH_2PO_4 . The pH was checked by using a pH meter.

PA-CoA and OA-CoA were purchased from Sigma Aldrich. Stock solution of 10 mM for each was made by diluting in 0.1 M phosphate buffer (pH 7.4). ACOD was purchased from Wako Japan at 100 Units, CAS # 61116-22-1 (Neuss, Germany). Each run contained 3 U/mL ACOD. This concentration was selected as it was the concentration stated in the Wako kit in the optical method.

The following SPE's were purchased from DropSens (Oviedo, Spain):

- Cobalt phthalocyanine (CoPc) SPE – model DRP-410. The working electrode (WE) is CoPc on carbon.
- Carbon (C) SPE – model DRP-C110. The WE is carbon.
- Single wall carbon nanotube (SWCNT) SPE – model DRP-110SWCNT. The WE consists of carboxyl functionalised SWCNT.

All the electrodes have a flat surface. The electrodes have a working electrode diameter of 0.40 cm and an area of 0.13 cm^2 . For all 3 DropSens electrodes, the reference electrode is silver/silver ion (Ag) and the counter electrode is carbon. The dimensions of all the electrodes are 3.40 x 1.00 x 0.05 cm (Length x Width x Height) respectively. These disposable electrodes were used as purchased with no pre-treatment required.

All interference work was done using C-SPE (DRP-C110). The ACOD was from the Roche kit, 30 μL was used per run. The concentration of ACOD in the commercial kit is not stated. Urea and bovine serum albumin (BSA) was purchased from Sigma Aldrich (Dorset, UK). Uric acid and ascorbic acid were purchased from Alfa Aesar (Heysham, Lancashire). Glucose was purchased from Fluka BioChemika (Dorset, UK). Stock solutions for each of these were made by diluting the relevant mass in 0.1 M phosphate buffer (pH 7.4). Acetaminophen (paracetamol) and aspirin were purchased from the pharmacy. The stock solutions were made after the active ingredient was calculated. The tablet was crushed, then dissolved in 0.1 M phosphate buffer (pH 7.4), then sonicated for 40 minutes. The percentage of interference was calculated by using 0.20

mM PA-CoA as a reference (with ACOD) and spiking this with the relative amount of each respective interference that is present in serum/plasma.

3.2.2 Electrochemical measurements

Electrochemical measurements were run on the Autolabs (PGSTAT101 and PGSTAT302) with NOVA 1.8 as the software package installed. Cyclic Voltammetry (CV) was done using a scan rate of either 5 mV s^{-1} , 50 mV s^{-1} , 100 mV s^{-1} or 500 mV s^{-1} . The potential range investigated was from -800 mV to 500 mV or up to 600 , 800 , 1000 , 1200 , 1400 and 1600 mV . Linear Sweep Voltammetry (LSV) was done using a scan rate of 1 mV s^{-1} . The potential range investigated was from 0 mV to 600 mV . Chronoamperometry (CA) was done at a set potential of 500 mV with a step potential of 0.25 seconds (s) and duration of 1500 s . 500 mV was the chosen potential because at this potential there was substantial oxidation of H_2O_2 , which was seen from the LSV.

All CA for interference work was done at a set potential of 500 mV with a step potential of 0.25 s and duration of 500 s . All CA calibration graphs in the study are shown at 500 s . This time was chosen for all the graphs to keep the representation of time consistent.

The electrolyte used throughout the work was 0.1 M phosphate buffer (pH 7.4 - same as blood).

All electrochemical experiments were done at room temperature, in at least duplicates wherever there are error bars. Error bars were worked out based on the average, the positive error was the most positive result minus the average, the negative error was the average minus the most negative result.

The experimental set-up is shown in Figure 3-3. The SPE was sealed in the cell shown by the four screws. This prevented solution leakage. The total volume of solution in the cell was $100 \mu\text{L}$.

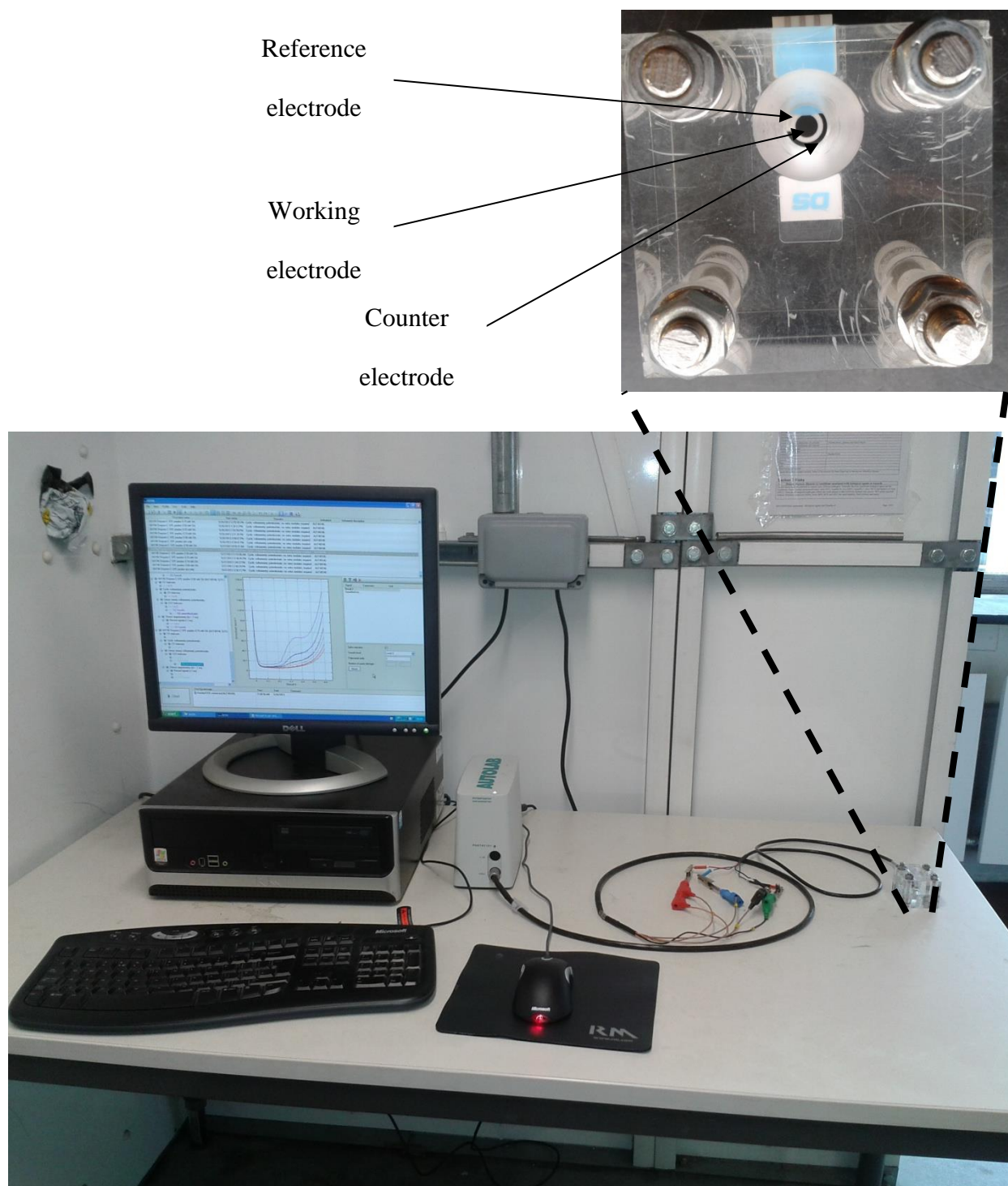


Figure 3-3: Experimental set-up for electrochemical experiments.

3.3 PA-CoA/OA-CoA detection electrochemically in solution

3.3.1 Detection using carbon screen printed electrode

Initially the LSV of different concentrations of H_2O_2 were detected on a C-SPE (Figure 3-4 and Figure 3-5). The sensitivity of the C-SPE towards H_2O_2 was determined to be $0.70 \mu\text{A}/\text{mM}$ at 500 mV . This would then be compared later with the data obtained from the acylated NEFAs investigated. The same concentration range of 0.00 mM to 3.00 mM will be investigated for acylated NEFA as this covers the NEFA range found in human blood. Testing the electrode with actual H_2O_2 proved that the electrode can be used for various concentrations of H_2O_2 , and produce a linear response (R^2 of 0.99). These C-SPE's are designed and sold as a detection tool for low concentrations of H_2O_2 detection. The lowest concentration investigated with H_2O_2 was 0.10 mM .

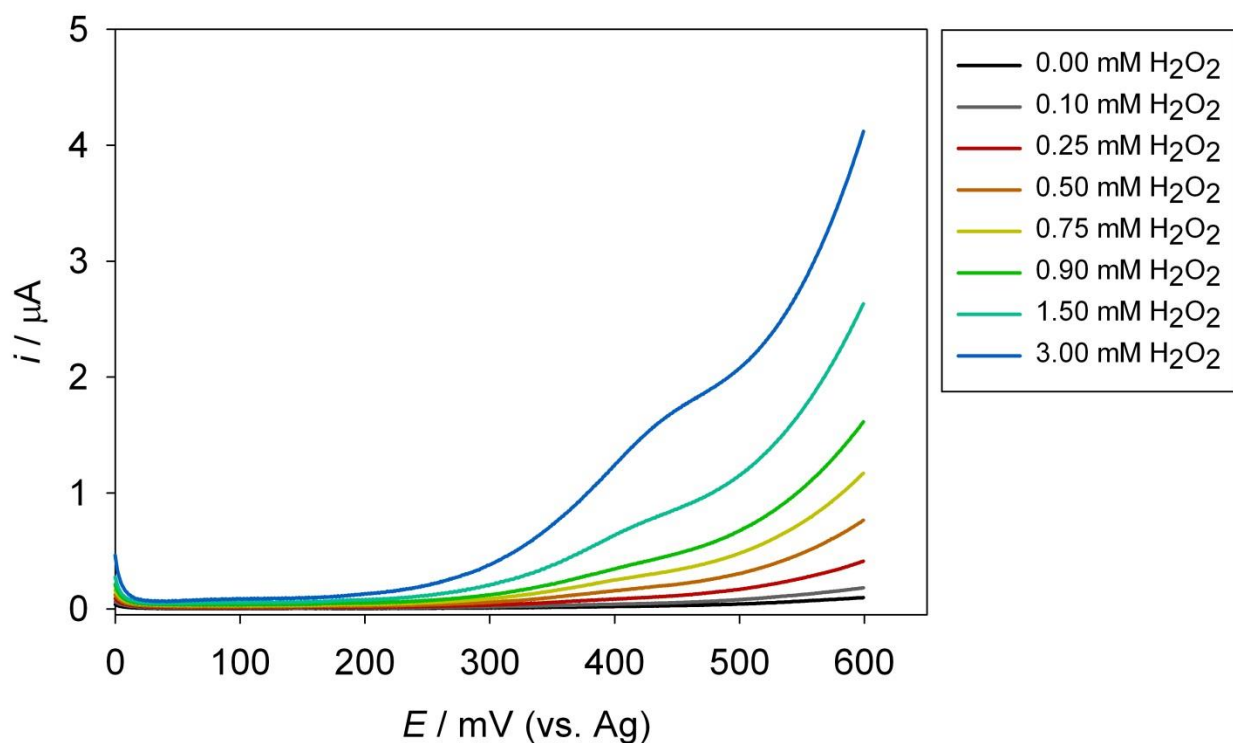


Figure 3-4: LSV for various concentrations of H_2O_2 measured at a C-SPE in 0.1 M phosphate buffer $\text{pH } 7.4$, scan rate 1 mV s^{-1} .

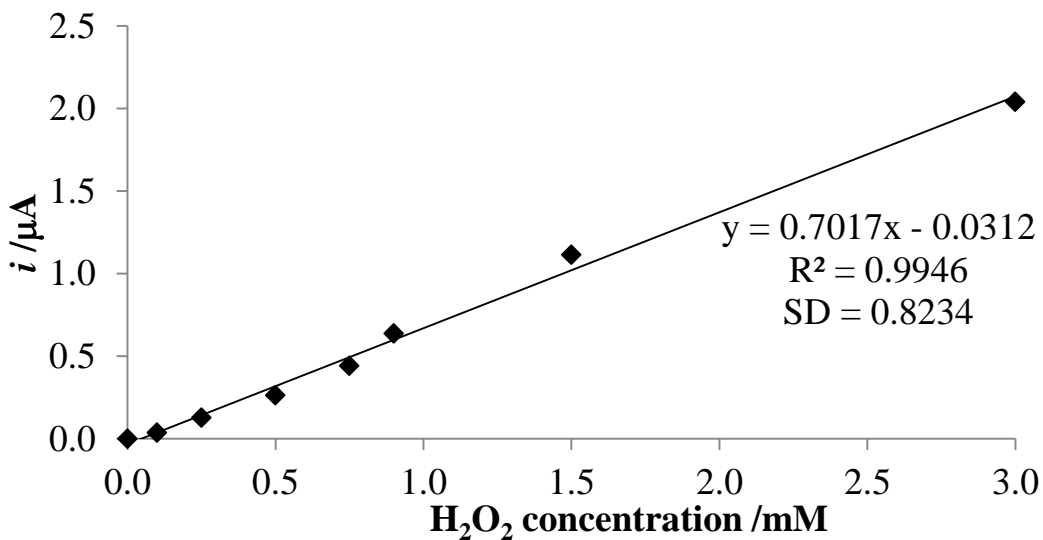


Figure 3-5: Calibration graph at 500 mV.

Figure 3-6 shows the $\log j$ (flux – which is the current produced divided by the surface area of the WE) vs. $\log H_2O_2$ plots for different potentials from 400 to 600 mV (vs. Ag). A slope of 0.95 to 1.03 was obtained for the entire $\log j$ (flux) vs. $\log H_2O_2$ range. This result indicates that the reaction is first-order with respect to $[H_2O_2]$ as the slope is ~ 1 . The only variant that is changing in this graph is the concentration of H_2O_2 . Calibration graphs can be made from the potentials of 400 to 600 mV, as this is the region in which the oxidation of H_2O_2 takes place on a C-SPE. The R^2 value was around 0.99 for each potential. This proves these electrodes are suitable for H_2O_2 detection.

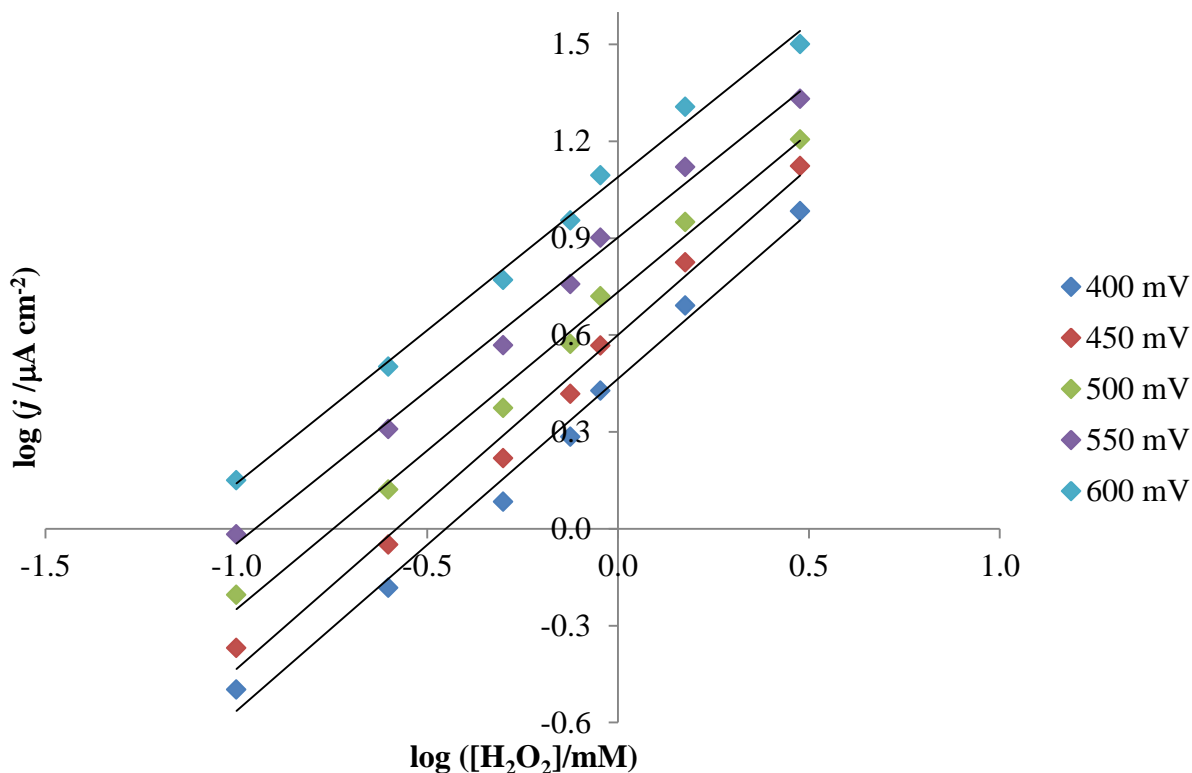


Figure 3-6: The relationship between $\log j$ and $\log \text{H}_2\text{O}_2$ concentration on the C-SPE at various electrode potentials in 0.1 M phosphate buffer pH 7.4.

The current produced at the potential of the calibration graphs is due to the oxidation of H_2O_2 . H_2O_2 has a very high overpotential for oxidation at the bare carbon surface (unmodified carbon electrode) [209, 269]. -47 mV is the formal potential for the oxidation of H_2O_2 at pH 7.4 in homogeneous solution. The current from the oxidation of H_2O_2 begins at ~ 300 mV. Applying this high voltage in a sensor the system may be susceptible to interference by other readily oxidizable compounds [277].

For an irreversible reaction (H_2O_2 oxidation) the kinetics has an important role [251]. A higher potential (overpotential) needs to be applied to overcome the activation barrier and allow the reaction to occur. The electrical current flowing through the electrode is proportional to the reaction rate and the electrode potential is proportional to the driving force [278]. The driving force for a chemical reaction is ΔG° (standard free energy of the reaction). This driving force can be modified by changing the electrode potential because $\Delta G = -nFE$, where n is the number of

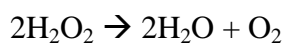
electrons, F is Faraday constant (charge on one mole of electrons, 96,484.6 coulombs) and E is the potential of the cell. For an oxidation reaction (the oxidation of H₂O₂), the driving force can be increased by applying a positive potential. Therefore all the calibration graphs for LSV in this study are at a chosen positive potential of 500 mV. All CA should also be done at 500 mV for consistency.

Different concentrations of PA-CoA and OA-CoA were then detected using the techniques LSV and CA. These experiments were performed with enzymes and substrate in solution. These experiments are crucial as they demonstrate the possibility of H₂O₂ detection in solution from its enzymatic production from acylated NEFA.

The LSV of PA-CoA is shown in Figure 3-7 (inset showing calibration graph at 500 mV), this graph shows H₂O₂ is detectable above the potential of 300 mV. 0.05 mM PA-CoA was also detected here, this low concentration also fitted into the general trend. The R² value was over 0.99 for 500 mV. With a sensitivity of ~1.13 μA/mM PA-CoA at 500 mV.

The sensitivity of PA-CoA detection was a lot higher than that of H₂O₂ detection (~1.13 μA/mM vs. ~0.70 μA/mM). This may be due to the decomposition of H₂O₂ which could be happening a lot more rapidly in H₂O₂ solution when compared to the H₂O₂ produced from PA-CoA oxidation.

Decomposition of H₂O₂:



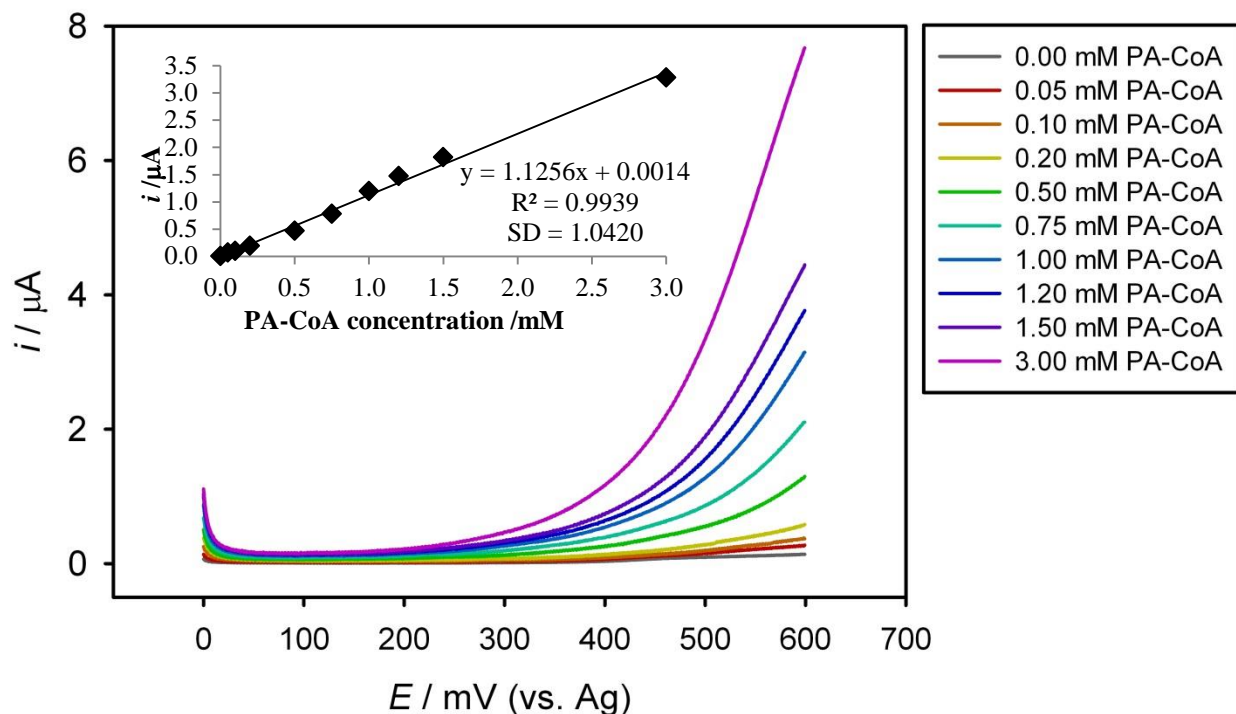


Figure 3-7: LSV for various concentrations of PA-CoA measured at a C-SPE with ACOD in 0.1 M phosphate buffer pH 7.4, scan rate 1 mV s^{-1} . Inset: calibration graph at a potential of 500 mV.

Figure 3-8 shows the $\log j$ vs. $\log \text{PA-CoA}$ plots for different potentials from 400 to 600 mV (vs. Ag). A slope of values between that of 0.73 to 0.87 was obtained for the entire $\log j$ vs. $\log \text{PA-CoA}$ range. This suggests a reaction order of approximately 1 with respect to PA-CoA concentration for the oxidation of H_2O_2 . This value is not as close to 1 as expected because one enzymatic reaction needs to occur before H_2O_2 is produced and oxidised on the electrode surface. R^2 value was above 0.97 for each potential.

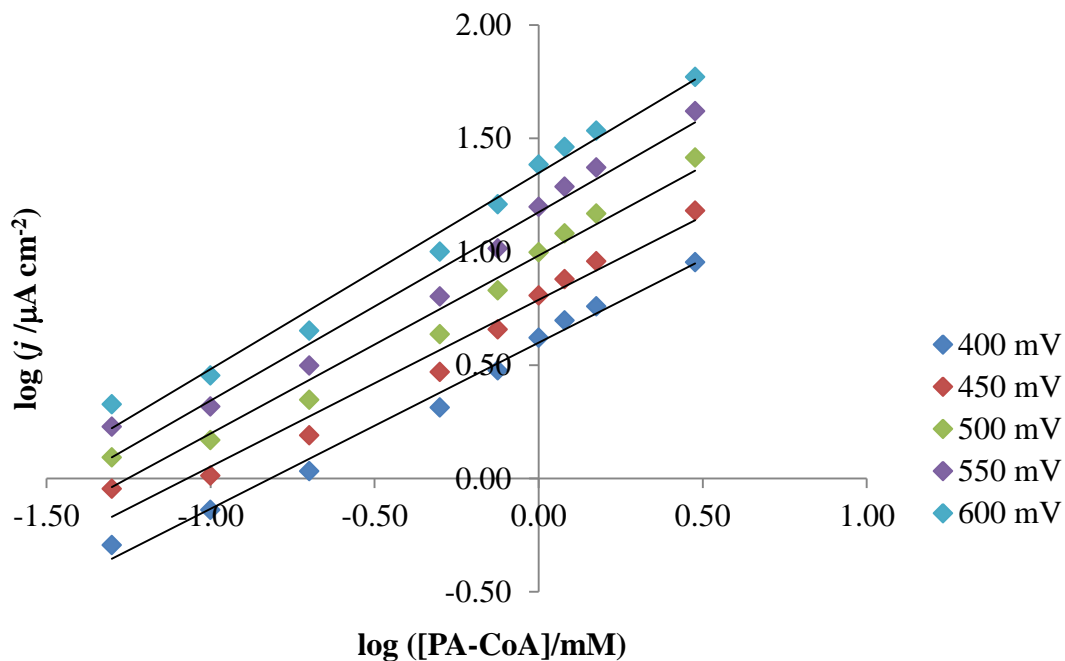


Figure 3-8: The relationship between $\log j$ and \log PA-CoA concentration at various electrode potentials in 0.1 M phosphate buffer pH 7.4.

Figure 3-9 shows the CA at the set potential of 500 mV for concentrations of PA-CoA up to 3.00 mM concentration. A calibration graph (Figure 3-10) was obtained from the current produced at 500 s. Linear increase of current was observed with increasing concentrations of PA-CoA. The amount of H_2O_2 produced from the reaction is proportional to the amount of PA-CoA to begin with, as this is a 1:1 molar reaction. The sensitivity of the C-SPE towards PA-CoA detection in solution is $0.6326 \mu\text{A}/\text{mM}$.

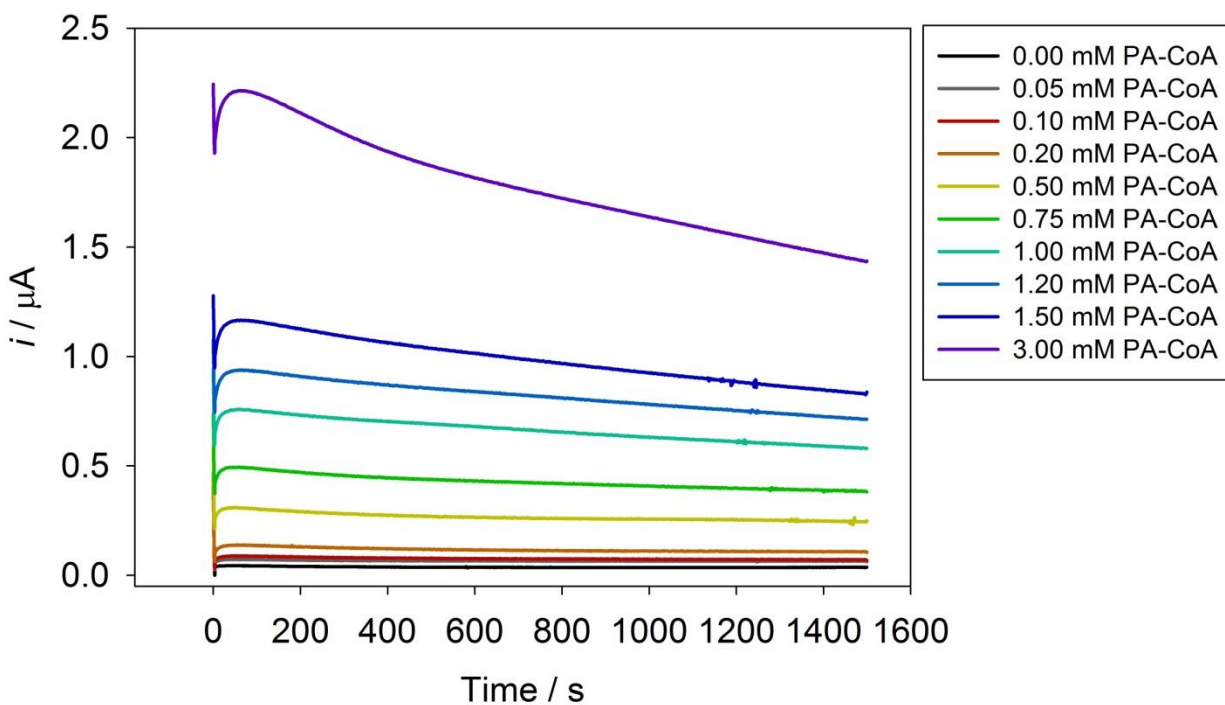


Figure 3-9: Chronoamperometry at 500 mV of various PA-CoA concentrations on C-SPE in 0.1 M phosphate buffer pH 7.4 with ACOD in solution.

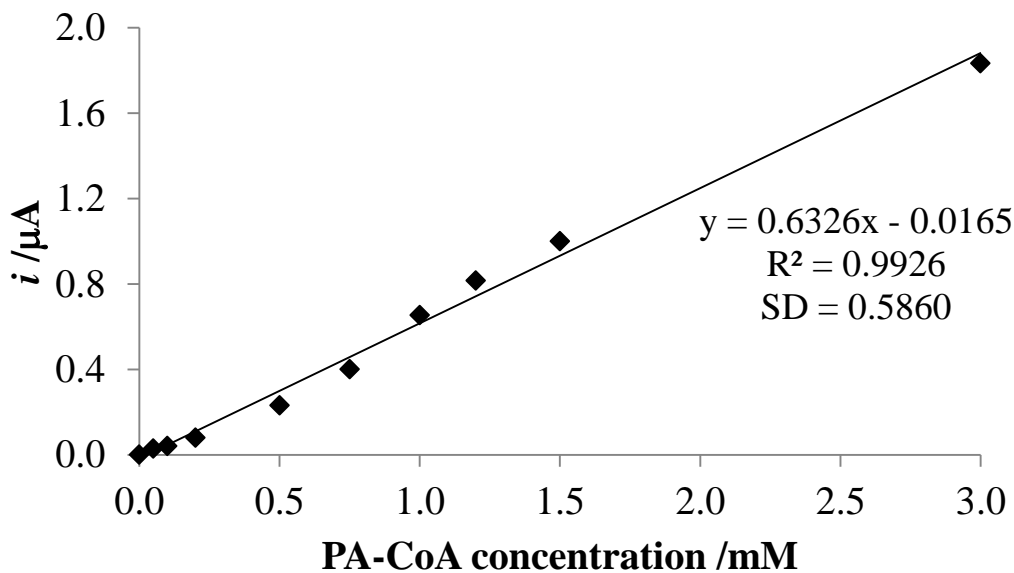


Figure 3-10: Calibration graph of current against PA-CoA concentration at 500 s.

The same CA was then done for the other acylated NEFA of interest OA-CoA, shown in Figure 3-11 and Figure 3-12 (calibration graph). With a similar sensitivity of $0.6519 \mu\text{A}/\text{mM}$ to that of PA-CoA. A bar chart showing the similarity of the current obtained from both acylated NEFAs is shown in Figure 3-13. This shows the current produced from the two acylated NEFAs is similar. The electrode is almost as sensitive to either of the two substrates. The slight difference may be due to error in experimentation, doing repeats and working out the standard deviation (SD) of error would help confirm this.

Step two (in Scheme 1) of the enzymatic reaction of acylated NEFA oxidation in the presence of ACOD can happen with any acylated NEFA. Both these acylated NEFAs are of interest for NEFA sensor development.

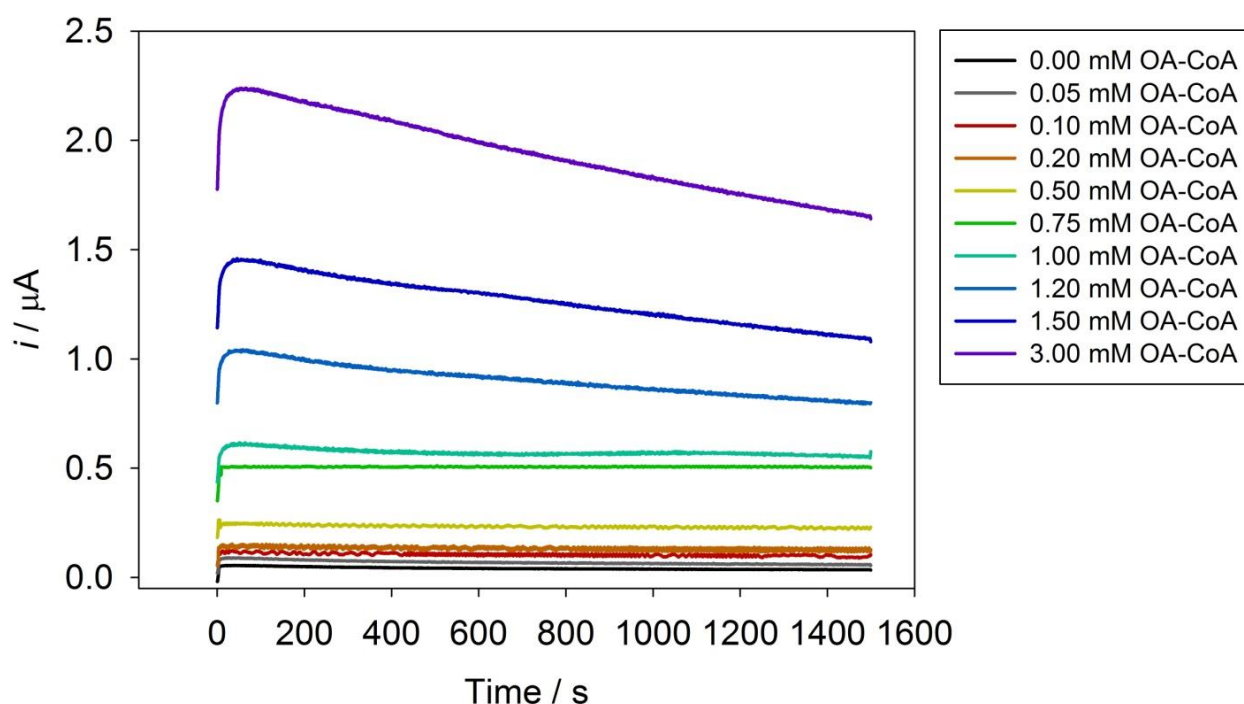


Figure 3-11: Chronoamperometry at 500 mV of various OA-CoA concentrations on C-SPE in 0.1 M phosphate buffer pH 7.4 with ACOD in solution.

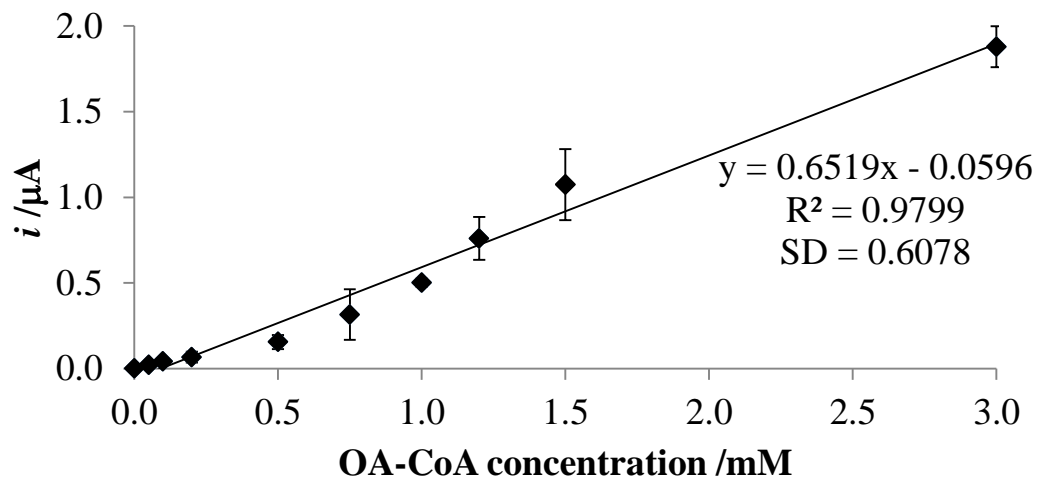


Figure 3-12: Calibration graph of current against OA-CoA concentration at 500 s.

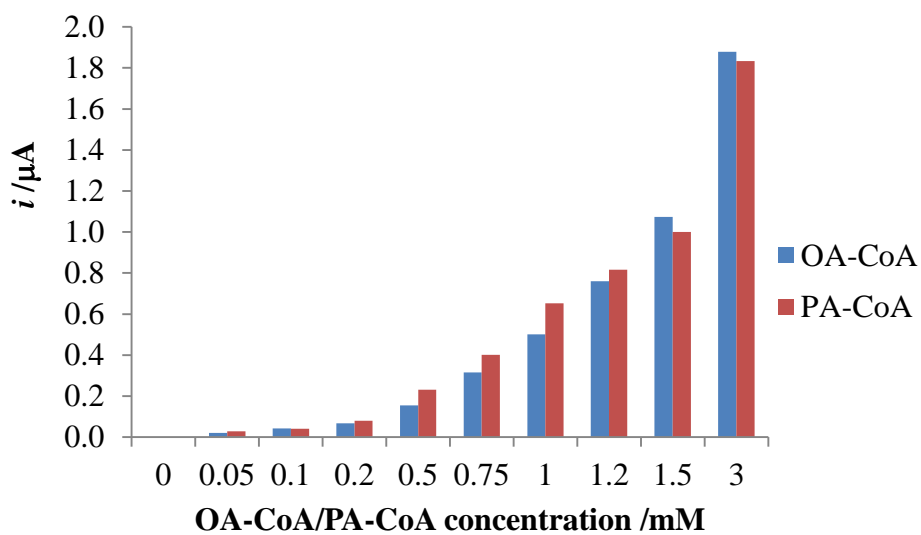


Figure 3-13: Bar chart comparing the current produced from the two different acylated NEFAs on SWCNT SPE. CA at 500 mV, current taken at 500 s.

As stated earlier, the driving force can be increased by applying a positive potential, this is proven by the CV's done at a scan rate of 100 mV s^{-1} , shown in Figure 3-14. The concentration of 0.50 mM PA-CoA was used for the investigation. To determine the potential limit required to sufficiently oxidise the electrode surface for the H_2O_2 oxidation, the switching potential was varied from 0.6 to 1.6 V . The amplitude of the oxidation current increased as the potential limit increased. As in the higher the positive potential the more H_2O_2 oxidised.



Table 3-1 shows the current produced for each scan rate ($5, 50, 100$ and 500 mV s^{-1}) at the upper potential for the same concentration of 0.50 mM PA-CoA . Maximum sensitivity was observed using a potential of 1.6 V . However, having a very high positive potential may result in charcoalization of the electrode. The surface of carbon at 1.0 V can be deeply oxidized and create surface oxygen groups which contribute to more effective H_2O_2 oxidation [265]. For ΔG° to be spontaneous at constant temperature and pressure it needs to be as negative as possible, therefore it is not ideal to go to such positive potentials.

Now that it has been confirmed that the oxidation of H_2O_2 is feasible and detectable on a C-SPE, optimisation for best results in terms of linear detection range and sensitivity needs to be explored. For this reason other SPE's (either incorporating carbon nanotubes (CNT) and/or catalysts such as cobalt) needed testing for H_2O_2 oxidation/production from the enzymatic reactions. These electrodes may detect the oxidation of H_2O_2 at lower potentials, reducing the overpotential and activation barrier required for reaction to take place.

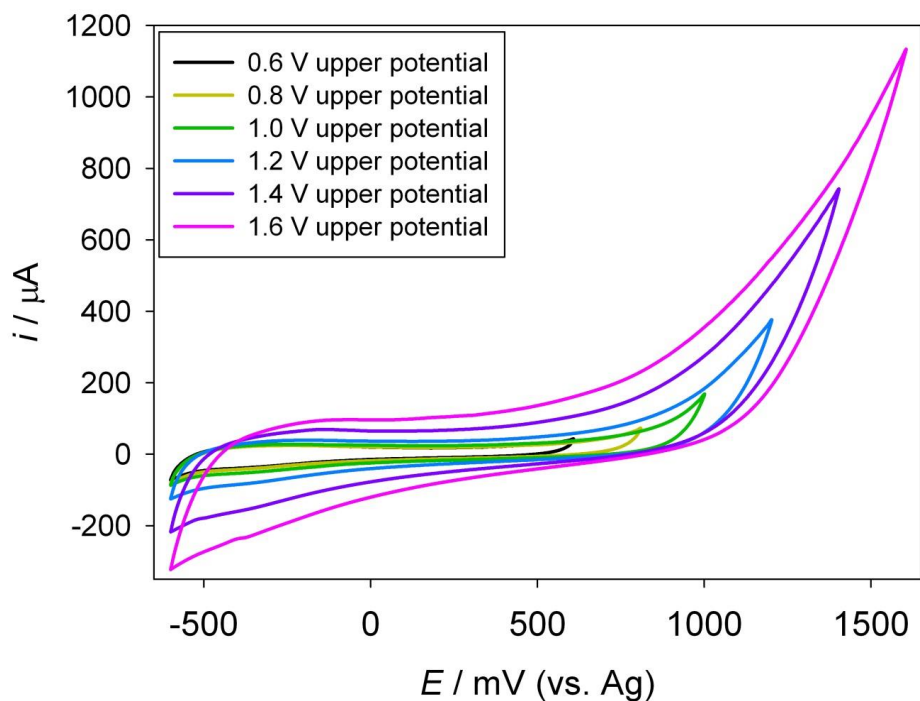


Figure 3-14: CV of 0.50 mM PA-CoA and ACOD at scan rate of 100 mV s^{-1} using a C-SPE with increasing upper limit potential varying from 0.6 V to 1.6 V.

Table 3-1: The current obtained for each scan rate for each upper potential for 0.50 mM PA-CoA. All data is background subtracted. Data given in 6 significant figures.

Upper potential (V)	Current produced (μA) for 0.50 mM PA-CoA at a scan rate at 5 mV s^{-1}	Current produced (μA) for 0.50 mM PA-CoA at a scan rate at 50 mV s^{-1}	Current produced (μA) for 0.50 mM PA-CoA at a scan rate at 100 mV s^{-1}	Current produced (μA) for 0.50 mM PA-CoA at a scan rate at 500 mV s^{-1}
0.6	4.35790	14.4195	18.9118	35.0036
0.8	8.06580	25.9156	33.8318	67.9018
1.0	35.9253	76.5684	84.4731	113.922
1.2	76.5690	147.949	168.457	211.579
1.4	119.293	238.830	273.773	332.641
1.6	80.8720	253.902	294.492	369.870

3.3.2 Detection using single wall carbon nanotube screen printed electrode

CNT have been extensively used since they were discovered by Iijima in 1991 [279]. CNT in electrochemical measurements provide a large surface area and enhance electron transfer in reactions for a great number of molecules (such as GOx) and have the possibility of miniaturization for further development of electrochemical biosensors [280-282].

The redox currents of inorganic, organic compounds/molecules, macrobiomolecules and biological cells can be improved by replacement of ordinary materials by CNT and reducing the redox overpotentials [209]. The next electrode investigated was the single wall carbon nanotube (SWCNT) SPE. Chronoamperometric results for PA-CoA are shown in Figure 3-15, with the corresponding calibration graph at 500 s in Figure 3-16. This gave a linear range up to 3.00 mM PA-CoA, with R^2 of 0.9960 and a sensitivity of 0.7358 $\mu\text{A}/\text{mM}$ at 500 mV. With the SWCNT electrode, there should have been an increase in current as the surface area increased when compared to plain C-SPE (Figure 3-9). The amount of current produced and sensitivity remained similar. However there was still a high overpotential for the oxidation of H_2O_2 .

Chronoamperometric results for OA-CoA are shown in Figure 3-17, with the corresponding calibration graph in Figure 3-18, showing a linear range up to 3.00 mM of OA-CoA too, R^2 of 0.9960 and a sensitivity of 1.0725 $\mu\text{A}/\text{mM}$, at the set potential of 500 mV.

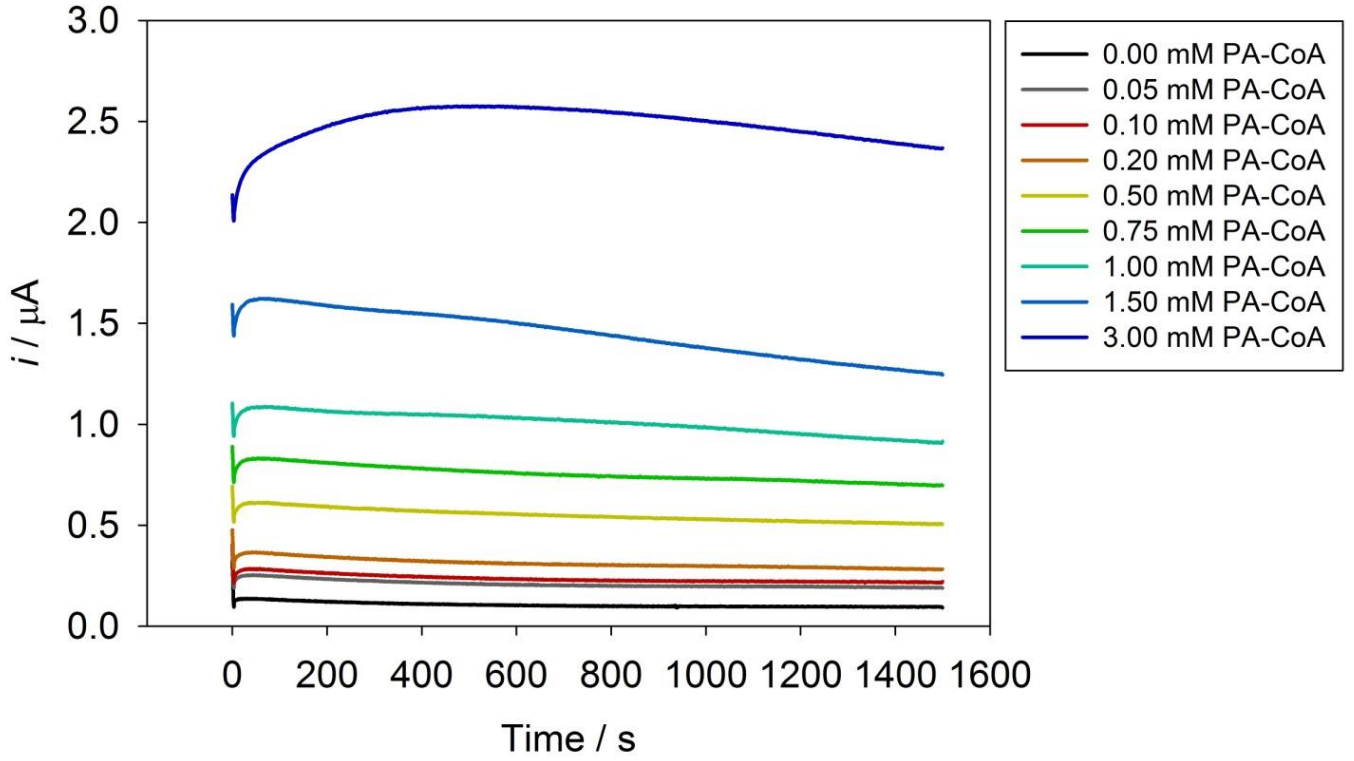


Figure 3-15: CA at 500 mV of various PA-CoA concentrations on SWCNT SPE in 0.1 M phosphate buffer pH 7.4 with ACOD in solution.

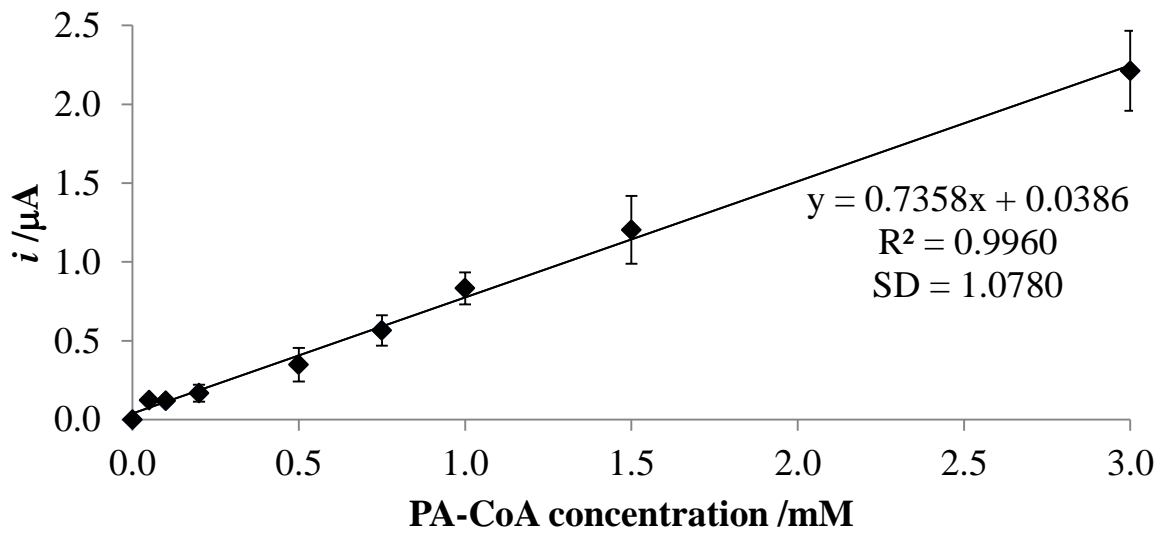


Figure 3-16: Calibration graph at 500 s.

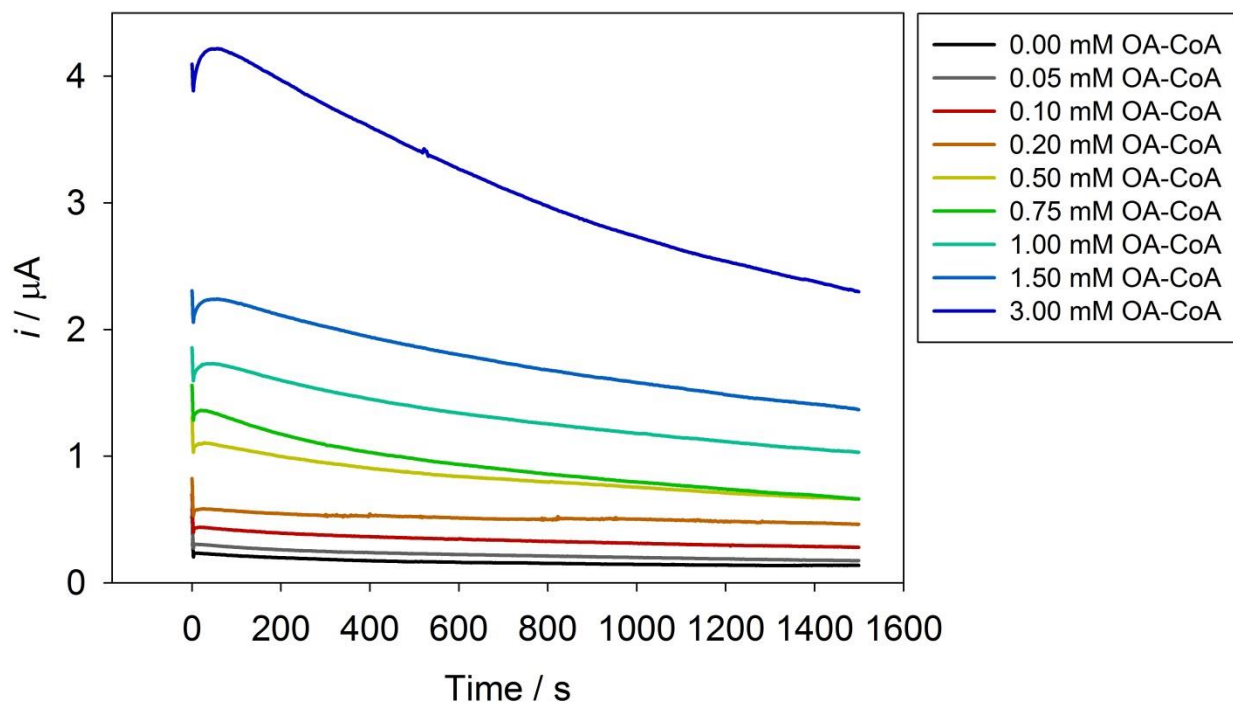


Figure 3-17: CA at 500 mV of various OA-CoA concentrations on SWCNT SPE in 0.1 M phosphate buffer pH 7.4 with ACOD in solution.

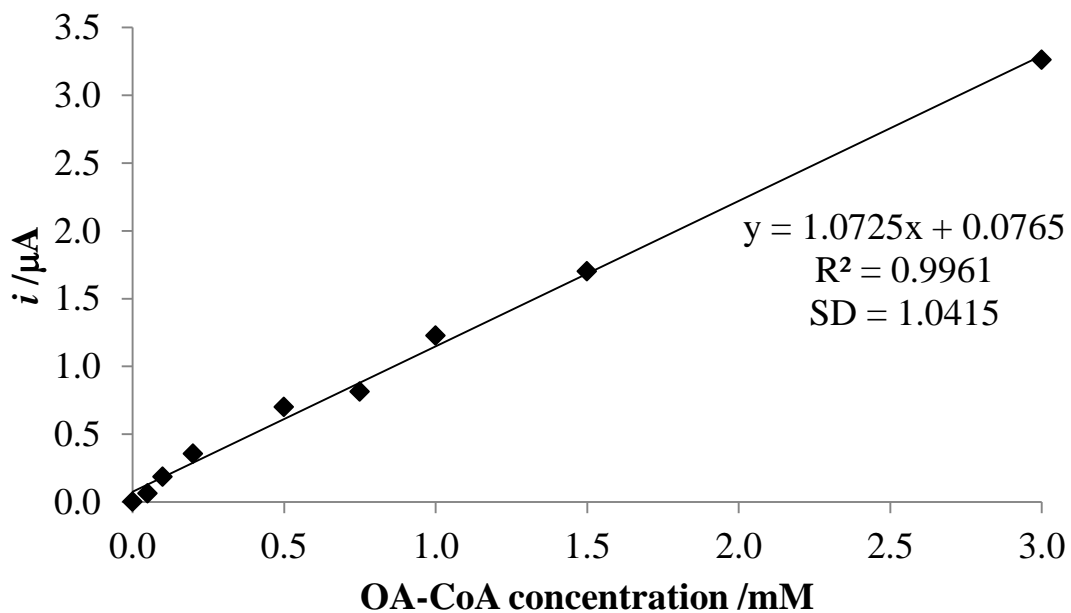


Figure 3-18: Calibration graph at 500 s.

The LSV of PA-CoA using this electrode is shown in Figure 3-19 (with Figure 3-20 showing the calibration graph at 500 mV). The response was linear up to 3.00 mM PA-CoA. The R^2 value was ~ 0.98 , with a sensitivity of $\sim 1.1 \mu\text{A}/\text{mM}$.

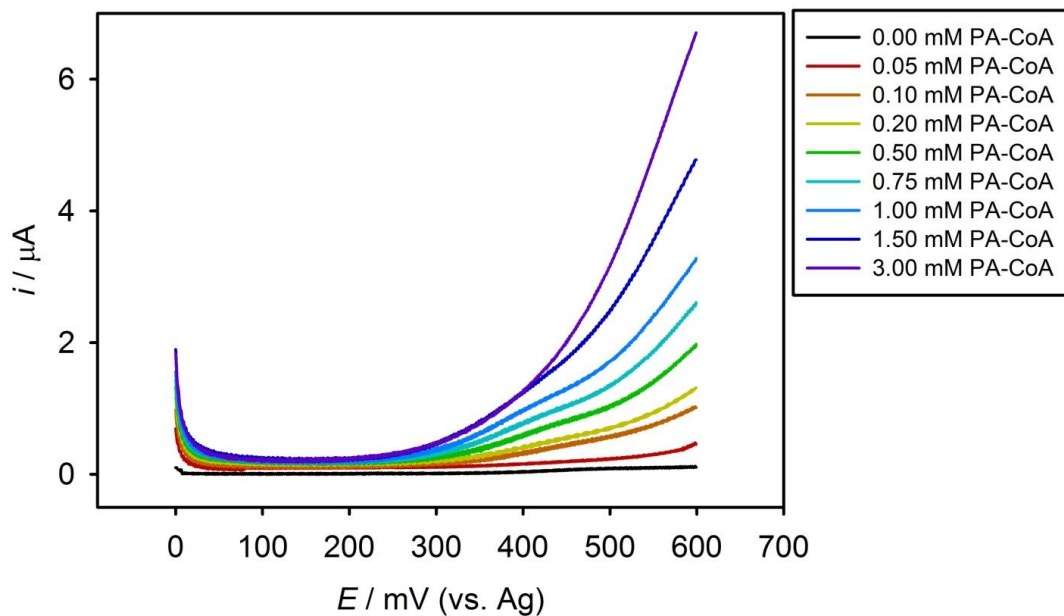


Figure 3-19: LSV for various concentrations of PA-CoA measured at a SWCNT SPE with ACOD in 0.1 M phosphate buffer pH 7.4 , scan rate 1 mV s^{-1} .

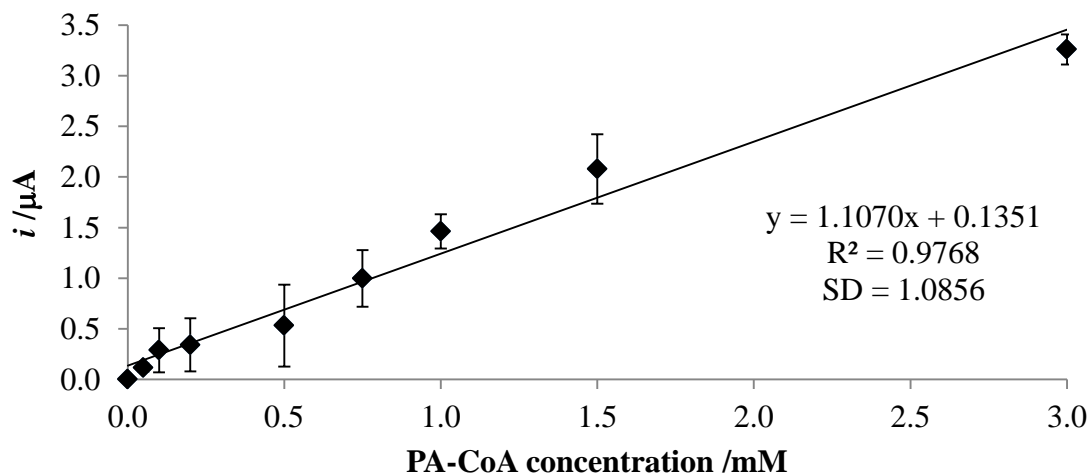


Figure 3-20: Calibration graph at 500 mV.

3.3.3 Detection using cobalt phthalocyanine screen printed electrode

Another electrode commonly used to detect H_2O_2 chronoamperometrically is the cobalt phthalocyanine (CoPc) SPE. The CA results are shown in Figure 3-21 and Figure 3-22. The CoPc SPE gave a linear range up to 3.00 mM PA-CoA, with R^2 of 0.99 and a sensitivity of $1.1664 \mu\text{A}/\text{mM}$ at 500 mV. This electrode gave the highest sensitivity and current. Due to its high catalytic activity, CoPc is the most sensitive material for detecting H_2O_2 [283].

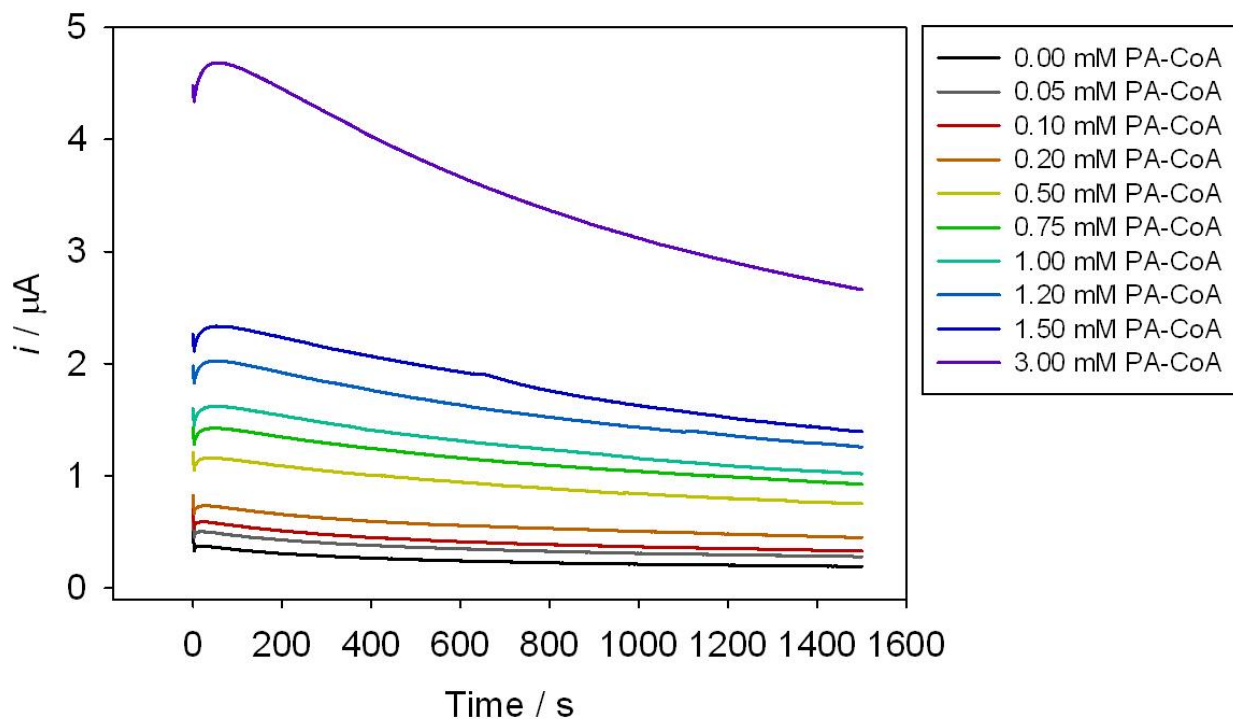


Figure 3-21: CA at 500 mV of various PA-CoA concentrations on CoPc SPE in 0.1 M phosphate buffer pH 7.4 with ACOD in solution.

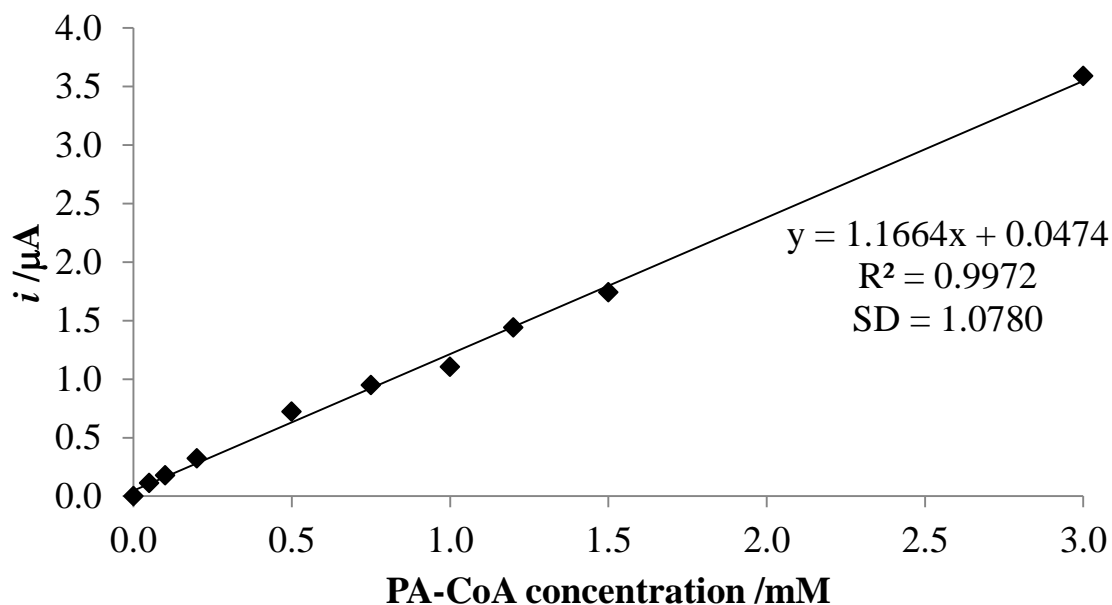
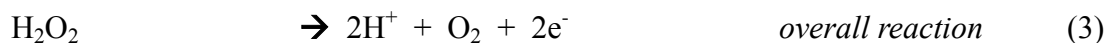
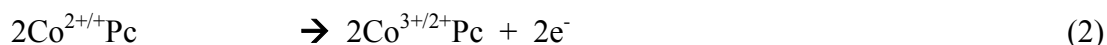


Figure 3-22: Calibration graph at 500 s.

Metallophthalocyanines are extremely versatile materials, due to their macrocyclic nature (extended π -system) they are capable of undergoing fast redox processes with minimal reorganizational energies and can also act as mediators in electron transfer processes involving many molecules [278]. Phthalocyanine electrodes act by lowering the overpotential of oxidation or reduction of the target molecules. Metallophthalocyanines act as catalysts in solution phase H_2O_2 electrochemical oxidation and reduction [283]. The catalytic activity is related to the central metal in the phthalocyanine, the frontier molecular orbitals of the reactant interact with the frontier orbitals situated on the metal centre, aiding the transfer of electron to and from the target molecule [284]. CoPc is a potent catalyst for H_2O_2 oxidation and reduction. In this study the CoPc SPE was shown to have reduced the activation energy and the reaction occurred faster, therefore H_2O_2 was oxidized at a lower potential (on CoPc SPE) compared to the C-SPE and SWCNT SPE. The reaction on CoPc electrodes can be written as follows:



CoPc is initially in the Co^{2+} oxidation state ($\text{Co}^{2+}\text{Pc}^{2-}$), it is subsequently electrochemically oxidized to Co^{3+} or reduced to Co^+ [277]. The structure of CoPc is shown in Figure 3-23.

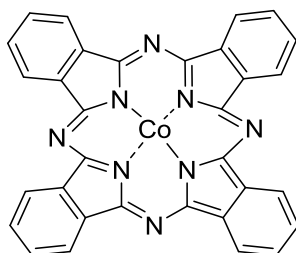


Figure 3-23: Chemical structure of CoPc.

The principle of operation of the proposed biosensor is illustrated in Figure 3-24. The enzymatic generation of H_2O_2 is achieved by PA-CoA reacting with O_2 to produce hexadecanoyl-CoA and H_2O_2 (which is then oxidized by Co^{2+} to produce Co^{3+}).

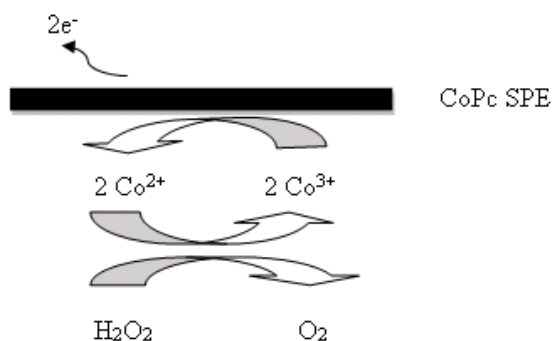


Figure 3-24: Schematic showing the principle of NEFA biosensor for H_2O_2 detection using CoPc SPE.

Similar data was obtained for OA-CoA using CoPc SPE in Figure 3-25, with its corresponding calibration graph in Figure 3-26. A bar chart highlighting the chronoamperometric currents at 500 s from both the acylated NEFAs is shown in Figure 3-27. PA-CoA produced more H_2O_2 compared to OA-CoA, this may be due to it being a saturated NEFA. In solution fatty acyl-CoA forms micelles, with the critical micelle concentration differing with the chain length, making it difficult for the determination of the kinetic parameters of these CoA esters [162].

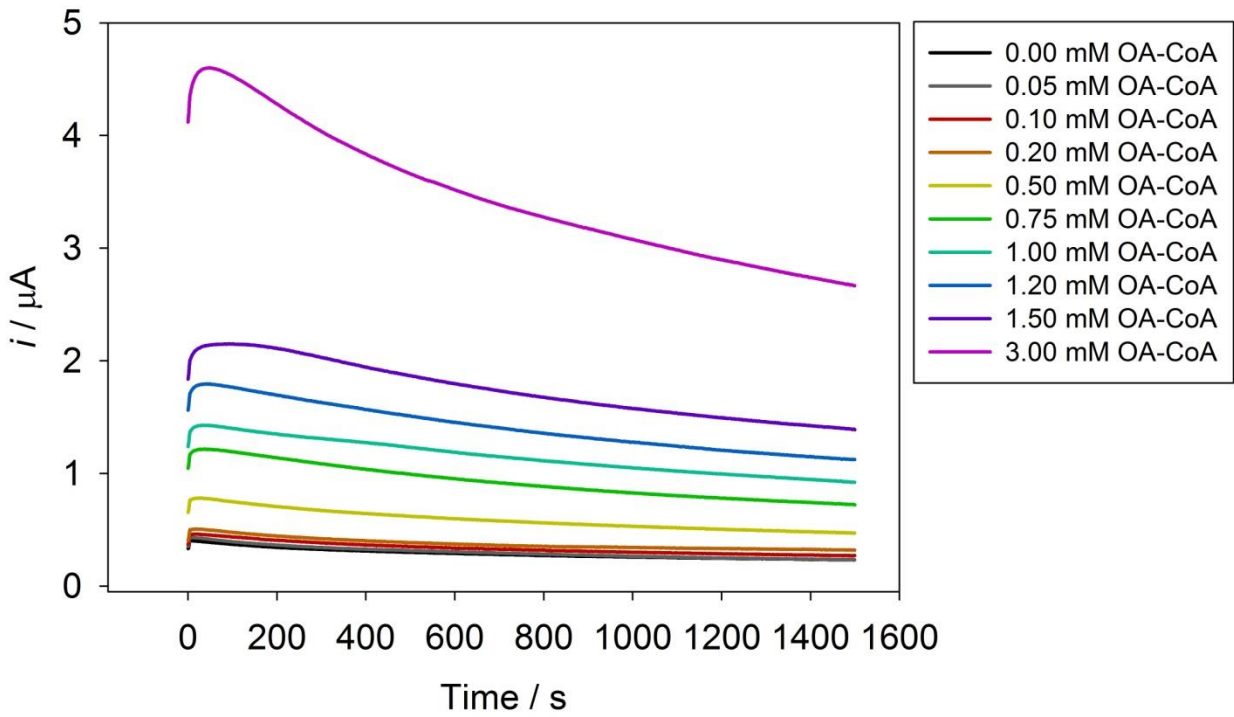


Figure 3-25: CA at 500 mV of various OA-CoA concentrations on CoPc SPE in 0.1 M phosphate buffer pH 7.4 with ACOD in solution.

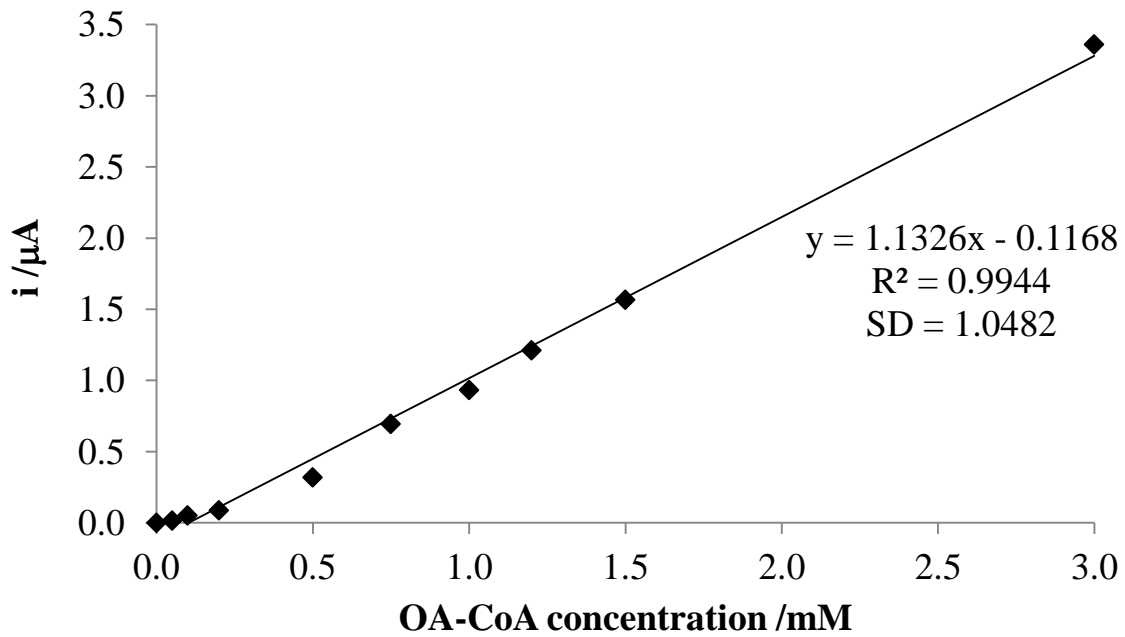


Figure 3-26: Calibration graph at 500 s.

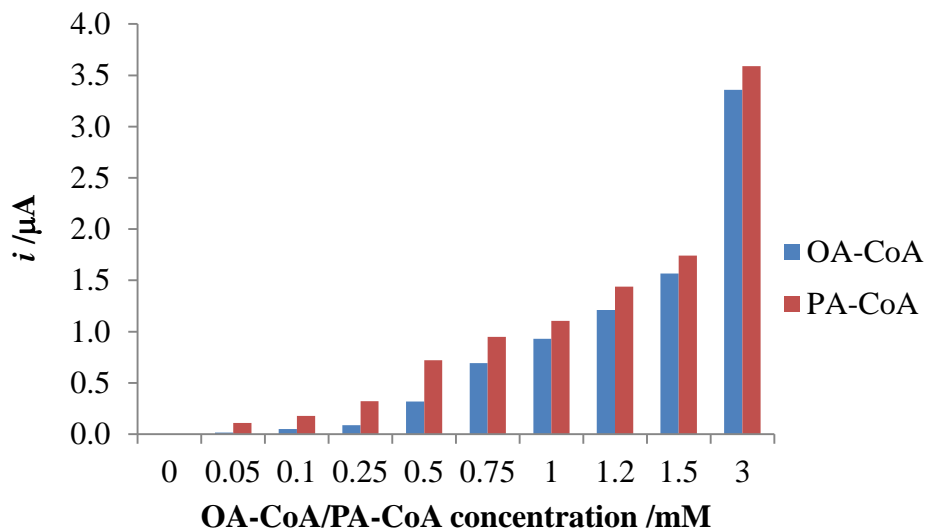


Figure 3-27: Bar chart comparing the current produced from the two different acylated NEFAs on CoPc SPE. CA at 500 mV, current taken at 500 s.

3.3.3.1 Activity of cobalt phthalocyanine lost over time

The activity of CoPc electrode was tested by multiple scans in 0.00 mM PA-CoA (as having no H_2O_2) and in 0.50 mM PA-CoA (in presence of H_2O_2 produced from the enzymatic reaction with ACOD). 75 CV scans were done in each solution at 50 mV s^{-1} scan rate. As the number of scans increased the activity of the CoPc SPE decreased, this is has been a feature of the metallophthalocyanine catalysts during cycling or long-term measurements attributed to the loss of adsorbed transition metal from the surface of the macrocycle [285, 286]. Figure 3-28 shows all the scans for 0.00 mM and 0.50 mM PA-CoA, the arrow points to the general pattern over consecutive scans. Work done by Van Veen and Colijn showed that oxidation of the macrocycle (Fe and Co) by O_2 or H_2O_2 caused the loss of activity [287]. Many catalysts are degraded by H_2O_2 , therefore successful potential scans are not fully reproducible, resulting in large number of studies with fresh electrode surfaces [288]. Whether or not all these fresh surfaces are identical, can complicate the study. So when using CoPc SPE, ideally a fresh electrode would be the best practice for each concentration of PA-CoA/ H_2O_2 .

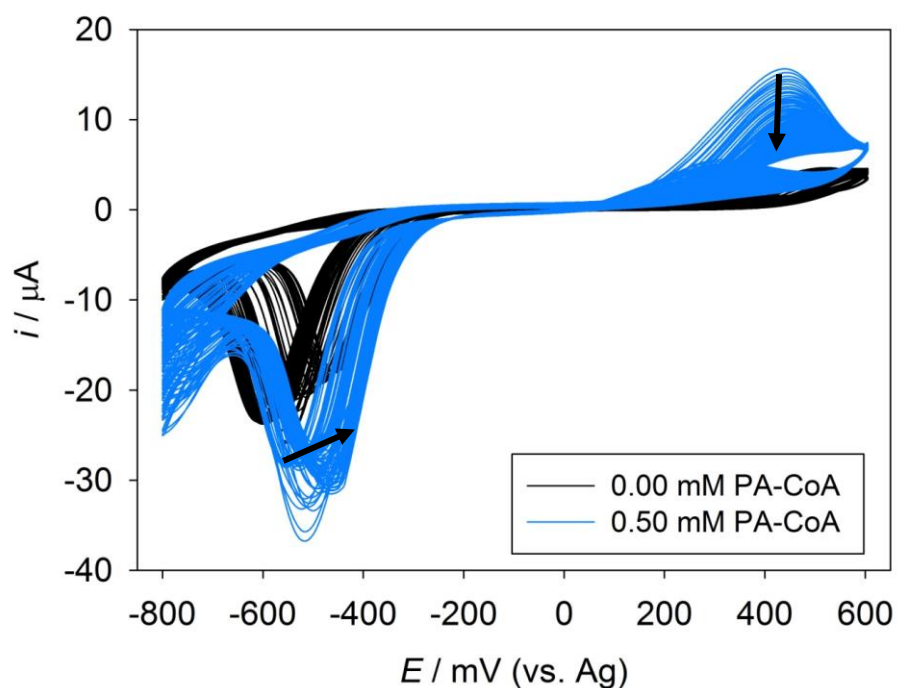


Figure 3-28: CV of 75 scans of 0.00 mM (black) and 0.50 mM (blue) PA-CoA with ACOD in solution, at scan rate of 50 mV s^{-1} using a CoPc SPE.

Parallel to Figure 3-14 and Table 3-1 are Figure 3-29 and Table 3-2 but using CoPc as the SPE. At 100 mV s^{-1} the CV shows that increasing to upper potential increases the amount of current produced. However Table 3-2 shows that only up to 1.0 V is this pattern observable over the whole range investigated on a different electrode. Having more scans loses the activity of the CoPc electrode, hence the drop in current at higher potentials. This could be due to desorption of CoPc from the electrode, macrocycle becoming destroyed in the presence of oxygen or demetallation of the phthalocyanine [285].

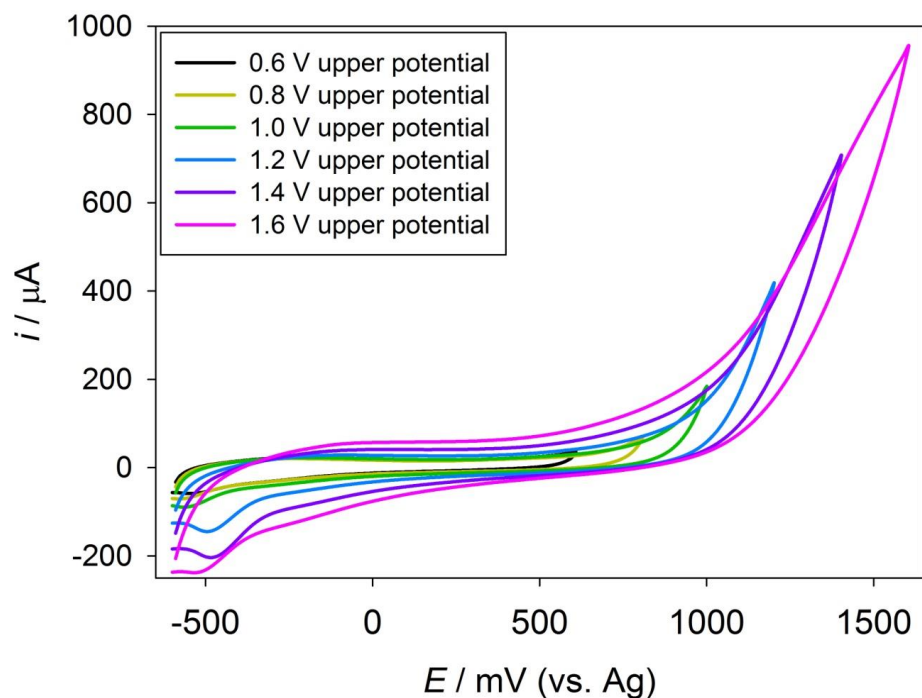


Figure 3-29: CV of 0.50 mM PA-CoA with ACOD in solution, at scan rate of 100 mV s^{-1} using a CoPc SPE with increasing upper limit potential varying from 0.6 V to 1.6 V.

Table 3-2: The current obtained for each scan rate for each upper potential for 0.50 mM PA-CoA. All data is background subtracted. Data given in 6 significant figures.

Upper potential (V)	Current produced (μA) for 0.50 mM PA-CoA at a scan rate at 5 mV s^{-1}	Current produced (μA) for 0.50 mM PA-CoA at a scan rate at 50 mV s^{-1}	Current produced (μA) for 0.50 mM PA-CoA at a scan rate at 100 mV s^{-1}	Current produced (μA) for 0.50 mM PA-CoA at a scan rate at 500 mV s^{-1}
0.6	2.95990	9.97620	15.2497	39.9872
0.8	6.92630	25.2899	34.0027	64.5289
1.0	20.5990	33.9960	41.9320	67.5050
1.2	11.4750	96.0700	40.0090	45.5930
1.4	-56.6710	76.1110	42.1150	-54.9320
1.6	-55.8470	-63.7810	-32.9590	-98.2600

3.3.4 Screen printed electrode comparison

A comparison table of the 3 substrates (H_2O_2 , PA-CoA and OA-CoA) and 3 electrodes is shown in Table 3-3. From the 3 electrodes investigated for electrochemical NEFA detection in solution, CoPc showed the highest sensitivity by far, for H_2O_2 production from NEFA. This is because CoPc SPE was the only catalyst modified electrode, thus reducing the excessive voltage required to drive the oxidation of H_2O_2 .

The current produced by H_2O_2 solution oxidation was always slightly lower, than that from H_2O_2 produced from PA-CoA/OA-CoA. However data from H_2O_2 solution oxidation was more linear (higher R^2 value). H_2O_2 readily decomposes, this could be the reason why its detection was lower from solution, as once the stock solution (10 mM) was made up, there was a bit of a wait to have all the concentration chronoamperometrically detected, compared to when PA-CoA/OA-CoA reacts with O_2 and it is detected without delay each time. All three electrodes had a linear detection range of 0.00 mM to 3.00 mM of PA-CoA/OA-CoA, covering well above the physiological range in human plasma.

Table 3-3: Comparison of 3 different electrodes for CA at 500 mV at 500 s, current for 0.75 mM PA-CoA/OA-CoA/ H_2O_2 .

Detection	C-SPE			CoPc SPE			SWCNT SPE		
	Current (μA)	Sensitivity ($\mu A/mM$)	R^2	Current (μA)	Sensitivity ($\mu A/mM$)	R^2	Current (μA)	Sensitivity ($\mu A/mM$)	R^2
PA-CoA	0.4011	0.6326	0.9926	0.9477	1.1664	0.9972	0.5651	0.7358	0.9960
OA-CoA	0.3155	0.6519	0.9799	0.6929	1.1326	0.9944	0.8125	1.0725	0.9961
H_2O_2	0.3127	0.5644	0.9943	0.7272	1.0539	0.9993	0.7275	1.2643	0.9963

C-SPE had the most consistent current produced for the 3 substrates at 0.75 mM, with a difference of only a minor 0.0884 μA . Whereas the SWCNT SPE had the largest difference between the substrates of 0.5285 μA . The variability between the amount of H_2O_2 detected by the different electrodes renders the C-SPE as the most reproducible and consistent electrode, it has no additional bonds on the surface (is a plain carbon electrode) and would be suitable for further optimization for NEFA detection.

3.3.5 Interferences

In literature, several molecules were found to cause interference with NEFA level determination (with standards and in blood), namely: phospholipids, bilirubin, albumin, haemoglobin, lecithin, lactic acid, acetic acid, ascorbic acid, β -hydroxybutyric acids, triglycerides, glutathione, cysteine and unreacted Coenzyme A [118, 121, 125, 127, 129-132]. The reason for the interference is mainly dependant on the method that is used to detect the NEFA. Details of this are given in Table 3-4 below.

Table 3-4: Suggested reasons why each interference may cause incorrect NEFA readings.

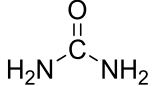
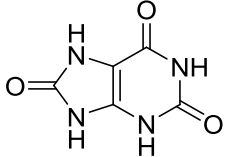
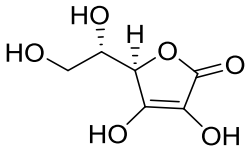
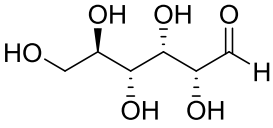
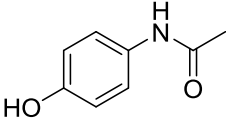
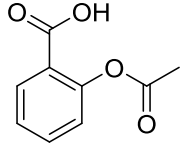
Interference	Method of NEFA detection	Result on reading	Suggested reason for interfering	References
Acetic acid	Paper chromatography	-	Traces from chromatographic solvent	[130]
Albumin	Optical enzymatic assay	Negative	Inhibits enzyme activity	[132]
	Paper chromatography	Positive	Bound fatty acids	[130]
	Colorimetric enzymatic assay	Negative	Bound fatty acids	[289]
Ascorbic acid	Optical enzymatic assay	Negative	Competition with POD for H ₂ O ₂	[132]
	Optical enzymatic assay	Positive	-	[121]
	Colorimetric enzymatic assay	Negative	-	[289]
Bilirubin	Optical enzymatic assay	Positive	-	[132]
	Colorimetric copper-soap method	Positive	Extracted as copper complex	[129]
	Colorimetric enzymatic assay	Negative	-	[289]
Coenzyme A	Colorimetric enzymatic assay	Negative	Unreacted Coenzyme A inhibits subsequent reaction	[120]
	Optical enzymatic assay	Negative		[132]
	Colorimetric enzymatic assay	Negative		[289]
Haemoglobin	Optical enzymatic assay	Positive	-	[132]
Heparin	Automated enzymatic determination by centrifugal analysis	Positive	Heparinized plasma falsely elevate by 10 %	[290]
Lecithin	Paper chromatography	Positive	Molar extinction produced is similar to that of NEFA	[123, 130]
	Radiochemical assay	Positive	-	[127]
Phospholipid	Colorimetric copper-soap method	Positive	Extracted as copper complex, tend to hydrolyse	[118, 129]

Electrochemically many compounds (e.g. acetaminophen, uric acid and ascorbic acid) can be oxidised at such high positively applied potentials (500 mV) and would cause interference with the H₂O₂ detection in real blood samples [291]. Adsorption of the listed compounds (or their derivatives) is undesirable on the analytical response, particularly on diffusion-controlled mass transport. Moreover, adsorption of interferences and/or their derivatives that are non-electroactive may deactivate the surface of the electrode [276]. Tests were done with selected compounds: albumin, urea, uric acid, ascorbic acid, glucose, acetaminophen and aspirin. Some general information on each of these is given in Table 3-5.

Acetaminophen (Paracetamol) was investigated as it is the most common pain killer in the world, naturally this would be present in the blood of people who take acetaminophen and then use the sensor [292]. The patients with T2D are also in danger of having high cholesterol and inevitably leading onto blood pressure problems, so aspirin was investigated, as it is commonly prescribed to patients with high blood pressure. Aspirin can also improve insulin sensitivity and lipid metabolism [293].

The concentrations selected for this study in Table 3-5 are typical ranges, in actual fact patients could have elevated concentrations of some of these interferences depending on their medical condition, e.g. concentration of urea increases in patients with kidney problems. The 'chosen concentrations' for urea, uric acid and aspirin were towards the higher end of the range of concentration found in blood. This was done to take the concentration fluctuation in different patients blood into consideration. The concentration of glucose was 10 mM, which was above the normal range. This was chosen to represent a patient with uncontrolled T2D, who would have a high glucose concentration.

Table 3-5: General information on the chosen interferences.

Interference	Chemical structure	Concentration in blood (mM)	Chosen concentration (mM)	References
Urea (NH ₂) ₂ CO		1 - 19 or 2.64-2.71	3.00	[294, 295]
Uric acid C ₅ H ₄ N ₄ O ₃		4 – 8.5	8.00	[294, 295]
Ascorbic acid C ₆ H ₈ O ₆		0.04 – 0.116 or 0.087 – 0.755	0.50	[294, 295]
Glucose C ₆ H ₁₂ O ₆		4– 8 Up to 30	10.0	[296]
Acetaminophen C ₈ H ₉ NO ₂		0.066 – 0.132	0.12	[297]
Aspirin C ₉ H ₈ O ₄		0.1 – 0.3 or 1.08 – 2.17	3.00	[295, 298]
Albumin	-	52 – 65% of total protein	0.60	[295]

Using chronoamperometry with C-SPE at 500 mV, the current at 500 s was compared with that of 0.20 mM PA-CoA and with that of 0.20 mM PA-CoA spiked with each interferant individually (each concentration used was the ‘chosen concentration’ in Table 3-5). The result is shown in Figure 3-30, along with a zoomed in version of lower current range.

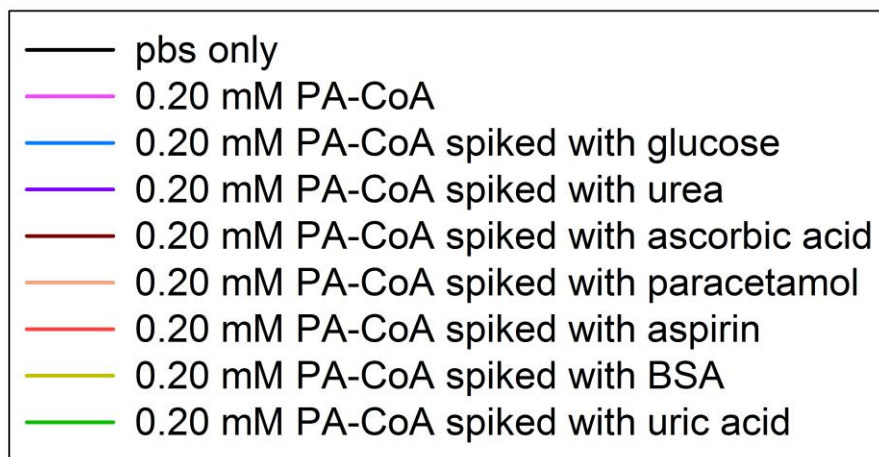
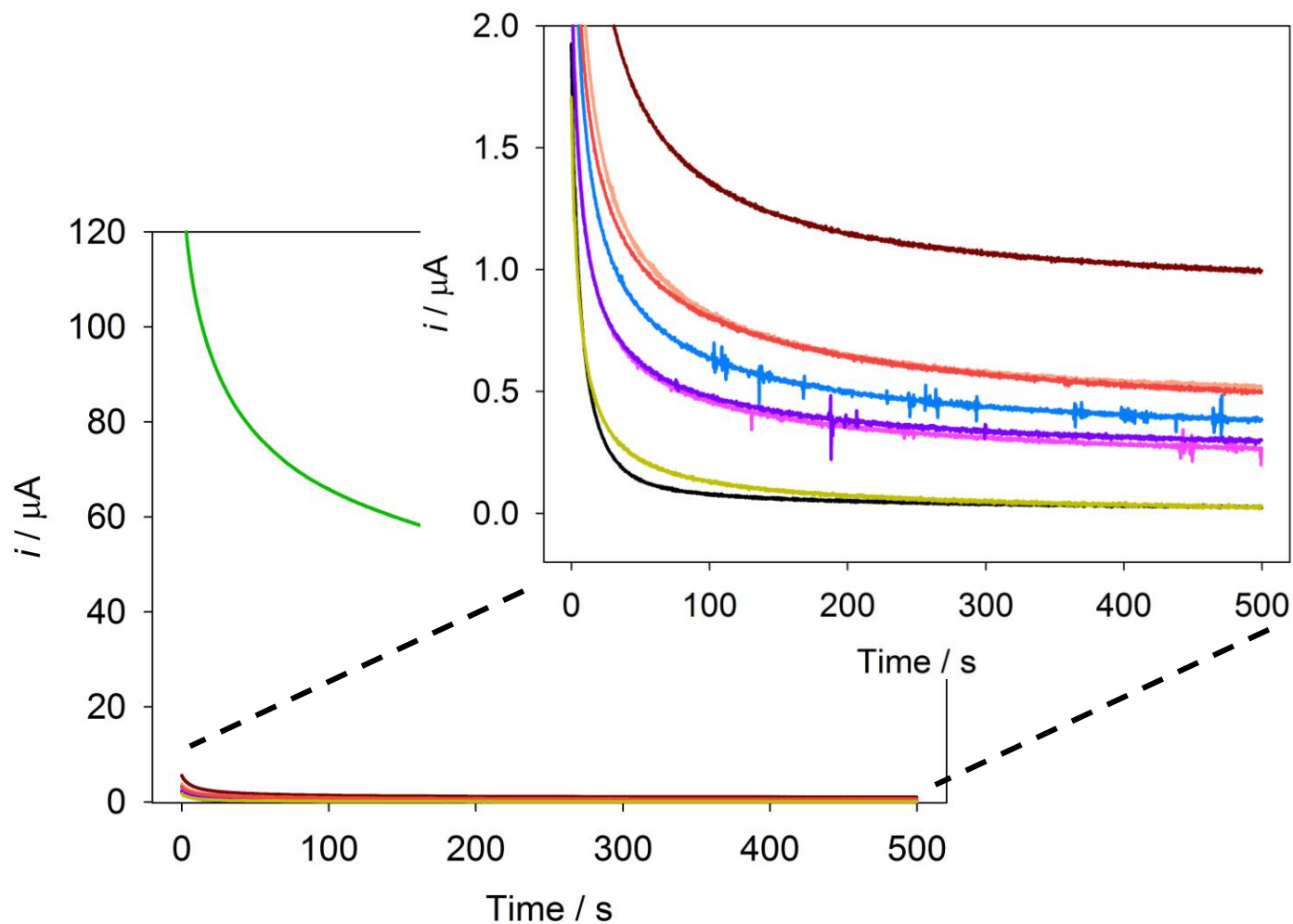


Figure 3-30: CA at 500 mV for 0.20 mM PA-CoA with ACOD, spiked with various interferences on C-SPE, in 0.1 M phosphate buffer pH 7.4. The concentration of each interference is that listed in Table 3-5.

Table 3-6 shows the percent interference worked out for each compound studied. This was calculated by the current produced with the spiked sample during CA at 500 s, divided by the current produced from 0.20 mM PA-CoA at 500 s, times 100 (to get a percentage interference).

Before this could be done, various concentrations of each interference only were tested on the C-SPE. This data is shown in the appendix (in Figure 7-2 to Figure 7-5) and the data is summarised in Table 3-6. The detection range given here is based on the linear detection of that interference on a C-SPE. The sensitivity is the sensitivity of C-SPE at various concentrations within the detection range.

Table 3-6: Each interference at 500 s CA at 500 mV.

Compound	Sensitivity ($\mu\text{A}/\text{mM}$)	R²	Detection range (mM)	% interference with 0.20 mM PA-CoA
Urea	0.0017	0.9675	0 - 10	4.6
Uric acid	4.5579	0.9808	1 - 10	15218
Ascorbic acid	1.3313	0.9777	0.1 - 1	218
Glucose	0.0026	0.7265	0 - 30	38.3
Acetaminophen	2.6588	0.9980	0 - 0.18	78.5
Aspirin	0.0043	0.9836	0 - 3	80
Albumin	0.0205	0.9968	0.2 – 0.6	-75

The increase in the percentage detection of 0.20 mM PA-CoA was caused by either the interference interacting with the enzymatic reaction or by the interference altering the surface of the electrode, leading to an increased current reading of H₂O₂ oxidation.

Most interference with NEFA detection was caused by uric acid and ascorbic acid due to the high overpotential required for the oxidation of H₂O₂ being similar to that of the oxidation of these compounds. The impact of uric acid and ascorbic acid will be discussed in more detail later.

All interferences studied caused an increase in the current except albumin. Bovine serum albumin (BSA) is a single polypeptide chain consisting of about 583 amino acid residues and no

carbohydrates. At pH 5-7 it contains 17 intrachain disulfide bridges and 1 sulfhydryl group [299, 300]. Each serum albumin protein molecule can carry seven fatty acid molecules [301]. Serum albumin interacts strongly with fatty acid anions [302]. The cationic sites on the albumin molecule is probably where the fatty acid anions bind to. The availability of such cationic sites will depend on their equilibrium with hydrogen ions. Albumin is the major vehicle for NEFA transport through the plasma [303]. Albumin hindered the activation of acylated NEFA by ACOD by forming a complex with the fatty acid, hence lower amount of H_2O_2 produced [155].

On a bare electrode the oxidations of ascorbic acid and uric acid occur at close potentials and the bare electrode very often suffers from fouling effects [304]. To reduce the potential interference and fouling effects of these compounds, the immobilization of the enzymes ACS and ACOD on the working electrode may be a step forward in the development of the NEFA electrochemical biosensor. Then oleic acid/palmitic acid can be used (step 1 from scheme 1) instead of OA-CoA/PA-CoA (step 2 from scheme 1), as they are the most abundant NEFAs present in the patient's blood.

Immobilization of enzymes on the WE would reduce the amount of enzyme used and increase the repeatability of using one electrode for multiple concentrations. This would bring the cost down in sensor development and in this research. Once the enzyme is bound to the surface of the SPE's WE, it is more likely to react with the substrate and cause H_2O_2 production and subsequent oxidation.

3.4 Conclusions

In this chapter H_2O_2 oxidation and H_2O_2 oxidation from the NEFA enzymatic reaction was tested on 3 SPE's (C-SPE, CoPc and SWCNT SPE) and compared. All electrodes had a good response to the various concentrations investigated (up to 3.00 mM PA-CoA/OA-CoA). Linear calibration graphs of LSV at 500 mV and CA at 500 s at 500 mV potential were obtained. In all 3 SPE's the limit of detection was 0.00 mM to 3.00 mM PA-CoA/OA-CoA. This covers the range of NEFA concentrations in human blood, for sensor development.

LSV's were used to determine the order of reaction by plotting $\log j$ vs. \log PA-CoA/OA-CoA concentration range for each electrode investigated. The potentials investigated (400 mV plus) proved to be first order, with correlation coefficient (R^2) around 0.99.

The current produced for H_2O_2 oxidation was evident at 300 mV plus. Which is why the set potential of 500 mV was chosen for all CA work.

Activity of CoPc electrode was lost over time, meaning that the SPE could only be used once to provide a reliable current.

Upper potential range was investigated for C-SPE and CoPc SPE. The higher the potential the more the current was produced using CV at 100 mV s^{-1} scan rate. But having a very high upper potential would have many side reactions too, so all LSV experiments were to be done up to 600 mV for future work.

The C-SPE electrode was taken forward and tested with common interferences that would be present in blood (urea, uric acid, ascorbic acid, glucose, acetaminophen, aspirin and albumin). From which urea had the least interference and uric acid had the most, as predicted from its highly oxidizable nature.

4 Enzyme electrode for NEFA detection

4.1 Introduction

The working electrode (WE) of screen printed electrodes (SPE's) can be readily modified to enhance selectivity and/or sensitivity by surface deposition of various substances, such as polymers and enzymes [305]. Carbon screen printed electrodes (C-SPE's) are suitable for a variety of applications, they are substrates for biosensors due to the large potential window of carbon, the low background current, chemical inertness and ease of derivitization and modification. The immobilization method may affect the sensitivity, response time, stability and reproducibility of biosensors [306]. The method needs to ensure the enzyme is retained on the support, with the active site maintaining its functionality and accessibility.

Carbon nanotubes (CNT) may be used to help achieve this, but they first need to be properly functionalized and immobilized [268]. Untreated CNT have high hydrophobicity and tend to assemble into bundles, limiting their usage and process ability [307]. Multiwall carbon nanotubes (MWCNT's) are coaxial assemblies of graphene cylinders with dimensions ranging from 2 to 30 nm and length of several microns [308]. CNT have poor solubility in usual solvents, so having polymer wrapped CNT improves solubility, is non-destructive and the electrocatalytic properties are retained [309]. Polymer/CNT composites prepared non-covalently retain their unique properties and can develop new materials [310]. Poly(dimethyldiallylammonium chloride) (PDA) is a water-soluble, quarternary ammonium, cationic polyelectrolyte (structure shown in Figure 5-2 later). This polymer when dissolved in aqueous solutions acts as a positively charged colloid [208]. It is a dispersant of MWCNT's and is readily coated on negatively charged surface of MWCNT's. The CNT have multiple roles [311]:

- they are a substrate to immobilize the enzyme
- electrocatalytic oxidation/reduction of H_2O_2 at the CNT surface, reduced over voltage and avoids interference from other co-existing interactive species
- enhance signal due to fast electron transfer and large working surface area.

The immobilization of biomolecules on electrodes is a big factor in the progress of electrochemical biosensors [312]. The functionality of the biomolecule must stay intact along with the ease of access to its active site. There are several immobilisation methods for biological

molecules, and no single method is right for all the different molecules or purposes [204]. Figure 4-1 schematically shows the various immobilization techniques.

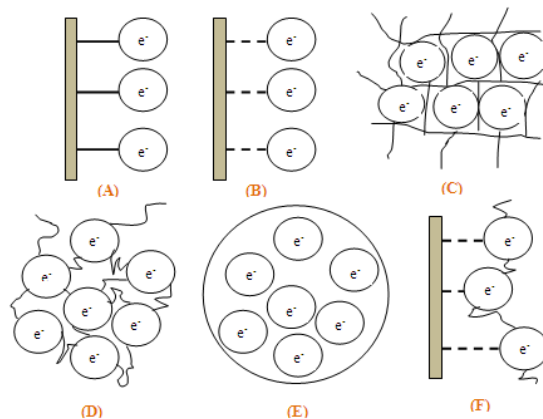


Figure 4-1: Schematic representation of various immobilization techniques: (A) covalent binding, (B) adsorption, (C) gel entrapment, (D) cross-linking, (E) microencapsulation and (F) adsorption-cross-linking [204].

The immobilization technique is responsible for the sensitivity, response time, long-term stability and reproducibility of the biosensor. Immobilization methods, for example physical adsorption, covalent binding, carrier binding, entrapment within a polymeric matrix, encapsulation and cross-linking, could engage in numerous point attachments, failure of biomolecule activity, biomolecule leaking, random biomolecule dis-configuration and great diffusion barriers [313]. These can consequently cause the biosensor to be poorly sensitive, unstable and have long response times. Which is not ideal for NEFA biosensor development.

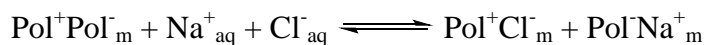
4.1.1 Layer-by-layer immobilization

The layer-by-layer (LbL) assembly technique for multicomposite films was first produced by Decher and group in 1991 [314]. LbL self-assembly technique is a simple procedure, with a wide choice of methods along with film composition, number of layers and thickness control. It takes advantage of the charge-charge interaction between the substrate and monolayers, creating multiple layers held together by strong electrostatic forces/interactions. LbL films provide favourable nanoenvironments for the enzymes/proteins and boost the direct exchange between the proteins and electrode [315]. In this work the multilayer assemblies consisted of alternating adsorption of anionic (the enzymes ACS and ACOD) and cationic (PDA-MWCNT) polyelectrolytes (electrostatic attraction of oppositely charged species) [316]. LbL method allows fine thickness control of enzymatic layers (at molecular or nanometer level), avoiding mass

transport problems between the analyte and electrode surface (this also affects the response time of biosensors) [216, 317, 318]. The adsorption of molecules having more than 1 equal charge allows charge reversal on the surface [314]. This gives:

- Repulsion of molecules that carry the same charge, the adsorption is therefore self-regulated and confined to a single layer
- On top of this layer, molecules with the opposite charge can be adsorbed. Building multiple films.

Salt (NaCl) is used in the solution in which polyelectrolyte multilayers are formed, known to participate in the formation and function of the layers [319]. The concentration of NaCl controls the thickness increment per deposition cycle, permeability and stability. NaCl counterions participate in charge neutralization leading to more equilibrated conformation of polymer chains [314]. The mobility of charge-paired polyelectrolyte chains are improved with higher NaCl concentrations. There is an equilibrium set-up between the “intrinsically” charge compensated polyelectrolyte complex, Pol^-Pol^+ , where the polymer segments balance the internal charge, and an “extrinsically” compensated form, $\text{Pol}^+\text{Cl}^-/\text{Pol}^-\text{Na}^+$.



$_m$ = multilayer phase

Addition of NaCl dramatically increases the amount of polyelectrolyte deposited [320].

There are four effects on the kinetic behaviour of an immobilized enzyme [321]:

1. Conformation and steric modification
2. Partitioning of reactant
3. Microenvironmental effects on intrinsic catalytic properties
4. Effects of diffusion or mass transfer

To understand characteristics of the immobilized enzymes, understanding the amount adsorbed, the kinetic behaviour of the enzyme regarding the support, the procedure used to immobilize the enzymes and the rate of substrate mass transport needs to be investigated [322].

4.1.2 H₂O₂ detection via layer-by-layer

A review paper was published by *Zhao et al.* highlighting the progress made on the electrochemical biosensors based on this LbL technique [216]. A few have been made to detect H₂O₂ oxidation/reduction from the enzymes that have been immobilized on the electrodes. Table 4-1 shows these selected sensors for H₂O₂ detection. There are multiple LbL assembly methods, the immobilization could be based on one of the following: electrostatic force, biological interaction (e.g. avidin-biotin, lectin-sugar, antibody-antigen), cross-linking, covalent binding and electrodeposition.

Table 4-1: Electrochemical biosensors based on LbL assembly methods for H₂O₂ detection.

Sensor for	Electrode fabrication	Electrode	Amperometric potential at H ₂ O ₂ oxidation/reduction	Abbreviations	Reference
Cholesterol	(PAH-MWCNT-GNPs/HRP)/(PAH-MWCNT-GNPs/ChOx)	gold	-0.15 V vs. calomel electrode - H ₂ O ₂ Reduction	PAH = poly(allylamine hydrochloride) GNPs = gold nanoparticles ChOx = cholesterol oxidase	[323]
Cholesterol	(PDA/ChOx)	gold	+ 0.70 V - H ₂ O ₂ Oxidation	PDA = poly(diallyldimethylammonium chloride)	[324]
Glucose	(PAH-MWCNT/HRP/ConA/GOx)	gold	-0.15 V vs. saturated calomel electrode - H ₂ O ₂ Reduction	HRP = horse radish peroxidase ConA = concanavalin A GOx = glucose oxidase	[325]
Glucose	(CNT/PDA/GOx/PDA)	glassy carbon	-0.10 V vs. Ag/AgCl - H ₂ O ₂ Reduction		[311]
Glucose	(MPS-PDA/PSS/PDA-MWCNT/GOx)	gold	-0.20 V - H ₂ O ₂ Reduction	MPS = 3-mercaptopropylsulfonic acid, sodium salt PSS = poly(sodium 4-styrenesulfonate)	[326]
Glucose	(HRP/GOx)	glassy carbon	-0.20 V vs. Ag/AgCl - H ₂ O ₂ Reduction		[327]
Acetylcholine	(PDA-AChE/GNPs/MWCNT)	platinum	+ 0.60 V vs. Ag/AgCl - H ₂ O ₂ Oxidation	AChE = acetylcholinesterase	[328]
Acetylcholine	(AChE/ChOx)	platinum	+ 0.60 V vs. Ag/AgCl - H ₂ O ₂ Oxidation	ChOx = choline oxidase	[329]
H ₂ O ₂	PVP-Os/HRP	gold	+ 0.35 V vs. saturated calomel electrode - H ₂ O ₂ Oxidation	PVP-Os = quaternized poly(4-vinylpyridine)	[330]

4.1.3 Experimental

Materials

Acyl-Coenzyme A synthetase (ACS) 4 U/mL of enzyme was purchased from Wako HR-series NEFA-HR(2) enzymatic NEFA assay kit (Neuss, Germany). In 30 μ L of solution, 0.12 U ACS was present. Oleic acid (OA) was the Wako NEFA standard solution (cat # 276-76491) also purchased from Wako HR-series NEFA-HR(2) enzymatic NEFA assay kit (Neuss, Germany). This comes as a 1 mM stock solution.

ACOD was purchased from Wako Japan at 100 Units, CAS # 61116-22-1 (Neuss, Germany). Stock solution of 4 U/mL with 0.20 M NaCl was prepared with phosphate buffer as the diluent.

PA-CoA, OA-CoA, ATP and Coenzyme A (CoA) were purchased from Sigma Aldrich (Dorset, UK). Stock solutions of the solutions PA-CoA (10 mM), OA-CoA (10 mM), ATP (20 mM) and CoA (20 mM) were made by diluting in 0.1 M phosphate buffer solution (PBS), pH 7.4 and stored at -20 $^{\circ}$ C until use.

Potassium ferricyanide (III) and potassium ferrocyanide was also purchased from Sigma Aldrich (Dorset, UK). 10 mM stock solution was prepared, for electrochemical impedance spectroscopy (EIS) measurements 5 mM 1:1 mixture of $K_3Fe(CN)_6$: $K_4[Fe(CN)_6]$ was used.

PDA solution consisted of 1 % PDA solution, with 0.20 M NaCl in 5 mL distilled water. PDA was purchased from Sigma-Aldrich (Germany).

A poly(dimethyldiallylammonium chloride)-MWCNT (PDA-MWCNT) solution was prepared by taking 3 mg of MWCNT's and placing in 5 mL of 1 % PDA solution, with 0.20 M NaCl and sonicating for 3 hours [309, 331]. The suspension was left overnight and the upper layer was used as the PDA-MWCNT solution. The bottom layer was discarded as it contained unbound MWCNT's. The dispersion of MWCNT in positively charged (polycation) PDA is possibly due to weak supramolecular interactions between them, which bind electrostatically to the negatively charged (polyanion) ACOD or ACS at pH 7.4, as the isoelectric point of ACOD is 5.5 and ACS is 6.27 [270, 307, 332].

The C-SPE (model DRP-C110), CoPc SPE (model DRP-410) and SWCNT SPE (model DRP-110SWCNT) were purchased from DropSens (Oviedo, Spain).

The electrodes have a WE diameter of 0.40 cm and an area of 0.13 cm². The reference electrode is silver/silver ion (Ag) and the counter electrode is carbon. The dimensions of the electrodes are 3.40 x 1.00 x 0.05 cm (Length x Width x Height) respectively. These disposable electrodes were used as purchased with no pre-treatment required.

Electrochemical measurements

Electrochemical measurements were run on the Autolabs (PGSTAT101 and PGSTAT302) with NOVA 1.8 as the software package installed. Cyclic Voltammetry (CV) was done using a scan rate of either 5 mV s⁻¹ or 50 mV s⁻¹. The potential range investigated was from -800 mV to 500 mV or to 600 mV. Linear Sweep Voltammetry (LSV) was done using a scan rate of 1 mV s⁻¹. The potential range investigated was from 0 mV to 600 mV. As stated in the previous section all calibration graphs will be at 500 mV. Chronoamperometry (CA) was done at a set potential of 500 mV with a step potential of 0.25 seconds (s) and duration of 1500 s. All CA calibration graphs will be at 500 s.

For EIS measurements a 5 mM 1:1 mixture of K₃[Fe(CN)₆] : K₄[Fe(CN)₆] was used as the redox probe, with the frequency range set between 0.1 – 100 000 Hz, along with 10 mV as the amplitude of alternating voltage. The fixed potential was 0.17 V.

The electrolyte used was 0.1 M phosphate buffer (pH 7.4).

All electrochemical experiments were done at room temperature, in at least duplicates wherever there are error bars. Error bars were worked out based on the average, the positive error was the most positive result minus the average, the negative error was the average minus the most negative result.

Fabrication of (PDA-CNT/ACOD)2 and (PDA/ACOD)2 electrodes

For electrode modification, an O-ring was used to expose just the surface of the WE and hide the reference electrode and counter electrode, to ensure immobilization occurred on the WE only.

To assemble enzyme electrode (PDA-MWCNT/ACOD)₂, 15 μL of PDA-MWCNT solution was dropped onto the WE, after 30 mins of storage in the fridge, the electrode was washed with 10 μL PBS solution (pH 7.4), then 30 μL of ACOD solution was dropped. The electrode was washed with 20 μL PBS solution (pH 7.4). The whole process was repeated once more to make (PDA-MWCNT/ACOD)₂ electrode. Between each addition the electrode was kept in the fridge at 4 °C for 30 minutes. Enzyme loading can be estimated to increase when there are more layers, but the exact amount cannot be worked out, as the electrode was washed with PBS before the next layer.

To assemble enzyme electrode (PDA/ACOD)₂, the same procedure as the (PDA-MWCNT/ACOD)₂ electrode was used, just the PDA-MWCNT solution was replaced with PDA solution. A schematic of this is shown in Figure 4-2 below.

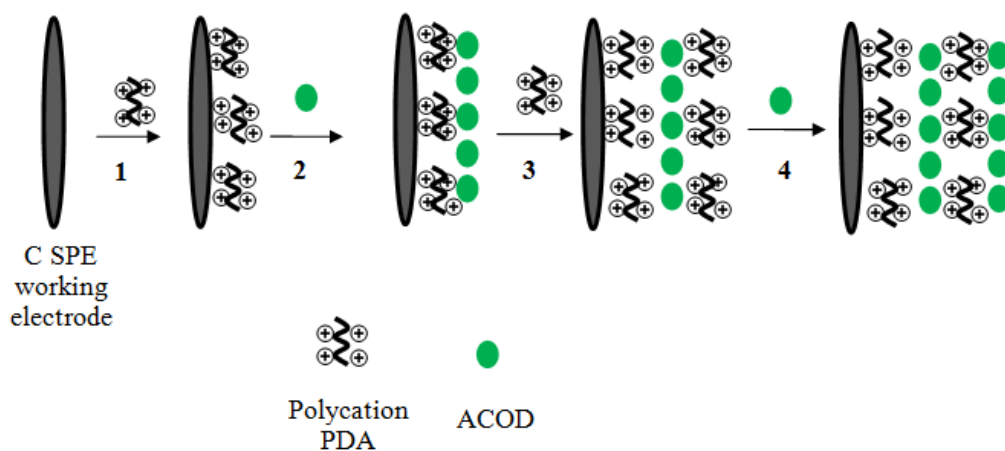


Figure 4-2: Schematic display of the LbL fabrication of (PDA/ACOD)₂ on C-SPE WE.

Fabrication of (PDA-MWCNT/ACOD/PDA-MWCNT/ACS)₁ electrodes

Again for electrode modification, an O-ring was used to expose just the surface of the WE. To assemble enzyme bilayers (PDA-MWCNT/ACOD/PDA-MWCNT/ACS)₁ on the electrodes, 15 μL of PDA-MWCNT solution was dropped onto the WE, then 30 μL of ACOD solution was dropped, then 15 μL of PDA-MWCNT solution and then lastly 30 μL of ACS. A schematic of this fabrication is shown in Figure 4-3. The electrode was washed with PBS solution (pH 7.4) between each dropping and the excess solution was removed as it was not properly bound to the

surface of the electrode. Between each addition the electrode was kept in the fridge at 4 °C for 30 minutes. The whole process was repeated another 3 times to make (PDA-MWCNT/ACOD/PDA-MWCNT/ACS)₄ electrode for the EIS measurements.

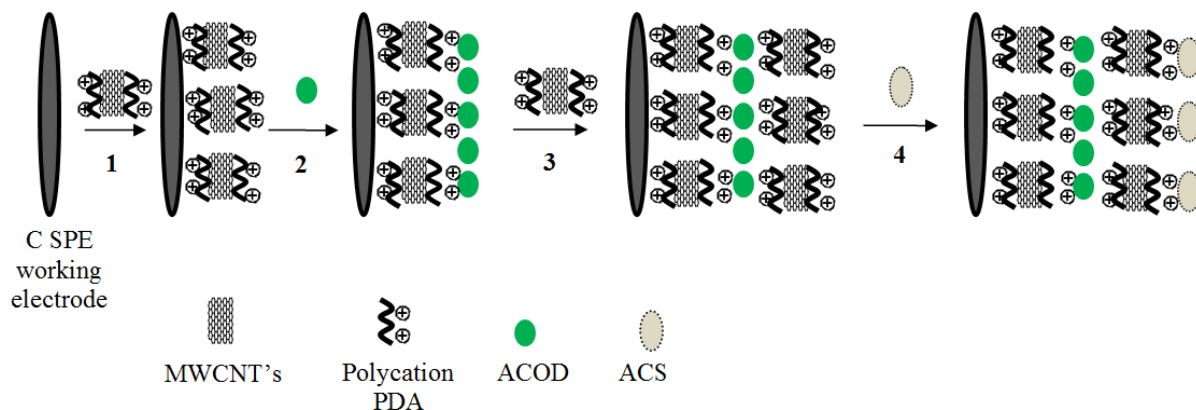


Figure 4-3: Schematic display of the LbL fabrication of (PDA-MWCNT/ACOD/PDA-MWCNT/ACS)₁ on C-SPE WE.

To assemble enzyme bilayers on the electrodes (PDA-MWCNT/ACS/PDA-MWCNT/ACOD)₁, the same procedure as above was repeated but with the enzyme order switched. This was done to optimise the enzyme electrode and to work out which configuration would give the best result in terms of sensitivity and current.

To assemble 1 single enzyme layer on the electrodes (PDA-MWCNT/ACOD+ACS)₁, 15 μL of PDA-MWCNT solution was dropped onto the WE, then 30 μL of ACS solution and 30 μL of ACOD solution was dropped together. Again the electrode was washed with PBS solution (pH 7.4) between each dropping. Between the two additions the electrode was kept in the fridge at 4 °C for 30 minutes immersing time. This electrode was tested for the same reasons as the (PDA-MWCNT/ACS/PDA-MWCNT/ACOD)₁ electrode and had an additional advantage of taking 1 hour less to fabricate.

For the (PDA/ACOD/PDA/ACS)₁ electrode, the same procedure as (PDA-MWCNT/ACOD/PDA-MWCNT/ACS)₁ was used but the PDA-MWCNT solution was replaced with PDA solution. This electrode was fabricated to test whether there are any additional benefits of incorporating MWCNT in this work and if not this would save money in the cost of fabrication.

4.2 Enzyme fabricated electrodes for PA-CoA/OA-CoA detection

Figure 4-4 shows the LSV at the C-SPE electrode modified with (PDA-MWCNT/ACOD)₂ film with different concentrations of OA-CoA (up to 1.50 mM). The current increased with increasing concentrations of OA-CoA. A calibration graph obtained at 500 mV exhibited a linear correlation ($R^2 = 0.98$) between the OA-CoA concentration (up to 0.75 mM) and the oxidation current, which is from the H₂O₂ produced by OA-CoA oxidation by ACOD and oxygen. This is in agreement with the solution study in section 3.3. It indicates that the activity of ACOD was retained within the PDA-MWCNT multilayer, and the enzyme electrode can be used to determine OA-CoA concentrations.

However the concentration range and the sensitivity here are much lower when compared to that of the work in solution. This could be due to the reduced volume/concentration of ACOD immobilised on the surface of the electrode compared to that which was present in solution. The same fabricated electrode was used for all the 8 concentrations investigated, over time ACOD was being used and could be lost to the solution and not be bound on the surface of the electrode.

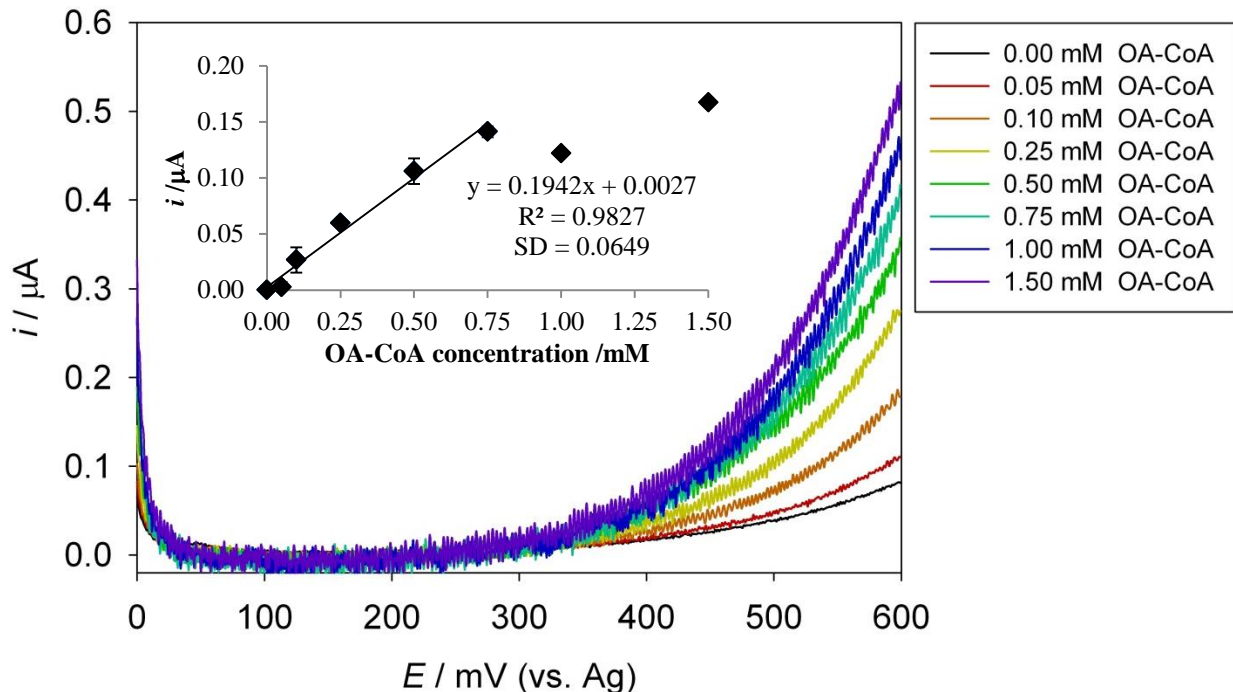


Figure 4-4: LSV for various concentrations of OA-CoA measured at a C-SPE modified with (PDA-MWCNT/ACOD)₂ in 0.1 M phosphate buffer pH 7.4, scan rate 1 mV s⁻¹. Inset: calibration graph at $E = 500 \text{ mV}$.

A slope of 0.42 was obtained at a potential of 500 mV from the plot of $\log j$ against $\log [\text{OA-CoA}]$ in Figure 4-5. Indicating that it's a second order rate of reaction. The R^2 was between ~ 0.88 and 0.99 for all the potentials in the graph.

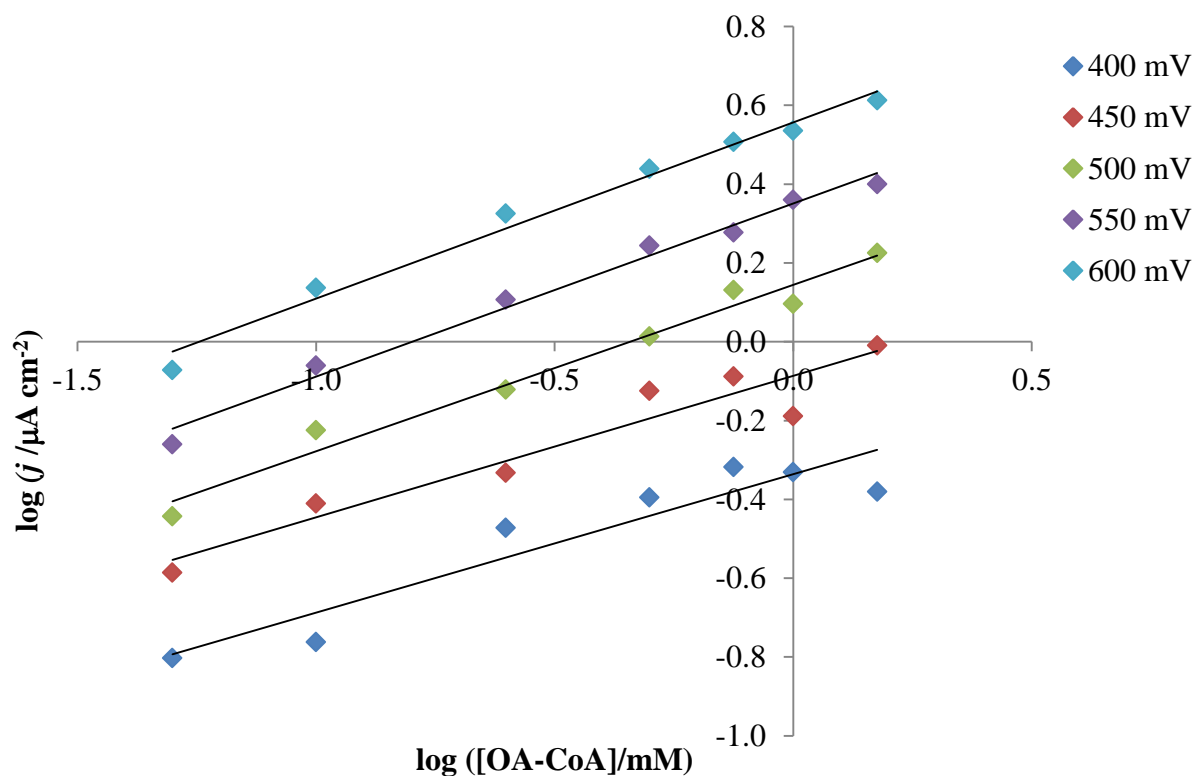


Figure 4-5: The relationship between $\log j$ and $\log \text{OA-CoA}$ concentration on the (PDA-MWCNT/ACOD)₂ electrode at various electrode potentials in 0.1 M phosphate buffer pH 7.4.

Parallel to Figure 4-4, linear sweep voltammetry were carried out in 0.1 M PBS with various PA-CoA concentrations, shown in Figure 4-6. The oxidation currents for potentials above 400 mV exhibited a linear increase as the PA-CoA concentration increased. A calibration curve obtained at 500 mV exhibited a linear range ($R^2 = 0.99$) in the same concentration range of PA-CoA (inset Figure 4-6).

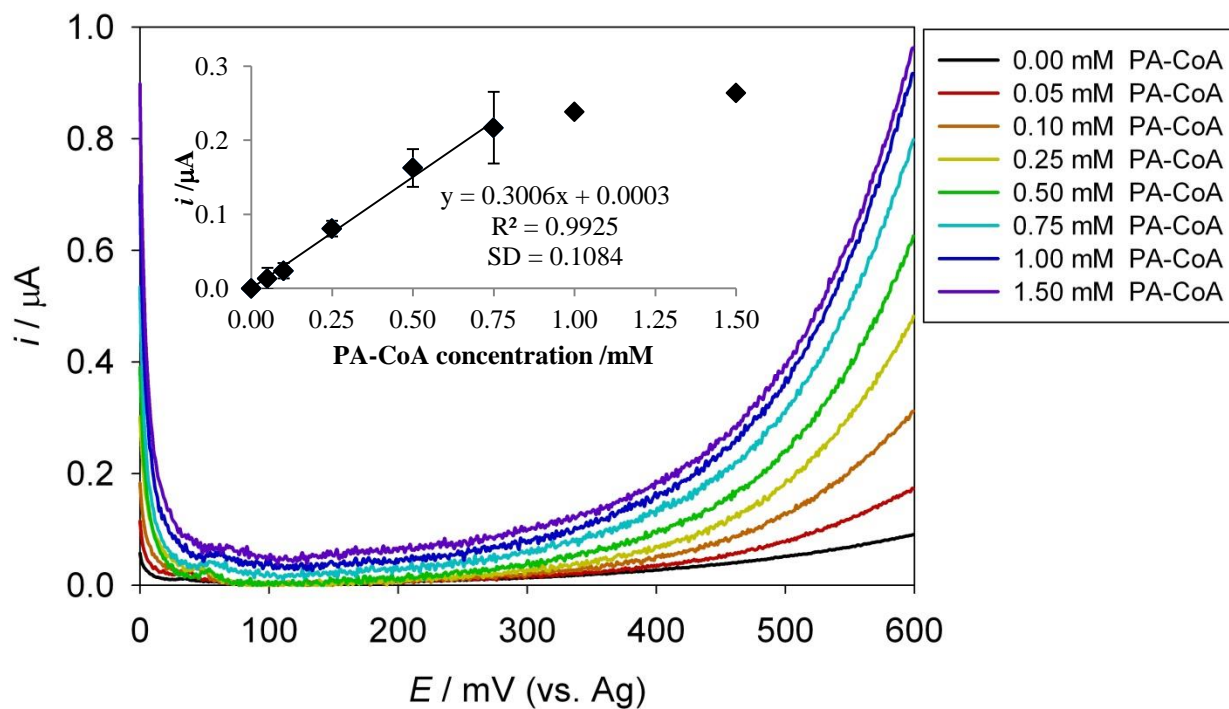


Figure 4-6: LSV for various concentrations of PA-CoA measured at a C-SPE modified with (PDA-MWCNT/ACOD)₂ in 0.1 M phosphate buffer pH 7.4, scan rate 1 mV s^{-1} . Inset: calibration graph at $E = 500 \text{ mV}$.

Slopes of ~ 0.5 were obtained at all the potentials investigated from the plot of $\log j$ against $\log [\text{PA-CoA}]$ in Figure 4-7. Indicating a reaction order of 0.5 with respect to PA-CoA. Same as that with OA-CoA. The R^2 value was between ~ 0.98 and 0.99 for all the potentials in the graph.

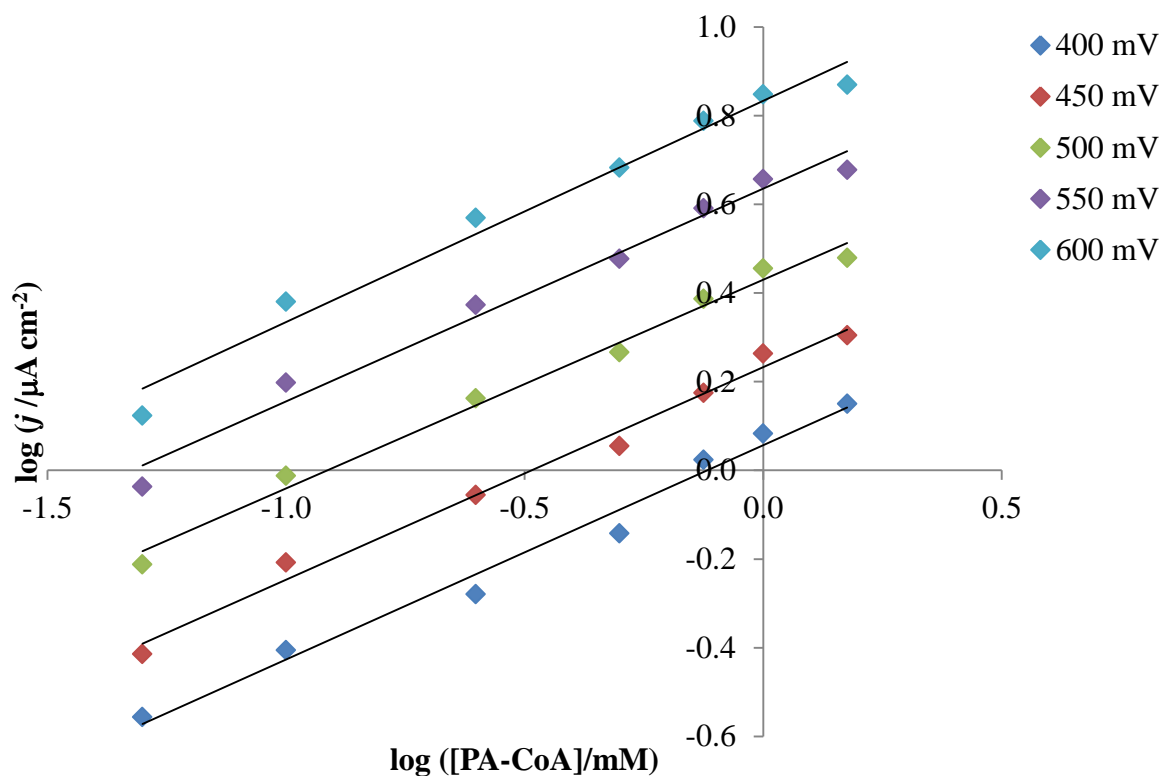


Figure 4-7: The relationship between $\log j$ and \log PA-CoA concentration on the (PDA-MWCNT/ACOD)₂ electrode at various electrode potentials in 0.1 M phosphate buffer pH 7.4.

The enzyme electrode (PDA-MWCNT/ACOD)₂ is selective for OA-CoA and PA-CoA detection individually. Figure 4-8 shows the current difference between the two different acylated NEFAs. The current obtained from PA-CoA was predominantly higher than that from OA-CoA, PA-CoA is from a saturated NEFA, this may have a better interaction with the enzyme electrode compared to the unsaturated OA-CoA. This difference in current production is higher than the current difference which was produced from the two acylated NEFAs in the solution work, indicating that immobilisation of ACOD results in even more selectivity. Another reason for this difference is, as more concentrations were run using the same immobilised electrode, more ACOD was being used and lost into solution rather than being retained on the surface of the WE, resulting in having less ACOD than there was to begin with in the subsequent concentrations. A better comparison would be to run each concentration on a freshly fabricated electrode, but this would use up resources.

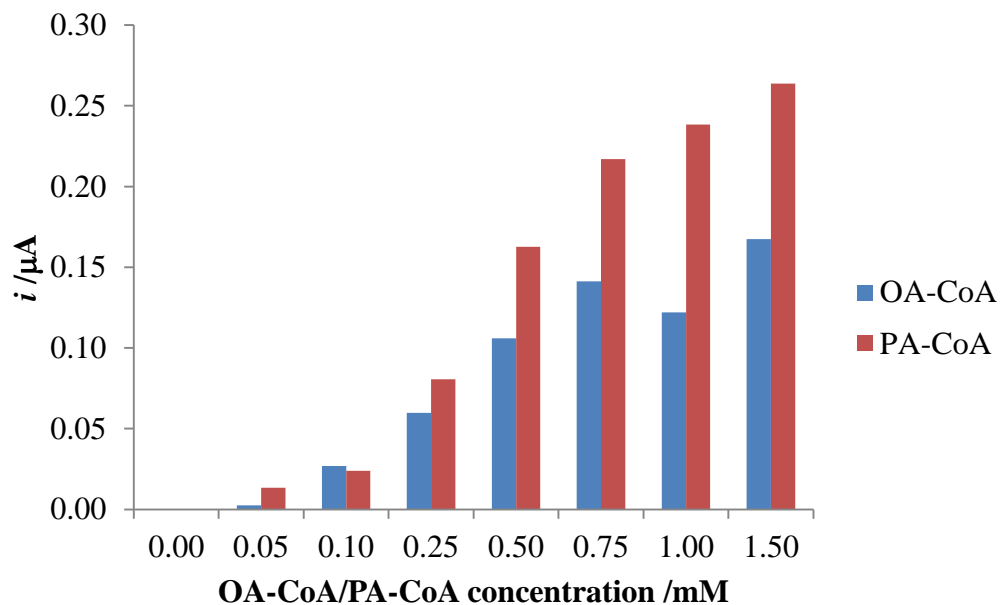


Figure 4-8: Bar chart comparing the current produced from the two different acylated NEFAs on (PDA-MWCNT/ACOD)₂ electrode. LSV at 1 mV s^{-1} , current taken at 500 mV .

The enzyme electrode (PDA-MWCNT/ACOD)₂ was fabricated to test whether the feasibility of immobilizing ACOD onto the WE of the C-SPE was possible. The next thing to consider would be to test whether having both ACOD and ACS immobilised on a C-SPE is possible. Then NEFA could be tested in one step, rather than relying on individual steps/reactions. A sensor is needed for the detection of NEFA and not for the detection of acylated NEFA, which is what the current (PDA-MWCNT/ACOD)₂ electrode does.

4.3 Enzyme fabricated electrodes for OA detection

4.3.1 Determination of OA using (PDA-MWCNT/ACOD/PDA-MWCNT/ACS) fabricated electrode

Both the enzymes ACOD and ACS were immobilized with PDA-MWCNT using the method described in Figure 4-3. The LSVs from various OA concentrations on C-SPE fabricated with (PDA-MWCNT/ACOD/PDA-MWCNT/ACS)¹ are shown in Figure 4-9. The calibration graph of this electrode (Figure 4-10) at 500 mV showed a good linear correlation between the different OA concentrations and the subsequent oxidation currents obtained, indicating a promising method for determining NEFA with one operating step. The average sensitivity of the data from Figure 4-9 was 1.7222 $\mu\text{A}/\text{mM}$ and the linear detection range was 0.10 – 0.90 mM OA.

The peak around 350 mV is due to the ACS enzyme used from the commercial Wako NEFA kit as it is not present in blank PBS only when the electrode is not fabricated. Confirmation of this is given in Figure 4-12. CV showed that this was not a redox peak. Wako solution A contains: 0.53 U/mL ACS (*Pseudomonas* sp.), 0.31 mM Coenzyme A (CoA, Candida), 4.30 mM ATP (*Bacterium* sp.), 1.50 mM 4-aminoantipyrine, 2.60 U/mL ascorbate oxidase (pumpkin), 0.062% sodium azide and 50 mM phosphate buffer, pH 7.0 [143]. The nature of the peak maybe due to any one of these compounds, as electrochemistry is a very sensitive technique, one of these compounds is being oxidised irreversibly at around 350 mV. By a process of elimination, buying each listed ingredient of Wako solution A individually and testing it via LSV on a C-SPE would help work out which compound this peak was originating from.

Figure 4-11 shows the plot of $\log j$ against $\log [\text{OA}]$. Indicating a reaction order of ~ 0.5 with respect to OA. The R^2 value was ~ 0.98 for all the potentials in the graph.

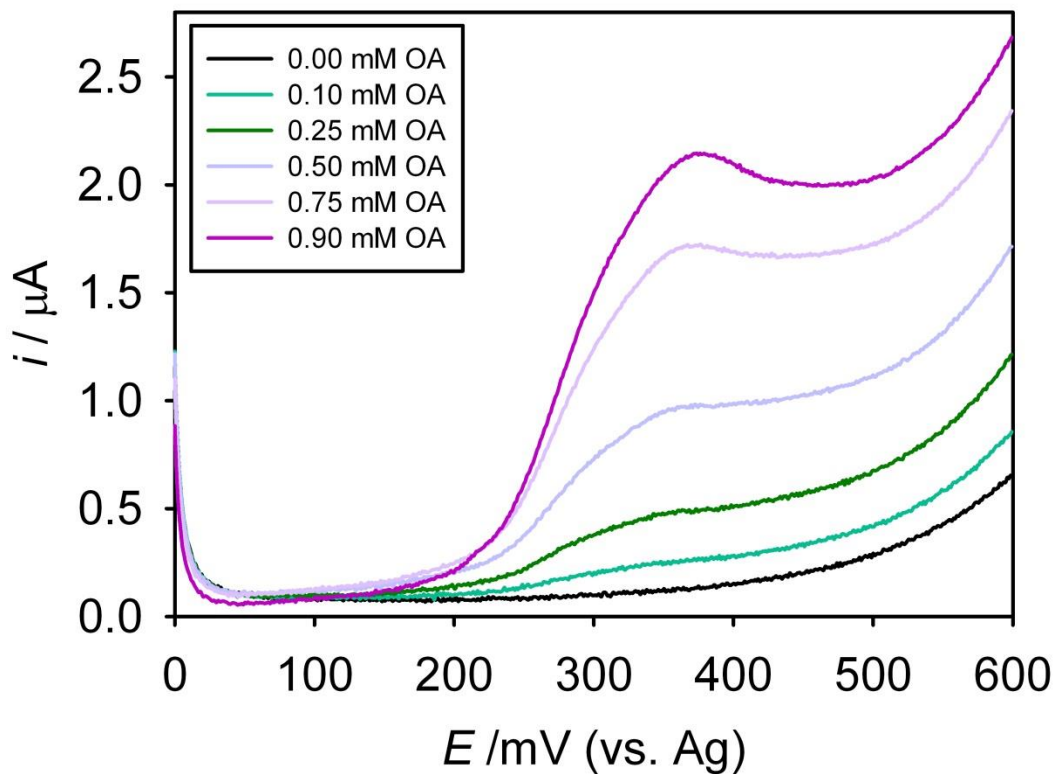


Figure 4-9: LSV of various concentrations of OA measured at a C-SPE modified with (PDA-MWCNT/ACOD/PDA-MWCNT/ACS)1 in 0.1 M phosphate buffer pH 7.4 and 1 mM ATP and CoA, scan rate 1 mV s⁻¹.

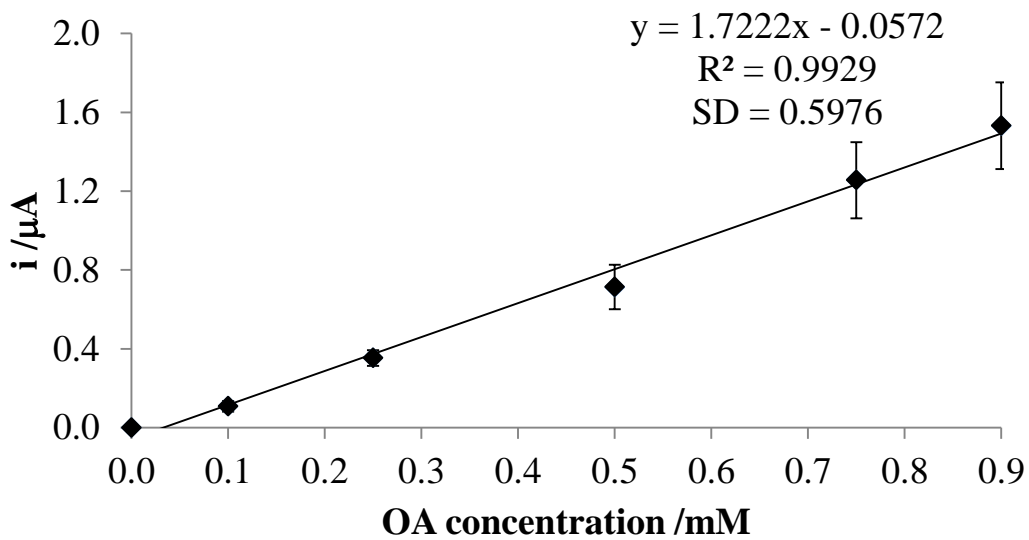


Figure 4-10: Calibration graph at 500 mV.

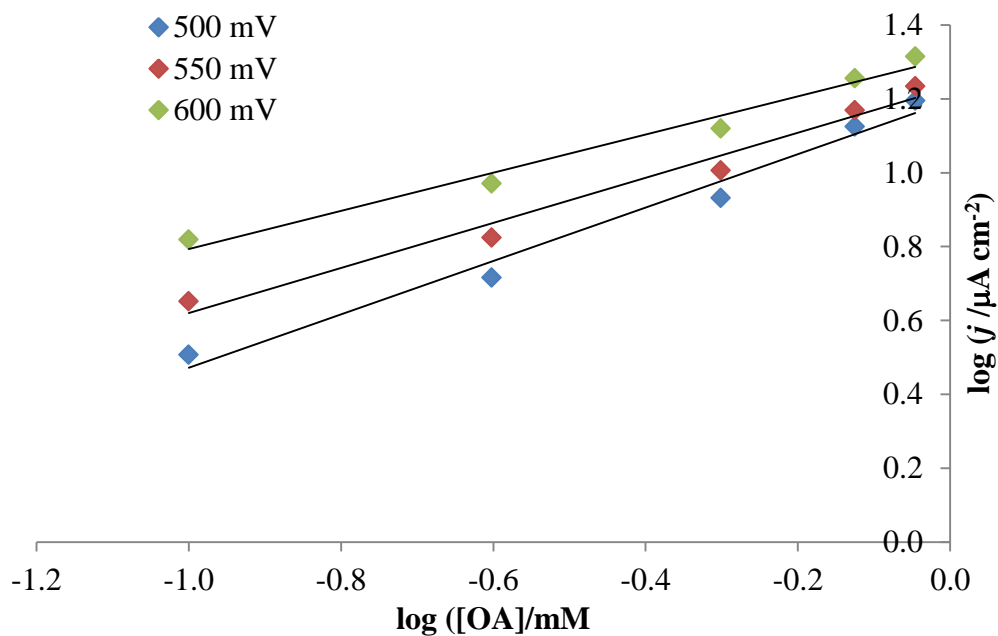


Figure 4-11: The relationship between $\log j$ and \log OA concentration on the (PDA-MWCNT/ACOD/PDA-MWCNT/ACS)1 electrode at various electrode potentials in 0.1 M phosphate buffer pH 7.4.

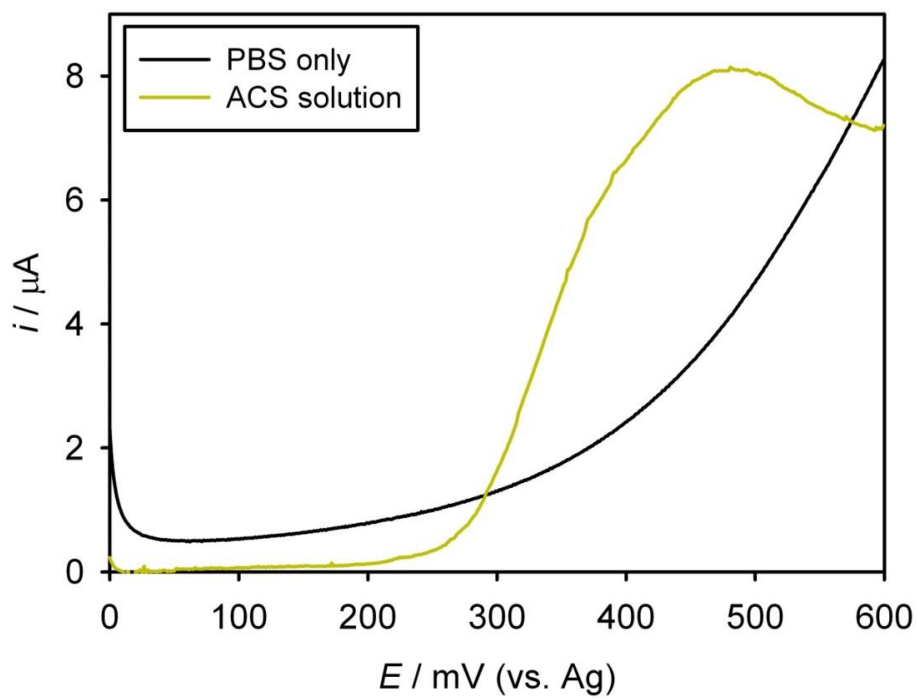


Figure 4-12: LSV at 1 mV s^{-1} on C-SPE with $100 \text{ }\mu\text{L}$ PBS only and with $100 \text{ }\mu\text{L}$ of ACS solution A from Wako kit.

Figure 4-9 consisted of around 1:1:1 molar ratio of OA:CoA:ATP, respectively. Although the maximum concentration of OA detected was 0.90 mM, so CoA and ATP were still 0.10 mM in excess. Validation of this enzyme electrode could be tested by LSV detection of different OA concentrations on a newly fabricated enzyme electrode and the current obtained by those electrodes plotted on a calibration graph of Figure 4-10. This addition has been shown in Figure 4-13. Two other OA concentrations (shown in green) were measured on a different electrode and plotted on the same graph. The error bars are due to repeats done on other immobilised electrodes (each concentration has been tested in twice on different electrodes – in total 4 electrodes used for this graph – 2 for the measurements in green and 2 for those in black). The results shown in green fitted well on the calibration graph, validating the electrode as a means of interpreting unknown OA concentrations.

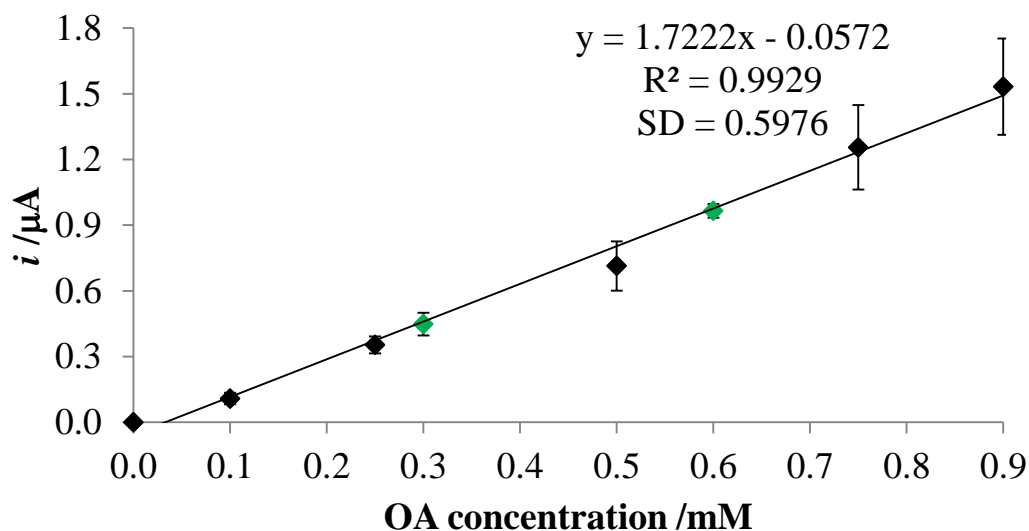


Figure 4-13: Calibration graph obtained by electrochemical measurement of various concentrations of OA at $E = 500$ mV (as shown in Figure 4-9). 0.30 mM and 0.60 mM were measured independently on a different electrode (shown in green).

The CA at 500 mV of this bienzyme fabricated electrode is shown in Figure 4-14, with the calibration graph having R^2 of 0.99 (Figure 4-15). Linear current responses were obtained in both the LSV and CA for OA detection parallel to the work in solution. This is the platform for the further detection of NEFA on immobilized electrodes. Both these electrochemical detection techniques are reproducible, with a R^2 of ~0.99.

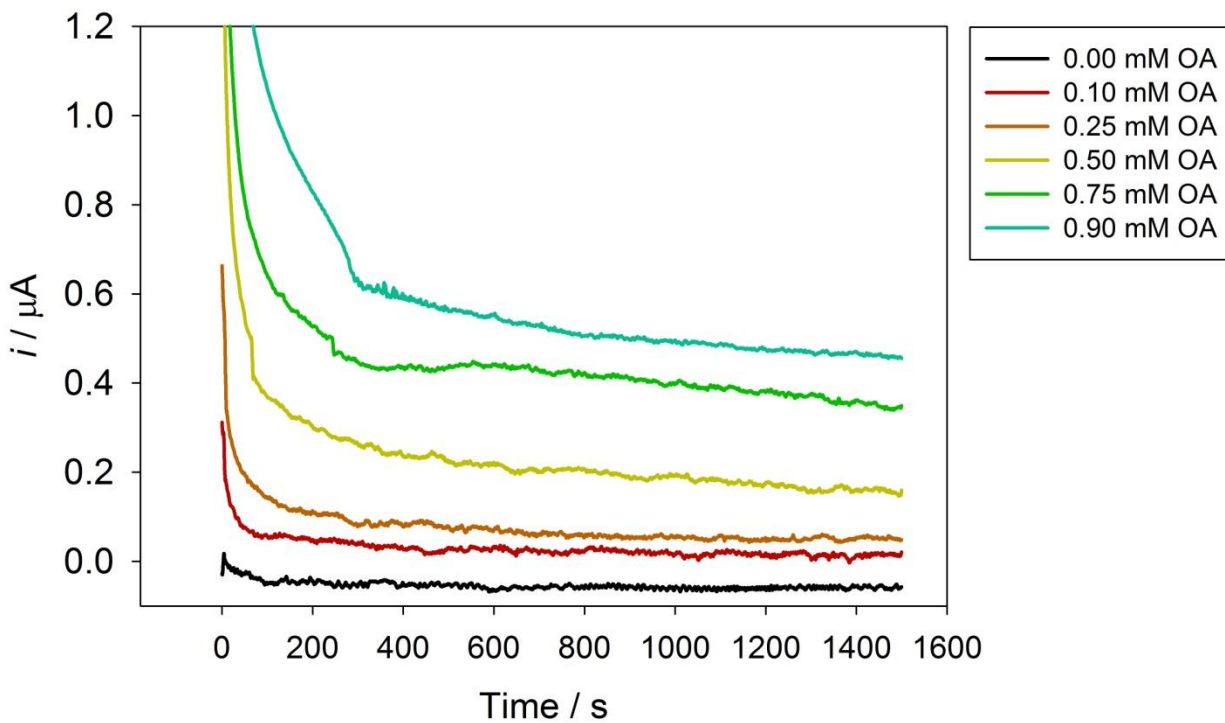


Figure 4-14: CA at 500 mV for various concentrations of OA measured at a C-SPE modified with (PDA-MWCNT/ACOD/PDA-MWCNT/ACS)1, in 0.1 M phosphate buffer pH 7.4 with 1 mM ATP and CoA.

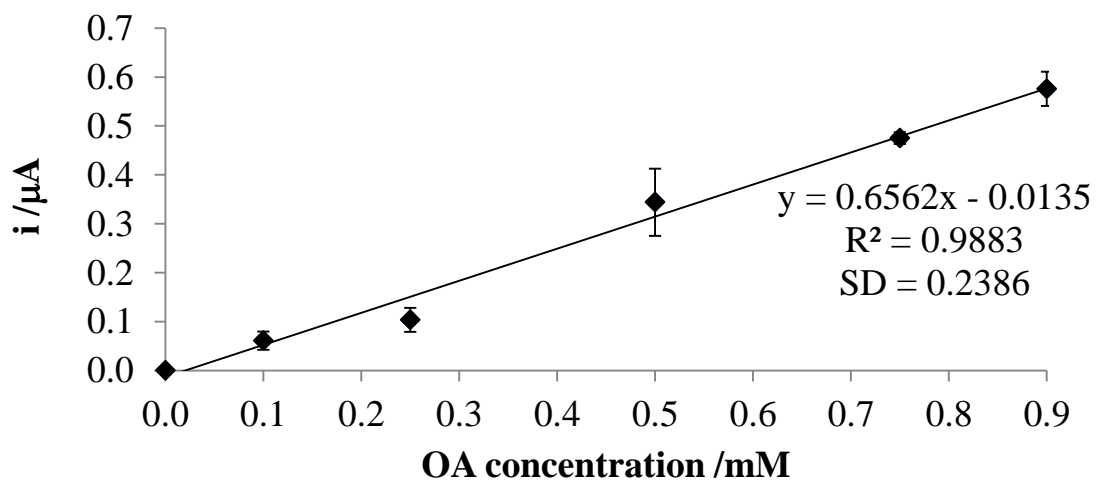


Figure 4-15: Calibration at 500 s.

To confirm that the enzymatic reaction needs all the substrates to work, several concentrations of OA were tested chronoamperometrically at 500 mV without 1 mM ATP and CoA. The bar chart in Figure 4-16 shows the current comparison at 500 s. This confirms that ATP and CoA are needed for the enzymatic reaction to take place and produce H₂O₂. The slight increase in current for 0.50 mM OA maybe due to the slight production of H₂O₂, as the Wako ACS solution which was used to immobilise the electrode contained a small amount of CoA and ATP. However this current was not as much as that produced with 1 mM ATP and CoA.

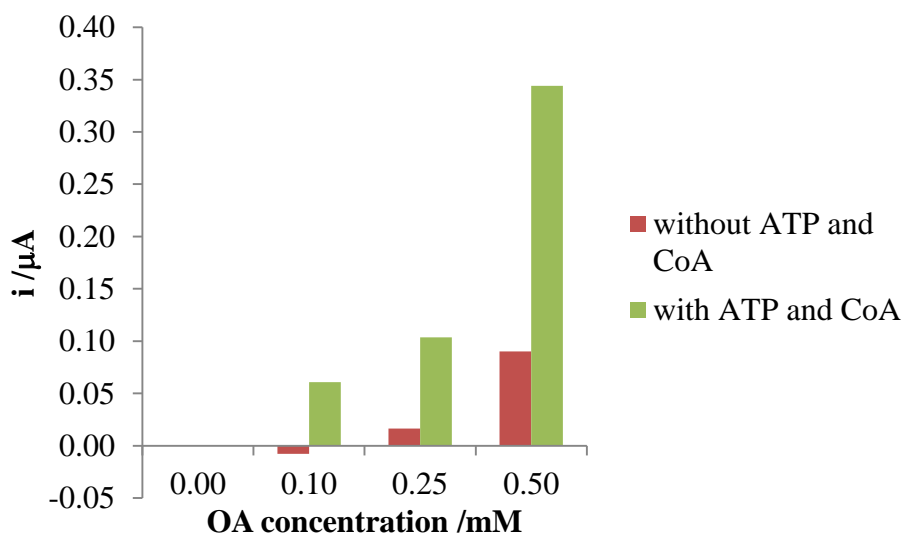


Figure 4-16: Current comparison with and without ATP and CoA on (PDA-MWCNT/ACOD/PDA-MWCNT/ACS)1 electrode, CA at 500 mV, current taken at 500 s.

Following from the fabrication of this electrode, other similar bienzyme electrodes were also fabricated. The electrode with (PDA-MWCNT/ACS/PDA-MWCNT/ACOD)1 fabrication showed linear correlation with H₂O₂ oxidation too as shown in Figure 4-17. The calibration graph is shown in Figure 4-18. However on this electrode the lower limit of detection dropped to 0.25 mM OA from 0.10 mM OA (0.00 mM and 0.10 mM were coeluted). Figure 4-19 shows the CA at 500 mV of (PDA-MWCNT/ACOD+ACS)1 fabricated electrode. This electrode contained less PDA-MWCNT yet still maintained good linearity with varying OA concentrations. The calibration graph (Figure 4-20) gave a R² value of ~0.98, almost the same as that of Figure 4-18.

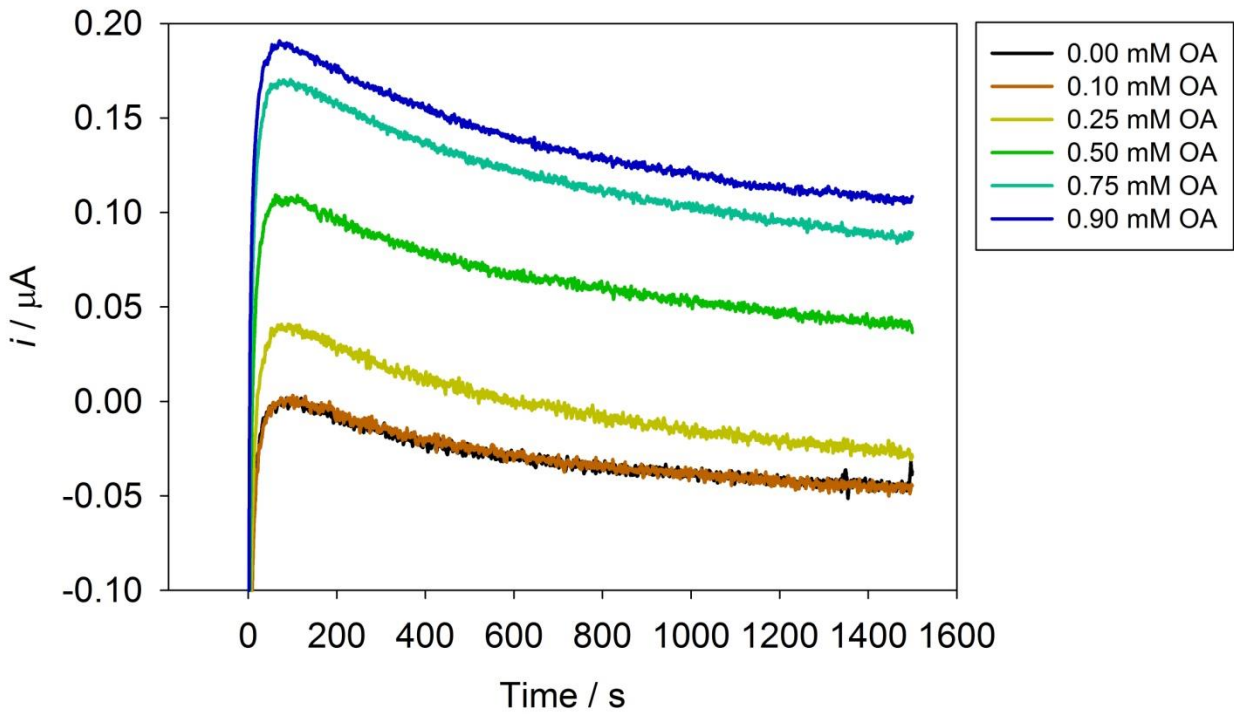


Figure 4-17: CA at 500 mV for various concentrations of OA measured at a C-SPE modified with (PDA-MWCNT/ACS/PDA-MWCNT/ACOD)1 in 0.1 M phosphate buffer pH 7.4 with 1 mM ATP and CoA.

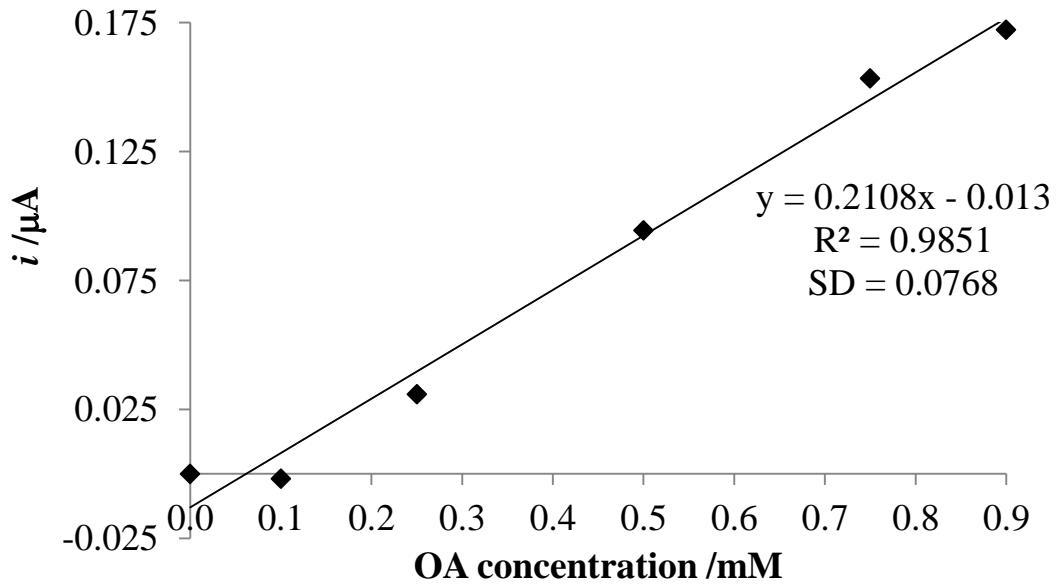


Figure 4-18: Calibration graph at 500 s.

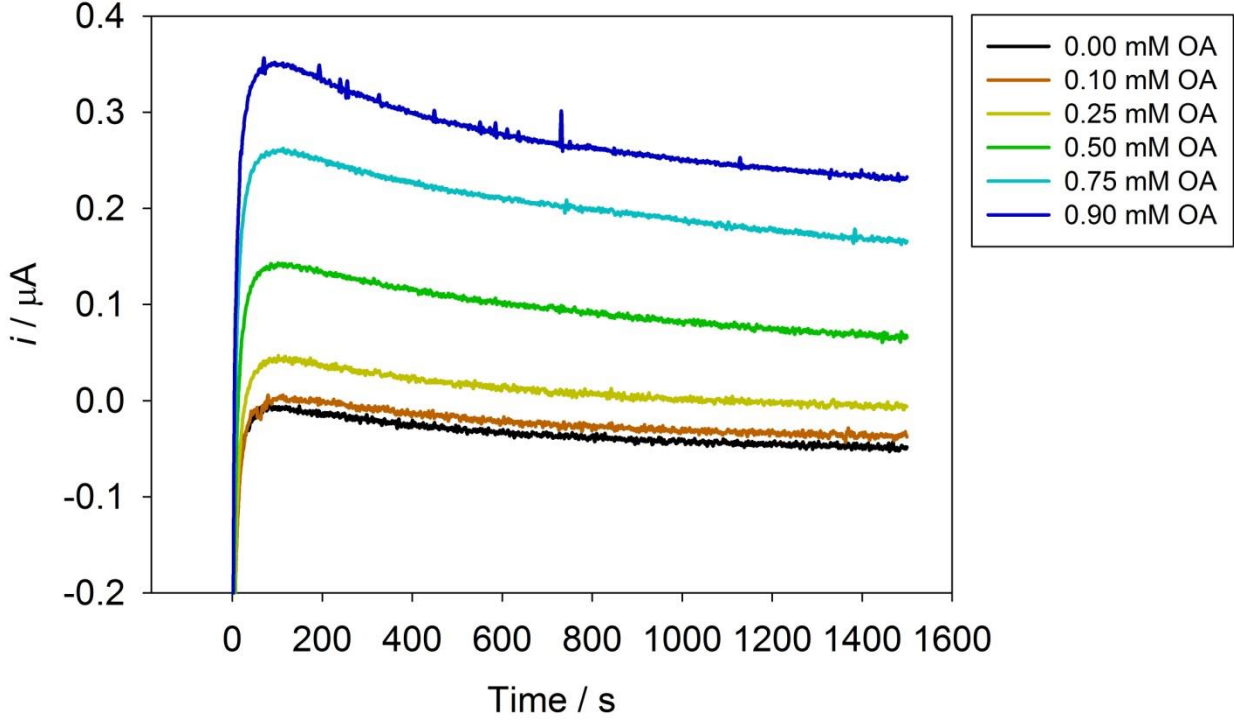


Figure 4-19: CA at 500 mV for various concentrations of OA measured at a C-SPE modified with (PDA-MWCNT/ACOD+ACS)1 in 0.1 M phosphate buffer pH 7.4 with 1 mM ATP and CoA.

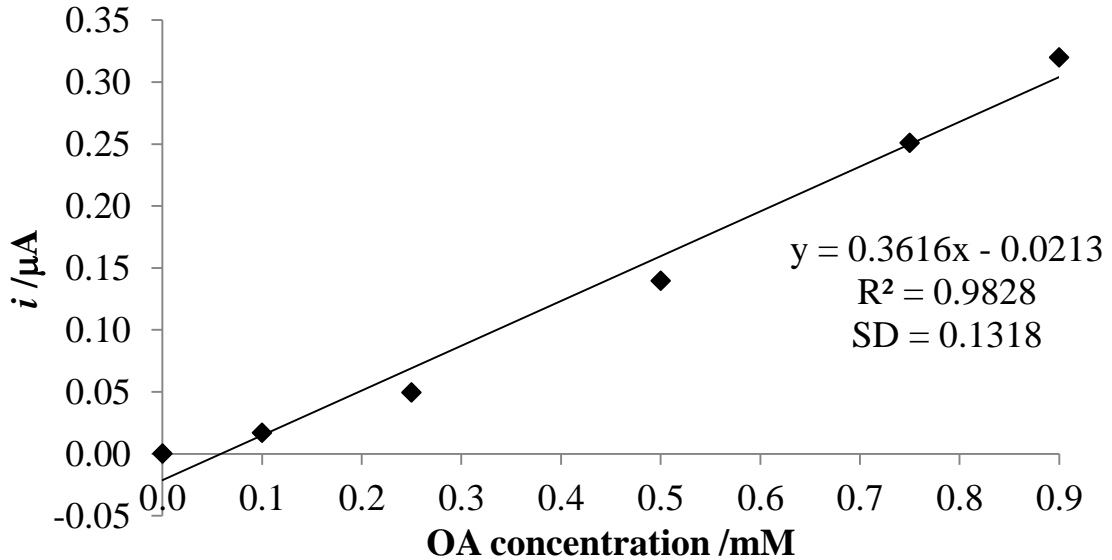


Figure 4-20: Calibration graph at 500 s.

Table 4-2 shows the comparison of the 3 different fabricated electrodes, the current produced from 0.90 mM OA is given as an example from each fabricated electrode. The electrode consisting of (PDA-MWCNT/ACOD/PDA-MWCNT/ACS) has the highest current produced for OA detection. This might be due to the fabrication being in the order of enzymatic reaction (ACS for acylation before ACOD for oxidation). This electrode also had the highest sensitivity and R^2 value.

Having both the enzymes mixed together (PDA-MWCNT/ACOD+ACS)1 had the second highest current produced. The PDA polymer was able to retain both enzymes on the surface of the electrode. For the fabrication of this electrode, both enzymes would be attracted to the positively charged polymer and would compete for the same area. Both enzymes have different isoelectric points, at pH 7.4, more ACOD would be attached to the polymer than ACS because it has a lower isoelectric point. The proportion of ACOD and ACS may not be equal on this electrode, which might be why this electrode had lower current and sensitivity when compared to (PDA-MWCNT/ACOD/PDA-MWCNT/ACS) electrode.

The (PDA-MWCNT/ACS/PDA-MWCNT/ACOD) electrode had the lowest sensitivity to OA detection, lowest current for 0.90 mM OA and the narrowest linear detection range (from 0.25 – 0.90 mM). Putting all this information together highlights the (PDA-MWCNT/ACOD/PDA-MWCNT/ACS) electrode as the one to take forward for NEFA sensor development. Although the layers of immobilized polymer and enzyme are very thin (1-2 nm) on the surface of the electrode, this configuration was favoured, this could be due to the thickness of layers and orientation of enzyme order favouring the reaction with OA [331].

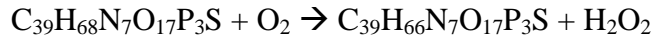
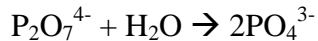
Table 4-2: Comparison of CA at 500 mV at 500 s for OA on 3 different fabricated electrodes.

Electrode fabrication	Sensitivity ($\mu\text{A}/\text{mM}$)	R^2 value	Linear detection range (mM)	Current for 0.90 mM OA (μA)
(PDA-MWCNT/ACOD/PDA-MWCNT/ACS)	0.6562	0.9883	0.10 – 0.90	0.5756
(PDA-MWCNT/ACS/PDA-MWCNT/ACOD)	0.2108	0.9851	0.25 – 0.90	0.1723
(PDA-MWCNT/ACOD+ACS)	0.3616	0.9828	0.10 – 0.90	0.3198

4.3.2 Comparison of different SPE's performance using molar ratios

As the detection of NEFA is based on an enzymatic reaction the effect of molar ratios were investigated. 1:2:2 molar ratio of OA:CoA:ATP was explored for C-SPE, CoPc SPE and SWCNT SPE. Both LSV and CA were carried out for this molar ratio. Using LSV the validation of 2 different concentrations (0.30 mM and 0.60 mM OA) on a different electrode were also independently tested.

The fully balanced molar reactions are shown below:



For the reaction to occur the molar ratio of OA: CoA: ATP should be 1:1:1. Theoretically to have a higher chance of reaction the OA: CoA: ATP molar ratio should be 1:2:2 (excess substrates increase likelihood of reaction). Table 4-3 and Table 4-4 show the comparison of the current produced at the different molar ratios on fabrication of (PDA-MWCNT/ACOD/PDA-MWCNT/ACS)1 bienzyme electrode on the 3 different electrodes investigated, along with each electrodes sensitivity and correlation coefficient determination (R^2). The 0.75 mM OA current values in the tables are averaged from two repeats. C-SPE produced the highest current in both the molar ratios. This would be the best electrode moving forward with the sensor, followed by the SWCNT SPE then the CoPc SPE. The CA showed almost 3 times higher current when switching the CoA and ATP to 2 mM for C-SPE. However as the maximum concentration that

can be detected when using 2 mM CoA and ATP is 0.75 mM OA, the 1:1:1 molar ratio is sufficient for good, reproducible NEFA detection electrochemically.

The highest sensitivity was given by the C-SPE in both the CA and LSV data, this was followed by the SWCNT SPE and then by the CoPc SPE. The highest R^2 value for the 1:1:1 molar ratio was for the C-SPE. The C-SPE showed the best data for the development of the NEFA sensor.

Table 4-3: Comparison of 3 different electrodes for CA at 500 mV at 500 s, current for 0.75 mM OA.

	C-SPE		CoPc SPE		SWCNT SPE	
	1:1:1	1:2:2	1:1:1	1:2:2	1:1:1	1:2:2
Molar ratio	1:1:1	1:2:2	1:1:1	1:2:2	1:1:1	1:2:2
Current (μ A)	0.4751	1.5514	0.2956	0.6527	0.4035	0.7588
Sensitivity (μ A/mM)	0.6562	2.0296	0.3372	0.9653	0.5380	1.0120
R^2	0.9883	0.9884	0.8675	0.9194	0.9869	0.9934
SD	0.2386	0.6095	0.1309	0.2965	0.3122	0.2987
Detection range (mM)	0.10 – 0.90	0.05 – 0.75	0.25 – 0.75	0.25 – 0.75	0.10 – 0.75	0.00 – 0.75

Table 4-4: Comparison of 3 different electrodes for LSV at 1 mV s^{-1} at 500 mV, current for 0.75 mM OA.

	C-SPE		CoPc SPE		SWCNT SPE	
	1:1:1	1:2:2	1:1:1	1:2:2	1:1:1	1:2:2
Molar ratio	1:1:1	1:2:2	1:1:1	1:2:2	1:1:1	1:2:2
Current (μ A)	1.2553	2.0726	0.8037	1.1171	0.7724	1.6919
Sensitivity (μ A/mM)	1.7222	2.6139	1.1929	1.5097	1.1404	2.2810
R^2	0.9929	0.9860	0.9795	0.9891	0.9745	0.9947
SD	0.5976	0.7680	0.4357	0.4471	0.3843	0.6873
Detection range (mM)	0.10 – 0.90	0.00 – 0.75	0.10 – 0.90	0.05 – 0.75	0.00 – 0.90	0.05 – 0.75

Each experiment was done in at least duplicates; the current shown in the tables is the average of 2 readings. Each electrode was also validated with 0.30 mM and 0.60 mM OA as shown in green on the calibration graphs below (Figure 4-21 and Figure 4-22). This shows all the electrodes have reproducibility. Validation was done in the same way as that described for Figure 4-13, in total 4 electrodes were used for each graph - 2 for the measurements shown in green and 2 for the measurements shown in black.

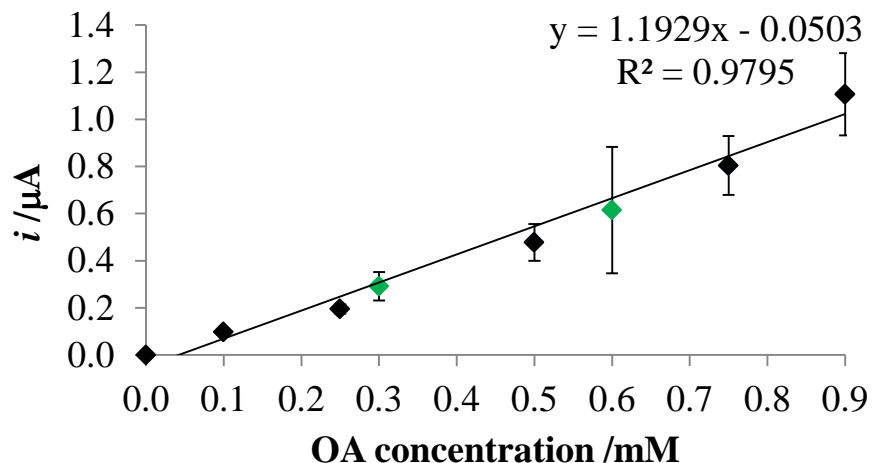


Figure 4-21: Calibration graph obtained by LSV of various concentrations of OA on a CoPc-SPE modified with (PDA-MWCNT/ACOD/PDA-MWCNT/ACS)1 in 0.1 M phosphate buffer pH 7.4 and 1 mM ATP and CoA, scan rate 1 mV s^{-1} .

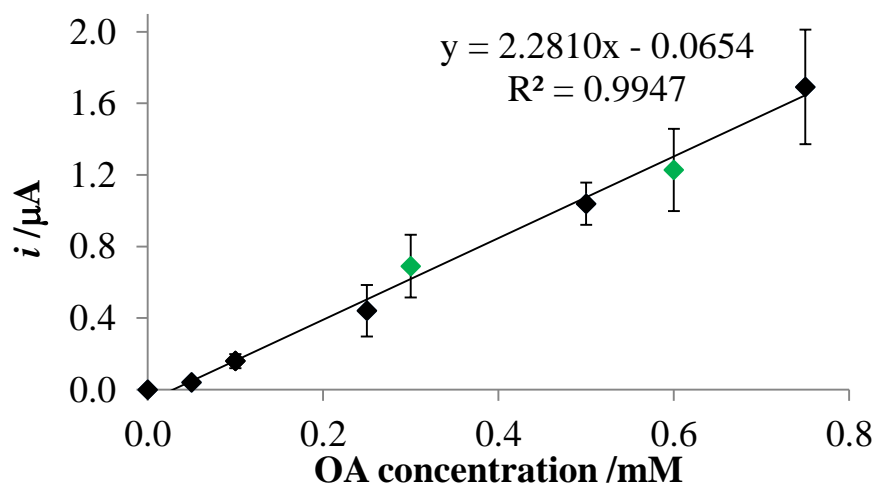


Figure 4-22: Calibration graph obtained by LSV of various concentrations of OA on a SWCNT SPE modified with (PDA-MWCNT/ACOD/PDA-MWCNT/ACS)1 in 0.1 M phosphate buffer pH 7.4 and 2 mM ATP and CoA, scan rate 1 mV s^{-1} .

4.3.3 Multiple Layer comparison of (PDA-MWCNT/ACOD/PDA-MWCNT/ACS) electrode

CA of (PDA-MWCNT/ACOD/PDA-MWCNT/ACS)1 and (PDA-MWCNT/ACOD/PDA-MWCNT/ACS)4 electrodes were spiked with 0.25 mM OA (shown in Figure 4-23). The set potential was 500 mV for each electrode. 125 μ L of 1 mM Wako OA standard solution was added to phosphate buffer solution containing 1 mM CoA and ATP at \sim 500 s, making the result of OA concentration at 0.25 mM. There was no time delay observed from both electrodes. Once OA was spiked, an instant current increase was obtained. This implies that the immobilization method produced fine thickness of polymer-bienzyme layers. These layers did not affect the mass transport of reactants cascading down the layers to fulfil two-step enzymatic reactions in sequence. The thickness of each layer has previously found to be 1-2 nm [331].

The higher the amount of bienzyme layers, the higher the current produced, as the amount of enzymes (ACS and ACOD) were quadrupled in (PDA-MWCNT/ACOD/PDA-MWCNT/ACS)4 compared to (PDA-MWCNT/ACOD/PDA-MWCNT/ACS)1. One unit of ACOD enzyme activity is defined as the amount of the enzyme which produces 1 μ mol H₂O₂ per min [270]. So naturally using less enzyme results in having less H₂O₂ production in (PDA-MWCNT/ACOD/PDA-MWCNT/ACS)1 when compared to (PDA-MWCNT/ACOD/PDA-MWCNT/ACS)4.

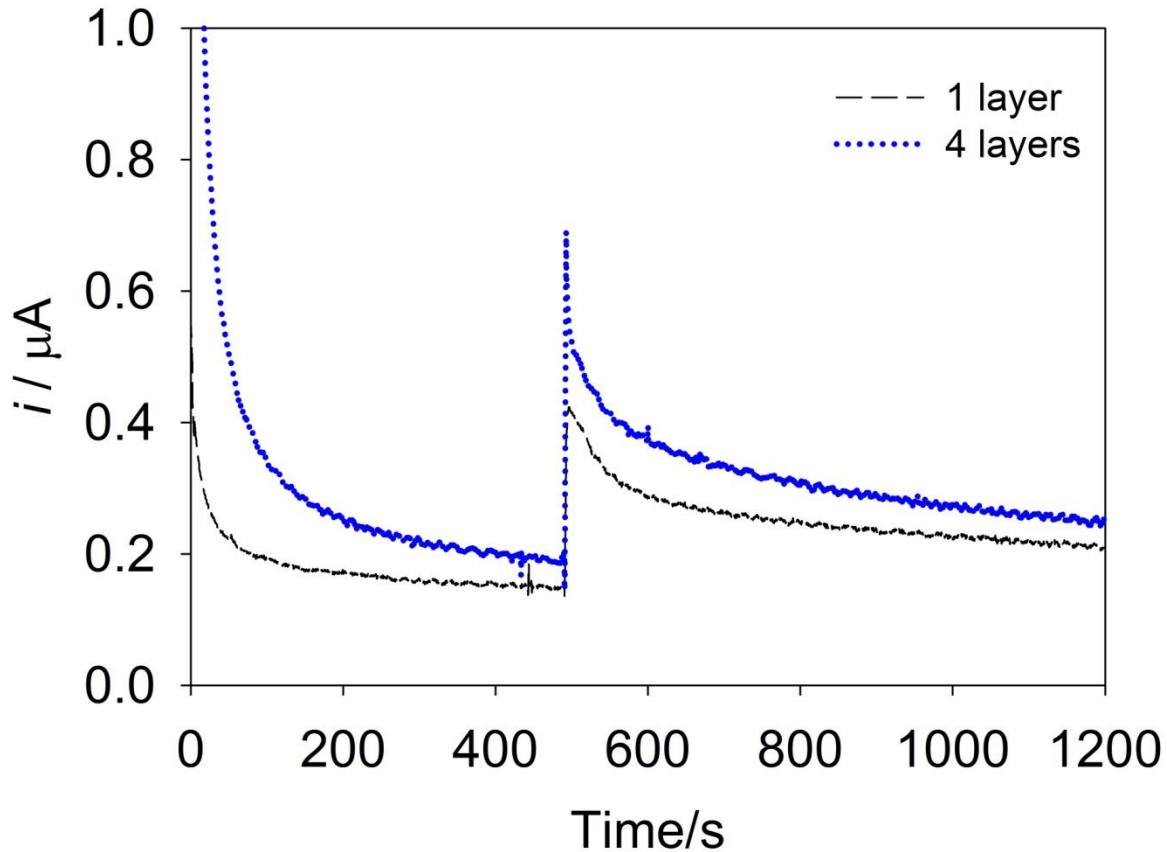


Figure 4-23: CA ($E = 500$ mV) of OA spiking on (PDA-MWCNT/ACOD/PDA-MWCNT/ACS)1 as black line and (PDA-MWCNT/ACOD/PDA-MWCNT/ACS)4 as blue line, in 0.1 M phosphate buffer pH 7.4 and 1 mM ATP and CoA. The concentration of OA before and after the spike is 0 mM and 0.25 mM, respectively.

However the amount of current produced was not directly proportional to the number of layers. Table 4-5 compares the current changes at 10 s and 100 s after spiking of OA on both electrodes. The current increases for one layer were 178 % at 10 s and 97.2 % at 100 s, respectively; for four-layer were 220 % and 99.8 %. The increase in current from both electrodes at 10 s and 100 s was similar, although the change on the four-layer electrode was slightly higher, but not proportionally as high as the amount of enzymes on the electrode (4 times higher).

Table 4-5: Comparison between (PDA-MWCNT/ACOD/PDA-MWCNT/ACS)1 and (PDA-MWCNT/ACOD/PDA-MWCNT/ACS)4 electrodes with OA spiking.

Time after OA added (s)	(PDA-MWCNT/ACOD/PDA-MWCNT/ACS)1 (μA)	Current difference with 0 s (%)	(PDA-MWCNT/ACOD/PDA-MWCNT/ACS)4 (μA)	Current difference with 0 s (%)
0	0.1492	-	0.1920	-
10	0.4153	178	0.6140	220
100	0.2942	97.2	0.3836	99.8

The electrochemical activity is not expected to increase linearly with the number of enzyme layers [333]. Rendering to the electron transfer theory, with increasing layers there is increasing distance from the electrode, the second layer plus of enzyme may not have its whole electrochemical activity. Another thing is thicker layers may increase electron-hopping distance and hinder diffusion of the supporting electrolyte [330]. So for future detection of NEFA the 1 layer of bienzyme electrode seems more practical and feasible for NEFA biosensor development, as it takes less time to make and does not use as much enzyme.

4.3.4 Confirmation of multiple layer configuration

EIS measurements were used to monitor the changes in charge transfer resistance (R_{ct}) during the assembly of the multilayer films for the bilayer electrode only (PDA-MWCNT/ACOD/PDA-MWCNT/ACS) during the modification process. The selection of 0.17 V is due to it being near the equilibrium of reductive and oxidative rates of the $\text{K}_3[\text{Fe}(\text{CN})_6] : \text{K}_4[\text{Fe}(\text{CN})_6]$ pair, and so that the redox species would not deplete near the electrode surface during the impedance measurements [309]. Measurements of the phase difference and the amplitude (i.e. the impedance) permits analysis of the electrode process in relation to contributions from diffusion, kinetics, double layer and/or coupled homogeneous reactions [251]. Figure 4-24 shows a strongly adsorbed intermediate in the absence of mass transport control. The Nyquist plot has two areas of interest, the high frequency region (electron-transfer properties) and the low frequency region (electrolyte diffusion controlled properties) [255, 334]. The semi-circle is related to the electron charge transfer resistance (R_{CT}). This resistance controls the redox probes

electron transfer kinetic process at the electrode interface [309]. The smaller it is the more conductive is the electrode or the materials used to modify the electrode. The R_{CT} depends on the dielectric and insulating features at the electrode/electrolyte interface [335]. As the number of bilayers increased so did the electron charge transfer resistance, from 2.31 K Ω (bare electrode) to 3.89 K Ω (1 bilayer) to 4.01 K Ω (2 bilayers) to 4.06 K Ω (4 bilayers), confirming step-wise assembly of the multi-layer films due to the polymer and enzyme deposition as shown in Table 4-6. The solution transfer resistance remained the same.

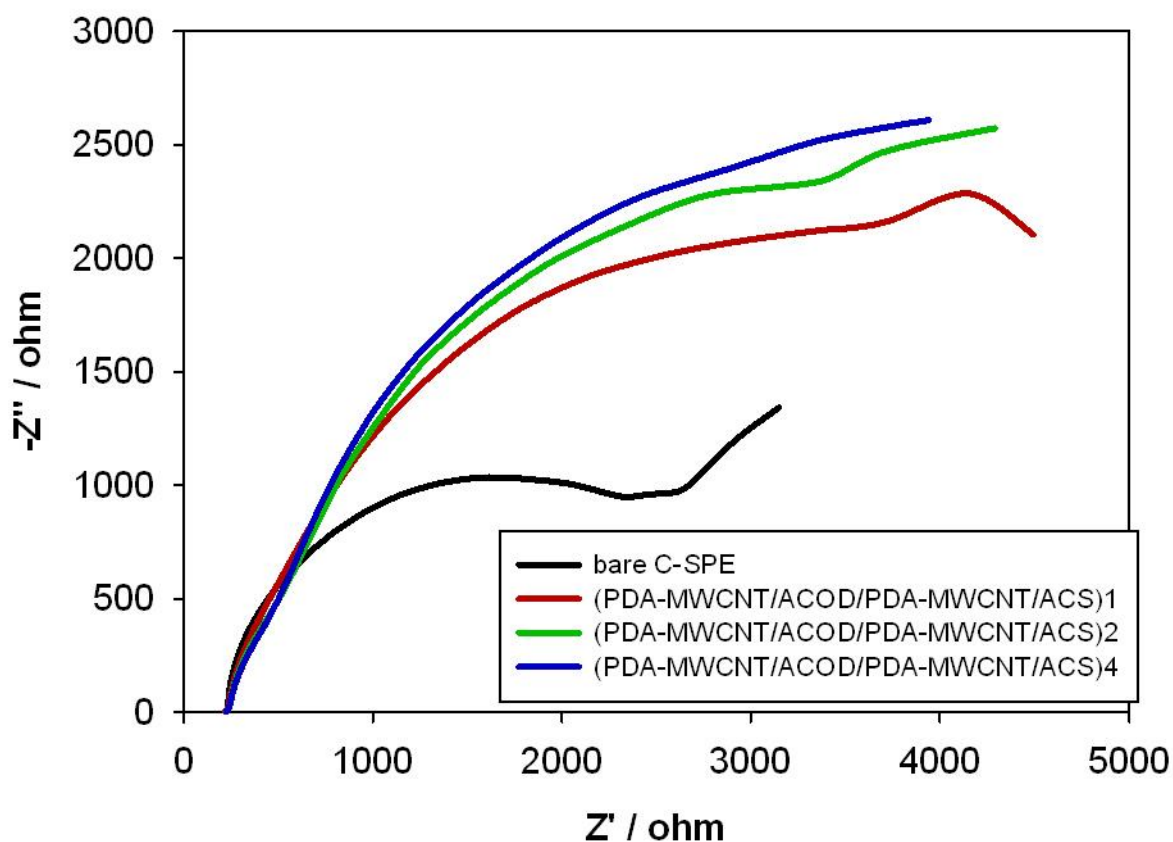


Figure 4-24: The Nyquist plots of C-SPE modified for: bare C-SPE; (PDA-MWCNT/ACOD/PDA-MWCNT/ACS)1; (PDA-MWCNT/ACOD/PDA-MWCNT/ACS)2 and (PDA-MWCNT/ACOD/PDA-MWCNT/ACS)4, all in 5 mM 1:1 mixture of $K_3[Fe(CN)_6]$: $K_4[Fe(CN)_6]$ at an applied voltage of 0.17 V.

Table 4-6: Properties determined by EIS of different enzyme layers.

Enzyme layer (PDA-MWCNT/ACOD/PDA- MWCNT/ACS)	0	1	2	4
Charge transfer resistance	2.31 k Ω	3.89 k Ω	4.01 k Ω	4.06 k Ω
Solution transfer resistance	235 Ω	236 Ω	243 Ω	243 Ω
Capacitance	34.1 μ F	59.1 μ F	89.4 μ F	116 μ F

LSV was done to confirm that having multiple layers shows as having more enzyme immobilized on the electrode. The normal ACS peak that was found at around 350 mV in Figure 4-9 is shown as being around 300 mV in Figure 4-25, this is for the electrode (PDA-MWCNT/ACOD/PDA-MWCNT/ACS)1, however the same peak shifted to a more negative potential in (PDA-MWCNT/ACOD/PDA-MWCNT/ACS)4 at around 140 mV. Adding 0.25 mM OA to each electrode showed a substantial increase in current for the electrode (PDA-MWCNT/ACOD/PDA-MWCNT/ACS)4, supporting the fact that more enzyme is there so more H₂O₂ oxidation can happen rapidly. Increasing the film thickness did not increase the difficulty for OA to diffuse through the film. At 500 mV the current produced for (PDA-MWCNT/ACOD/PDA-MWCNT/ACS)1 was 0.0146 μ A compared to that of (PDA-MWCNT/ACOD/PDA-MWCNT/ACS)4 which was 0.4294 μ A (both background subtracted).

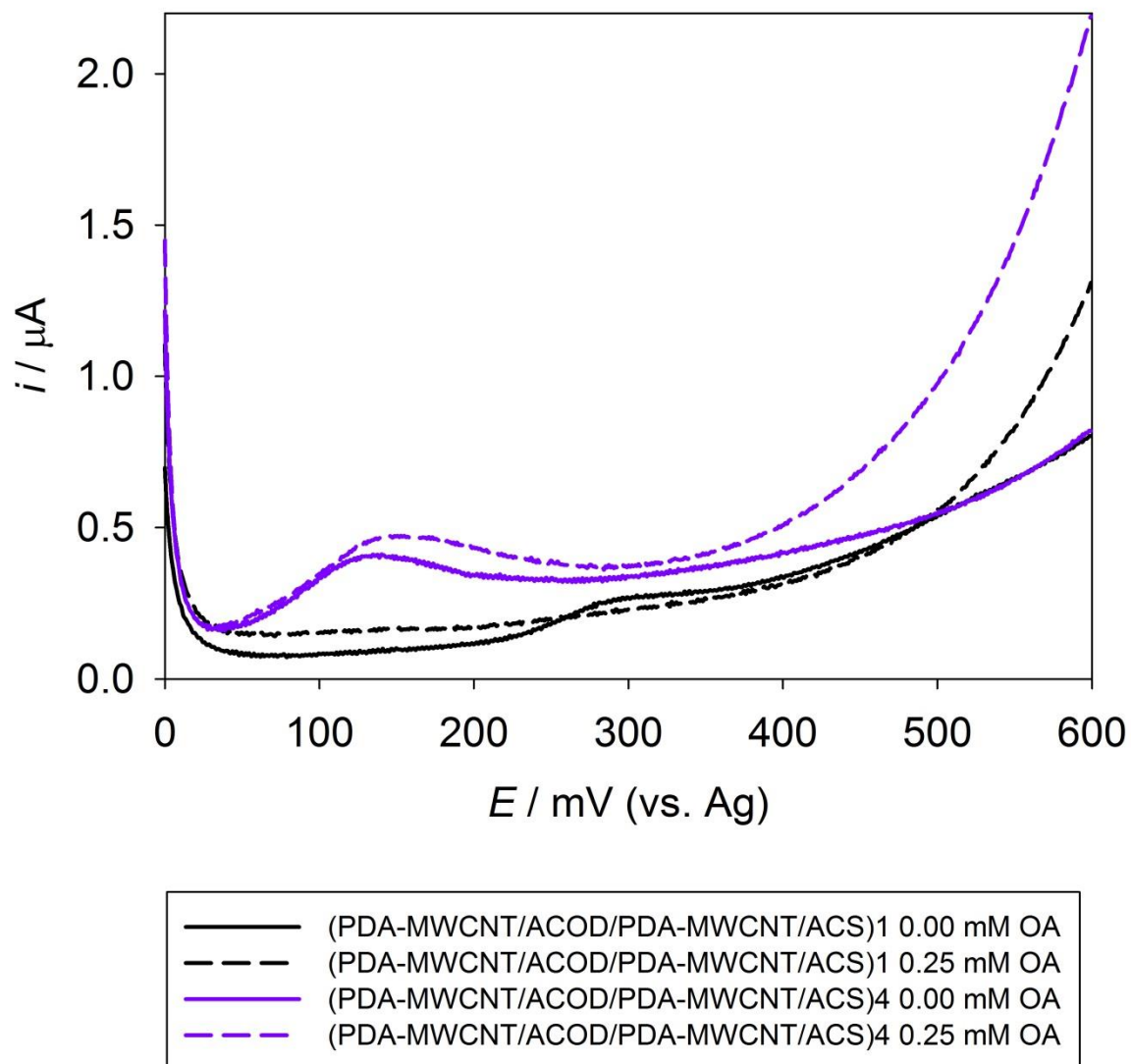


Figure 4-25: LSV at 1 mV s^{-1} showing (PDA-MWCNT/ACOD/PDA-MWCNT/ACS)1 as black line and (PDA-MWCNT/ACOD/PDA-MWCNT/ACS)4 as purple line, in 0.1 M phosphate buffer pH 7.4 and 1 mM ATP and CoA. The same electrode with 0.25 mM OA is then shown as the dashed line respectively.

4.3.5 Use of N-ethyl-maleinimide and effect of excess CoA

In some optical commercial methods of NEFA detection, the compound N-ethyl-maleinimide (NEM) is added to remove excess CoA, as the presence of non-reacted free CoA inhibits the reaction with POD, the sulfhydryl group of any remaining CoA is blocked with NEM after the first step [132].



The company Roche Applied Science for example adds 50 μL of NEM solution (this is the same volume of plasma/serum in the reaction), stating that NEM is necessary for the 'removal of an existing surplus of CoA' before the oxidation of the activated fatty acids by ACOD [336]. Whether or not NEM is needed in the electrochemical method, and what the excess amount of CoA is, needs to be investigated.

Two bienzyme electrodes of (PDA-MWCNT/ACOD/PDA-MWCNT/ACS)₁ were fabricated at the same time and tested with 0.10 mM OA at a 1:2 molar ratio with 0.20 mM CoA and at a 1:20 molar ratio with 2.00 mM CoA. 0.10 mM OA was selected as it is the lowest amount of NEFA detectable on the electrode, so its response to excess CoA would aid in the investigation without using too much substrate. Figure 4-26 shows the LSV at 1 mV s^{-1} , with ATP having the same molar ratio as CoA, in PBS.

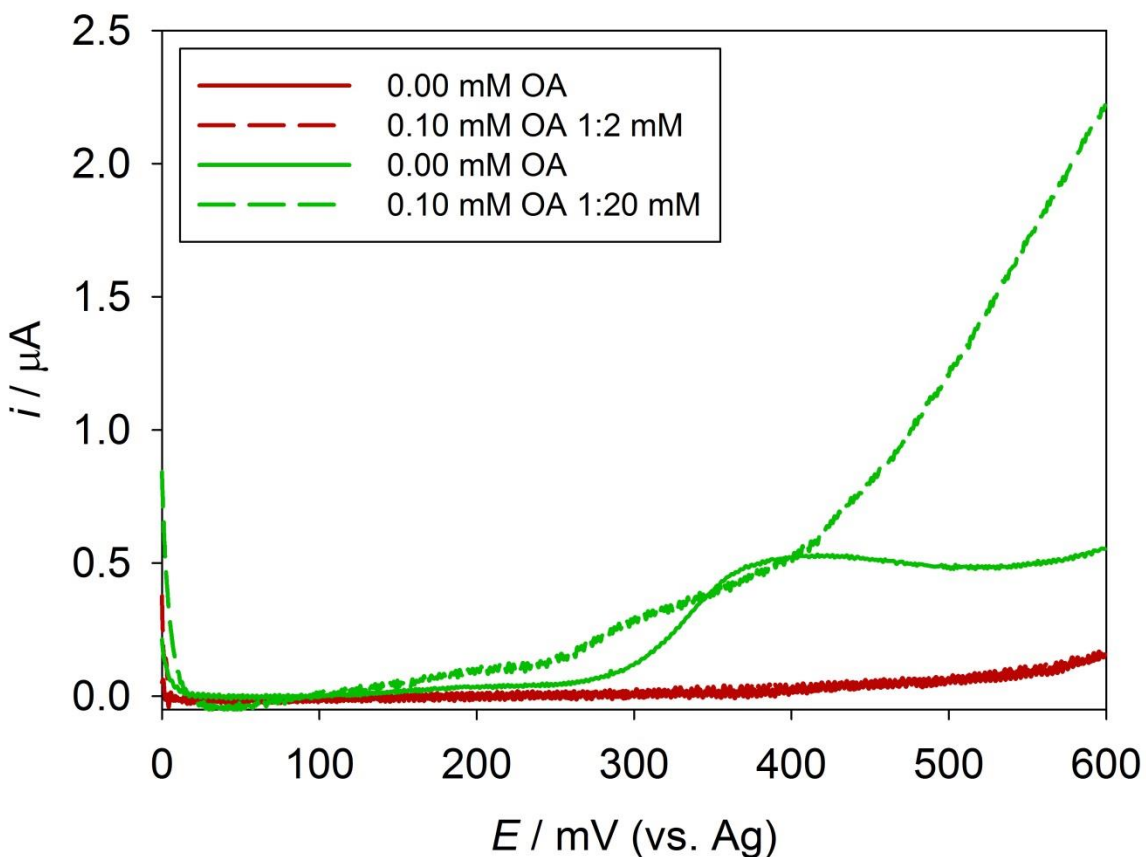


Figure 4-26: LSV for 0.10 mM OA measured on two C-SPE's modified with (PDA-MWCNT/ACOD/PDA-MWCNT/ACS)1 (one electrode shown in green and one electrode shown in red) in 0.1 M phosphate buffer pH 7.4, scan rate 1 mV s^{-1} .

Excess CoA meant that more H_2O_2 could be produced and detected electrochemically. 20 times higher CoA ratio produced $0.7569 \mu\text{A}$ compared to $0.0005 \mu\text{A}$ at 1:2 molar ratio, at the potential of 500 mV. When the concentration of CoA was 0.20 mM, there was not substantial H_2O_2 production, concluding that excess CoA is needed in order for the reaction to occur.

However the LSV for both the electrodes in 0.00 mM OA shows a very different profile and current production at 500 mV. A solid conclusion with regards to having excess CoA or not cannot be drawn from this data alone. More repeats are needed.

The effect of NEM electrochemically in the enzyme reaction was investigated via chronoamperometry by adding 5.25 μL NEM (same volume ratio as that in Roche optical method) to 120 μL of total solution containing 0.10 mM OA, ATP, CoA and PBS (Figure 4-27). Firstly 0.10 mM OA was detected at each electrode, followed by the addition of NEM. At 500 s 1:20 showed a 0.0801 μA reduction in current, whereas 1:2 showed a 0.0729 μA reduction. Addition of NEM did not increase the amount of H_2O_2 detected, both the molar ratios showed similar reduction in current, concluding that NEM is not needed for the electrochemical detection of NEFA.

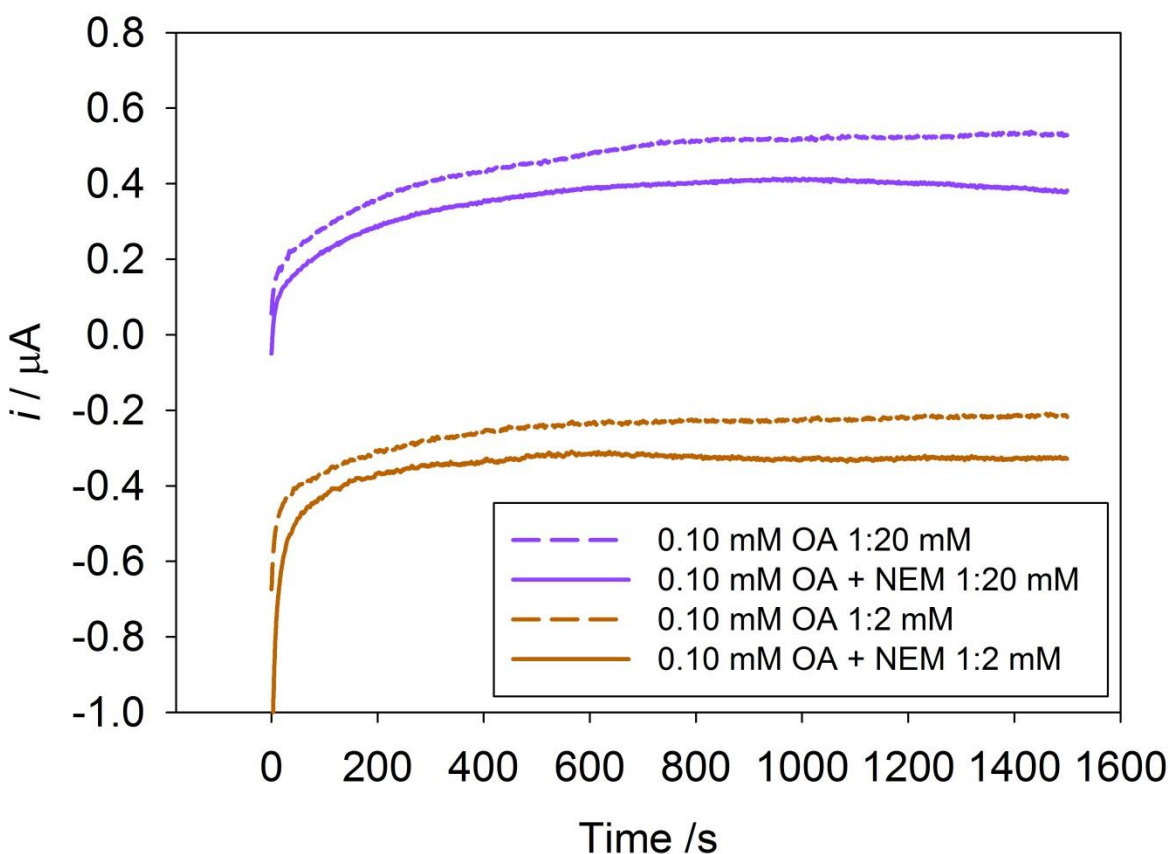


Figure 4-27: CA ($E = 500$ mV) of OA with and without NEM on (PDA-MWCNT/ACOD/PDA-MWCNT/ACS)1 at different molar ratios of CoA and ATP. All background subtracted.

4.3.6 Stability

The stability of the electrode was tested by immobilizing four different enzyme electrodes (PDA-MWCNT/ACOD/PDA-MWCNT/ACS)1 at the same time (Figure 4-28). The electrodes were stored under the same conditions (in PBS at 4 °C).

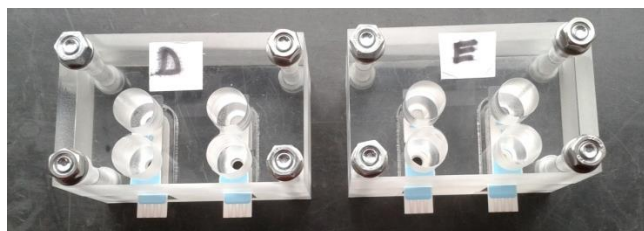


Figure 4-28: Set-up for 4 C-SPE's immobilized at the same time.

One electrode was tested at each period (via chronoamperometry at 500 mV) using 0.00 mM OA and 0.75 mM OA. All the tests contained PBS, 1 mM ATP and 1 mM CoA. The electrodes were tested on four different days (on the day of fabrication, 1 day, 3 days and 6 days later). Between the tests the electrodes were stored in the cell with the last layer of enzyme still fabricated on, therefore the electrodes were stored wet. They were rinsed with PBS as usual to remove the excess unbound enzyme and polymer, before the experiment was done. The data is shown in Table 4-7. The 'current difference' was worked out by the current produced at 0.75 mM OA minus the current at 0.00 mM OA for each day. The 'percentage difference from day 0' was worked out by the current difference on the other days divided by the current difference of day 0 (0.4139 μ A). After 1 day, the electrode lost 2 % activity. The electrode was stable for 3 days (retaining over 90 % activity), beyond which the enzymes had lost activity and denatured (resulting in a negative reading for current difference at day 6).

Table 4-7: Chronoamperometry at 500 mV, readings taken at 500 s.

Day (at 500 s)	Current (μ A) for 0.75 mM	Current (μ A) for 0.00 mM	Current (μ A) difference	% difference from day 0
0	0.6900	0.2761	0.4139	-
1	0.4664	0.0610	0.4054	2.05
3	0.8452	0.4675	0.3777	8.75
6	2.9601	5.0308	-2.0707	600

4.3.7 Reproducibility

The reproducibility of the electrode was tested by CA of one fabricated electrode with the concentration of 0.00 mM OA and 0.75 mM OA on the day of fabrication and 1 day later. The electrode was stored wrapped in foil in the fridge at 4 °C over night. The electrode was rinsed with PBS before the re-run. Figure 4-29 shows the chronoamperometric comparison of the same electrode 1 day after fabrication and use. The response dropped to that below 0.00 mM OA. Therefore the enzyme fabricated electrode is not re-usable the next day. Most commercially available sensors have disposable one use only electrodes. The same would apply for electrodes for NEFA detection.

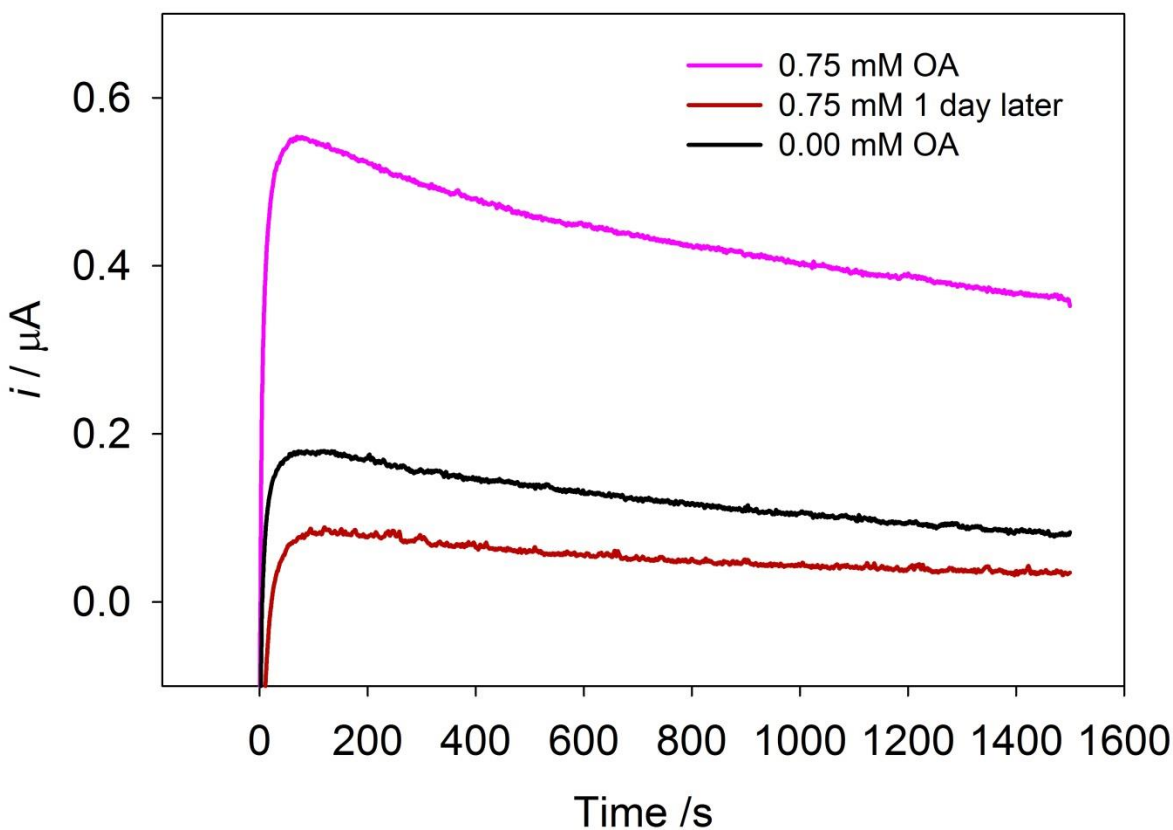


Figure 4-29: CA ($E = 500$ mV) of 0.75 mM OA (PDA-MWCNT/ACOD/PDA-MWCNT/ACS)1 electrode in 0.1 M phosphate buffer pH 7.4 with 1 mM ATP and CoA. 0.00 mM OA consisted of 0.1 M phosphate buffer pH 7.4 with 1 mM ATP and CoA only.

4.3.8 Determination of OA using (PDA/ACOD/PDA/ACS) fabricated electrode

The use of CNT in the immobilization of ACS and ACOD may not be necessary as there is no redox activity of the enzymes, unlike in glucose sensors (using GOx) which rely on CNT to shuttle electrons. The enzyme electrode (PDA/ACOD/PDA/ACS)1 was fabricated and tested with OA concentrations on C-SPE. LSV at 1 mV s^{-1} is shown in Figure 4-30. The calibration graph compared with the previously fabricated bienzyme electrode (PDA-MWCNT/ACOD/PDA-MWCNT/ACS)1 is shown in Figure 4-31, as can be seen, there was more linearity established with using CNT than without (higher R^2 value). Although the current produced without CNT is slightly higher, for the purpose of the sensor, CNT will be taken forward. Both the fabricated electrodes had the same linear detection range of 0.10 – 0.90 mM OA.

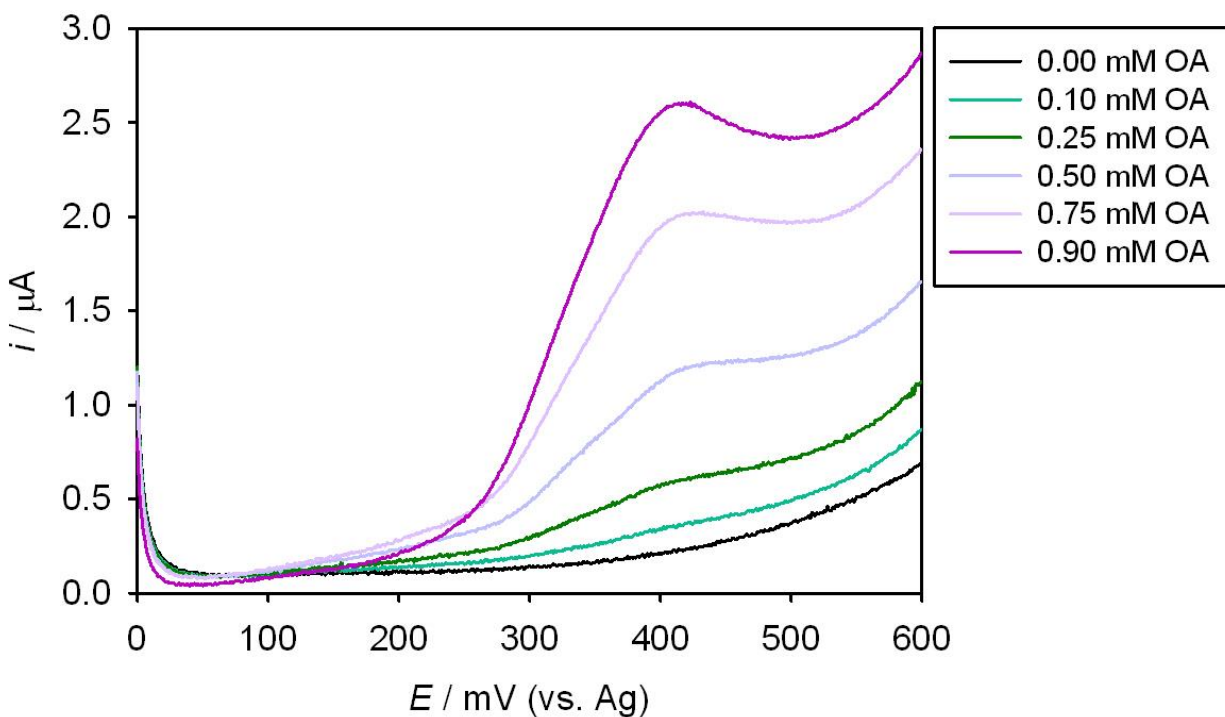


Figure 4-30: LSV of various concentrations of OA measured at a C-SPE modified with (PDA/ACOD/PDA/ACS)1 in 0.1 M phosphate buffer pH 7.4 and 1 mM ATP and CoA, scan rate 1 mV s^{-1} .

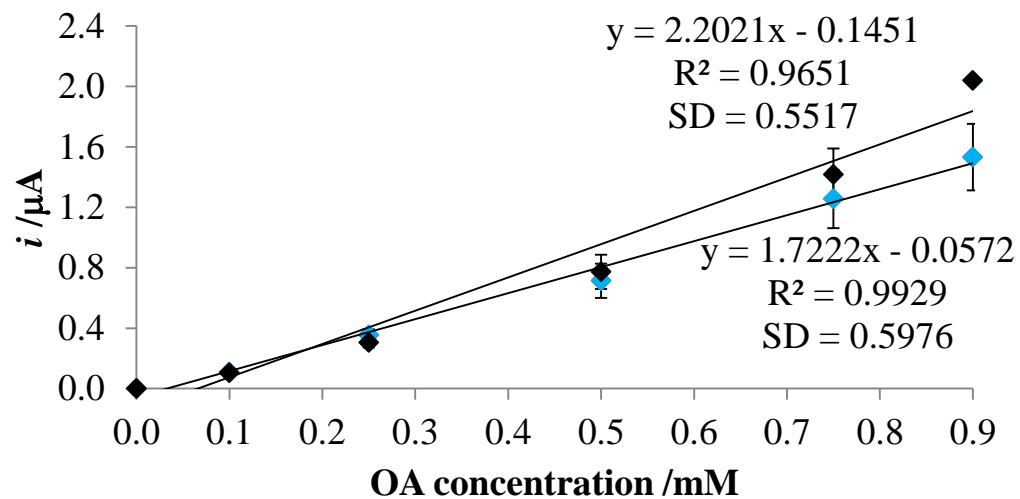


Figure 4-31: Comparison of calibration graphs at 500 mV of LSV's obtained from (PDA/ACOD/PDA/ACS)1 in black and (PDA-MWCNT/ACOD/PDA-MWCNT/ACS)1 in blue on C-SPE.

4.3.9 Interferences

The effects of these interferences needed to be investigated to further the development of the NEFA biosensor. The enzyme fabricated electrode was tested individually with urea (3 mM), uric acid (8 mM), ascorbic acid (0.5 mM), glucose (10 mM), albumin (0.6 mM), paracetamol (120 μ M) and aspirin (3 mM), in a similar manner to that described in section 3.3.5. The reasons behind investigating these interferences, is the same as those given in that section.

LSV and CA (at 500 mV) were carried out for each interference, using 0.25 mM OA as the reference to compare the current to. Table 4-8 shows the sensitivity, correlation coefficient (R^2), detection range and percent interference for each compound studied. The detection range given here is the linear detection range in which the compound was detectable during the CA at 500 mV. The compounds with very low sensitivity (urea, glucose, aspirin and albumin) may not be fully detectable on the enzyme fabricated electrode.

Table 4-8: Each interference at 500 s CA at 500 mV.

Compound	Sensitivity (μA/mM)	R^2	Detection range (mM)	% interference with 0.25 mM OA	Comparison to work in solution
Urea	- 0.0037	0.5387	0.5 – 10	-28.3	Up
Uric acid	1.3106	0.9931	0 – 8	5004	Down
Ascorbic acid	2.6352	0.9787	0.1 – 1.0	1497	Up
Glucose	- 0.0009	0.846	2 - 30	27.2	Down
Acetaminophen	1.5325	1.000	0 – 0.12	938	Up
Aspirin	- 0.0807	0.4039	1 - 3	-15.5	Down
Albumin	- 0.0491	0.7111	0.2 -0.6	2	Down

Looking at the table, 4/7 of the interferences were reduced with the immobilized electrode when compared to the work in solution. As expected uric acid, ascorbic acid and acetaminophen showed the highest interference, as they are readily oxidizable compounds. However the interference from uric acid had decreased over 3 fold with the enzymes immobilized.

Chronoamperometric response at 500 mV of uric acid on the modified electrode is shown in Figure 4-32. Above 5 mM uric acid, the electrode was unable to detect increasing concentrations of uric acid. In human plasma, uric acid is one of the most important kidney calculus indices [337]. So this will most definitively be present in blood detection of NEFA.

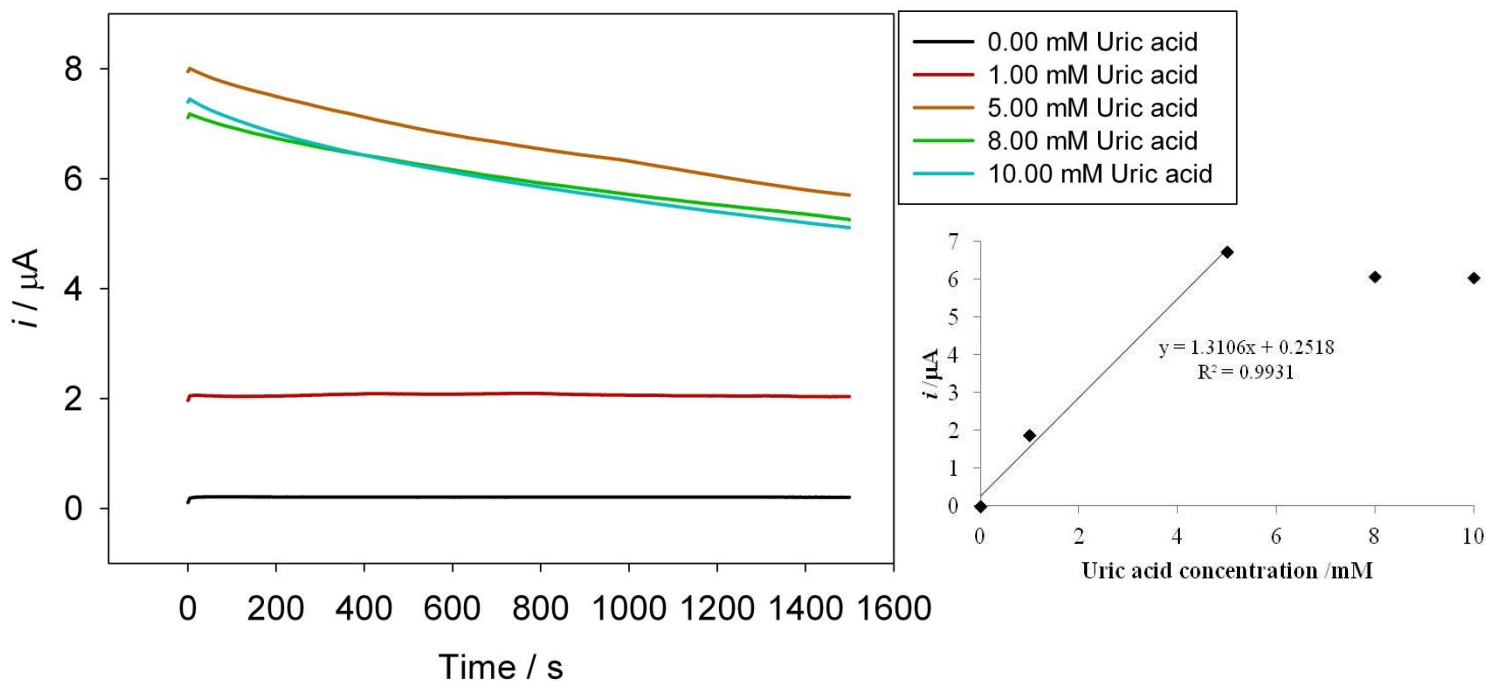


Figure 4-32: CA at 500 mV for various concentrations of Uric acid measured at a C-SPE modified with (PDA-MWCNT/ACOD/PDA-MWCNT/ACS)1 in 0.1 M phosphate buffer pH 7.4. Inset: Calibration graph at 500 s.

The electrode surface has been fouled by the oxidation product of uric acid, this is shown by the CV in Figure 4-33. Only the first concentration (1 mM) gave the usual voltammetric peak at 200 mV. All the other concentrations of uric acid gave a peak which showed the electrode surface had been fouled. This would mean that uric acid would interfere with the NEFA detection, as it would block the site on the C-SPE, where H_2O_2 would be oxidised. Each fabricated electrode would be usable once.

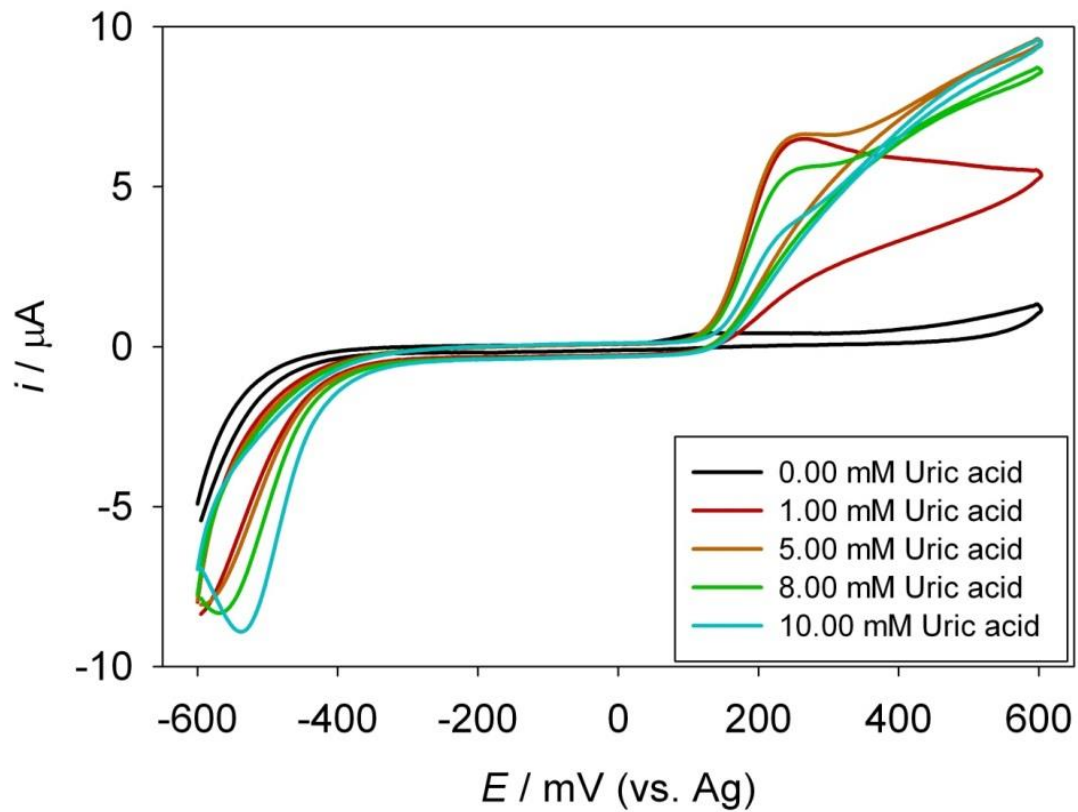


Figure 4-33: CV of various concentration of uric acid at scan rate of 5 mV s^{-1} using a C-SPE modified with (PDA-MWCNT/ACOD/PDA-MWCNT/ACS)1 in 0.1 M phosphate buffer pH 7.4.

The chronoamperometric response at 500 mV of ascorbic acid on the modified electrode is shown in Figure 4-34. Linear response was obtained up to 1 mM ascorbic acid.

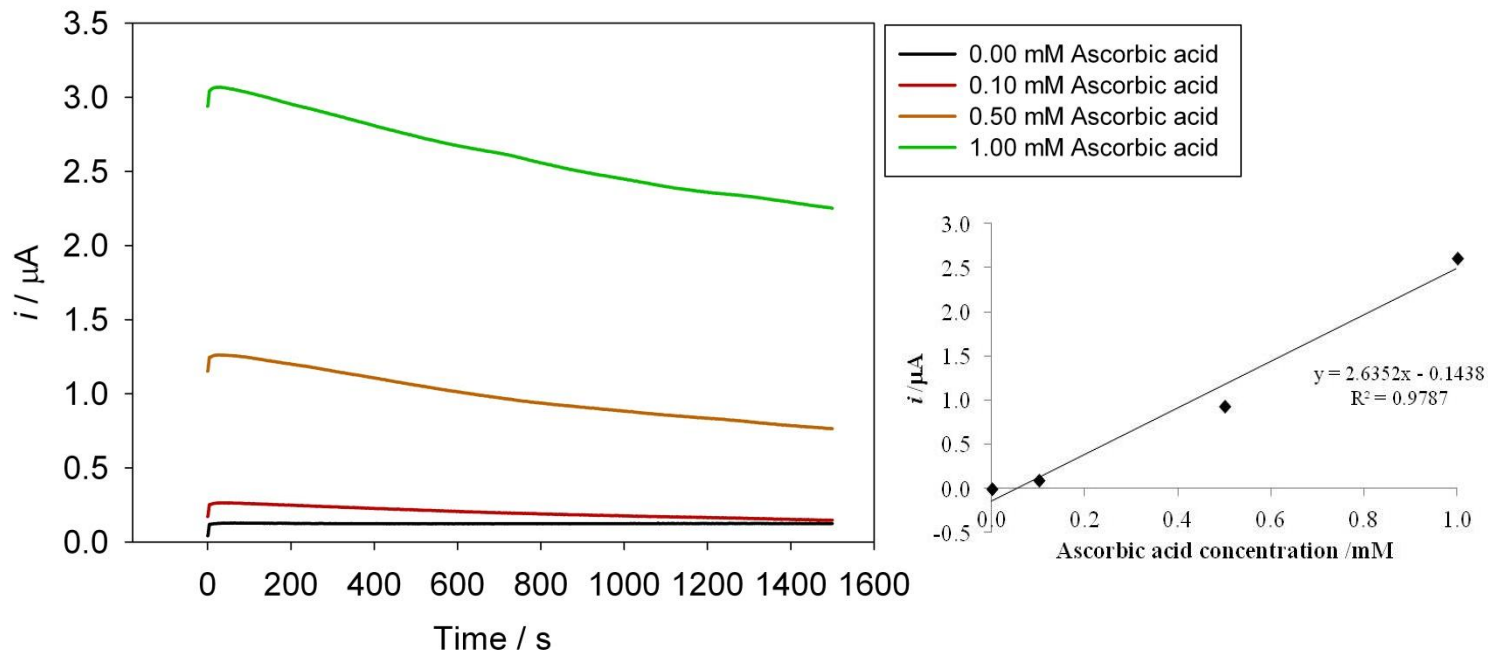


Figure 4-34: CA at 500 mV for various concentrations of Ascorbic acid measured at a C-SPE modified with (PDA-MWCNT/ACOD/PDA-MWCNT/ACS)1 in 0.1 M phosphate buffer pH 7.4. Inset: Calibration graph at 500 s.

A (PDA-MWCNT/ACOD/PDA-MWCNT/ACS)1 electrode was fabricated and 1 mM ascorbic acid was added into the solution containing; PBS, 1 mM ATP and 1 mM CoA. The electrode was tested with varying concentrations of OA. The barchart in Figure 4-35 gives the comparison of the current response (500 s) of CA at 500 mV with ascorbic acid in the solution compared with the data from Figure 4-14. Excluding the reading of 0.25 and 0.50 mM OA, ascorbic acid is predicted to be an interference in the study in blood, in some cases by giving two fold higher current (0.10 and 0.90 mM OA). This is still not as high as that was predicted in Table 4-8. This experiment was only done once. There is no systematic increase in current production with the same concentration of ascorbic acid (1 mM) and varying

concentrations of OA. This experiment shows that the current production at 500 mV will fluctuate when ascorbic acid is in solution with the fabricated electrode.

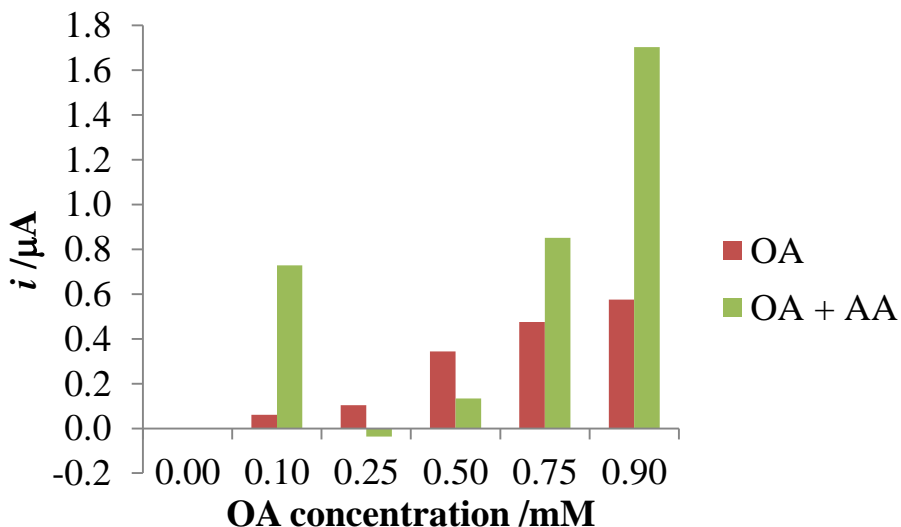


Figure 4-35: Bar chart of current obtained at 500 s of CA at 500 mV for 1 mM ascorbic acid added in as interference measured at a C-SPE modified with (PDA-MWCNT/ACOD/PDA-MWCNT/ACS)1 in 0.1 M phosphate buffer pH 7.4, 1 mM ATP and CoA with varying concentrations of OA.

Chronoamperometric response at 500 mV of acetaminophen on the modified electrode is shown in Figure 4-36. The oxidation of acetaminophen was linear for concentrations up to 0.12 mM acetaminophen. The subsequent LSV is shown in Figure 4-37. There is a profound oxidation peak present with acetaminophen, which increases as the concentration increases. This would interfere with H₂O₂ oxidation at 500 mV. Therefore is a problem for NEFA detection.

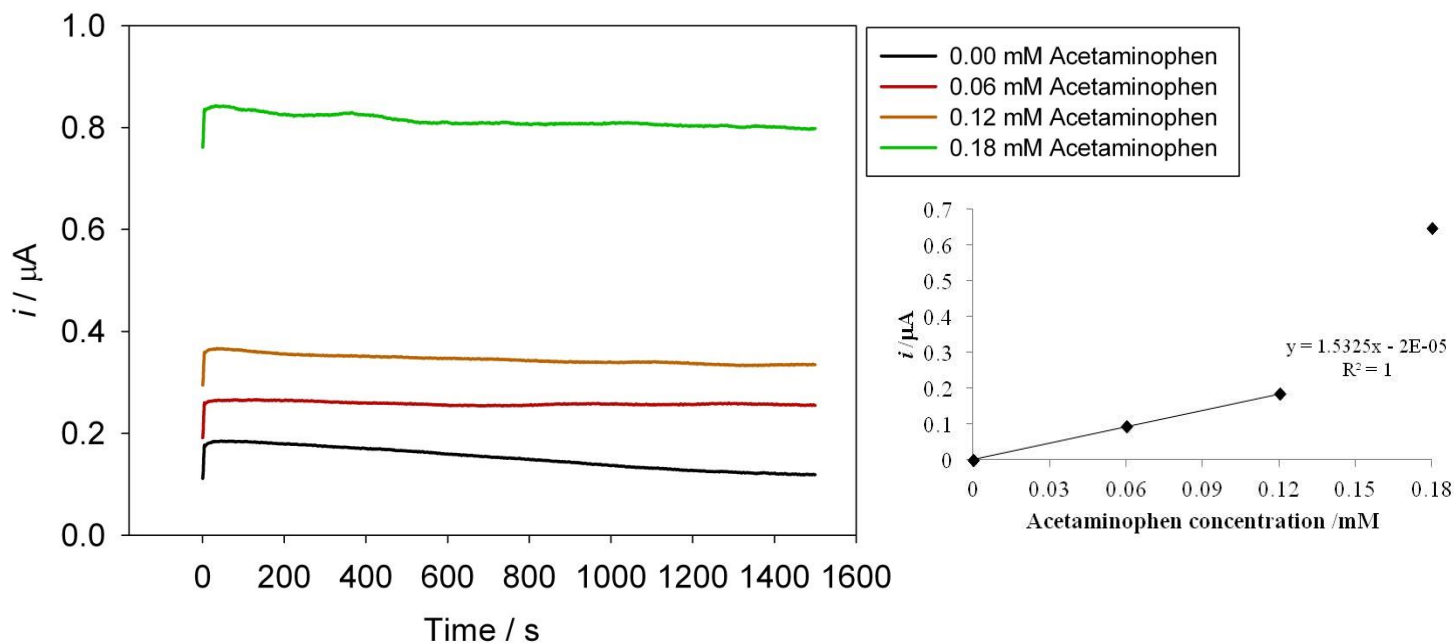


Figure 4-36: CA at 500 mV for various concentrations of Acetaminophen measured at a C-SPE modified with (PDA-MWCNT/ACOD/PDA-MWCNT/ACS)1 in 0.1 M phosphate buffer pH 7.4. Inset: Calibration graph at 500 s.

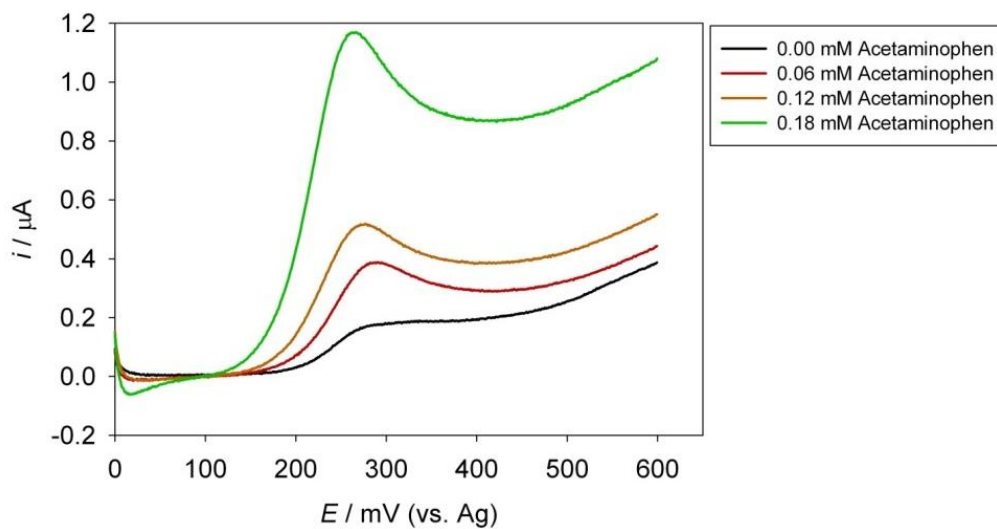


Figure 4-37: LSV of various concentrations of acetaminophen measured at a C-SPE modified with (PDA-MWCNT/ACOD/PDA-MWCNT/ACS)1 in 0.1 M phosphate buffer pH 7.4, scan rate 1 mV s^{-1} .

On a new fabricated electrode, 5 mM glucose was added into the solution and tested with the bienzyme electrode with varying concentrations of OA. The barchart below (Figure 4-38) gives the comparison of the current response (500 s) of CA at 500 mV with glucose (present as an interference) in the solution compared with the data from Figure 4-14. For the higher concentrations of OA (0.50 mM OA plus), glucose showed a 7 % plus increase in current. Meaning it would interfere in NEFA detection.

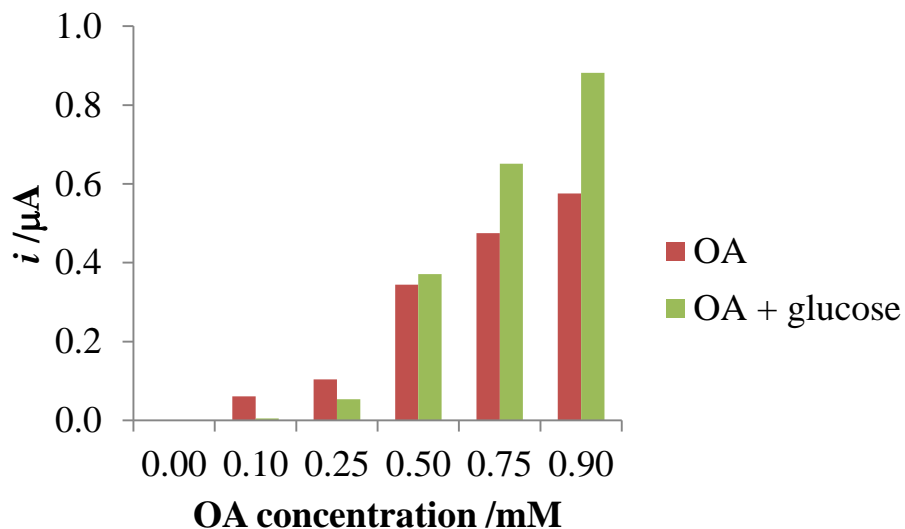


Figure 4-38: Barchart of current obtained at 500 s of Chronoamperometry at 500 mV for 5 mM glucose added in as interference, measured at a C-SPE modified with (PDA-MWCNT/ACOD/PDA-MWCNT/ACS)1 in 0.1 M phosphate buffer pH 7.4, 1 mM ATP and CoA with varying concentrations of OA.

4.4 Conclusions

In this chapter many enzyme electrodes were fabricated using LbL method on different SPE (C-SPE, CoPc and SWCNT SPE). Firstly, the (PDA-MWCNT/ACOD)₂ fabricated electrode was made and tested with concentrations of OA-CoA and PA-CoA (up to 1.5 mM). Then the bienzyme electrode (PDA-MWCNT/ACOD/PDA-MWCNT/ACS)₁ was fabricated and various concentration of OA were tested (up to 0.90 mM). Linear calibration graphs of LSV at 500 mV (with R^2 of ~0.99) and CA at 500 s at 500 mV chosen potential (with R^2 of ~0.99) were obtained and will be used as the reference graphs for future comparisons. The linear detection range of OA was found to be 0.10 mM to 0.90 mM. Multiple layer comparison and confirmation was done using the electrochemical techniques of CA, EIS and LSV.

Other similar fabricated electrodes were also made and tested with the same concentration of OA as a reference, these electrodes were (PDA-MWCNT/ACS/PDA-MWCNT/ACOD)₁ and (PDA-MWCNT/ACOD+ACS)₁. These electrodes had lower linear detection ranges, so were not to be taken forward in NEFA sensor development.

The molar ratio of ATP and CoA was also investigated on all 3 SPE (C-SPE, CoPc and SWCNT SPE) for the fabricated enzyme electrode (PDA-MWCNT/ACOD/PDA-MWCNT/ACS)₁. 1:1:1 molar ratio was found to be sufficient for linearity and reproducibility of this work. The use of NEM and effect of excess CoA was also investigated as literature stated they would be a problem for NEFA detection. This was invalid for electrochemical NEFA detection. The stability of the electrodes was up to 3 days. There was no reproducibility found for re-using the same enzyme fabricated electrode the next day.

The C-SPE (PDA-MWCNT/ACOD/PDA-MWCNT/ACS)₁ enzyme electrode was taken forward and tested with common interferences that would be present in blood. This data was a comparison with that in the previous chapter.

5 Enzyme fabricated electrodes for blood NEFA detection

5.1.1 Introduction

This section will look at fabrication of the electrode to keep common interferences in blood to a minimum. A schematic of what should be happening in each layer of the LbL fabricated electrode is illustrated in Figure 5-1. The last layer, should not only reduce the likelihood of biofouling, but also regulate the diffusion of NEFA [338]. The outer membranes role is particularly important in sensor function [229]. The desired role of the last layer is shown in the figure below. It should hypothetically allow the diffusion of O_2 , CoA, ATP and NEFA, but withhold the penetration of interferences such as ascorbic acid, uric acid and acetaminophen.

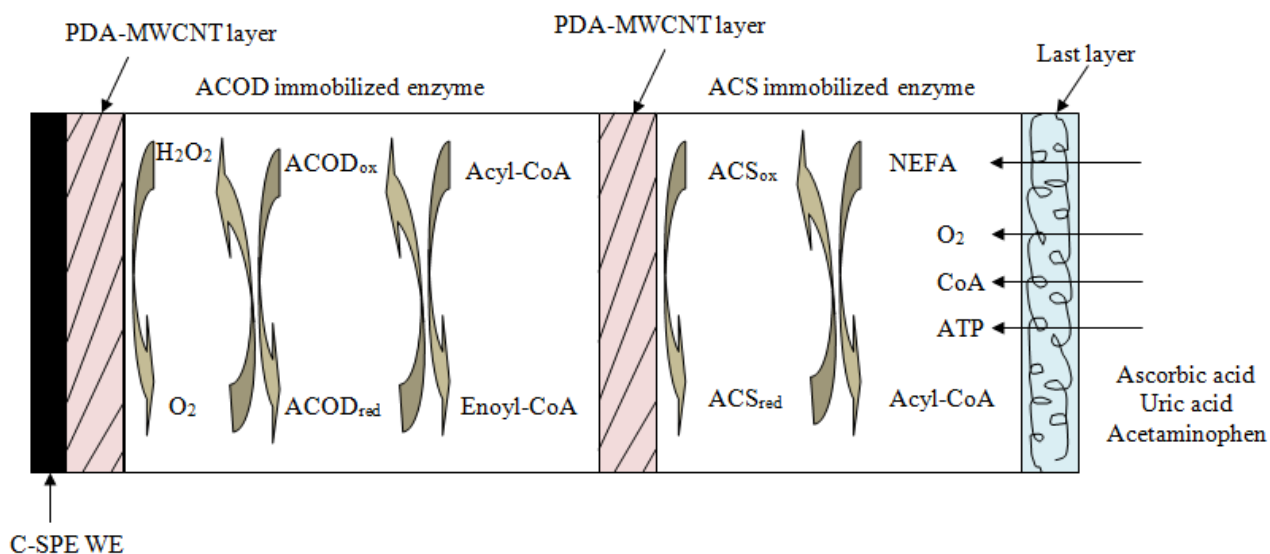
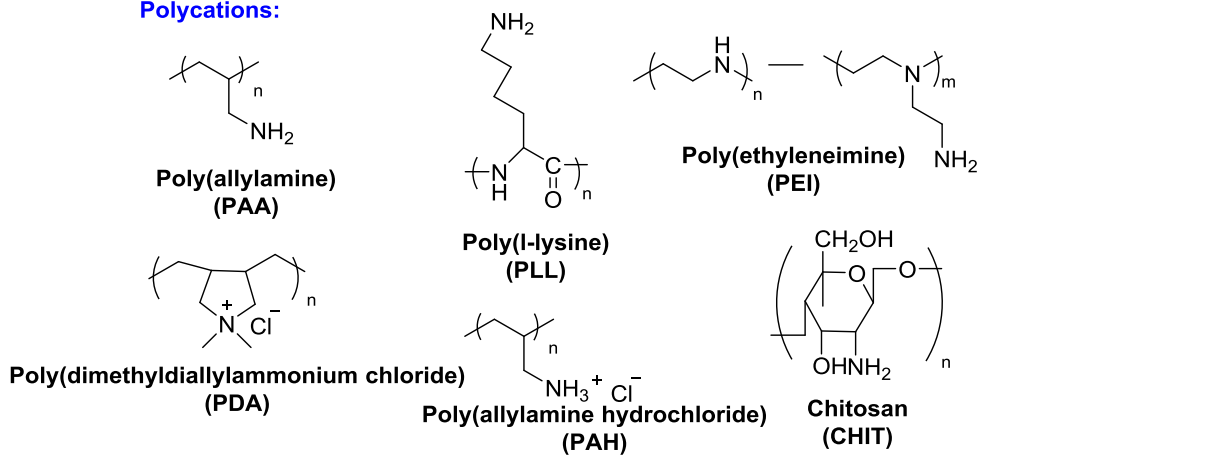


Figure 5-1: Various chemical, electrochemical and diffusion processes on the LbL electrode of the current NEFA sensor. Adapted from [338].

Figure 5-2 shows chemical structures of common polymeric materials [216]. These can be incorporated in the current LbL configuration (as the last layer) to attempt to reduce interferences that would be present in blood.

Polycations:



Polyanions:

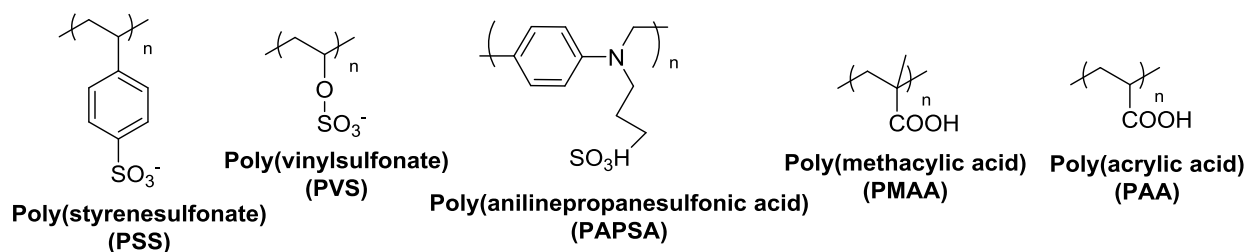


Figure 5-2: Chemical structure of commonly used polyelectrolytes.

Immobilization usually perturbs the microenvironment of the active site of the enzyme, resulting in alterations of the enzymes intrinsic kinetic characteristics [322]. Alkaline shifts could be due to negatively charged surface or a loss of positive charge on the enzyme because of the immobilization procedure. An acidic shift may be caused by positively charged surface or negative charge lost on enzyme, or both reasons combined.

5.1.2 Experimental

5.1.2.1 Materials

Roche free fatty acids, Half-micro test assay kit (cat no. 11 383 175 001) was purchased from Roche Applied Science (West Sussex, UK). The Wako HR series NEFA-HR (2) kit was purchased from Wako Diagnostics (Neuss, Germany). Oleic acid (OA) was the Wako NEFA standard solution used again in this work.

Serum and plasma samples were kindly donated by Newcastle University Medical School, from Professor Mike Trenell's group. Blood samples were collected by a cannula inserted into a forearm vein. Blood samples were spun in a centrifuge (Harrier 18/80R; MSE Ltd, London, UK) for 10 minutes at a speed of 3000 rpm at 4 °C. Plasma was then pipetted off each sample and stored at -40 °C. The samples were then stored at -80 °C until use. Once the centrifugation was complete and even after storage, the serum/plasma samples needed to be checked for haemolysis [339]. If there was any obvious haemolysis those samples were discarded, all samples are shown in Figure 5-3.



Figure 5-3: Samples of serum and plasma (some haemolysed).

Poly [2-methacryloyloxyethyl phosphorylcholine – co-*n*-butyl methacrylate – co-*p*-nitrophenyloxycarbonyl poly(ethylene glycol) methacrylate] (PMBN) 5 % solution in ethanol was provided by Dr. Yu (structure is shown later in Figure 5-10). This was made by the method described in work done by *Konno et al.* [340]. It was prepared by random copolymerization of 2-methacryloyloxyethyl phosphorylcholine (MPC), *n*-butyl methacrylate and *p*-nitrophenylester bearing methacrylate.

Bovine serum albumin (BSA) was purchased from Sigma Aldrich (Dorset, UK). BSA solution consisted of 1 mM BSA concentration in PBS. Sodium poly(styrenesulfonate) (PSS) was also purchased from Sigma Aldrich (Germany). Poly(methacrylic acid sodium salt) (PMAA) was purchased from Polysciences Inc (Eppelheim, Germany). Both polymer solutions consisted of 1 % polymer in solution, with 0.20 M NaCl in 5 mL distilled water.

5.1.2.2 Optical measurements

The UV spectrophotometer used was Ultrospec 3000 (Pharmacia Biotech). The Roche protocol titled 'Free fatty acids, Half-micro test', was used to obtain a calibration graph with OA Wako NEFA standard solution 1 mM with N-ethyl-maleinimide (NEM) [142]. The different OA concentrations were made by diluting the standard 1 mM OA standard solution with double distilled water. Each run was done in triplicates and then averaged. 6 plasma samples were then tested optically, and the concentrations of NEFA were determined by reading against this calibration graph obtained by using OA standard.

The Wako protocol was used for the rest of the serum/plasma samples [143]. The unknown blood samples were read-off against the calibration graph obtained using OA standard.

Both optical methods were validated with 0.30 mM and 0.60 mM OA, made up in the same manner but ran separately to the bulk OA concentrations (Figure 5-4 and Figure 5-5). The figure shows the great level of reproducibility and linearity obtained from the current optical method.

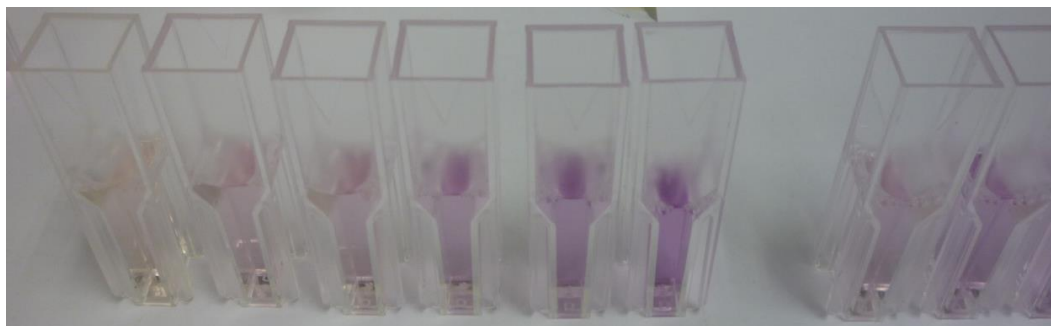


Figure 5-4: Optical validation. Concentrations 0.00 mM to 0.90 mM OA from left to right respectively. Far right concentrations 0.30 mM and 0.60 mM OA.

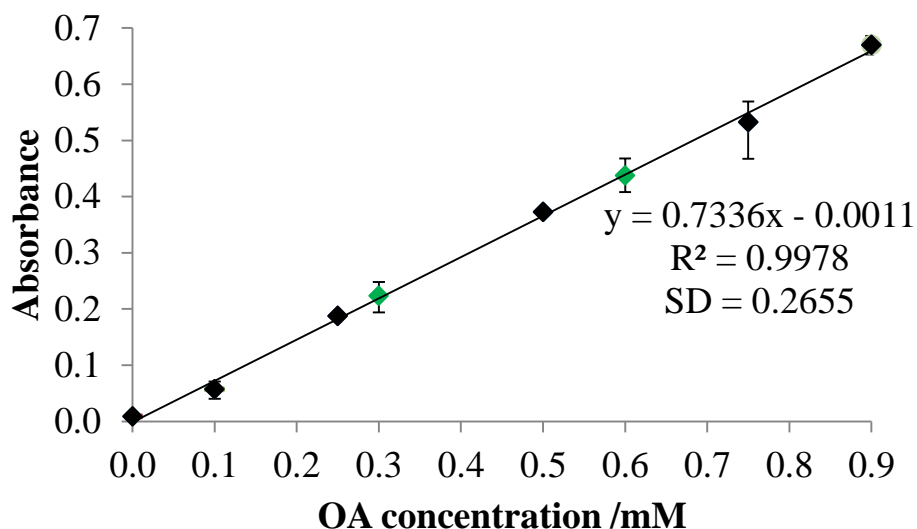


Figure 5-5: Calibration graph obtained by measurement of various concentrations of OA by the Roche colorimetric method. The fitting is based on average values obtained from three measurements ($\lambda=546$ nm). 0.30 mM and 0.60 mM were measured independently (shown in green).

5.1.2.3 Electrochemical measurements

Each experiment was first done with the individual fabricated electrode with various concentration of Wako OA standard (0.00, 0.10, 0.25, 0.50, 0.75 and 0.90 mM). Once this calibration graph was obtained, then the serum/plasma experiments were done and compared to this calibration graph.

Fabrication of electrodes

The (PDA/ACOD/PDA/ACS)1 electrode was fabricated in the same way as described in section 4.1.3. The rest of the specific electrodes were fabricated following adaptation from the original electrode (PDA-MWCNT/ACOD/PDA-MWCNT/ACS)1.

The PMBN fabricated electrodes consisted of 8 μ L of PMBN 5 % solution in ethanol. This was deposited directly on the WE of the C-SPE after the original fabrication, forming a gel-like layer as shown in Figure 5-6. The experiments were done with either 1 mM ATP and 1 mM CoA

mixed into the PMBN layer (PDA-MWCNT/ACOD/PDA-MWCNT/ACS/PMBN+ATP+CoA)¹ or without (PDA-MWCNT/ACOD/PDA-MWCNT/ACS/PMBN)¹.



Figure 5-6: Electrode with PMBN layer.

The (PDA-MWCNT/ACOD/PDA-MWCNT/ACS/BSA)¹ electrode was fabricated following the original protocol, then depositing 10 μL of BSA solution. Although BSA has been listed as interference in the UV method, it is used as an outer membrane layer in other glucose sensor work, which is why it was incorporated into this sensor too.

(PDA-MWCNT/ACOD/PDA-MWCNT/ACS/PDA-MWCNT/PSS)¹ and (PDA-MWCNT/ACOD/PDA-MWCNT/ACS/PDA-MWCNT/PMAA)¹ were fabricated as the original electrode, then 15 μL of PDA-MWCNT solution, then 15 μL of PSS/PMAA solution was deposited. These polymers were chosen because at pH 7.4, both of these polymers would have a negative charge, as their isoelectric point is below that of the pH. As negatively charged polymers they would be able to electrostatically bind to the positively charged PDA-MWCNT layer and in theory reduce interference.

Each electrode was left in the fridge after each additional step (for 30 minutes) and washed with PBS before the next step.

5.1.3 Serum vs. plasma

The decision between collecting and testing in plasma or serum is based on the distinctive requirement that the sample is needed for. Table 5-1 states the advantages and disadvantages of one over the other. For this study both serum and plasma samples were analysed. Firstly plasma was used, but as plasma contains fibrinogens, which are thought to affect the electrochemical measurements, serum samples were used as they were thought to be more ‘cleaner’.

Table 5-1: Advantages and disadvantages of plasma over serum [341].

Advantages of plasma over serum	Disadvantages of plasma over serum
Quicker process – the wait for blood to clot is eliminated	Method-dependent interference from anticoagulants
Higher yield – from whole blood ~15-20 % more plasma than serum will be attained	Cation interference – lithium/ammonium might increase due to contamination with heparinates usage
Essentially no interference from the postcentrifugal coagulation that happens in serum	Fibrinogen changes protein electrophoresis results
<i>In vivo</i> is more representative from plasma results than serum	
Reduced chance of haemolysis and thrombocytolysis	

5.2 Detection of plasma samples

Six different plasma samples (from different patients) were tested optically with the commercial Roche kit, the NEFA concentrations were read against the calibration graph obtained in Figure 5-5. The respective NEFA concentration in plasma came to 0.15 mM, 0.23 mM, 0.25 mM, 0.31 mM, 0.35 mM and 0.53 mM. The same plasma samples were then tested electrochemically using the enzyme fabricated electrode (PDA-MWCNT/ACOD/PDA-MWCNT/ACS)¹ and compared to the calibration graph previously obtained in Figure 4-14 in Figure 5-7 (data taken from 500 s). A comparison of the values obtained is shown in Table 5-2. The NEFA value obtained electrochemically was at least twice as high as that compared to the optical method in five out of the six samples. This is due to the multiple interferences in human plasma. However the interference from blood is not as high as what was predicted from the interference study in section 4.3.9, where individual concentrations of each interference were tested on the fabricated electrodes (e.g. 8 mM uric acid).

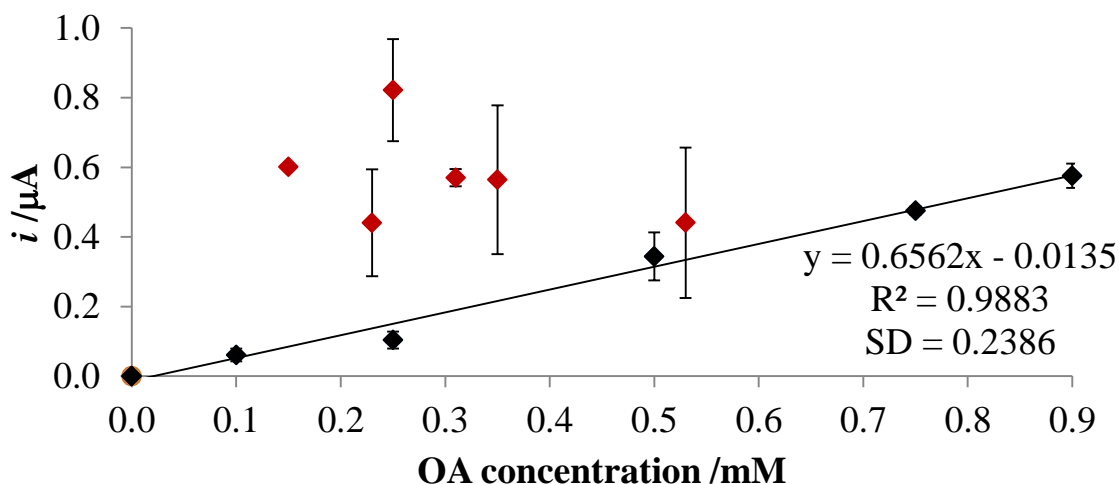


Figure 5-7: CA at 500 mV for various concentrations of OA measured at a C-SPE modified with (PDA-MWCNT/ACOD/PDA-MWCNT/ACS)1 in 0.1 M phosphate buffer pH 7.4, with 1 mM ATP and CoA (in black) along with 6 plasma concentrations measured independently in duplicates (in red).

Table 5-2: Comparison of the NEFA values obtained in 6 plasma samples from the two different detection methods.

Concentration using optical method (mM)	Concentration using electrochemical method (mM)
0.15	0.900
0.23	0.725
0.25	1.190
0.31	0.890
0.35	0.875
0.53	0.700

5.3 Detection of serum samples

Figure 5-8 shows the chronoamperometric results for serum samples run at 500 mV for the fabricated electrode (PDA-MWCNT/ACOD/PDA-MWCNT/ACS)1. The calibration graph in Figure 5-9 shows the results from CA at 500 s (from Figure 4-14), along with those of 5 serum samples run from the two patients. The UV concentrations of 0.114, 0.122, 0.171, 0.342 and 0.513 mM came to 0.70, 0.85, 0.50, 0.76 and 1.05 mM electrochemically. This is a 514, 597, 192, 122 and 105 % increase respectively. The lower the concentration of NEFA was the higher the increase in current due to interference. However both plasma and serum did not give consistent/reproducible NEFA concentrations. The electrode now needs further fabrication, as shown in Figure 5-1 earlier.

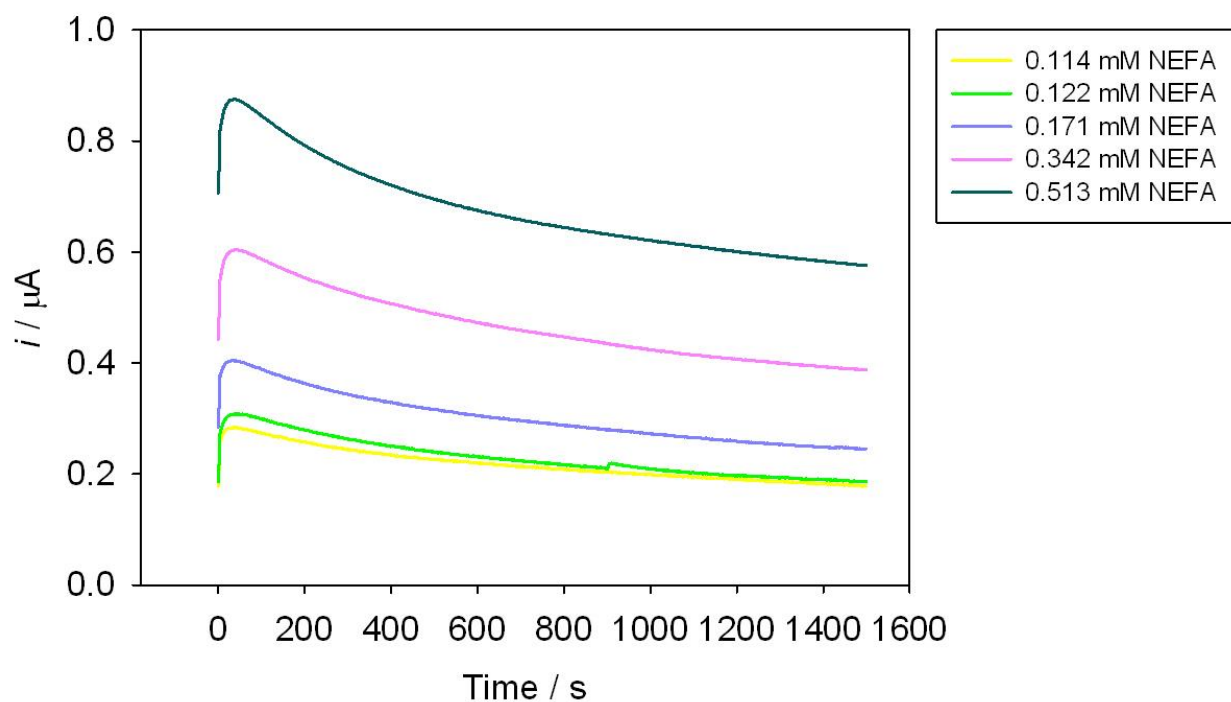


Figure 5-8: CA at 500 mV for various concentrations of serum NEFA (from 2 patients) measured at a C-SPE modified with (PDA-MWCNT/ACOD/PDA-MWCNT/ACS)1 in 1 mM ATP and CoA and 0.1 M phosphate buffer pH 7.4.

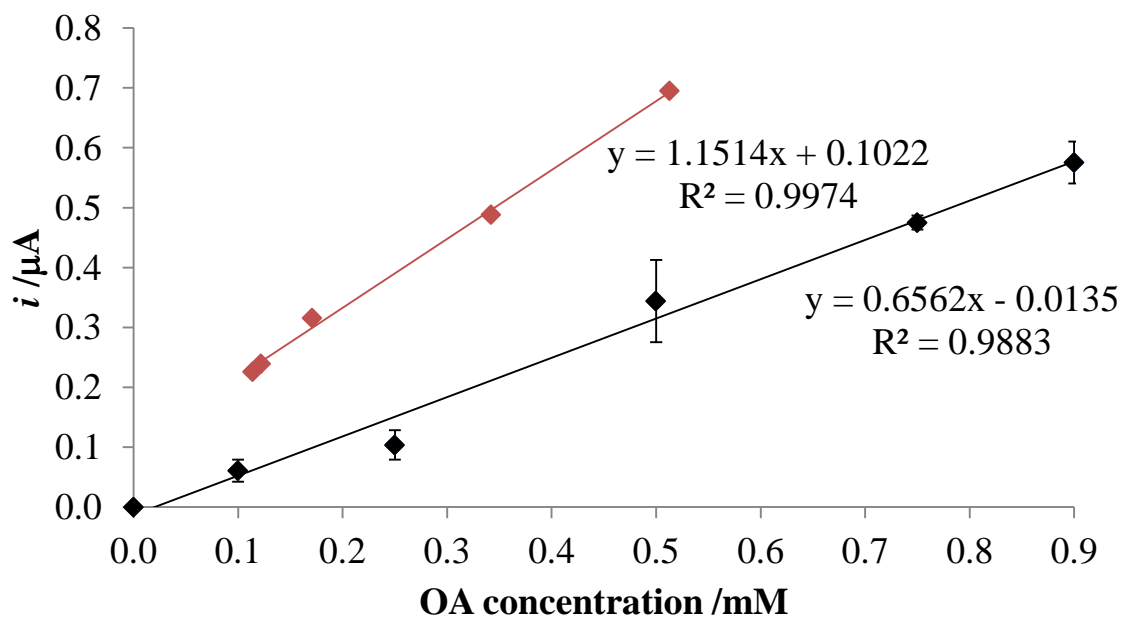


Figure 5-9: CA at 500 mV for various concentrations of OA measured at a C-SPE modified with (PDA-MWCNT/ACOD/PDA-MWCNT/ACS)1 in 0.1 M phosphate buffer pH 7.4, with 1 mM ATP and CoA (in black) along with 5 serum concentrations (in red).

5.4 Comparison of different fabricated electrodes performance using human blood

After using plasma and serum samples, the interference detected on the (PDA-MWCNT/ACOD/PDA-MWCNT/ACS) electrode is high, as expected. However, it is not as high as was predicted from the interference work done on the fabricated enzyme electrode in section 4.3.9. In order to make a commercial biosensor for blood NEFA detection, the sensor needs to work in blood in a reliable and reproducible manner. To do this the current enzyme electrode needs further fabrication to reduce the interferences. The last layer as shown in Figure 5-1 needs to be incorporated.

Table 5-3 shows the CA data at 500 mV for the various fabricated electrodes, and the current for 0.90 mM OA at 500 s, the percentage difference was worked out by using current from the standard (PDA-MWCNT/ACOD/PDA-MWCNT/ACS) electrode as the reference (data shown in Figure 4-15). The individual CA for each electrode and their calibration graphs at 500 seconds are given in the appendix (in Figure 7-6 to Figure 7-17), along with some explanation of the actual result produced.

Table 5-4 shows the respective LSV at 1 mV s^{-1} for each electrode, the current for comparison is at 500 mV for 0.90 mM OA. The reference data for the LSV comparison was taken from Figure 4-10.

The different electrodes fabricated contained either PMBN (results shown in appendix as Figure 7-8 to Figure 7-11) or BSA (Figure 7-12 and Figure 7-13) as the last layer after (PDA-MWCNT/ACOD/PDA-MWCNT/ACS) or the polymers PSS or PMAA (shown in Figure 7-14 to Figure 7-17) after (PDA-MWCNT/ACOD/PDA-MWCNT/ACS/PDA-MWCNT). The LbL fabrication of electrodes had an additional PDA-MWCNT layer for the negatively charged polymers PSS and PMAA because the PDA-MWCNT layer is positively charged. Each fabricated electrode was tested with the various concentrations of OA, and then a new electrode was fabricated for the different blood samples.

From both the tables (hence both the methods CA and LSV), using PMBN gave the best results when compared to the standard bienzyme electrode (PDA-MWCNT/ACOD/PDA-MWCNT/ACS)¹. This was the only method that did not rely on LbL deposition but was instead a gel-like layer on top of the pre-immobilized LbL enzyme electrode. The phospholipid polymer,

(poly [2-methacryloyloxyethyl phosphorylcholine (MPC) – co-n-butyl methacrylate (BMA) – co-p-nitrophenyloxycarbonyl poly(ethylene glycol) methacrylate (MEONP)]) (PMBN) has positively charged groups that bind electrostatically to negatively charged groups [342]. PMBN is a deacylated derivative of polymyxin B (PMB), which is a polycationic drug. Structure of PMBN is shown in Figure 5-10, it consists of three polymer chain segments.

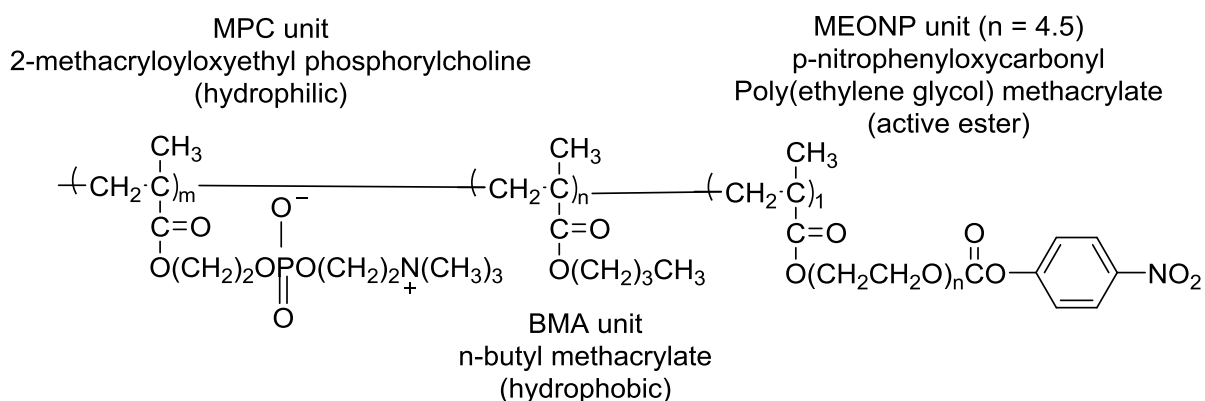


Figure 5-10: Chemical structure of water-soluble PMBN polymer [343, 344].

The outer layer of PMBN contains polar phosphorylcholine group, this suppresses non-specific adsorption of particular proteins (BSA and γ -globulin) [345]. The orientation of these groups at the external surface of the bilayer, gives a neutral, zwitterionic interface, having little or no attraction for proteins on the extracellular environment.

MPC polymers have acted as surface modifiers to improve biocompatibility in several medical devices [346]. The active ester group in the MEONP side chain makes PMBN conjugate to any material containing ester bonds. PMBN is known to maintain its enzyme activity [343]. PMBN has good biocompatibility, inhibiting the adhesion and activation of blood cells, resulting in it reducing blood coagulation when in contact with blood [343]. So incorporating PMBN into the enzyme electrode could help reduce the interference with blood, yet maintain PMBN's activity. The electrode (PDA-MWCNT/ACOD/PDA-MWCNT/ACS/PMBN+ATP+CoA) had ATP and CoA incorporated into the PMBN layer, this electrode gave the lowest interference with blood (+14 %) compared to the electrode that had ATP and CoA in solution (+78 %).

Another electrode of interest was the (PDA-MWCNT/ACOD/PDA-MWCNT/ACS/BSA)1 fabricated electrode which gave 64 % plus interference. Human serum albumin (HSA) and BSA

have approximately 76 % sequence homology, with a similar three-dimensional structure [347]. BSA is a single polypeptide chain with around 583 amino acid residues and no carbohydrates [299, 300, 348]. At the pH range of 5-7 it comprises of 17 intrachain disulfide bridges and only 1 sulfhydryl group (free thiol), positioned in a repeating series of 9 loop-like structures centred on 8 sequential cys-cys pairs [349]. Albumins contain an excess of amino acids [350]. Serum and plasma albumin comprises of 55-62 % of the protein present.

BSA is used in biosensor fabrication because it is inert, lysine rich and inexpensive, and makes films more stable and sensitive [351]. It has a strong affinity for various types of surfaces and does not interfere in many biochemical reactions [349].

Molecular interactions between NEFA and plasma albumins from various species can have differences [352]. Studies by *Spector et al.* have been done to compare NEFA binding to human, bovine and rabbit albumin [303]. Results for palmitate showed a small difference in the binding constants (bovine > rabbit > human). To human albumin laurate and oleate were bound more tightly than to bovine albumin [352]. Hydrophobic interactions are responsible for the binding energy for fatty acids binding to albumin. The BSA fabricated electrode had +64 % interference in plasma when compared to the electrodes performance with the OA standard.

The PMAA based fabricated electrode gave the lowest current (highest difference compared to (PDA-MWCNT/ACOD/PDA-MWCNT/ACS)1 electrode), and its interference was so high that it was unreadable off the graph (shown in Figure 7-17 in the appendix), this was because PMAA was the weakest polyelectrolyte used ($pK_a = 6-7$), so its attraction was not as strong as the other polyelectrolytes. Its carboxylic acid groups degree of ionization depends on the pH [353]. There is significant influence on the complex that is formed of the interacting polymer with its nature and molecular weight [354]. Environmental factors such as the solvent (it is in), pH, ionic strength, temperature and polymer concentration also play a part. Poly[(meth)acrylic acid]s make interpolymer complexes with:

- Non-ionic proton accepting polymers and their derivatives
- Cationic polyelectrolytes in media (aqueous and organic)

Table 5-3: Electrode comparison for CA at 500 mV, current taken at 500 s.

Electrode fabrication	Sensitivity (μA/mM)	R² value	Linear detection range (mM)	Current for 0.90 mM OA (μA)	% difference with (PDA-MWCNT/ACOD/PDA-MWCNT/ACS)	Tested with plasma/serum	Sensitivity (μA/mM)	R² value	% interference
(PDA-MWCNT/ACOD/PDA-MWCNT/ACS)	0.6562	0.9883	0.1 – 0.9	0.7480	-	5 serum	1.1514	0.9974	105 % +
(PDA/ACOD/PDA/ACS)	1.4969	0.9620	0.1 – 0.9	1.3543	81	4 serum	3.7640	0.9864	16.8 % +
(PDA-MWCNT/ACOD/PDA-MWCNT/ACS/PMBN)	0.8335	0.9516	0.1 – 0.9	0.8089	8	5 plasma	0.1149	0.3358	78 % +
(PDA-MWCNT/ACOD/PDA-MWCNT/ACS/PMBN+ATP+CoA)	0.8613	0.9464	0.1 – 0.9	0.8557	14	5 plasma	-0.6584	0.5083	14 % +
(PDA-MWCNT/ACOD/PDA-MWCNT/ACS/BSA)	0.6790	0.9510	0.1 – 0.9	0.5985	-20	5 plasma	0.3904	0.3562	64 % +
(PDA-MWCNT/ACOD/PDA-MWCNT/ACS/PDA-MWCNT/PSS)	0.4810	0.9639	0.1 – 0.9	0.4192	-44	4 serum	1.4308	0.9474	208 % +
(PDA-MWCNT/ACOD/PDA-MWCNT/ACS/PDA-MWCNT/PMAA)	0.2571	0.9108	0.1 – 0.9	0.2588	-65	4 serum	1.6474	0.9922	-

Table 5-4: Electrode comparison for LSV at 1 mV s⁻¹, current taken at 500 mV.

Electrode fabrication	Sensitivity (μA/mM)	R² value	Linear detection range (mM)	Current for 0.90 mM OA (μA)	% difference with (PDA-MWCNT/ACOD/PDA-MWCNT/ACS)	Tested with plasma/serum	Sensitivity (μA/mM)	R² value
(PDA-MWCNT/ACOD/PDA-MWCNT/ACS)	1.7222	0.9929	0.1 – 0.9	1.5320	-	5 serum	2.6738	0.9972
(PDA/ACOD/PDA/ACS)	2.2021	0.9651	0.1 – 0.9	2.0387	33	4 serum	3.8001	0.9661
(PDA-MWCNT/ACOD/PDA-MWCNT/ACS/PMBN)	1.4505	0.9776	0.1 – 0.9	1.3211	-14	5 plasma	4.7975	0.4555
(PDA-MWCNT/ACOD/PDA-MWCNT/ACS/PMBN+ATP+CoA)	1.7383	0.9278	0.1 – 0.9	1.7107	12	5 plasma	-1.2018	0.4256
(PDA-MWCNT/ACOD/PDA-MWCNT/ACS/BSA)	1.0190	0.9840	0.1 – 0.9	0.9094	-41	5 plasma	-0.1047	0.0155
(PDA-MWCNT/ACOD/PDA-MWCNT/ACS/PDA-MWCNT/PSS)	0.8144	0.9909	0.1 – 0.9	0.7168	-53	4 serum	2.3723	0.9134
(PDA-MWCNT/ACOD/PDA-MWCNT/ACS/PDA-MWCNT/PMAA)	0.5372	0.9629	0.1 – 0.9	0.5080	-67	4 serum	1.9237	0.9884

5.4.1 Problems with working in blood

Even after the incorporation of the last layer (as shown as a pictorial scheme in Figure 5-1) in to the standard bienzyme electrode, the interferences were not significantly reduced. Biological variation of some metabolites (in plasma NEFA) makes the status of healthy individuals hard to define in just one reading [355]. There is conflicting information in literature regarding the correct time to detect NEFA from patients blood and this varies depending on the method that is used for NEFA determination.

Once the blood is withdrawn from the patient, the NEFA should be analysed at once, this has been emphasised by many authors [356-358]. If there is a delay in NEFA extraction and detection the results are not representative of the actual NEFA concentration of the patient at the time it was withdrawn. Table 5-5 lists the different techniques in literature that have come across this problem and the optimum conditions derived for NEFA storage and accurate determination that was found. Some studies were done in which two or more techniques of NEFA detection were compared, and in which the concentration of NEFA detected increased over time [359, 360]. Over the other methods, the enzymatic method was chosen in hospitals as it was the easiest to do (low training needed) and took the least time, the method could be easily automated, reducing the amount of reagents needed and the cost for each analysis, so this was the method chosen in hospitals till today [360]. However this enzyme method gives total NEFA levels, and the concentration of each fatty acid is unknown [1]. The data obtained from Figure 5-7 has been incorporated into the table, the pattern observed in this work follows the norm with regards to fluctuations in NEFA detection in blood.

Table 5-5: Different methods of NEFA detection and concentration difference during storage.

Detection of NEFA in	Method of NEFA detection	Time after which analysed	Storage	Information found	References
Plasma and serum of healthy adults	Extraction, TLC and methylation, then quantitated via GC column with flame ionization detector	1-3 days after methylation and extraction	at 4 °C under nitrogen	3 % change in NEFA concentration	[361]
Whole blood	Extraction, TLC and methylation, then quantitated via GC column with flame ionization detector	2 hours	at room temperature	At 24 hours in room temperature for the unsaturated NEFA the % of control value was twice as high as for the saturated NEFA. Storage at -20 °C without nitrogen led to oxidation of double bonds in unsaturated NEFA.	[358, 361]
Plasma		48 hours	at 4 °C		
		6 hours	at room temperature		
		48 hours	at 4°C		
		10 days	at -20 °C under nitrogen		
Serum	Extraction then titration [362]	1 hour	at room temperature	Increase of total NEFA serum concentrations in both samples by 50 %	[363]
		1 hour	frozen		
Plasma	Comparative study of calorimetric method and titration method	Immediately upon separation	at room temperature	NEFA level rose	[364]
		2-48 hours after separation	at room temperature	Increase by 100 % within 24 hours	
		1-60 days later	at -20 °C	Reduction of NEFA after 2-3 days, greatest after 30-50 days. Further storage had no additional loss.	

Plasma	Extraction into organic phase, purification with silica, dried then derivatised via GC column with dual flame ionization detectors	Immediately upon extraction and assay	at room temperature	Used as control	[158]
		24 hours	at 4 °C	8 % increase	
		1 hour	at room temperature	22 % increase	
		1 month	at 15 °C	6 % decrease	
Plasma	Commercial NEFA-C test Wako enzymatic kit	1 month	at -18 °C	No change in the total amount of NEFA	[360]
Plasma	Extraction then titration [362]	6 months	at room temperature	4 fold increase in NEFA concentrations	[359]
	Extracted, saponified, dissolved and titrated [365]	6 months	at room temperature	NEFA concentrations fell sharply and activity disappeared after 2/3 months	
Serum	Ether extraction		at 4 °C	Storage in fridge resulted in rise in NEFA level	[366]
Plasma and serum	Separation and titration	Immediately upon separation	at room temperature	Best	[367]
		1 hour	at 4 °C	Gave lower reading	
		24 hours to 4 days	at 4 °C	Once sample is separated, similar results within this time period	
Plasma	Extraction, then quantitated via GC column with mass spectroscopy	10 hours	at 4 °C	Stable	[58]
		1 to 7 days	at -20 °C	Stable	
		3 months	at -80 °C	Increase levels by 30 %	
Plasma	Chronoamperometry	1 hour	at -80 °C	In 3/6 of samples increase in concentrations by over 100 %	This work

5.4.2 Why does NEFA concentration increase over time?

NEFA binding with albumin, can cause underestimation of plasma NEFA [368]. Therefore a small percentage of NEFA in plasma cannot be dissociated from albumin, and cannot take part in the reaction to quantify the NEFA concentration.

Lipoprotein lipase (LPL) is released by heparin from the endothelium and causes the breakdown of circulating triglycerides to NEFA via hydrolysis [369, 370]. This lipolysis continues *in vitro*, producing artificially high NEFA concentrations [82]. The lipolytic activity needs to be inhibited to stop this, for example with the use of tetrahydrolipstatin during storage of sample [369]. Once the sample is taken, instant freezing of the plasma sample does not limit the *in vitro* lipolysis. Structure of the compound is shown in Figure 5-11 below.

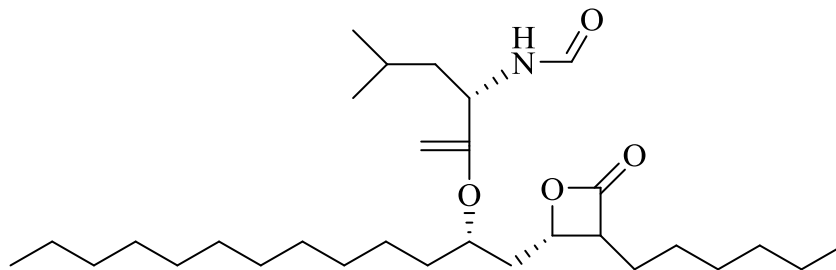


Figure 5-11: Structure of tetrahydrolipstatin [371].

There have been different results reported for the breakdown of phospholipids once plasma has been incubated [372]. Work done by Dole showed that before extraction, plasma incubated at 37 °C increased the acidity by 35 $\mu\text{Eq/L}$ [362]. The cause was found to be enzymatic hydrolysis of esterified fatty acids. The increase was prevented by adding 0.1 M CuSO_4 or ethanol. The conversion of lecithin to lysolecithin accounted for the rate of release of the fatty acids [373]. In many of the experiments, most of the acidity determined is a feature of the albumin-bound fatty acids, as there is little/no hydrolysis of triglyceride happening in the extraction or titration steps that follow [362]. A few proteins other than albumin can bind to NEFA, however none bind as much or as tightly as albumin [352]. Numerous intracellular proteins such as the cytoplasmic fatty-acid binding protein can bind to NEFA, the same with fructose 1,6-diphosphate-1-phosphatase and acetyl coenzyme A carboxylase. Catecholamines (e.g. norepinephrine and isoproterenol) are key stimulating agents of lipolysis [374]. They have been infused *in vivo* to

study the release of NEFA in plasma, and can be used *in vitro* to stimulate the release of NEFA in adipose tissue or adipocytes in culture.

The norm concentration of NEFA also differs depending on what nutritional state of the patients the samples are collected in. As in, whether the patients are healthy or diabetic, whether they were fasting or not and whether they were exercising at the time of sampling or not. The variety of means has resulted in the widespread of norm values in literature [356]. After a carbohydrate meal, the metabolism of carbohydrates provides the heart with its energy, and the NEFA levels drop low, with myocardial extraction of NEFA decreasing, but in a fasting scenario, non-carbohydrates (fatty acids) provide myocardial energy [375]. In a study by *Rothlin and Bing*, random patients plasma samples were taken from a hospital after a 12 hour fast, oleic acid concentration was found higher in these patients compared to the study done by *Dole et al.* in which similar concentrations of palmitic and palmitoleic acid concentrations were found in healthy subjects [86, 376]. The changes are due to different rates in myocardial uptake of individual NEFA. Plasma NEFA concentrations are higher in patients with T2D, obesity or insulin resistance [369]. As NEFA provide immediate supply of energy to muscles and the heart, this also needs to be considered when quoting concentrations of NEFA from different patients.

There is a lack of relationship between plasma NEFA concentrations and other measurable variables, questioning the daily reproducibility within individuals of NEFA concentrations [49]. Both the NEFA concentration and its flux through the circulation varies widely from hour-to-hour, dependant on nutritional state and physical activity (greatly controlled by hormonal, metabolic and neural signals) [81]. In one study fasting samples were taken from 12 healthy individuals on consecutive mornings and NEFA was determined using the Roche Applied Science colorimetric method [355]. The same method used in the optical validation work in section 5.2. The results in that study had very high variability (within person the biological coefficient of variation was 45 % for NEFA, compared with lactate 31 %, triglycerides 21 % and glucose 4.8 %). The results implied that plasma NEFA concentrations generate ‘almost random numbers!’ [49]. Biological variation may be due to variation in: assays, technique (e.g. patient blood sampling), day-to-day conditions and biological status of an individual. Making NEFA concentrations not the ideal marker for epidemiology [72].

Another important factor is time. The quality of the result is degraded if the sample is not transported and analysed in time [339]. 5 % stability loss is the maximum permissible storage time [341]. An elevated concentration *in vitro* is not just a problem for NEFA determination. Other research has been done on other biomarkers such as glucose and lactate in which the concentration of the analyte shifted over time. With limited oxygen supply glucose is converted to lactic acid by anaerobic metabolism, reducing glucose concentration and subsequently increasing concentrations of lactate and H⁺ [339]. The reaction speed is proportional to the temperature, time and amount of metabolically active cells in the sample. To stop these metabolic changes, glycolysis inhibitors should be present in the sampling tube. Albumin and other plasma proteins are very stable, so will still be present as interference in the work. Always resulting in a lower current response.

Factors influencing measured NEFA biomarker levels [84, 85]:

- Age and sex – effects of growth hormone and oestrogen levels
- Dietary intake
- Supplement use by individual
- Sampling site, procedure, amount sampled (detection limits), sample handling and storage
- Analytical method
- Lipolysis/fasting state of individual
- Status of nutrition
- Lipogenesis
- Diseases affecting measurement (e.g. cystic fibrosis, liver cirrhosis, diabetes, zellweger syndrome).

All these factors need to be taken into consideration when working out NEFA biomarker concentrations. Having a study that is consistent in the group/type of people who donate plasma/serum for NEFA detection is paramount to the future of any NEFA biosensor development.

It is unknown what disease state these donors (people who donated their blood for this study) were in/if any, leading to the complication in getting a consistent reading with varying NEFA concentrations. The donors may have been in completely different disease states, or having elevated concentrations of other compounds in their blood which would have caused interference on the fabricated electrode, e.g. ascorbic acid.

In future taking blood from the same sample of donors would provide more consistent data for the sensor in reading concentrations of blood NEFA within certain conditions. In a practical application, some sensors are prone to certain interferences which are present at high enough concentrations in the patients blood. These sensors would state in the information manual provided that the sensor would not be suitable for patients suffering from that disease because of a specific interference or increase in concentration of a compound.

It would have been useful to have had the concentration of glucose/ascorbic acid/uric acid worked out (via assays) for each plasma/serum sample. This would have shown how much the concentrations of each patients had differed and if that difference was causing the difference in NEFA levels determined via CA.

Having a finger prick sensor would give instantaneous results of NEFA, when compared to the current method used in hospitals which involves transportation of sample across a city or region to get it tested via the optical UV method. In addition, compare the time taken for CA at 500 mV after 500 s vs. the 35 minutes plus for the current UV method to give the NEFA reading in the concentration of blood sample.

5.5 Conclusions

The aim of this chapter was to fabricate an enzyme electrode based on the original bienzyme electrode (PDA-MWCNT/ACOD/PDA-MWCNT/ACS)¹ to keep interferences in blood to a minimum.

Many enzyme electrodes were fabricated using LbL method on C-SPE, including the use of PMBN, BSA and the polymers PSS and PMAA. Calibration plots were first obtained with different concentrations of OA standard using CA at a set potential of 500 mV for each fabricated electrode. After the original electrode, (PDA-MWCNT/ACOD/PDA-MWCNT/ACS/PDA-MWCNT/PSS)¹ had the highest linearity for CA (with R^2 of 0.96) and LSV (with R^2 of 0.99).

The linear detection range of each of the new fabricated electrodes was the same as the reference electrode, 0.1 mM to 0.9 mM OA.

The choice of whether to test in serum or plasma was also investigated. Serum and plasma samples were tested electrochemically to detect the NEFA concentrations. The actual NEFA concentration in each blood sample was pre-determined using the UV method from following either Roche Applied Science or Wako Diagnostics protocols.

The problems of working in blood for NEFA detection were highlighted, along with reasons as to why there are major fluctuations within reproducibility using the same blood sample. This problem had been encountered by many authors for a range of NEFA detection techniques.

6 Conclusions and recommendations for future work

6.1 Conclusions

The development of an electrochemical biosensor for NEFA is feasible. The oxidation of H_2O_2 was detected using 3 SPE's from the enzymatic reaction of acylated NEFA and the enzyme ACOD (step 2 of scheme 1). This showed linear, reproducible calibration graphs.

Enzyme electrodes were fabricated to lose having the enzyme ACOD in solution. (PDA-MWCNT/ACOD)² was the first enzyme electrode fabricated based on LbL method. This also gave linear corresponding current which was detectable using LSV. The main bienzyme electrode was (PDA-MWCNT/ACOD/PDA-MWCNT/ACS)¹ which was used throughout the study as the standard enzyme electrode, due to its reproducibility and linearity. This fabricated electrode now eradicated the use of both ACOD and ACS in solution, only leaving the addition of solutions of ATP and CoA to complete the enzymatic reaction and produce H_2O_2 . The different electrode combinations and enzyme ratios were investigated leaving a chosen method for future work. The compound NEM was dropped from the NEFA sensor development as it was not needed for electrochemical NEFA detection (saving potential cost and time).

Multiple enzyme electrodes were fabricated on C-SPE and tested with serum/plasma samples for NEFA detection. The most promising electrode was with the addition of PMBN as a blocking agent to potential interferences in human blood.

The expected product will help researchers know more about the metabolic information in the patients and ultimately improve their lifestyle by helping them track and monitor their blood NEFA levels in addition to their blood glucose levels. NEFA detection is much less studied in comparison with glucose. Opening up a pathway for a new market for this sensor development. But before the sensor can be developed any further, work needs to be done on the reproducibility of NEFA concentrations in blood, in both the optical method (as validation) and in the electrochemical method presented. The optimal method of blood extraction, storage and reproducibility needs addressing, as this has been found as missing in literature.

6.2 Recommendations for future work

The most simplest and common types of biosensors consist of H_2O_2 detection [377]. So with keeping this in mind, further work can be suggested.

As there was no effective blocking membrane found for NEFA detection, other compounds could be investigated. Nafion could be used as a blocking membrane to prevent interferences passing through [378]. It contains two different regions (hydrophilic polymer backbone and outside the hydrophobic region, the hydrophilic sulfonate groups) [209]. Nafion provides electrostatic repulsion, by being a negatively-charged perfluorinated ionomer, successfully limiting the anionic interferences from adhering to its surface [379]. It also reduces the rate of biofouling [380]. Nafion has been used extensively in amperometric biosensors (e.g. in glucose sensors as the outer coating [338]) and can be applied to this current fabrication system. Nafion can be used to solubilize CNT giving effective electrocatalytic action of CNT towards H_2O_2 [268]. Also alternate deposition of nafion and cellulose acetate can be used to eliminate interferences [381].

As ACOD contains FAD, the well defined direct electrochemical behaviour of flavoprotein-oxidase systems is extremely difficult due to the FAD moiety deeply embedded in a protective protein shell [274]. Direct electron transfer cannot occur from the enzyme to the electrode. Mediators are therefore needed. Co-immobilization of enzyme and electron mediator on the electrodes surface can give a mediator based biosensor [377]. Mediators can be used to shuttle electrons to and from the enzyme and electrode. The mediator is free to move between the enzyme active site and the electrode surface, reducing the electron tunnelling distance. A redox mediator could oxidize H_2O_2 or the enzyme ACOD, and then be reduced in turn by the surface of the electrode [269]. Good redox mediators should be:

- small in size and molecular weight
- independent of pH
- having its electron transfer properties reversible
- chemically stable in both forms (oxidized and reduced)
- immobilized easily

Common class of redox mediators used for H₂O₂ detection is the ferrocenes (Figure 6-1). The molecule bis-cyclopentadienyl iron(II) (the full name of ferrocene) has a sandwich-type structure, here the iron atom is sandwiched in the middle of two five-membered carbon rings [250].

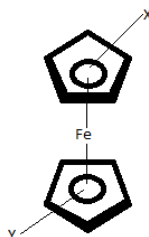
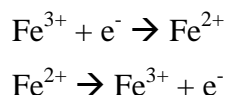


Figure 6-1: Structure of Ferrocene (its derivatives have different functional groups on X/Y).

Ferrocene just as common iron centred inorganic complexes can undertake reversible 1 e⁻ oxidation / reduction, with the electron transfer rate being extremely quick.



However direct electron transfer (without mediators) would be more advantageous, as it helps develop reagentless biosensors [382].

Due to the high interference of readily oxidizable compounds in blood at 500 mV, CA could be done at a lower potential of 300 mV (shown in Figure 6-2). The calibration graph of this at 500 s is shown in Figure 6-3. At the lower potential there is lower H₂O₂ oxidized, however the sensor would be less susceptible to interferences such as ascorbic acid, uric acid and acetaminophen. The linear detection range at this potential was 0.0 to 0.9 mM OA (the same as that of 500 mV), the sensitivity was 0.5072 μA/mM and the R² value was 0.9988. Repeating the blood experiments at this lower potential may have been good to provide a comparison. Further work could explore the avenue of having a reduced potential of 300 mV.

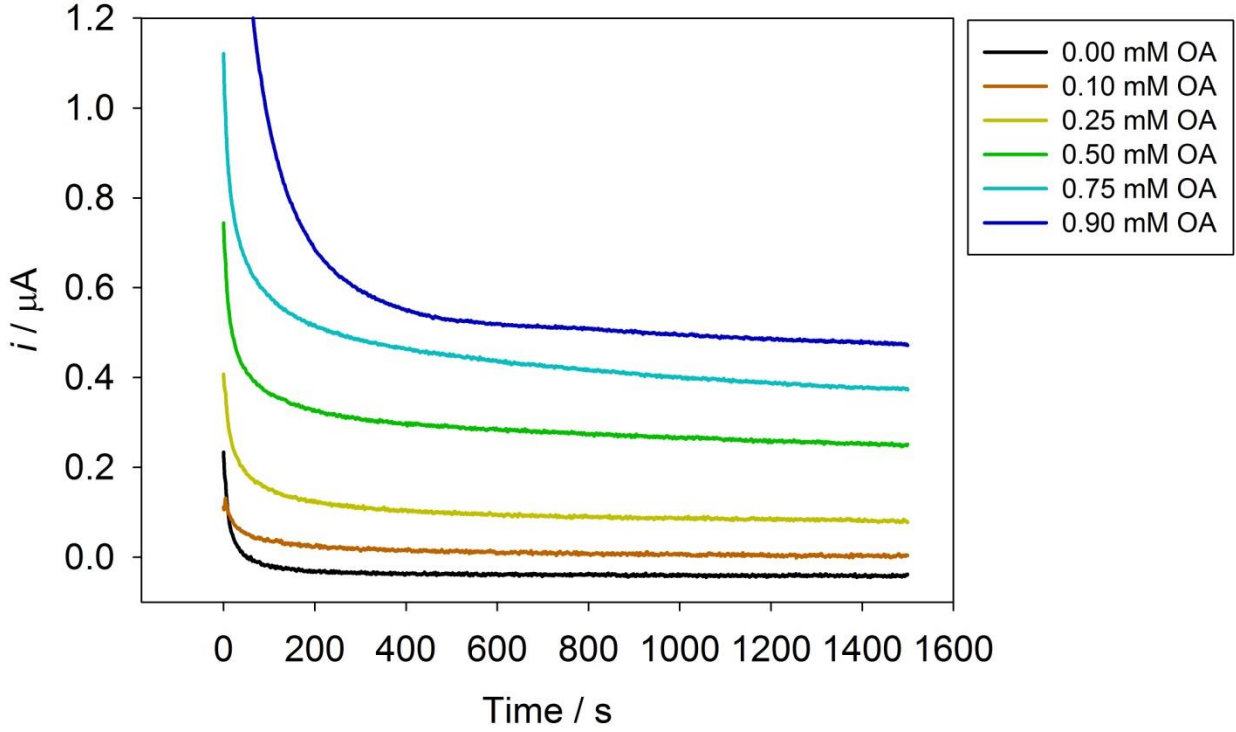


Figure 6-2: CA at 300 mV for various concentrations of OA measured at a C-SPE modified with (PDA-MWCNT/ACOD/PDA-MWCNT/ACS)1 in 1 mM ATP and CoA and 0.1 M phosphate buffer pH 7.4.

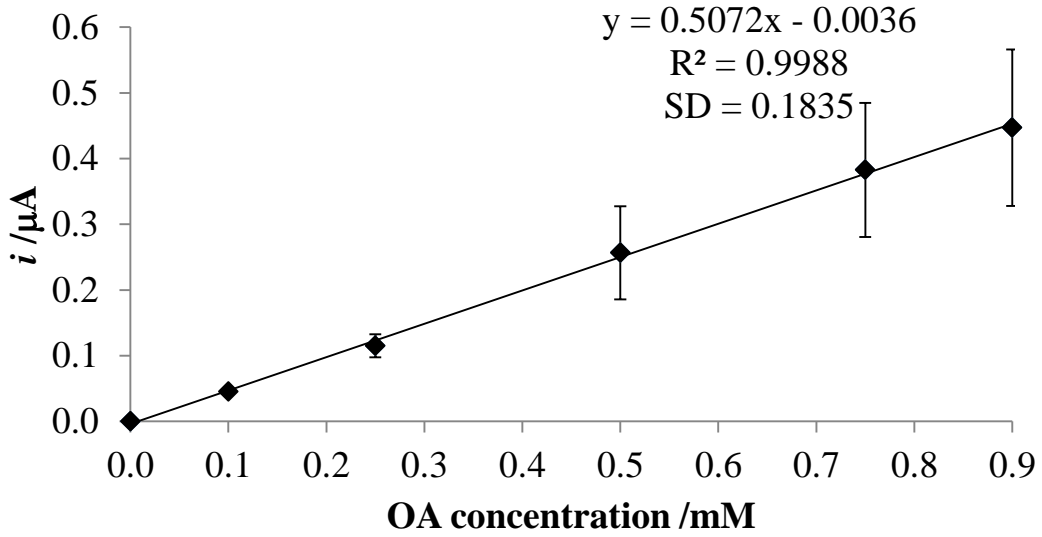


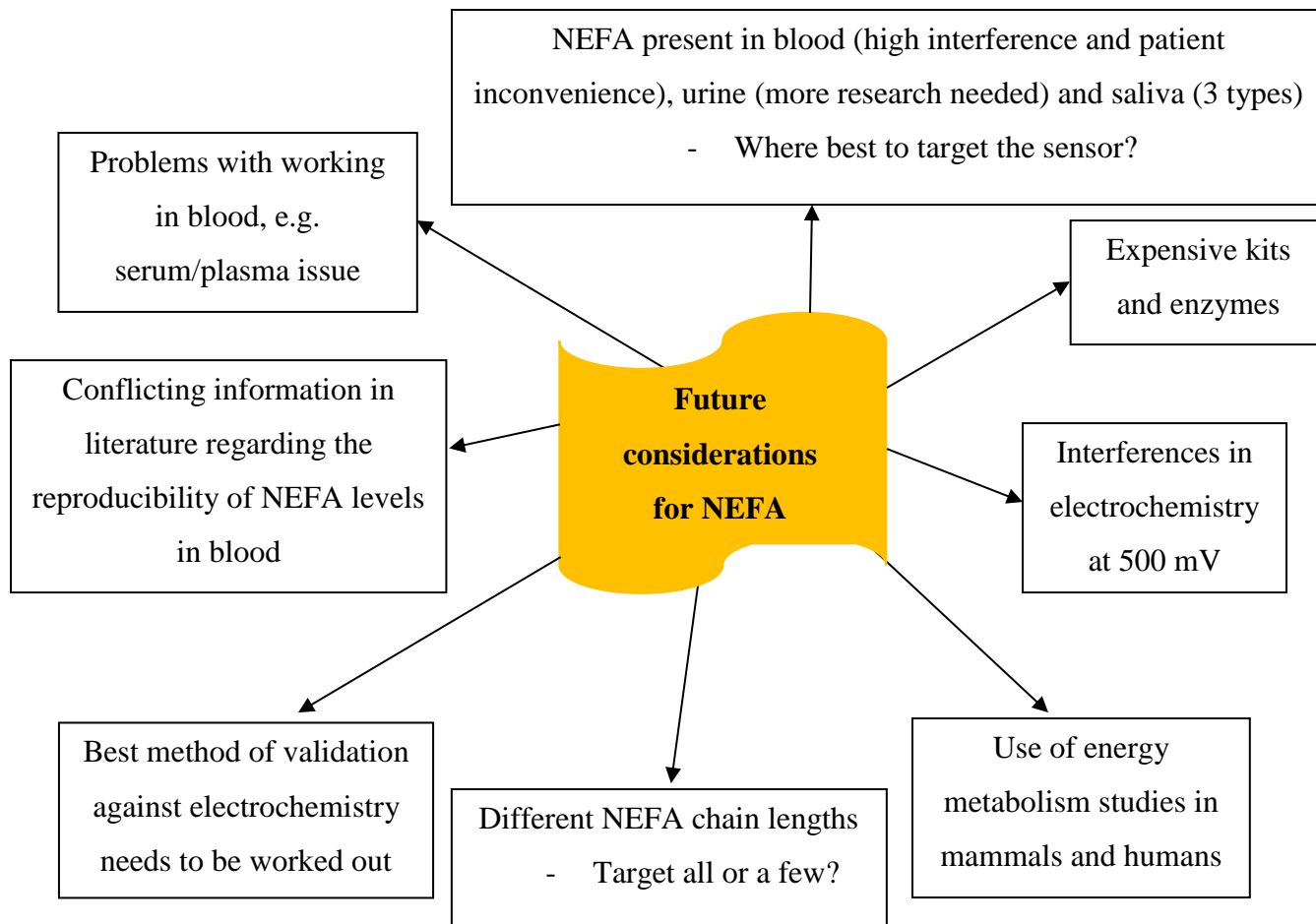
Figure 6-3: Calibration graph at 500 s.

The reduction of H_2O_2 can also be investigated. As the potential at which H_2O_2 oxidises causes large interferences, the reduction does not have this disadvantage. H_2O_2 can be reduced at ~ 0.0 V by metalized carbon (e.g. rhodium or ruthenium on carbon working electrode) transducers [383]. At this potential most undesirable electrochemical reactions of potentially interfering substrates are insignificant.

Currently, the only fatty acids investigated were palmitic and oleic acid. There are many fatty acids present in the blood and plasma, which may or may not have an influence on patients with T2D or for metabolism studies in general. The structure of the fatty acid will have an effect on its detection. Other fatty acids that will may also need to be investigated are linoleic acid (C 18:2), which has two double bonds and stearic acid (C 18:0), which is a longer saturated chain compared to palmitic acid.

There has been an increased demand of multianalyte sensing devices [384]. This is very useful for energy metabolism biomarkers, or in combining the detection of the different biomarkers in one simple sensor, which would work by just one finger prick of blood. Another research interest may be to combine NEFA (lipid store) and glucose (carbohydrate store) and have one sensor that can detect both, helping the patient manage and control their diabetes better. This is ideal as patients already monitor their glucose and there are already third generation glucose sensing kits based on electrochemical methods. Personalised intervention programmes for treatment and management of T2D would find this sensor useful. Offering more comprehensive information of the patients metabolic profile for both patient and clinician, leading to better disease management.

The future considerations in NEFA sensor development are shown in the mind map below:



7 Appendix

Publications from this work:

- Kang J, Hussain A T, Catt M, Trenell M, Haggett B and Yu E H, 'Electrochemical detection of non-esterified fatty acid by layer-by-layer assembled enzyme electrodes', (2013) 190 *Sensors and Actuators B: Chemical*.

Oral presentations at conferences:

- Northern Postgraduate Chemical Engineering conference (NPCEC), Newcastle from 8-9th August 2013. Presentation titled 'Development of non-esterified fatty acid (NEFA) electrochemical biosensor for patients with type-2-diabetes'.

Poster presentations at conferences:

- Biosensors 2012, Cancun Mexico from 15-18th May 2012. Poster titled 'Electrochemical biosensor development for non-esterified fatty acid (NEFA) detection'.
- Diabetes UK 2014, Liverpool UK from 5-7th March 2014. Poster titled 'Development of electrochemical non-esterified fatty acid (NEFA) biosensor for patient management of type-2-diabetes'.

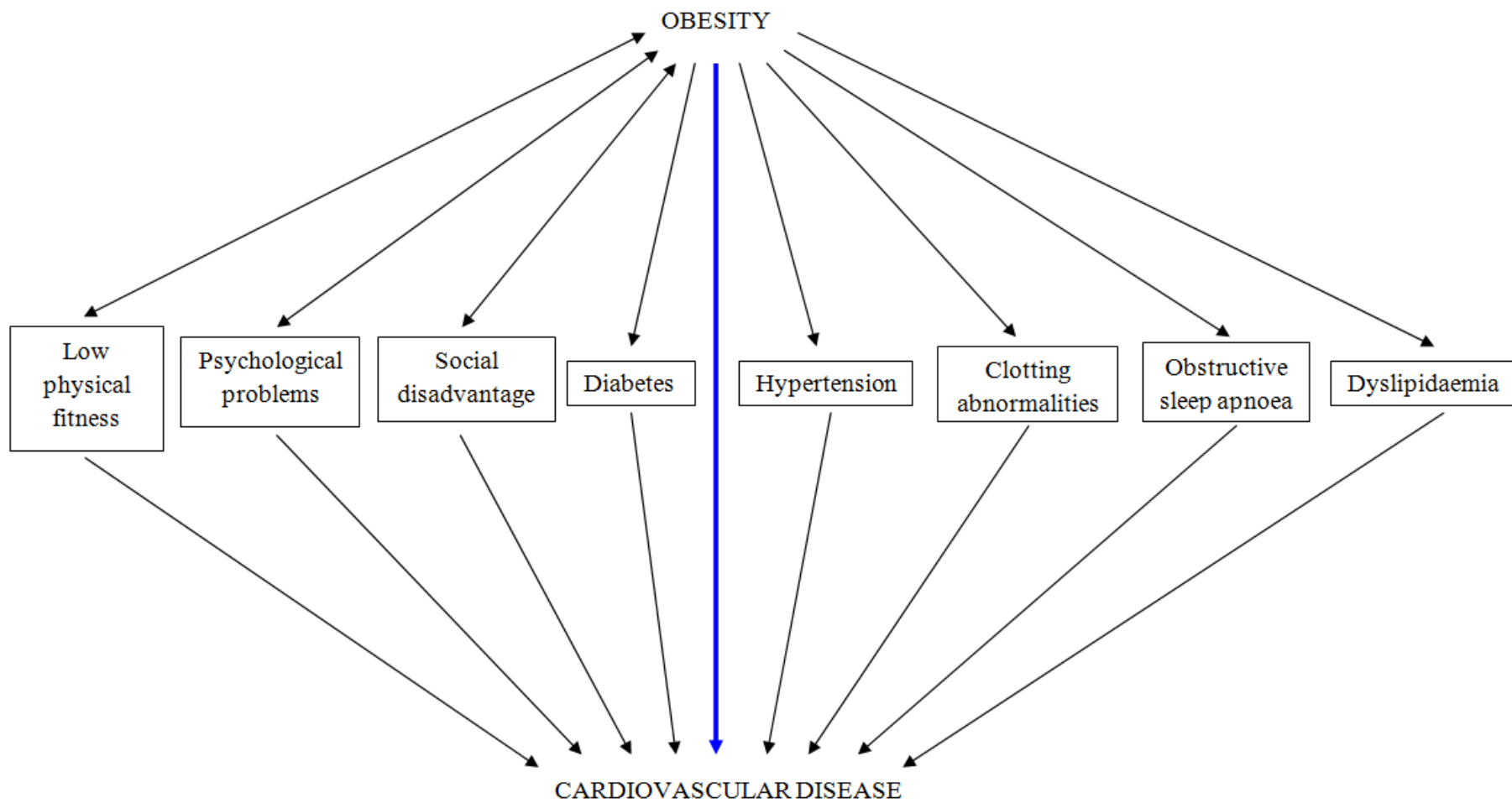


Figure 7-1: The factors that contribute towards cardiovascular disease in obesity [385].

Uric acid

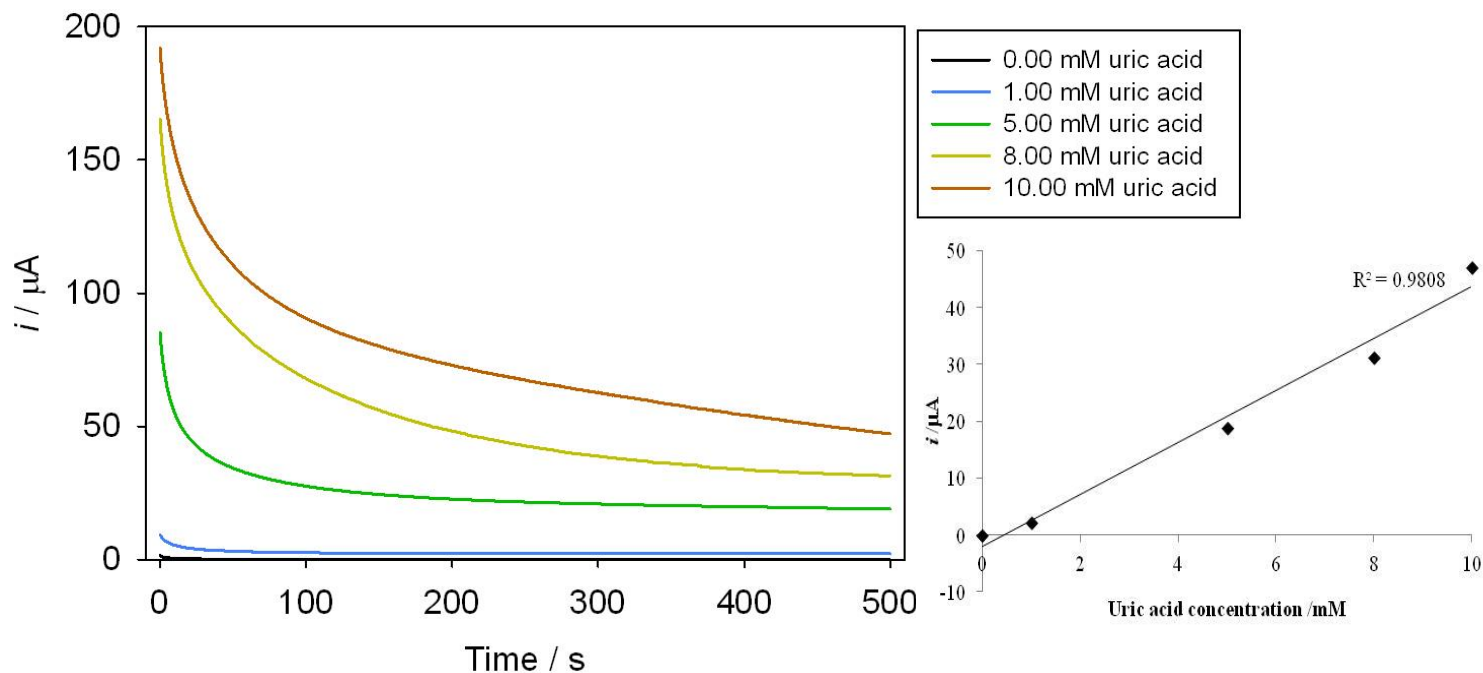


Figure 7-2: CA at 500 mV for various concentrations of Uric acid measured at a C-SPE in 0.1 M phosphate buffer pH 7.4. Inset: Calibration graph at 500 s.

Figure 7-2 shows the CA at 500 mV for uric acid on the C-SPE. The inset shows a linear calibration graph obtained at 500 s. In humans, the end product of purine metabolism is uric acid [386]. The major purine nucleosides, adenosine and guanosine get converted to uric acid via an intermediate. High serum uric acid is linked with higher risk of T2D, this is independent of obesity, dyslipidemia and hypertension [387].

The electrochemical oxidation of uric acid occurs at approximately 460 mV, the electrode surface is fouled by the oxidation product [304]. Its oxidation is irreversible at glassy carbon and metal electrodes and quasi-reversible at a graphite electrode. At pH 7.4 approximately 98 % of uric acid is in the form of monosodium salt [388].

Uric acid is oxidized (Figure 7-3) in a $2e^-2H^+$ reaction to an unstable quinonoid diimine species (half-life ≤ 22 ms), which in a step-wise fashion gets attacked by water molecules forming an anionic imine-alcohol, then uric acid-4,5 diol [304, 389]. This uric acid-4,5 diol is unstable, and

depending on the pH it decomposes to various products. The end decomposition product is allantoin [282].

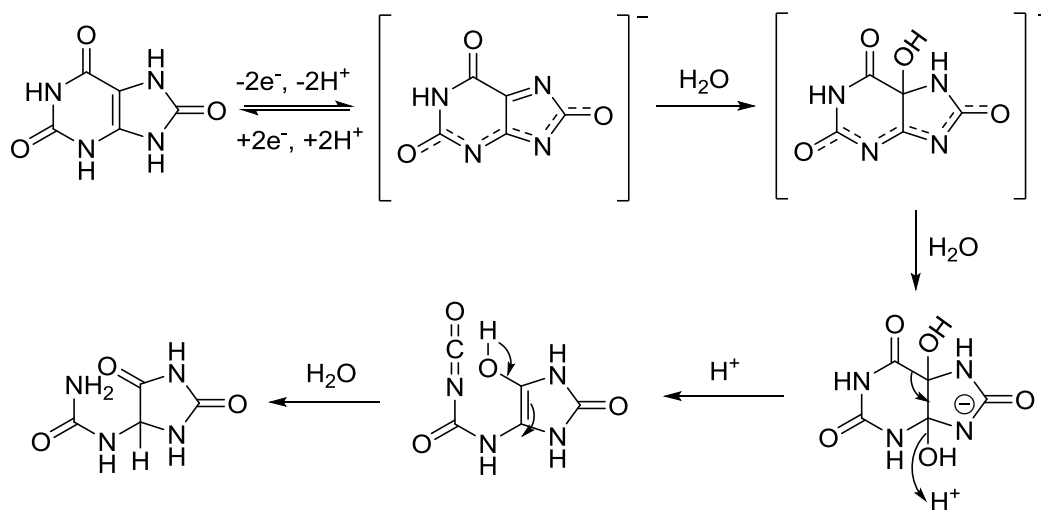
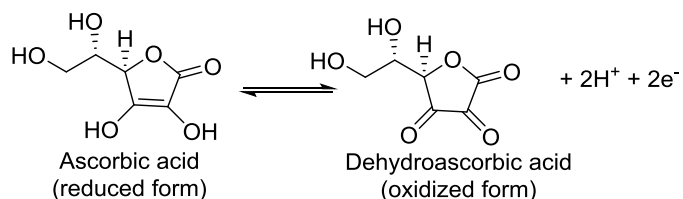


Figure 7-3: Series of reactions that occur with uric acid oxidation [389].

This is what would have fouled the surface of the C-SPE, rendering it unusable for other uric acid concentrations.

Ascorbic acid

Ascorbic acid exists in two ketone tautomers below:



The enol form is less stable. On a bare electrode, the oxidation of ascorbic acid is totally irreversible and requires high overpotential [304]. No reproducible electrode response is found due to the electrode surface getting fouled by the adsorption of the oxidized product of ascorbic acid. Figure 7-4 shows the CA at 500 mV for ascorbic acid on the C-SPE. The inset shows a linear calibration graph obtained at 500 s, the electrode surface has not been fouled by the oxidation product.

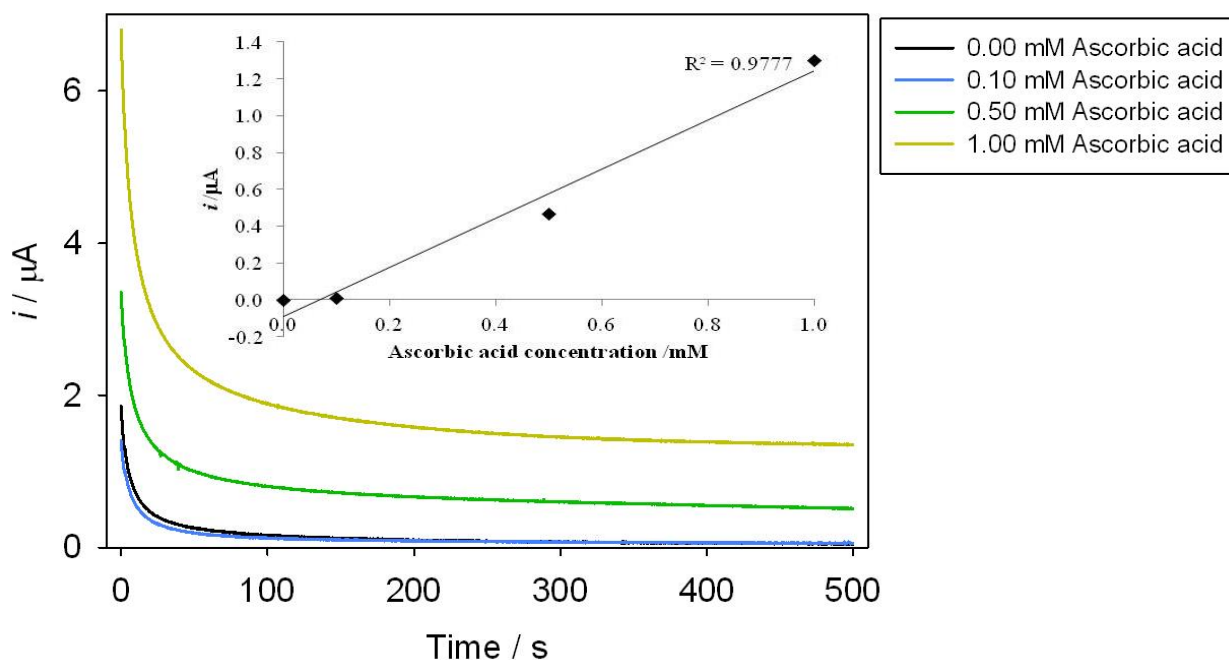


Figure 7-4: CA at 500 mV for various concentrations of Ascorbic acid measured at a C-SPE in 0.1 M phosphate buffer pH 7.4. Inset: Calibration graph at 500 s.

Acetaminophen

Figure 7-5 shows the CA at 500 mV for acetaminophen on the C-SPE. The inset shows a very linear calibration graph obtained at 500 s.

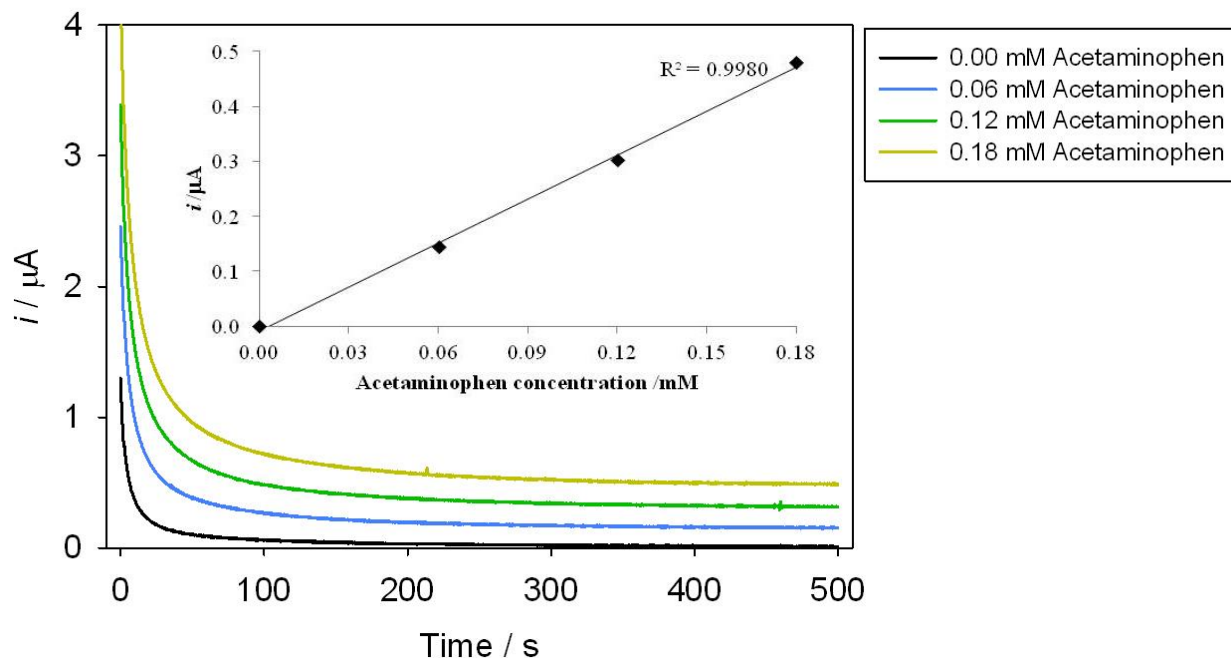
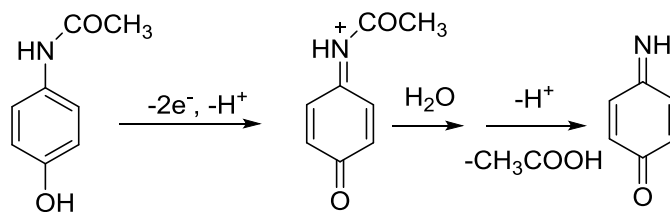


Figure 7-5: CA at 500 mV for various concentrations of Acetaminophen measured at a C-SPE in 0.1 M phosphate buffer pH 7.4. Inset: Calibration graph at 500 s.

Acetaminophen is electroactive and previously voltammetric mechanistic studies for the electrode processes of the acetaminophen/N-acetyl-p-quinoneimine redox system have been done [390]. Its oxidation is reversible during CV. Acetaminophen oxidation is also a $2e^-2H^+$ process, shown below:



Acetaminophen causes a large interference on C-SPE due to its highly oxidizable nature.

PDA based electrode for blood detection

Figure 7-6 shows the chronoamperometric results for OA at 500 mV for the fabricated electrode (PDA/ACOD/PDA/ACS)1. The calibration graph in Figure 7-7 shows the results from CA at 500 s, along with those of 4 serum samples run from the same patient. The UV serum concentrations of 0.107, 0.160, 0.240 and 0.360 mM came to 0.125, 0.210, 0.390 and 0.740 mM electrochemically. This is a 16.8, 31.25, 62.5 and 106 % increase respectively. The higher the concentration of NEFA the higher was the increase of interference.

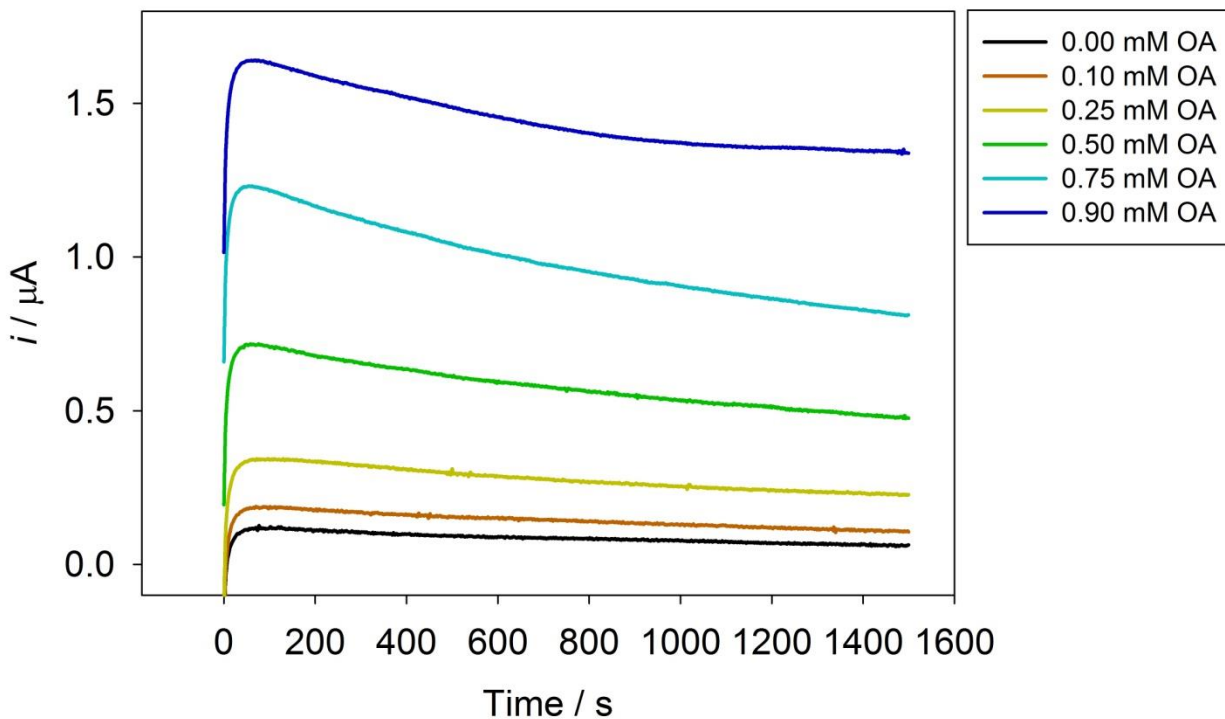


Figure 7-6: CA at 500 mV for various concentrations of OA measured at a C-SPE modified with (PDA/ACOD/PDA/ACS)1 in 1 mM ATP and CoA and 0.1 M phosphate buffer pH 7.4.

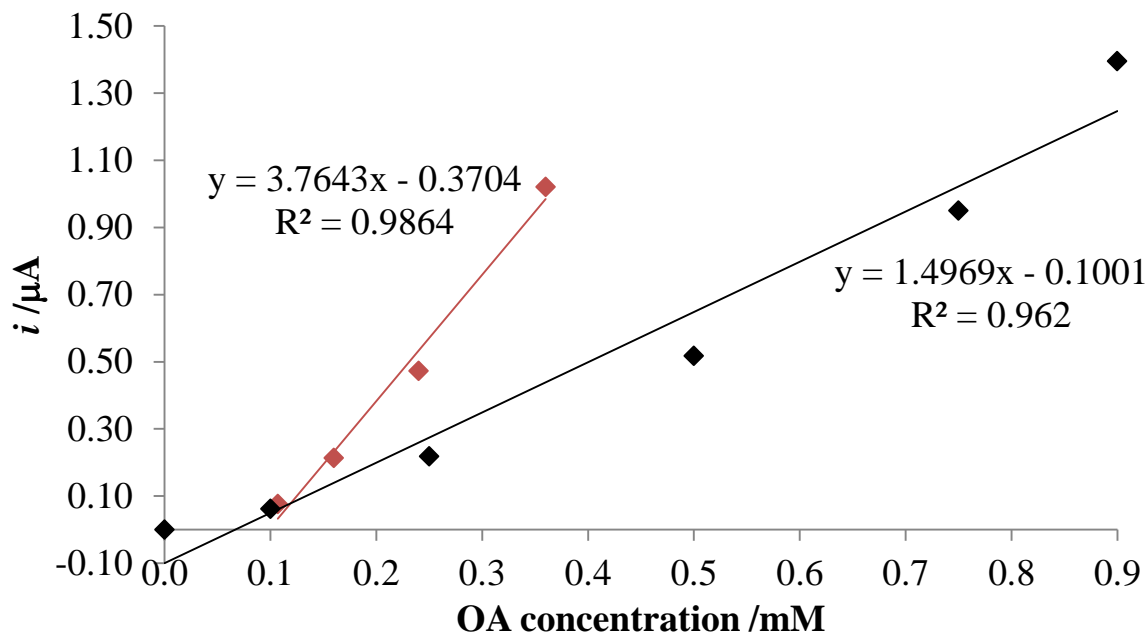


Figure 7-7: Calibration graph at 500 s. 4 serum samples from the same patient in red.

PMBN based electrode for blood detection

Figure 7-8 shows the chronoamperometric results for OA at 500 mV for the fabricated electrode (PDA-MWCNT/ACOD/PDA-MWCNT/ACS/PMBN)¹. The calibration graph in Figure 7-9 shows the results from CA at 500 s, along with those of 5 plasma samples run from the different patients. The UV plasma concentrations of 0.090, 0.216, 0.239, 0.495 and 0.522 mM came to 0.900, 0.875, 0.940, 0.930 and 0.930 mM electrochemically. This is a 900, 305, 293, 88 and 78 % increase respectively. All the plasma samples read to similar values electrochemically. The interferences were too large to detect the difference in the NEFA concentrations for different patients.

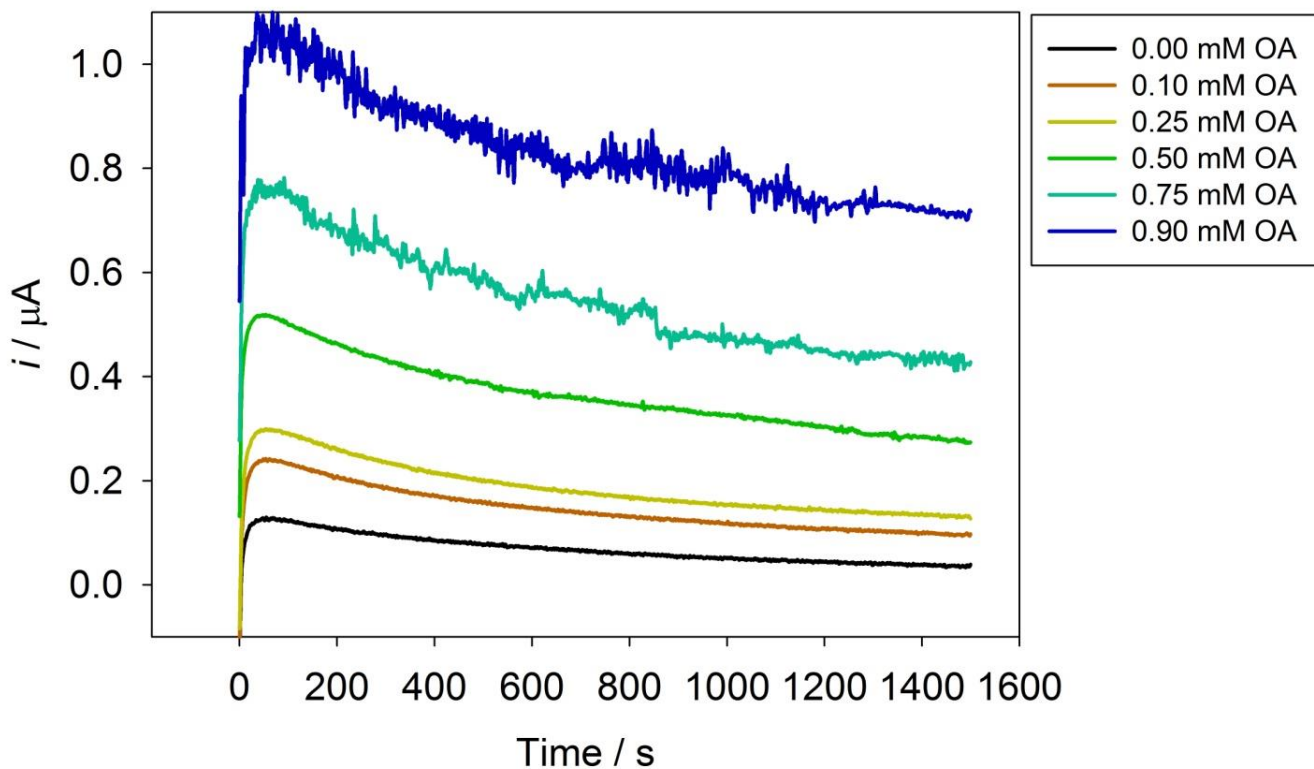


Figure 7-8: CA at 500 mV for various concentrations of OA measured at a C-SPE modified with (PDA-MWCNT/ACOD/PDA-MWCNT/ACS/PMBN)1 in 1 mM ATP and CoA and 0.1 M phosphate buffer pH 7.4.

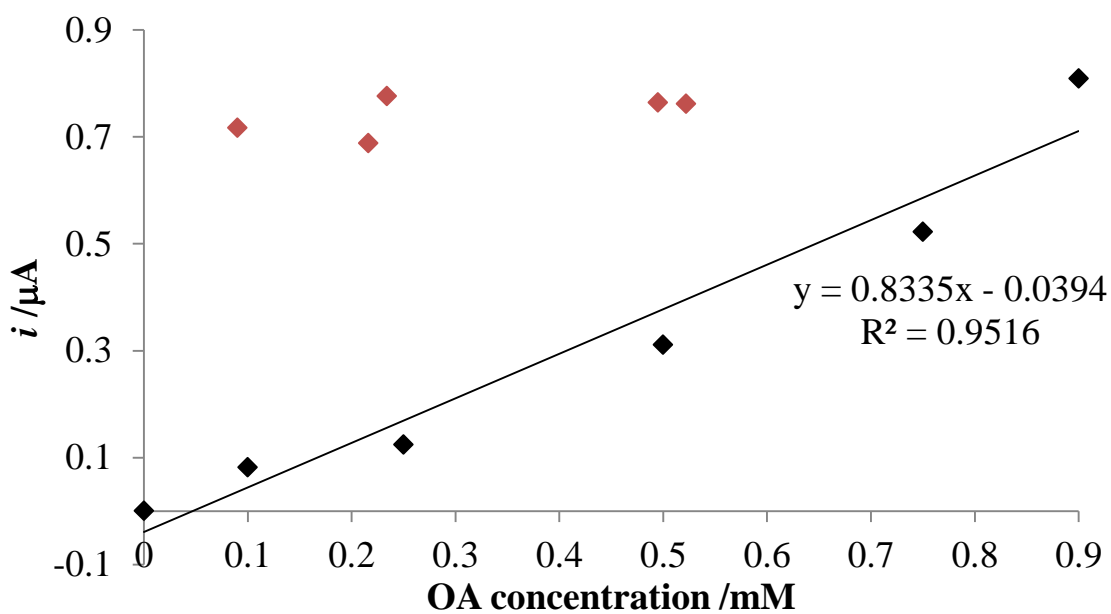


Figure 7-9: Calibration graph at 500 s. 5 plasma samples from the same patient in red.

Figure 7-10 shows the chronoamperometric results for OA at 500 mV for the fabricated electrode (PDA-MWCNT/ACOD/PDA-MWCNT/ACS/PMBN+ATP+CoA)¹. The calibration graph in Figure 7-11 shows the results from CA at 500 s, along with those of 5 plasma samples run from one patient. The UV plasma concentrations of 0.240, 0.265, 0.550, 0.580 and 0.610 mM came to 0.775, 1.080, 0.660, 0.660 and 0.720 mM electrochemically. This is a 223, 308, 20, 14 and 18 % increase respectively. This was a great improvement compared to the electrode (PDA-MWCNT/ACOD/PDA-MWCNT/ACS/PMBN)¹. However similar NEFA concentrations (0.550 and 0.580 mM) that are distinguishable in the UV method, are not distinguishable in the electrochemical method (both showed as 0.660 mM). Increase in concentration of NEFA by 14-20 % in blood compared to OA standard is the best result in all the fabricated electrodes.

The molecular size of phospholipids is < than of proteins, and the molar concentration of phospholipids is > than proteins, therefore phospholipid molecules diffuse from plasma to the polymer surface more readily than proteins [391]. On the MPC copolymers surface, phospholipids are adsorbed immediately undergoing self-organization and forming a stable adsorbed layer that has a surface similar to a biomembrane.

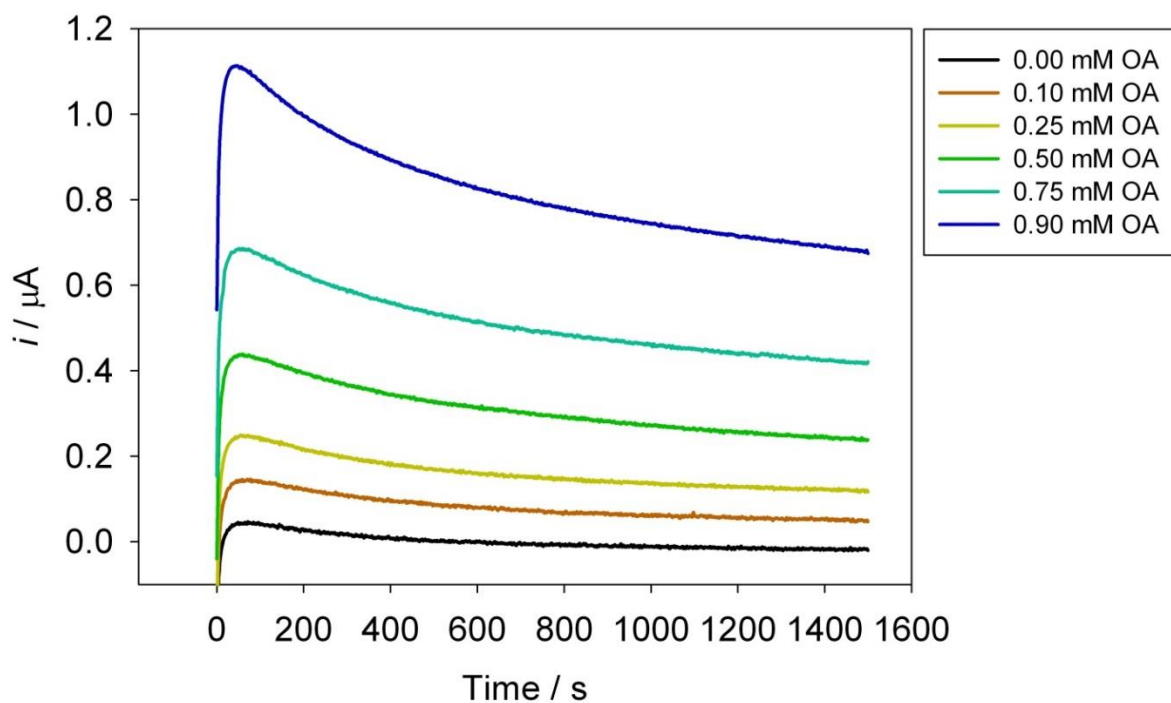


Figure 7-10: CA at 500 mV for various concentrations of OA measured at a C-SPE modified with (PDA-MWCNT/ACOD/PDA-MWCNT/ACS/PMBN)1 in 0.1 M phosphate buffer pH 7.4 (1 mM ATP and CoA in the PMBN layer).

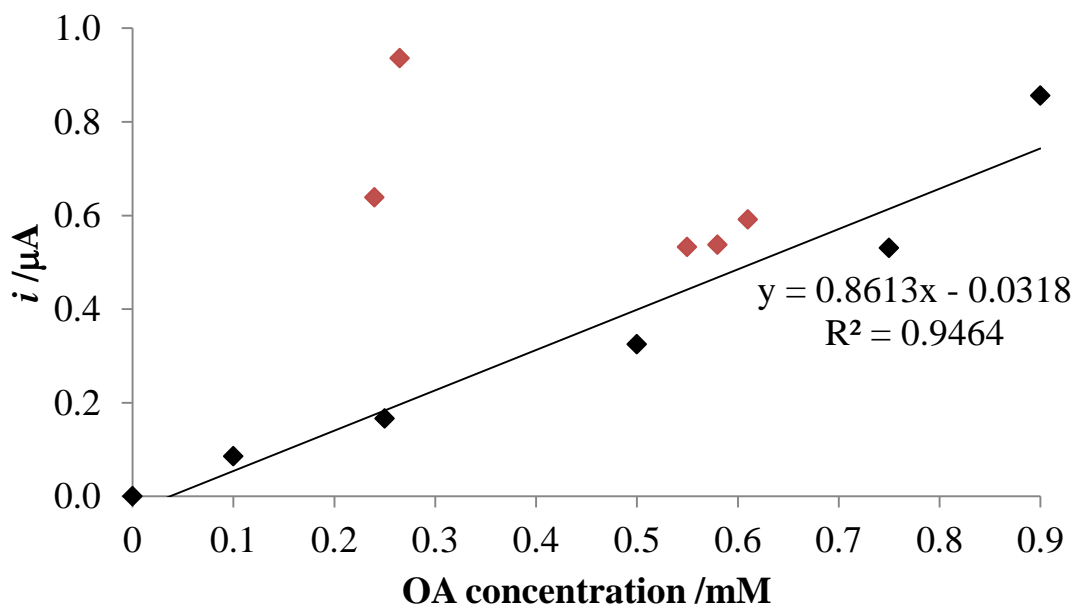


Figure 7-11: Calibration graph at 500 s. 5 plasma samples from the same patient in red.

BSA based electrode for blood detection

Figure 7-12 shows the chronoamperometric results for OA at 500 mV for the fabricated electrode (PDA-MWCNT/ACOD/PDA-MWCNT/ACS/BSA)¹. The calibration graph in Figure 7-13 shows the results from CA at 500 s, along with those of 5 plasma samples run from different patients. The UV plasma concentrations of 0.189, 0.279, 0.405, 0.477 and 0.639 mM came to 0.750, 1.125, 0.870, 0.780 and 1.160 mM electrochemically. This is a 297, 303, 115, 64 and 82 % increase respectively. Again the interference being highest for the lower concentrations of NEFA.

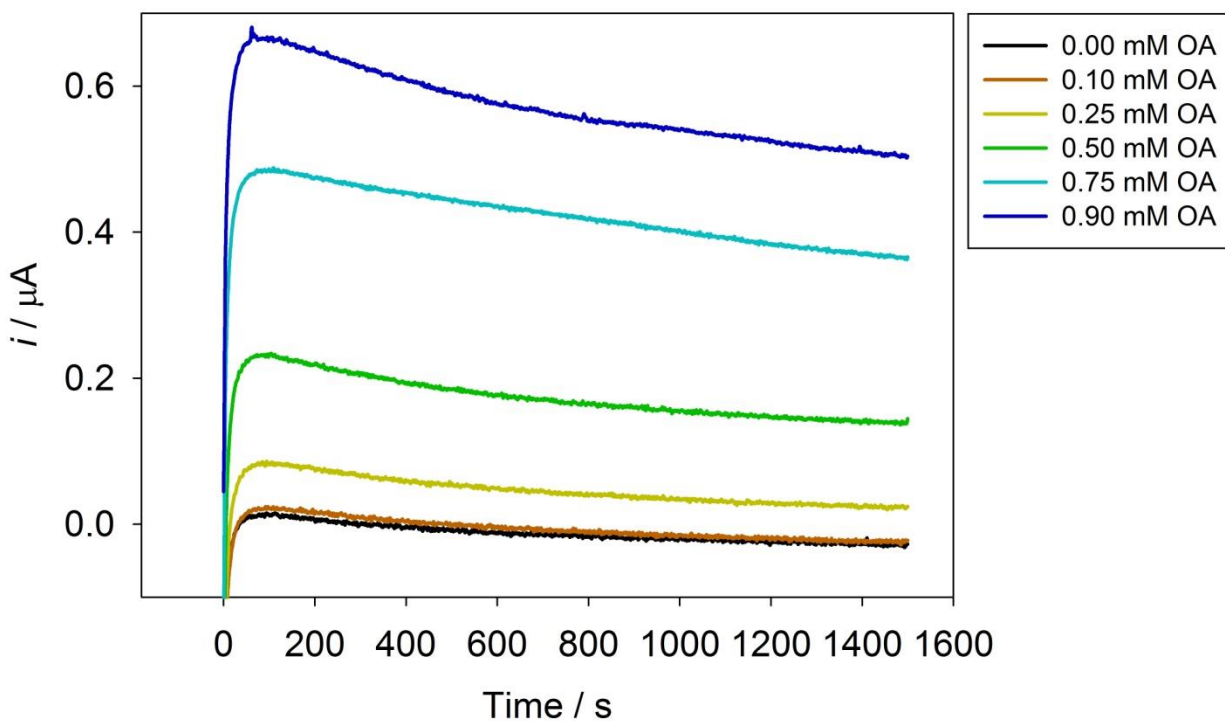


Figure 7-12: CA at 500 mV for various concentrations of OA measured at a C-SPE modified with (PDA-MWCNT/ACOD/PDA-MWCNT/ACS/BSA)¹ in 1 mM ATP and CoA and 0.1 M phosphate buffer pH 7.4.

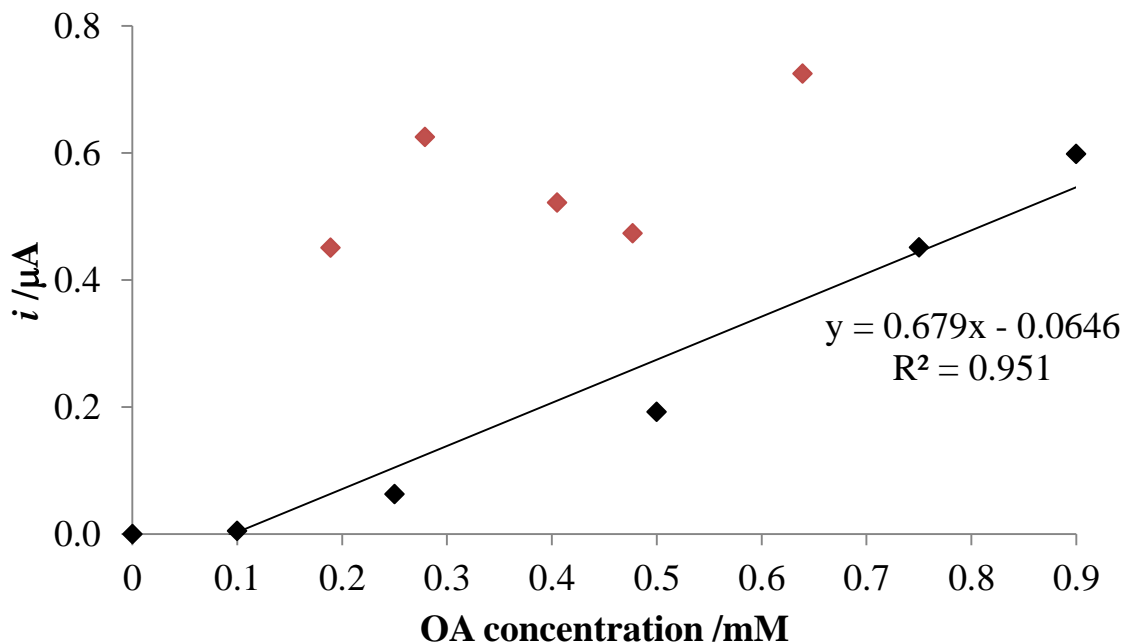


Figure 7-13: Calibration graph at 500 s. 5 different patient's plasma samples in red.

PSS based electrode for blood detection

Figure 7-14 shows the chronoamperometric results for OA at 500 mV for the fabricated electrode (PDA-MWCNT/ACOD/PDA-MWCNT/ACS/PDA-MWCNT/PSS)1. The calibration graph in Figure 7-15 shows the results from CA at 500 s, along with those of 4 serum samples run from the same patient. The UV serum concentrations of 0.107, 0.160, 0.240 and 0.360 mM came to 0.480, 0.625, 0.740 and 1.225 mM electrochemically. This is a 349, 291, 208 and 240 % increase respectively. Using serum samples for the same patient did not reduce the interference significantly. The electrode (PDA-MWCNT/ACOD/PDA-MWCNT/ACS/PDA-MWCNT/PSS)1 relies on electrostatic interaction only between the polymers. In comparison to the PMBN electrodes, which create a surface similar to a biomembrane, and therefore reduces interference significantly.

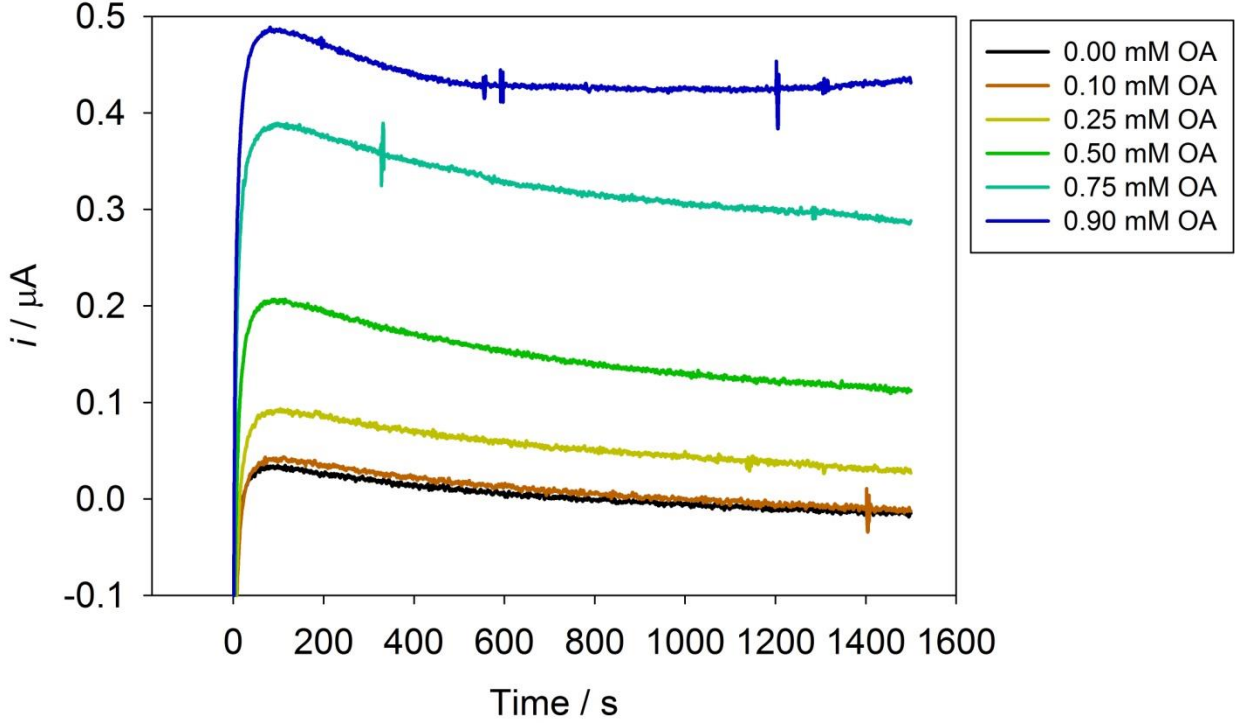


Figure 7-14: CA at 500 mV for various concentrations of OA measured at a C-SPE modified with (PDA-MWCNT/ACOD/PDA-MWCNT/ACS/PDA-MWCNT/PSS)1 in 1 mM ATP and CoA and 0.1 M phosphate buffer pH 7.4.

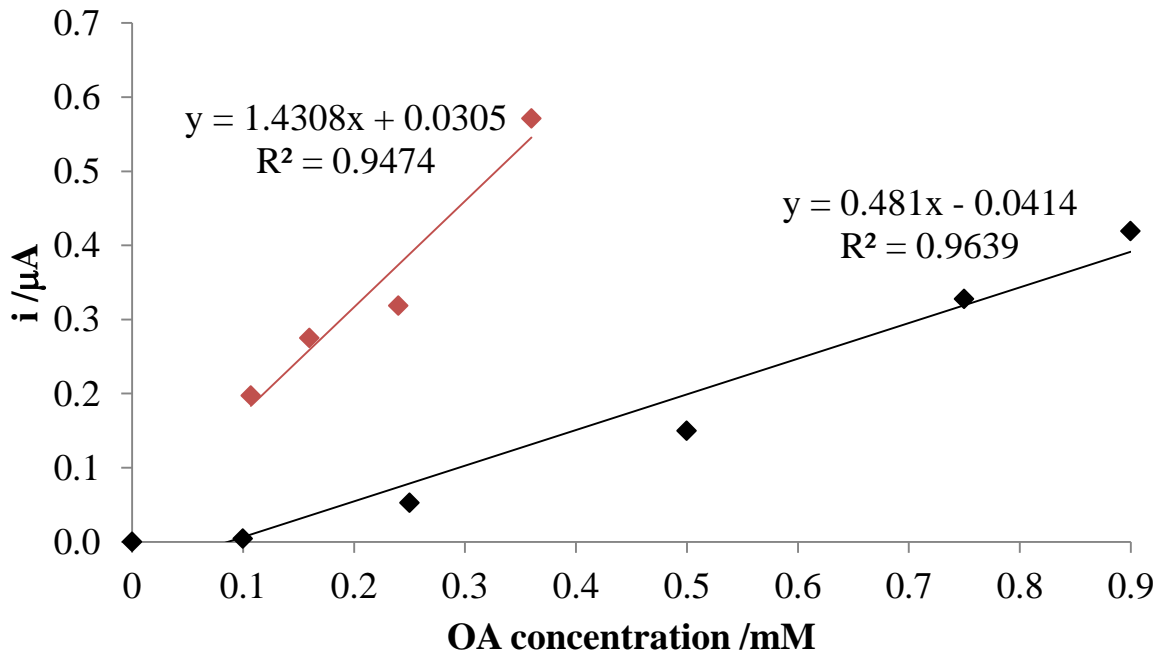


Figure 7-15: Calibration graph at 500 s. 4 serum samples from the same patient in red.

PMAA based electrode for blood detection

Figure 7-16 shows the chronoamperometric results for OA at 500 mV for the fabricated electrode (PDA-MWCNT/ACOD/PDA-MWCNT/ACS/PDA-MWCNT/PMAA)¹. The calibration graph in Figure 7-17 shows the results from CA at 500 s, along with those of 4 serum samples run from the same patient. The UV serum concentrations of 0.107, 0.160, 0.240 and 0.360 mM were too high to be detected electrochemically. This electrode was not suitable for NEFA detection.

With polyelectrolytes which are weak the interaction becomes more complicated, PMAA has more negative charges at the pH of 8 compared to that at the pH of 5 [353]. Normally there is a 1:1 ratio of anionic and cationic groups in polyelectrolyte multilayers, however for weak polyelectrolytes (such as in the case of PMAA), overall ratio can differ from 1:1 as not all of the monomers need to have a charge [314]. Hence why the performance of this electrode was the poorest.

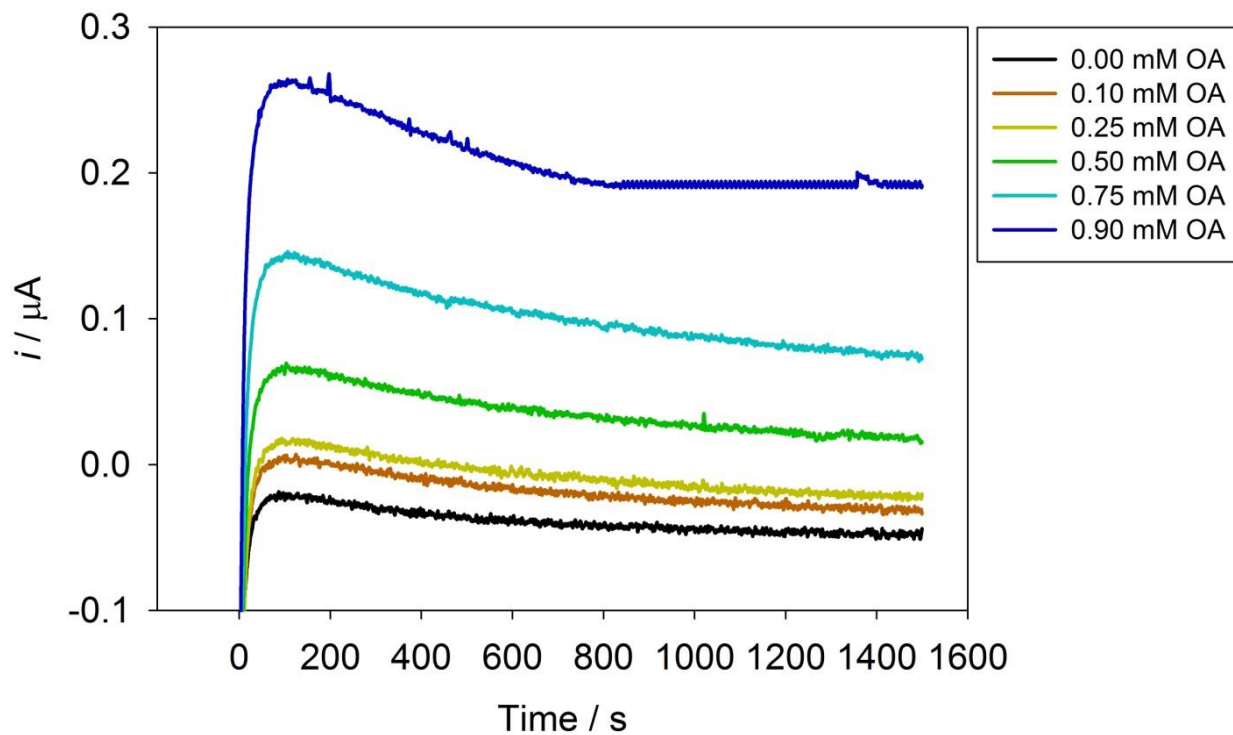


Figure 7-16: CA at 500 mV for various concentrations of OA measured at a C-SPE modified with (PDA-MWCNT/ACOD/PDA-MWCNT/ACS/PDA-MWCNT/PMAA)1 in 1 mM ATP and CoA and 0.1 M phosphate buffer pH 7.4.

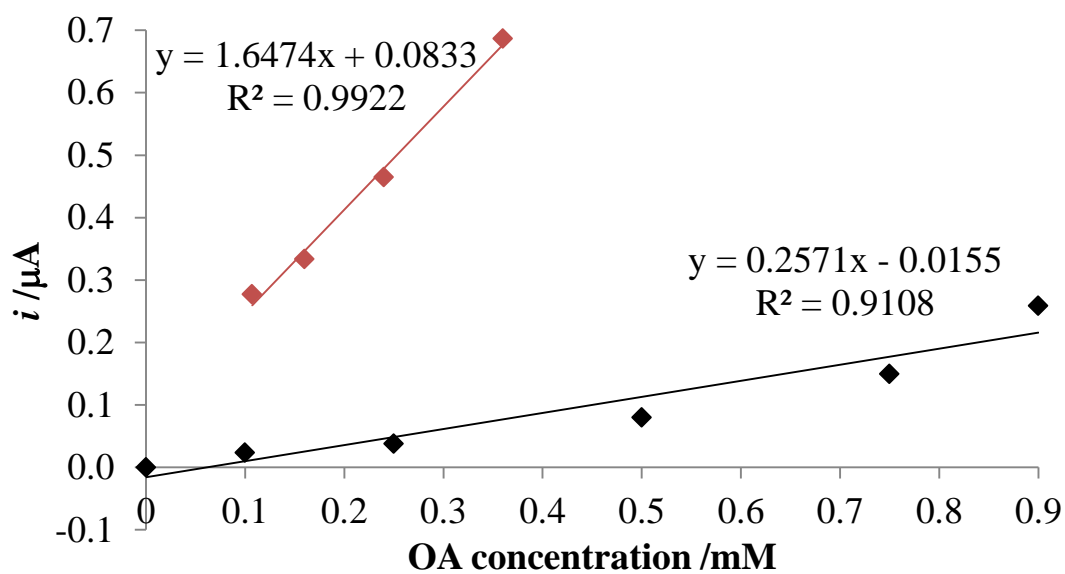


Figure 7-17: Calibration graph at 500 s. 4 serum samples from the same patient in red.

8 References

1. Yi, L., et al., *Simultaneously quantitative measurement of comprehensive profiles of esterified and non-esterified fatty acid in plasma of type 2 diabetic patients*. Chemistry and Physics of Lipids, 2007. **150**(2): p. 204-216.
2. Diabetes and UK. <http://www.londondiabetes.nhs.uk/content.aspx?pageid=100770>. [18/07/11].
3. The, et al., *The effect of intensive treatment of diabetes on the development and progression of long-term complications in insulin-dependent diabetes mellitus*. . New England Journal of Medicine, 1993. **329**(14): p. 977-986.
4. Cnop, M., *Fatty acids and glucolipotoxicity in the pathogenesis of Type 2 diabetes*. Biochemical Society Transactions, 2008. **36**(3): p. 348.
5. Scheuermann-Freestone, M., et al., *Abnormal Cardiac and Skeletal Muscle Energy Metabolism in Patients With Type 2 Diabetes*. Circulation, 2003. **107**(24): p. 3040-3046.
6. Hill, J.O. and J.C. Peters, *Biomarkers and functional foods for obesity and diabetes*. British Journal of Nutrition, 2002. **88**(2): p. S213–S218.
7. Oliver, N.S., et al., *Glucose sensors: a review of current and emerging technology*. Diabetic Medicine, 2009. **26**(3): p. 197-210.
8. Turner, A.P.F., B. Chen, and S.A. Piletsky, *In Vitro Diagnostics in Diabetes: Meeting the Challenge*. Clinical Chemistry, 1999. **45**(9): p. 1596-1601.
9. Grieshaber, D., et al., *Electrochemical Biosensors - Sensor Principles and Architectures*. Sensors, 2008: p. 1400-1458.
10. Weber, J.-M. and S.P. Reidy, *Extending food deprivation reverses the short-term lipolytic response to fasting: role of the triacylglycerol/fatty acid cycle*. Journal of Experimental Biology, 2012. **215**(9): p. 1484-1490.
11. van Meijl, L.E.C. and R.P. Mensink, *Low-fat dairy consumption reduces systolic blood pressure, but does not improve other metabolic risk parameters in overweight and obese subjects*. Nutrition Metabolism and Cardiovascular Diseases, 2011. **21**(5): p. 355-361.
12. Ruperez, A.I., et al., *Adipocyte fatty acid-binding protein plasma levels are increased in children with metabolic syndrome and correlate with non-esterified fatty acids concentration*. International Journal of Obesity, 2011. **35**: p. S163-S163.
13. Pears, A.D., J.W. Rankin, and Y.W. Lee, *Effects of acute ingestion of different fats on oxidative stress and inflammation in overweight and obese adults*. Nutrition Journal, 2011. **10**.
14. Faerch, K. and A. Vaag, *Metabolic inflexibility is a common feature of impaired fasting glycaemia and impaired glucose tolerance*. Acta Diabetologica, 2011. **48**(4): p. 349-353.
15. Tobin, L., et al., *Vascular and metabolic effects of adrenaline in adipose tissue in type 2 diabetes*. Nutrition & Diabetes, 2012. **2**.
16. Morita, S., et al., *Effect of exposure to non-esterified fatty acid on progressive deterioration of insulin secretion in patients with Type 2 diabetes: a long-term follow-up study*. Diabetic Medicine, 2012. **29**(8): p. 980-985.
17. Kehlenbrink, S., et al., *Elevated NEFA levels impair glucose effectiveness by increasing net hepatic glycogenolysis*. Diabetologia, 2012. **55**(11): p. 3021-3028.
18. Grapov, D., et al., *Type 2 Diabetes Associated Changes in the Plasma Non-Esterified Fatty Acids, Oxylipins and Endocannabinoids*. Plos One, 2012. **7**(11).

19. Becarevic, M., et al., *Adiponectin, non-esterified fatty acids and antiphospholipid antibodies in type 2 diabetes mellitus*. Journal of Medical Biochemistry, 2012. **31**(3): p. 199-204.
20. Ensling, M., W. Steinmann, and A. Whaley-Connell, *Hypoglycemia: A Possible Link between Insulin Resistance, Metabolic Dyslipidemia, and Heart and Kidney Disease (the Cardiorenal Syndrome)*. Cardiorenal Medicine, 2011. **1**(1): p. 67-74.
21. Penesova, A., et al., *Insulin resistance in young, lean male subjects with essential hypertension*. Journal of Human Hypertension, 2011. **25**(6): p. 391-400.
22. Radovic, B., E. Aflaki, and D. Kratky, *Adipose triglyceride lipase in immune response, inflammation, and atherosclerosis*. Biological Chemistry, 2012. **393**(9): p. 1005-1011.
23. Yee, M.S., et al., *The effects of rosiglitazone on atherosclerotic progression in patients with Type 2 diabetes at high cardiovascular risk*. Diabetic Medicine, 2010. **27**(12): p. 1392-1400.
24. Mas, S., et al., *Local Non-Esterified Fatty Acids Correlate With Inflammation in Atheroma Plaques of Patients With Type 2 Diabetes*. Diabetes, 2010. **59**(6): p. 1292-1301.
25. Patel, J.V., et al., *Diabetes Health, Residence & Metabolism in Asians: the DHRMA study, research into foods from the Indian subcontinent - a blinded, randomised, placebo controlled trial*. BMC Cardiovascular Disorders, 2011. **11**.
26. Pal, S., V. Ellis, and S. Ho, *Acute effects of whey protein isolate on cardiovascular risk factors in overweight, post-menopausal women*. Atherosclerosis, 2010. **212**(1): p. 339-344.
27. Santo, A.S., et al., *Postprandial Lipemia Detects the Effect of Soy Protein on Cardiovascular Disease Risk Compared with the Fasting Lipid Profile*. Lipids, 2010. **45**(12): p. 1127-1138.
28. Scorletti, E., P.C. Calder, and C.D. Byrne, *Non-alcoholic fatty liver disease and cardiovascular risk: metabolic aspects and novel treatments*. Endocrine, 2011. **40**(3): p. 332-343.
29. Kahraman, A., et al., *Fetuin-A mRNA expression is elevated in NASH compared with NAFL patients*. Clinical Science, 2013. **125**(7-8): p. 391-400.
30. Kawano, Y. and D.E. Cohen, *Mechanisms of hepatic triglyceride accumulation in non-alcoholic fatty liver disease*. Journal of Gastroenterology, 2013. **48**(4): p. 434-441.
31. Martinez, J.G., et al., *Membrane-targeted synergistic activity of docosahexaenoic acid and lysozyme against Pseudomonas aeruginosa*. Biochemical Journal, 2009. **419**: p. 193-200.
32. Kafi, M., et al., *Relationships between thyroid hormones and serum energy metabolites with different patterns of postpartum luteal activity in high-producing dairy cows*. Animal, 2012. **6**(8): p. 1253-1260.
33. Stockigt, J.R. and C.-F. Lim, *Medications that distort in vitro tests of thyroid function, with particular reference to estimates of serum free thyroxine*. Best Practice & Research Clinical Endocrinology & Metabolism, 2009. **23**(6): p. 753-767.
34. Kumar, A., et al., *Non-Esterified Fatty Acids Generate Distinct Low-Molecular Weight Amyloid-beta (A beta 42) Oligomers along Pathway Different from Fibril Formation*. Plos One, 2011. **6**(4).
35. Astarita, G., et al., *Elevated Stearoyl-CoA Desaturase in Brains of Patients with Alzheimer's Disease*. Plos One, 2011. **6**(10).

36. Hon, G.M., et al., *Non-esterified fatty acids in blood cell membranes from patients with multiple sclerosis*. European Journal of Lipid Science and Technology, 2012. **114**(7): p. 703-709.
37. Hon, G.M., et al., *Plasma non-esterified fatty acids in patients with multiple sclerosis*. Neurology Asia, 2011. **16**(3): p. 217-222.
38. Babushkina, T.A., et al., *Study of High-Resolution H-1 Nuclear Magnetic Resonance Spectra of the Serum and Its Albumin Fraction in Patients with the First Schizophrenia Episode*. Bulletin of Experimental Biology and Medicine, 2012. **152**(6): p. 748-751.
39. Ciccoli, L., et al., *Morphological changes and oxidative damage in Rett Syndrome erythrocytes*. Biochimica Et Biophysica Acta-General Subjects, 2012. **1820**(4): p. 511-520.
40. Guebre-Egziabher, F., et al., *Ectopic lipid accumulation: A potential cause for metabolic disturbances and a contributor to the alteration of kidney function*. Biochimie, 2013. **95**(11): p. 1971-1979.
41. Smelt, A.H.M., *Triglycerides and gallstone formation*. Clinica Chimica Acta, 2010. **411**(21-22): p. 1625-1631.
42. Jankovec, Z., et al., *Influence of Physical Activity on Metabolic State Within a 3-h Interruption of Continuous Subcutaneous Insulin Infusion in Patients with Type 1 Diabetes*. Diabetes Technology & Therapeutics, 2011. **13**(12): p. 1234-1239.
43. Jang, T.R., et al., *Effects of carbohydrate, branched-chain amino acids, and arginine in recovery period on the subsequent performance in wrestlers*. Journal of the International Society of Sports Nutrition, 2011. **8**.
44. Hamzah, S., et al., *The effect of glycaemic index of high carbohydrate diets consumed over 5 days on exercise energy metabolism and running capacity in males*. Journal of Sports Sciences, 2009. **27**(14): p. 1545-1554.
45. Rigamonti, A.E., et al., *Changes in plasma levels of ghrelin, leptin, and other hormonal and metabolic parameters following standardized breakfast, lunch, and physical exercise before and after a multidisciplinary weight-reduction intervention in obese adolescents*. Journal of Endocrinological Investigation, 2010. **33**(9): p. 633-639.
46. Smith, J., et al., *The beta-1 adrenergic antagonist, atenolol, decreases acylation stimulating protein, exercise capacity and plasma free fatty acids in men with type 2 diabetes*. Nutrition Metabolism and Cardiovascular Diseases, 2012. **22**(6): p. 495-502.
47. Ortega-Senovilla, H., et al., *Enhanced circulating retinol and non-esterified fatty acids in pregnancies complicated with intrauterine growth restriction*. Clinical Science, 2010. **118**(5-6): p. 351-358.
48. Jarvie, E., et al., *Lipotoxicity in obese pregnancy and its potential role in adverse pregnancy outcome and obesity in the offspring*. Clinical Science, 2010. **119**(3-4): p. 123-129.
49. Karpe, F., J.R. Dickmann, and K.N. Frayn, *Fatty Acids, Obesity, and Insulin Resistance: Time for a Reevaluation*. Diabetes, 2011. **60**(10): p. 2441-2449.
50. Tan, Y., et al., *Chinese herbal extracts (SK0506) as a potential candidate for the therapy of the metabolic syndrome*. Clinical Science, 2011. **120**(7-8): p. 297-305.
51. Yao, H.T., et al., *Effect of Shengmai San on Insulin Resistance, Tumor Necrosis Factor-Alpha and Oxidative Stress in Rats Fed on a High-Fat Diet*. Journal of Food and Drug Analysis, 2011. **19**(1): p. 40-48.

52. Jovanovic, A., et al., *The second-meal phenomenon is associated with enhanced muscle glycogen storage in humans*. *Clinical Science*, 2009. **117**(3-4): p. 119-127.
53. Verbrugge, M., et al., *Quantification of hydrophilic ethoxylates in polysorbate surfactants using diffusion H-1 NMR spectroscopy*. *Journal of Pharmaceutical and Biomedical Analysis*, 2010. **51**(3): p. 583-589.
54. Boruckowska, H., et al., *The obtaining of starch and oleic acid based ester and its properties*. *Zywnosc-Nauka Technologia Jakosc*, 2012. **19**(4): p. 98-107.
55. Namgaladze, D., et al., *Phospholipase A(2)-modified low density lipoprotein induces mitochondrial uncoupling and lowers reactive oxygen species in phagocytes*. *Atherosclerosis*, 2010. **208**(1): p. 142-147.
56. Han, L.-D., et al., *Plasma esterified and non-esterified fatty acids metabolic profiling using gas chromatography-mass spectrometry and its application in the study of diabetic mellitus and diabetic nephropathy*. *Analytica Chimica Acta*, 2011. **689**(1): p. 85-91.
57. Tsikas, D., A.A. Zoerner, and J. Jordan, *Oxidized and nitrated oleic acid in biological systems: Analysis by GC-MS/MS and LC-MS/MS, and biological significance*. *Biochimica Et Biophysica Acta-Molecular and Cell Biology of Lipids*, 2011. **1811**(11): p. 694-705.
58. Kopf, T. and G. Schmitz, *Analysis of non-esterified fatty acids in human samples by solid-phase-extraction and gas chromatography/mass spectrometry*. *Journal of Chromatography B-Analytical Technologies in the Biomedical and Life Sciences*, 2013. **938**: p. 22-26.
59. Morgan, L.T., et al., *Thrombin-activated human platelets acutely generate oxidized docosahexaenoic-acid-containing phospholipids via 12-lipoxygenase*. *Biochemical Journal*, 2010. **431**: p. 141-148.
60. Trufelli, H., et al., *Profiling of non-esterified fatty acids in human plasma using liquid chromatography-electron ionization mass spectrometry*. *Analytical and Bioanalytical Chemistry*, 2011. **400**(9): p. 2933-2941.
61. Hinder, A., et al., *Investigation of the Molecular Structure of the Human Stratum Corneum Ceramides NP and EOS by Mass Spectrometry*. *Skin Pharmacology and Physiology*, 2011. **24**(3): p. 127-135.
62. Wang, Z., et al., *Labelled antibody-based one-step time-resolved fluoroimmunoassay for measurement of free thyroxine in serum*. *Annals of Clinical Biochemistry*, 2011. **48**: p. 550-557.
63. Tenllado, D., G. Reglero, and C.F. Torres, *A combined procedure of supercritical fluid extraction and molecular distillation for the purification of alkylglycerols from shark liver oil*. *Separation and Purification Technology*, 2011. **83**: p. 74-81.
64. Berdeaux, O., et al., *A detailed identification study on high-temperature degradation products of oleic and linoleic acid methyl esters by GC-MS and GC-FTIR*. *Chemistry and Physics of Lipids*, 2012. **165**(3): p. 338-347.
65. Leaf, A., *Plasma Nonesterified Fatty Acid Concentration as a Risk Factor for Sudden Cardiac Death*. *Circulation*, 2001. **104**(7): p. 744-745.
66. McNaught, A.D. and A. Wilkinson, *Compendium of Chemical Terminology*. Second ed. 1997: Blackwell Scientific Publications, Oxford
67. Hallaq, Y., et al., *Use of Acetyl Chloride/Methanol for Assumed Selective Methylation of Plasma Nonesterified Fatty Acids Results in Significant Methylation of Esterified Fatty Acids*. *Lipids*, 1993. **28**(4): p. 355-360.

68. French, M.A., K. Sundram, and M.T. Clandinin, *Cholesterolaemic effect of palmitic acid in relation to other dietary fatty acids*. Asia Pacific Journal of Clinical Nutrition, 2002. **11**: p. S401-S407.
69. Bender, D.A., *A dictionary of food and nutrition*. 2005, Oxford University Press. p. 201, 369.
70. Weber, J.M. and S.P. Reidy, *Extending food deprivation reverses the short-term lipolytic response to fasting: role of the triacylglycerol/fatty acid cycle*. Journal of Experimental Biology, 2012. **215**(9): p. 1484-1490.
71. Syamsunarno, M., et al., *A Critical Role of Fatty Acid Binding Protein 4 and 5 (FABP4/5) in the Systemic Response to Fasting*. PLoS One, 2013. **8**(11): p. 13.
72. Frayn, K.N., *Plasma non-esterified fatty acids: why are we not measuring them routinely?* Annals of Clinical biochemistry, 2005. **42**(6): p. 413-414.
73. Taggart, P. and M. Carruthers, *Endogenous hyperlipidemia induced by emotional stress of racing driving*. The Lancet, 1971. **297**(7695): p. 363-366.
74. Arbogast, B.W., et al., *Transient loss of serum protective activity following short-term stress: A possible biochemical link between stress and atherosclerosis*. Journal of Psychosomatic Research, 1994. **38**(8): p. 871-884.
75. Groop, L.C., et al., *Role of free fatty acids and insulin in determining free fatty acid and lipid oxidation in man*. Journal of Clinical Investigation, 1991. **87**(1): p. 83-89.
76. Cascio, G., G. Schiera, and I. Di Liegro, *Dietary fatty acids in metabolic syndrome, diabetes and cardiovascular diseases*. Current diabetes reviews, 2012. **8**(1): p. 2-17.
77. Martins, A.R., et al., *Mechanisms underlying skeletal muscle insulin resistance induced by fatty acids: importance of the mitochondrial function*. Lipids in Health and Disease, 2012. **11**.
78. Dumas, M.-E., J. Kinross, and J.K. Nicholson, *Metabolic Phenotyping and Systems Biology Approaches to Understanding Metabolic Syndrome and Fatty Liver Disease*. Gastroenterology, 2013(0).
79. Boden, G., *Obesity and Free Fatty Acids*. Endocrinology & Metabolism Clinics of North America, 2008. **37**(3): p. 635-646.
80. Drew, B.G., et al., *Reconstituted high-density lipoprotein infusion modulates fatty acid metabolism in patients with type 2 diabetes mellitus*. Journal of Lipid Research, 2011. **52**(3): p. 572-581.
81. Frayn, K.N., *Non-esterified fatty acid metabolism and postprandial lipaemia*. Atherosclerosis, 1998. **141**, **Supplement 1**(0): p. S41-S46.
82. Beysen, C., et al., *Interaction between specific fatty acids, GLP-1 and insulin secretion in humans*. Diabetologia, 2002. **45**(11): p. 1533-1541.
83. Borra, C., et al., *Reliable measurement of non-esterified long-chain fatty-acid pattern in blood-plasma*. Journal of Chromatography, 1984. **311**(1): p. 9-15.
84. Rogiers, V., *Long chain nonesterified fatty acid patterns in plasma of healthy children and young adults in relation to age and sex*. Journal of Lipid Research, 1981. **22**(1): p. 1-6.
85. Arab, L., *Biomarkers of Fat and Fatty Acid Intake*. The Journal of Nutrition, 2003. **133**(3): p. 925S-932S.
86. Dole, V.P., et al., *The fatty acid patterns of plasma lipids during alimentary lipemia*. The Journal of clinical investigation, 1959. **38**: p. 1544-54.

87. Miles, B. *Fatty Acid Catabolism*. 2003 [cited 2013 14/08/2013]; Available from: tamu.edu/faculty/bmiles/lectures/fatcatii.pdf
88. Berg, J.M., J.L. Tymoczko, and L. Stryer., *Biochemistry*. 5th ed. 2002, New York: W H Freeman.
89. Il'yasova, D., et al., *Prospective association between fasting NEFA and type 2 diabetes: impact of post-load glucose*. *Diabetologia*, 2010. **53**(5): p. 866-874.
90. Frayn, K.N., *Fat as a fuel: emerging understanding of the adipose tissue-skeletal muscle axis*. *Acta Physiologica*, 2010. **199**: p. 509-518.
91. van Loon, L.J.C., et al., *The effects of increasing exercise intensity on muscle fuel utilisation in humans*. *Journal of Physiology-London*, 2001. **536**(1): p. 295-304.
92. van Hall, G., et al., *Regional fat metabolism in human splanchnic and adipose tissues; the effect of exercise*. *Journal of Physiology-London*, 2002. **543**(3): p. 1033-1046.
93. Romijn, J.A., et al., *Regulation of endogenous fat and carbohydrate metabolism in relation to exercise intensity and duration*. *American Journal of Physiology*, 1993. **265**(3): p. E380-E391.
94. Lambert, J.E. and E.J. Parks, *Postprandial metabolism of meal triglyceride in humans*. *Biochimica et Biophysica Acta (BBA) - Molecular and Cell Biology of Lipids*, 2012. **1821**(5): p. 721-726.
95. *β -oxidation*. 2013 [cited 2013 21/01/13]; Available from: <http://www.bioinfo.org.cn/book/biochemistry/chapt16/sim2.htm>.
96. Rossignol, D.A. and R.E. Frye, *Mitochondrial dysfunction in autism spectrum disorders: a systematic review and meta-analysis*. *Mol Psychiatry*, 2011.
97. Mathews, C.K., K.E.v. Holde, and K.G. Ahern, *Biochemistry*. Third ed. 2000, San Francisco: Addison-Wesley Publishing Company. 1186.
98. Burrows, A., et al., *Chemistry³ introducing inorganic, organic and physical chemistry*. 2009: Oxford University Press. 1397.
99. *Chapter 17: Fatty Acid Catabolism*, in *Solutions manual*. 2008, EQA. p. S199-S210.
100. Yi, L.-Z., et al., *Plasma fatty acid metabolic profiling and biomarkers of type 2 diabetes mellitus based on GUMS and PLS-LDA*. *FEBS Letters*, 2006. **580**(30): p. 6837-6845.
101. Tillil, H. and J. Kobberling, *Age-corrected empirical genetic risk estimates for first-degree relatives of IDDM patients*. *Diabetes*, 1987. **36**(1): p. 93-9.
102. Ali, O., *Genetics of type 2 diabetes*. *World Journal of Diabetes*, 2012. **4**(4): p. 114-123.
103. Jouven, X., et al., *Circulating Nonesterified Fatty Acid Level as a Predictive Risk Factor for Sudden Death in the Population*. *Circulation*, 2001. **104**(7): p. 756-761.
104. Stefan, N., et al., *Circulating Palmitoleate Strongly and Independently Predicts Insulin Sensitivity in Humans*. *Diabetes Care*, 2010. **33**(2): p. 405-407.
105. Mathew, M., E. Tay, and K. Cusi, *Elevated plasma free fatty acids increase cardiovascular risk by inducing plasma biomarkers of endothelial activation, myeloperoxidase and PAI-1 in healthy subjects*. *Cardiovascular Diabetology*, 2010. **9**(9): p. 1-9.
106. Steven, S., E.L. Lim, and R. Taylor, *Dietary reversal of Type 2 diabetes motivated by research knowledge*. *Diabetic Medicine*, 2010. **27**(6): p. 724-725.
107. Taylor, R., *Type 2 Diabetes Etiology and reversibility*. *Diabetes Care*, 2013. **36**(4): p. 1047-1055.

108. Pan, X.R., et al., *Effects of diet and exercise in preventing NIDDM in people with impaired glucose tolerance - The Da Qing IGT and diabetes study*. Diabetes Care, 1997. **20**(4): p. 537-544.
109. Eriksson, K.F. and F. Lindgarde, *Prevention of type 2 (non-insulin-dependent) diabetes mellitus by diet and physical exercise: the 6-year Malmo feasibility study*. Diabetologia, 1991. **34**(12): p. 891-898.
110. Tuomilehto, J., et al., *Prevention of type 2 diabetes mellitus by changes in lifestyle among subjects with impaired glucose tolerance*. New England Journal of Medicine, 2001. **344**(18): p. 1343-1350.
111. Lim, E., et al., *Reversal of type 2 diabetes: normalisation of beta cell function in association with decreased pancreas and liver triacylglycerol*. Diabetologia, 2011. **54**(10): p. 2506-2514.
112. Steven, S., E.L. Lim, and R. Taylor, *Population response to information on reversibility of Type 2 diabetes*. Diabetic Medicine, 2013. **30**(4): p. e135-e138.
113. Wing, R.R., *Long-term effects of a lifestyle intervention on weight and cardiovascular risk factors in individuals with type 2 diabetes mellitus: four-year results of the Look AHEAD trial*. Arch Intern Med, 2010. **170**(17): p. 1566-75.
114. Albu, J.B., et al., *Metabolic Changes Following a 1-Year Diet and Exercise Intervention in Patients With Type 2 Diabetes*. Diabetes, 2010. **59**(3): p. 627-633.
115. Newsholme, P., et al., *Life and death decisions of the pancreatic beta-cell: the role of fatty acids*. Clinical Science, 2007. **112**(1-2): p. 27-42.
116. Gordon, R.S., A. Cherkes, and H. Gates, *Unesterified fatty acid in human blood plasma. the transport function of unesterified fatty acid*. Journal of Clinical Investigations, 1957. **36**: p. 810-815.
117. Carlson, L.A. and L.B. Wadstrom, *A colorimetric method of determining unesterified fatty acids in plasma*. Journal of clinical laboratory investigations, 1958. **10**(4): p. 407-414.
118. Dole, V.P. and H. Meinertz, *Microdetermination of long-chain fatty acids in plasma and tissues*. J Biol Chem, 1960. **235**: p. 2595-9.
119. Shimizu, S., et al., *Enzymatic microdetermination of serum free fatty acids*. Analytical Biochemistry, 1979. **98**(2): p. 341-345.
120. Mizuno, K., et al., *A new enzymatic method for colorimetric determination of free fatty acids*. Analytical Biochemistry, 1980. **108**(1): p. 6-10.
121. Hosaka, K., et al., *A New Colorimetric Method for the Determination of Free Fatty Acids with Acyl-CoA Synthetase and Acyl-CoA Oxidase*. Journal of Biochemistry, 1981. **89**: p. 1799-1803.
122. Duncombe, W.G., *The colorimetric micro-determination of non-esterified fatty acids in plasma*. Clinica Chimica Acta, 1964. **9**(2): p. 122-125.
123. Itaya, K. and M. Ui, *Colorimetric determination of free fatty acids in biological fluids*. Journal of Lipid Research, 1965. **6**: p. 16-20.
124. Milan, N., *Colorimetric ultramicro method for the determination of free fatty acids*. Journal of Lipid Research, 1965. **6**: p. 431-433.
125. Trout, D.L., E.H. Estes, and S.J. Friedberg, *Titration of free fatty acids of plasma: a study of current methods and a new modification*. J Lipid Res, 1960. **1**: p. 199-202.
126. Barreto, R.C.R. and D.B. Mano, *A colorimetric method for the assay of some higher fatty acids in blood and serum*. Clinica Chimica Acta, 1961. **6**(6): p. 887-889.

127. Ho, R.J., *Radiochemical assay of long-chain fatty acids using ⁶³Ni as tracer*. Analytical Biochemistry, 1970. **36**(1): p. 105-113.
128. Debrabander, H.F. and R. Verbeke, *Radiochemical assay of long-chain fatty-acids using ⁶³Ni*. Analytical Biochemistry, 1981. **110**(1): p. 240-241.
129. Brunk, S.D. and J.R. Swanson, *Colorimetric method for free fatty-acids in serum validated by comparison with Gas-Chromotography*. Clinical Chemistry, 1981. **27**(6): p. 924-926.
130. Duncombe, W.G., *The Colorimetric Micro-Determination of Long-Chain Fatty Acids*. Journal of Biochemistry, 1963. **88**.
131. Elphick, M.C., *Modified colorimetric ultramicro method for estimating Nefa in serum*. J Clin Pathol, 1968. **21**(5): p. 567-70.
132. Okabe, H., et al., *Enzymic Determination of Free Fatty Acids in Serum*. Clinical Chemistry, 1980. **26**(11): p. 1540-1543.
133. Sode, K., et al., *Sensor for free fatty acids based on acyl coenzyme-a synthetase and acyl coenzyme-a oxidase*. Analytica Chimica Acta, 1989. **220**(0): p. 251-255.
134. Buerk, D.G., *Biosensors: Theory and Applications*. 1993: Technomic Publishing AG. 221.
135. Sode, K., et al., *Amperometric determination of free fatty acids by utilizing five sequential enzyme reactions*. Electroanalysis, 1989. **1**(1): p. 69-74.
136. Catachem. *Nonesterified fatty acids (NEFA) reagent*. 2013 [cited 2013 25/10/13]; Available from: http://www.catacheminc.com/index_files/Page13486.htm.
137. Company, C.C. *Free Fatty Acid Assay Kit*. 2013 [cited 2013 25/10/13]; Available from: <https://www.caymanchem.com/pdfs/700310.pdf>.
138. DiaSys. *NEFA FS Non-esterified fatty acids*. 2013 [cited 2013 25/10/13]; Available from: http://www.metabolic-syndrome.de/fileadmin/downloads/Print_Material/Reagenzbroschueren/DiaSys_NEFA_FS.pdf.
139. DiaSys. *Liquid-stable reagent for measurement of free fatty acids*. 2013 [cited 2013 25/10/13]; Available from: <http://www.alere.co.uk/pdf/220310040721-DiaSys%20NEFA%20Paper.pdf>.
140. Inc., C.B., *Free Fatty Acid Assay Kit (Colorimetric)*. 2013.
141. Inc., C.B., *Free Fatty Acid Assay Kit (Fluorometric)*. 2013.
142. Roche. https://e-labdoc.roche.com/LFR_PublicDocs/ras/11383175001_en_09.pdf. 2004 18/07/11].
143. Wako. [http://www.wakodiagnosics.com/pi/pi_hr_seriese_nefa-hr\(2\).pdf](http://www.wakodiagnosics.com/pi/pi_hr_seriese_nefa-hr(2).pdf). [cited 2010 29/10/10].
144. Zen-Bio, *96-well Serum/Plasma Fatty Acid Kit Non-esterified Fatty Acids Detection 1,000 Point kit*. 2013.
145. Zen-Bio, *96-well Serum/Plasma Fatty Acid Kit Non-esterified Fatty Acids Detection 100 Point kit*. 2013.
146. Zen-Bio, *96-well Serum/Plasma Fatty Acid and Glycerol Kit for the detection of both Non-esterified Fatty Acids and Free Glycerol*. 2013.
147. Zen-Bio, *Cellulite Treatment Screening Kit Human Adipocyte Lipolysis Assay for Both Free Glycerol and Non-esterified Fatty Acids*. 2013.
148. Randox, *Nefa (non-esterified fatty acids) assay*. 2013.

149. Cusabio. *Bovine non-ester fatty acid (NEFA) ELISA Kit*. 2013 [cited 2013 25/10/13]; Available from: [http://www.cusabio.com/Instructions/CSB-E13165B_Bovine_non-ester_fatty_acid_\(NEFA\)_ELISA_Kit.pdf](http://www.cusabio.com/Instructions/CSB-E13165B_Bovine_non-ester_fatty_acid_(NEFA)_ELISA_Kit.pdf).
150. BioVision. *Free Fatty Acid Quantification Colorimetric/Fluorometric Kit*. 2013 [cited 2013 25/10/13]; Available from: <http://www.biovision.com/manuals/K612-100.pdf>
151. Laboratory, B.T., *Bovine Non-esterified fatty acid (NEFA) ELISA Kit*. 2013.
152. Sigma-Aldrich, *Free Fatty Acid Quantitation Kit*. 2013.
153. abcam. *ab65341 Free Fatty Acid Quantification Kit*. 2013 [cited 2013 25/10/13]; Available from: [http://www.abcam.com/ps/products/65/ab65341/documents/ab65341%20Free%20Fatty%20Acid%20Quantification%20Kit%20Protocol%20v2%20\(Website\).pdf](http://www.abcam.com/ps/products/65/ab65341/documents/ab65341%20Free%20Fatty%20Acid%20Quantification%20Kit%20Protocol%20v2%20(Website).pdf).
154. Johnson, M.M. and J.P. Peters, *Technical note: an improved method to quantify nonesterified fatty acids in bovine plasma*. J Anim Sci, 1993. **71**(3): p. 753-6.
155. Matsubara, C., et al., *A spectrophotometric method for the determination of free fatty acid in serum using acyl-coenzyme A synthetase and acyl-coenzyme A oxidase*. Analytical Biochemistry, 1983. **130**(1): p. 128-133.
156. Catachem. *Nonesterified fatty acids (NEFA) Product/Service Information*. 2013 [cited 2013 25/10/13]; Available from: <http://www.catacheminc.com/nefa%20pdf.pdf>.
157. Beattie, J. and R. Carachi, eds. *Practical paediatric problems*. 2005, Hodder Arnold. 477.
158. Sampson, D. and W.J. Hensley, *A rapid gas chromatographic method for the quantitation of underivatized individual free fatty acids in plasma*. Clinica Chimica Acta, 1975. **61**(1): p. 1-8.
159. Wierzbicki, et al., *Influence of plasma phytanic acid levels in Refsum's disease on the behaviour of the erythrocyte membrane sodium–lithium countertransporter*. European Journal of Clinical Investigation, 1998. **28**(4): p. 334-338.
160. Knaap, M.S.v.d., *Magnetic resonance of myelination and myelin disorders*. 2005, Springer: New York. p. 191-194.
161. Wanders, R.J.A., H.R. Waterham, and B.P. Leroy. *Refsum Disease*. 2010 [cited 2013 19/08/2013]; Available from: <http://www.ncbi.nlm.nih.gov/books/NBK1353/>.
162. Ferdinandusse, S., et al., *Clinical, biochemical, and mutational spectrum of peroxisomal acyl-coenzyme a oxidase deficiency*. Human Mutation, 2007. **28**(9): p. 904-912.
163. Slomiany, B.L., V.L. Murty, and A. Slomiany, *Salivary lipids in health and disease*. Prog Lipid Res, 1985. **24**(4): p. 311-24.
164. Actis, A.B., et al., *Fatty acid profile of human saliva: a possible indicator of dietary fat intake*. Arch Oral Biol, 2005. **50**(1): p. 1-6.
165. Larsson, B., G. Olivecrona, and T. Ericson, *Lipids in human saliva*. Arch Oral Biol, 1996. **41**(1): p. 105-10.
166. Alam, S.Q. and B.S. Alam, *Effect of Dietary Lipids on Saliva Composition*. The Journal of Nutrition, 1982. **112**(5): p. 990-996.
167. Kulkarni, B. and R. Mattes, *Evidence for Presence of Nonesterified Fatty Acids as Potential Gustatory Signaling Molecules in Humans*. Chemical Senses, 2013. **38**(2): p. 119-127.
168. Kulkarni, B.V., K.V. Wood, and R.D. Mattes, *Quantitative and qualitative analyses of human salivary NEFA with gas-chromatography and mass spectrometry*. Front Physiol, 2012. **3**: p. 328.

169. Poette, J., et al., *Fat sensitivity in humans: oleic acid detection threshold is linked to saliva composition and oral volume*. Flavour and Fragrance Journal, 2013.
170. Tucker, R.M., et al., *The Effect of Short, Daily Oral Exposure on Non-esterified Fatty Acid Sensitivity*. Chemosensory Perception, 2013. **6**(2): p. 78-85.
171. Mattes, R.D., *Oral detection of short-, medium-, and long-chain free fatty acids in humans*. Chem Senses, 2009. **34**(2): p. 145-50.
172. Khan, N.A. and P. Besnard, *Oro-sensory perception of dietary lipids: New insights into the fat taste transduction*. Biochimica et Biophysica Acta (BBA) - Molecular and Cell Biology of Lipids, 2009. **1791**(3): p. 149-155.
173. Coste, T.C., et al., *An overview of monitoring and supplementation of omega 3 fatty acids in cystic fibrosis*. Clinical Biochemistry, 2007. **40**(8): p. 511-520.
174. Rungroj, K., et al., *Determination of non-esterified fatty acids in bovine serum: evaluation of a modified Randox NEFA® kit with reduced sample and reagent volumes*. Journal of the Thai Veterinary Medical Association, 2009. **60**(1-3): p. 9-16.
175. Ospina, P.A., et al., *Evaluation of nonesterified fatty acids and β -hydroxybutyrate in transition dairy cattle in the northeastern United States: Critical thresholds for prediction of clinical diseases*. Journal of Dairy Science, 2010. **93**(2): p. 546-554.
176. Kaufmann, T.B., et al., *Correlations between periparturient serum concentrations of non-esterified fatty acids, beta-hydroxybutyric acid, bilirubin, and urea and the occurrence of clinical and subclinical postpartum bovine endometritis*. BMC Veterinary Research, 2010. **6**.
177. Ospina, P.A., et al., *Associations of elevated nonesterified fatty acids and β -hydroxybutyrate concentrations with early lactation reproductive performance and milk production in transition dairy cattle in the northeastern United States*. Journal of Dairy Science, 2010. **93**(4): p. 1596-1603.
178. Ospina, P.A., et al., *Association between the proportion of sampled transition cows with increased nonesterified fatty acids and β -hydroxybutyrate and disease incidence, pregnancy rate, and milk production at the herd level*. Journal of Dairy Science, 2010. **93**(8): p. 3595-3601.
179. Miksa, I.R., C.L. Buckley, and R.H. Poppenga, *Detection of nonesterified (free) fatty acids in bovine serum: comparative evaluation of two methods*. Journal of Veterinary Diagnostic Investigation, 2004. **16**(2): p. 139-144.
180. Gonzalez, F.D., et al., *Relationship among blood indicators of lipomobilization and hepatic function during early lactation in high-yielding dairy cows*. J Vet Sci, 2011. **12**(3): p. 251-5.
181. Oetzel, G.R., *Herd-Based Biological Testing For Metabolic Disorders*, in American Association of Bovine Practitioners, 36th Annual Conference. 2003: Columbus.
182. Khan, J.R. and R.S. Ludri, *Changes in Maternal Blood Glucose and Plasma Non-Esterified Fatty Acid during Pregnancy and around Parturition in Twin and Single Fetus Bearing Crossbred Goats*. Asian - Australasian Journal of Animal Sciences 2002. **15**(4): p. 504-508.
183. Suagee, J.K., et al., *A 90-day adaptation to a high glycaemic diet alters postprandial lipid metabolism in non-obese horses without affecting peripheral insulin sensitivity*. Journal of Animal Physiology and Animal Nutrition, 2013. **97**(2): p. 245-254.

184. Gray, S.M., P.A. Bartell, and W.B. Staniar, *High glycemic and insulinemic responses to meals affect plasma growth hormone secretory characteristics in Quarter Horse weanlings*. Domestic Animal Endocrinology, 2013. **44**(4): p. 165-175.
185. Delavaud, C., et al., *Plasma leptin, glucose and non-esterified fatty acid variations in dromedary camels exposed to prolonged periods of underfeeding or dehydration*. Comparative Biochemistry and Physiology a-Molecular & Integrative Physiology, 2013. **166**(1): p. 177-185.
186. Seki, Y., et al., *Minireview: Epigenetic Programming of Diabetes and Obesity: Animal Models*. Endocrinology, 2012. **153**(3): p. 1031-1038.
187. King, A.J.F., *The use of animal models in diabetes research*. British Journal of Pharmacology, 2012. **166**(3): p. 877-894.
188. Cefalu, W.T., *Animal Models of Type 2 Diabetes: Clinical Presentation and Pathophysiological Relevance to the Human Condition*. ILAR Journal, 2006. **47**(3): p. 186-198.
189. Bertram, C.E. and M.A. Hanson, *Animal models and programming of the metabolic syndrome: Type 2 diabetes*. British Medical Bulletin, 2001. **60**(1): p. 103-121.
190. Cafazzo, S., et al., *Effect of short road journeys on behaviour and some blood variables related to welfare in young bulls*. Applied Animal Behaviour Science, 2012. **139**(1-2): p. 26-34.
191. Kenny, F.J. and P.V. Tarrant, *The reaction of young bulls to short-haul road transport*. Applied Animal Behaviour Science, 1987. **17**(3-4): p. 209-227.
192. Hansen, P.D., et al., *Biological analysis (Bioassays, Biomarkers, Biosensors)*, in *Sustainable Management of Sediment Resources*, P.D. Barceló and D.M. Petrovic, Editors. 2007, Elsevier. p. 131-161.
193. Crimmins, E., et al., *Biomarkers related to aging in human populations*. Advances in clinical chemistry, 2008. **46**: p. 161-216.
194. Lebovitz, H., *Therapy for Diabetes Mellitus and Related Disorders*. 2009, American Diabetes Association.
195. Wang, J., *Electrochemical Glucose Biosensors*. Chemical Reviews, 2008. **108**(2): p. 814-825.
196. Andreux, P.A., R.H. Houtkooper, and J. Auwerx, *Pharmacological approaches to restore mitochondrial function*. Nat Rev Drug Discov, 2013. **12**(6): p. 465-483.
197. Fulati, A., et al., *An intracellular glucose biosensor based on nanoflake ZnO*. Sensors and Actuators B: Chemical, 2010. **150**(2): p. 673-680.
198. Li, Y.C., et al., *Application of shielding boronate affinity chromatography in the study of the glycation pattern of haemoglobin*. Journal of Chromatography B-Analytical Technologies in the Biomedical and Life Sciences, 2002. **776**(2): p. 149-160.
199. Gaborit, B., et al., *Comparison of performances of various HbA1c methods in Haemoglobin Camperdown variant detection: Consequences in diabetes management*. Clinica Chimica Acta, 2009. **403**(1-2): p. 262-263.
200. Bhat, V., K. Dewan, and P. Krishnaswamy, *Diagnostic Dilemma of HbA1c Detection in Presence of a Hemoglobinopathy: A Case Report* Indian Journal of Clinical Biochemistry, 2011. **26**(1): p. 91-95.
201. Jeppsson, J.O., et al., *Approved IFCC reference method for the measurement of HbA1c in human blood*. Clinical Chemistry and Laboratory medicine, 2002. **40**(1): p. 78-79.

202. Thevarajah, M., M.N. Nadzimah, and Y.Y. Chew, *Interference of hemoglobinA1c (HbA1c) detection using ion-exchange high performance liquid chromatography (HPLC) method by clinically silent hemoglobin variant in University Malaya Medical Centre (UMMC)--A case report*. *Clinical Biochemistry*, 2009. **42**(4-5): p. 430-434.
203. Bennett, C.M., M. Guo, and S.C. Dharmage, *HbA1c as a screening tool for detection of Type 2 diabetes: a systematic review*. *Diabetic Medicine*, 2007. **24**(4): p. 333-343.
204. Malhotra, B.D. and A. Turner, *Advances in Biosensors : Perspectives in Biosensors*. 2003: JAI Press.
205. Ricardo Romero, M., et al., *Amperometric Biosensor for Direct Blood Lactate Detection*. *Analytical Chemistry*, 2010. **82**(13): p. 5568-5572.
206. Wei, F., et al., *Serum Creatinine Detection by a Conducting-Polymer-Based Electrochemical Sensor To Identify Allograft Dysfunction*. *Analytical Chemistry*, 2012. **84**(18): p. 7933-7937.
207. Wang, Y., et al., *Electrochemical sensors for clinic analysis*. *Sensors*, 2008. **8**: p. 2043-2081.
208. Eguilaz, M., et al., *Gold nanoparticles: Poly(diallyldimethylammonium chloride) - carbon nanotubes composites as platforms for the preparation of electrochemical enzyme biosensors: Application to the determination of cholesterol*. *Journal of Electroanalytical Chemistry*, 2011. **661**(1): p. 171-178.
209. Hu, C. and S. Hu, *Carbon Nanotube-Based Electrochemical Sensors: Principles and Applications in Biomedical Systems*. *Journal of Sensors*, 2009: p. 1-40.
210. Vengatajalabathy Gobi, K. and F. Mizutani, *Layer-by-layer construction of an active multilayer enzyme electrode applicable for direct amperometric determination of cholesterol*. *Sensors and Actuators B: Chemical*, 2001. **80**(3): p. 272-277.
211. Branzoi, V., A. Musina, and F. Branzoi, *Amperometric urea biosensor based platinum electrode modified with a composite film*. *Revue Roumaine de Chimie*, 2011. **56**(9): p. 883-893.
212. Maher, J.J., *Retinol binding protein 4 and fatty liver: A direct link?* *Hepatology*, 2013. **58**(2): p. 477-479.
213. Lee, S.J., et al., *ssDNA Aptamer-Based Surface Plasmon Resonance Biosensor for the Detection of Retinol Binding Protein 4 for the Early Diagnosis of Type 2 Diabetes*. *Analytical Chemistry*, 2008. **80**(8): p. 2867-2873.
214. Saki, F., S. Ashkani-Esfahani, and Z. Karamizadeh, *Investigation of the Relationship Between Retinol Binding Protein 4, Metabolic Syndrome and Insulin Resistance in Iranian Obese 5-17 Year Old Children*. *Iranian Journal of Pediatrics*, 2013. **23**(4): p. 396-402.
215. Graham, T.E., et al., *Retinol-binding protein 4 and insulin resistance in lean, obese, and diabetic subjects*. *New England Journal of Medicine*, 2006. **354**(24): p. 2552-2563.
216. Zhao, W., J.-J. Xu, and H.-Y. Chen, *Electrochemical Biosensors Based on Layer-by-Layer Assemblies*. *Electroanalysis*, 2006. **18**(18): p. 1737-1748.
217. Balkau, B., et al., *High Blood Glucose Concentration Is a Risk Factor for Mortality in Middle-Aged Nondiabetic Men: 20-year follow-up in the Whitehall Study, the Paris Prospective Study, and the Helsinki Policemen Study*. *Diabetes Care*, 1998. **21**(3): p. 360-367.

218. Heianza, Y., et al., *Longitudinal Trajectories of HbA1c and Fasting Plasma Glucose Levels During the Development of Type 2 Diabetes: The Toranomon Hospital Health Management Center Study 7 (TOPICS 7)*. Diabetes Care, 2012.
219. Takebayashi, K., et al., *Retinol Binding Protein-4 Levels and Clinical Features of Type 2 Diabetes Patients*. Journal of Clinical Endocrinology & Metabolism, 2007. **92**(7): p. 2712-2719.
220. Seo, J.A., et al., *Serum retinol-binding protein 4 levels are elevated in non-alcoholic fatty liver disease*. Clinical Endocrinology, 2008. **68**(4): p. 555-560.
221. Li, G., et al., *Study of carbon nanotube modified biosensor for monitoring total cholesterol in blood*. Biosensors & Bioelectronics, 2005. **20**: p. 2140–2144.
222. Ziegelmeier, M., et al., *Serum levels of adipokine retinol-binding protein-4 in relation to renal function*. Diabetes Care, 2007. **30**(10): p. 2588-2592.
223. O'Byrne, S.M. and W.S. Blaner, *Retinol and retinyl esters: biochemistry and physiology*. Journal of Lipid Research, 2013. **54**(7): p. 1731-1743.
224. Cho, Y.M., et al., *Plasma Retinol-Binding Protein-4 Concentrations Are Elevated in Human Subjects With Impaired Glucose Tolerance and Type 2 Diabetes*. Diabetes Care, 2006. **29**(11): p. 2457-2461.
225. Hansen, P.D., *Chapter 6 Biomarkers*, in *Trace Metals and other Contaminants in the Environment*, B.A. Markert, A.M. Breure, and H.G. Zechmeister, Editors. 2003, Elsevier. p. 203-220.
226. Zhang, S., G. Wright, and Y. Yang, *Materials and techniques for electrochemical biosensor design and construction*. Biosensors and Bioelectronics, 2000. **15**(5-6): p. 273-282.
227. Clark, L.C., Jr. and C. Lyons, *Electrode systems for continuous monitoring in cardiovascular surgery*. Annals of the New York Academy of Sciences, 1962. **102**: p. 29-45.
228. Park, S., H. Boo, and T. Chung, *Electrochemical non-enzymatic glucose sensors*. Analytica Chimica Acta, 2006. **556**(1): p. 46-57.
229. Wilson, G.S., et al., *Progress toward the development of an implantable sensor for glucose*. Clinical Chemistry, 1992. **38**(9): p. 1613-7.
230. Zhang, X., H. Ju, and J. Wang, *Electrochemical Sensors, Biosensors and Their Biomedical Applications*. 2011, Academic Press. p. 57-69.
231. Abbott. *Precision Xceed Pro Blood Glucose & β -Ketone Monitoring System*. 2008 [cited 2013 12/12/13]; Available from: <https://www.abbottdiabetescare.com/products/hospital/precision-xceed-pro.html>.
232. Abbott, *Precision Exceed Pro*. 2007.
233. Abbott, *FreeStyle Freedom Lite*. 2010.
234. Bayer, *Ascensia Elite XL Diabetes Care System*. 2002.
235. LifeScan, *SureStep Owners booklet*. 1998.
236. LifeScan, *One Touch Ultra*. 2005.
237. Diagnostics, R., *Accu-Check users manual*. 2006.
238. London, R.C.o.P.o., *TYPE 2 DIABETES: National clinical guideline for management in primary and secondary care (update)*. 2008, The Lavenham Press Ltd: Suffolk.
239. Boren, S.A. and W.L. Clarke, *Analytical and Clinical Performance of Blood Glucose Monitors*. Journal of Diabetes Science and Technology, 2010. **4**(1): p. 84–97.

240. Newman, J.D. and A.P.F. Turner, *Home blood glucose biosensors: a commercial perspective*. *Biosensors & Bioelectronics*, 2005. **20**(12): p. 2435-2453.
241. Heller, A. and B. Feldman, *Electrochemical glucose sensors and their applications in diabetes management*. *Chemical Reviews*, 2008. **108**(7): p. 2482-2505.
242. Tack, C., et al., *Accuracy evaluation of five blood glucose monitoring systems obtained from the pharmacy: a European multicenter study with 453 subjects*. *Diabetes Technol Ther*, 2012. **14**(4): p. 330-7.
243. Lunt, H., et al., *Capillary glucose meter accuracy and sources of error in the ambulatory setting*. *N Z Med J*, 2010. **123**(1310): p. 74-85.
244. Thomas, L.E., et al., *A glucose meter accuracy and precision comparison: the FreeStyle Flash Versus the Accu-Chek Advantage, Accu-Chek Compact Plus, Ascensia Contour, and the BD Logic*. *Diabetes Technol Ther*, 2008. **10**(2): p. 102-10.
245. Arabadjief, D. and J.H. Nichols, *Assessing glucose meter accuracy*. *Curr Med Res Opin*, 2006. **22**(11): p. 2167-74.
246. Peel, E., et al., *Blood glucose self-monitoring in non-insulin-treated type 2 diabetes: a qualitative study of patients' perspectives*. *British Journal of General Practice*, 2004. **54**(500): p. 183-188.
247. Wang, J., *Electrochemical biosensors: Towards point-of-care cancer diagnostics*. *Biosensors and Bioelectronics*, 2006. **21**(10): p. 1887-1892.
248. Groves, P.D., *Electrochemistry*. 1974, London: John Murray Ltd.
249. Crow, D.R., *Principles and applications of electrochemistry*. 4th ed. 1998: Stanley Thornes Ltd.
250. Tsierkezos, N., *Cyclic Voltammetric Studies of Ferrocene in Nonaqueous Solvents in the Temperature Range from 248.15 to 298.15 K*. *Journal of Solution Chemistry*, 2007. **36**(3): p. 289-302.
251. Brett, C.M.A. and A.M.O. Brett, *Electrochemistry principles, methods and applications*. 1993: Oxford Science Publications. 427.
252. Kertesz, V., J.Q. Chambers, and A.N. Mullenix, *Chronoamperometry of Surface-Confining Redox Couples for Irreversible Two-Step and Three-Step Consecutive Reaction Mechanisms*. *Analytical Chemistry*, 1999. **71**: p. 3905-3909.
253. BASi. http://www.basinc.com/mans/EC_epsilon/Techniques/ChronoI/ca_analysis.html. 28/03/11].
254. Kondo, T., M. Horitani, and M. Yuasa, *Sensitive Electrochemical Detection of Glucose at Glucose Oxidase-Cobalt Phthalocyanine-Modified Boron-Doped Diamond Electrode*. *International Journal of Electrochemistry*, 2012.
255. Mashazi, P., et al., *The effects of carbon nanotubes on the electrocatalysis of hydrogen peroxide by metallo-phthalocyanines*. *Talanta*, 2011. **85**(4): p. 2202-2211.
256. Arduini, F., et al., *Carbon Black-Modified Screen-Printed Electrodes as Electroanalytical Tools*. *Electroanalysis*, 2012. **24**(4): p. 743-751.
257. Tripathi, V.S., V.B. Kandimalla, and H. Ju, *Amperometric biosensor for hydrogen peroxide based on ferrocene-bovine serum albumin and multiwall carbon nanotube modified ormosil composite*. *Biosensors and Bioelectronics*, 2006. **21**(8): p. 1529-1535.
258. Roberts, J.G., et al., *Voltammetric detection of hydrogen peroxide at carbon fiber microelectrodes*. *Society for Neuroscience Abstract Viewer and Itinerary Planner*, 2010. **40**: p. 5205-5210.

259. Chen, W., et al., *Recent advances in electrochemical sensing for hydrogen peroxide: a review*. Analyst, 2012. **137**(1): p. 49-58.
260. Zagal, J.H., *Metallophthalocyanines as catalysts in electrochemical reactions*. Coordination Chemistry Reviews, 1992. **119**: p. 89-136.
261. Xu, J.-Z., et al., *An Amperometric Biosensor Based on the Coimmobilization of Horseradish Peroxidase and Methylene Blue on a Carbon Nanotubes Modified Electrode*. Electroanalysis, 2003. **15**(3): p. 219-224.
262. Zhang, L., et al., *Direct Electrocatalytic Oxidation of Hydrogen Peroxide Based on Nafion and Microspheres MnO₂ Modified Glass Carbon Electrode*. International Journal of Electrochemical Science, 2009. **4**: p. 407 - 413.
263. Aguilar, G. and R.A. Guzman, *Hydrogen Peroxide*. Biochemistry Research Trends. 2013, New York: Nova Science Publishers Inc.
264. Bockris, J.O.M. and L.F. Oldfield, *The oxidation-reduction reactions of hydrogen peroxide at inert metal electrodes and mercury cathodes*. Transactions of the Faraday Society, 1955. **51**(0): p. 249-259.
265. Dominguez, C.M., et al., *The use of cyclic voltammetry to assess the activity of carbon materials for hydrogen peroxide decomposition*. Carbon, 2013. **60**(0): p. 76-83.
266. Wroblowa, H.S., Y.C. Pan, and G. Razumney, *Electroreduction of oxygen: A new mechanistic criterion*. Journal of Electroanalytical Chemistry, 1976. **69**(2): p. 195-201.
267. Prakash, J., D.A. Tryk, and E.B. Yeager, *Kinetic investigations of oxygen reduction and evolution reactions on lead ruthenate catalysts*. Journal of the Electrochemical Society, 1999. **146**(11): p. 4145-4151.
268. Wang, J., *Carbon-Nanotube Based Electrochemical Biosensors: A Review*. Electroanalysis, 2005. **17**(1): p. 7-14.
269. Nowall, W.B. and W.G. Kuhr, *Detection of hydrogen peroxide and other molecules of biological importance at an electrocatalytic surface on a carbon fiber microelectrode*. Electroanalysis, 1997. **9**(2): p. 102-109.
270. Shimizu, S., et al., *Acyl-CoA oxidase from Candina-Tropicalis*. Biochemical and Biophysical Research Communications, 1979. **91**(1): p. 108-113.
271. Kim, J.J.P. and R. Miura, *Acyl-CoA dehydrogenases and acyl-CoA oxidases Structural basis for mechanistic similarities and differences*. Eur. J. Biochem., 2004(271): p. 483-493.
272. Zeng, J., G.S. Deng, and D. Li, *Intrinsic enoyl-CoA isomerase activity of rat acyl-CoA oxidase I*. Biochimica Et Biophysica Acta-General Subjects, 2006. **1760**(1): p. 78-85.
273. Inestrosa, N.C., M. Bronfman, and F. Leighton, *Detection of peroxisomal fatty acyl-Coenzyme-A oxidase activity*. Biochemical Journal, 1979. **182**(3): p. 779-788.
274. Abe, T., et al. <http://jb.oxfordjournals.org/content/111/1/123.full.pdf+html> [4/3/11].
275. Zeng, J., et al., *Oct-2-en-4-ynoyl-CoA as a specific inhibitor of acyl-CoA oxidase*. Organic Letters, 2008. **10**(19): p. 4287-4290.
276. Uslu, B. and S.A. Ozkan, *Electroanalytical Application of Carbon Based Electrodes to the Pharmaceuticals*. Analytical Letters, 2007. **40**(5): p. 817-853.
277. Gilmartin, M.A.T., et al., *Voltammetric and photoelectron spectral elucidation of the electrocatalytic oxidation of hydrogen peroxide at screen-printed carbon electrodes chemically modified with cobalt phthalocyanine*. Electroanalysis, 1995. **7**(6): p. 547-555.

278. Zagal, J.H., et al., *Metallophthalocyanine-based molecular materials as catalysts for electrochemical reactions*. Coordination Chemistry Reviews, 2010. **254**(23-24): p. 2755-2791.
279. Iijima, S., *Helical microtubules of graphitic carbon*. Nature, 1991. **354**(6348): p. 56-58.
280. Trojanowicz, M., *Analytical applications of carbon nanotubes: a review*. Trac-Trends in Analytical Chemistry, 2006. **25**(5): p. 480-489.
281. Fanjul-Bolado, P., et al., *Manufacture and evaluation of carbon nanotube modified screen-printed electrodes as electrochemical tools*. Talanta, 2007. **74**(3): p. 427-433.
282. Ye, J.-S., et al., *Selective Voltammetric Detection of Uric Acid in the Presence of Ascorbic Acid at Well-Aligned Carbon Nanotube Electrode*. Electroanalysis, 2003. **15**(21): p. 1693-1698.
283. Bohrer, F.I., et al., *Selective Detection of Vapor Phase Hydrogen Peroxide with Phthalocyanine Chemiresistors*. Journal of the American Chemical Society, 2008. **130**(12): p. 3712-3713.
284. Geraldo, D., et al., *Volcano correlations between formal potential and Hammett parameters of substituted cobalt phthalocyanines and their activity for hydrazine electro-oxidation*. Electrochemistry Communications, 2002. **4**(2): p. 182-187.
285. Baranton, S., et al., *Oxygen reduction reaction in acid medium at iron phthalocyanine dispersed on high surface area carbon substrate: tolerance to methanol, stability and kinetics*. Journal of Electroanalytical Chemistry, 2005. **577**(2): p. 223-234.
286. Yeager, E., *Dioxygen electrocatalysis: mechanisms in relation to catalyst structure*. Journal of Molecular Catalysis, 1986. **38**(1-2): p. 5-25.
287. van Veen, J.A.R. and H.A. Colijn, *Oxygen reduction on transition-metal porphyrins in acid electrolyte II. Stability*. Berichte der Bunsengesellschaft/Physical Chemistry Chemical Physics, 1981. **85**(8): p. 700-704.
288. Kobayashi, N., P. Janda, and A.B.P. Lever, *Cathodic reduction of oxygen and hydrogen peroxide at cobalt and iron crowned phthalocyanines adsorbed on highly oriented pyrolytic graphite electrodes*. Inorganic Chemistry, 1992. **31**(25): p. 5172-5177.
289. Shimizu, S., et al., *Enzymatic determination of serum-free fatty acids: A colorimetric method*. Analytical Biochemistry, 1980. **107**(1): p. 193-198.
290. Knox, D.P. and D.G. Jones, *Automated enzymatic determination of plasma free fatty acids by centrifugal analysis*. Journal of Automatic Chemistry, 1984. **6**(2): p. 152-154.
291. Jia, W., et al., *Electrocatalytic oxidation and reduction of H₂O₂ on vertically aligned Co₃O₄ nanowalls electrode: Toward H₂O₂ detection*. Journal of Electroanalytical Chemistry, 2009. **625**: p. 27-32.
292. R Ben-Shachar, et al., *The biochemistry of acetaminophen hepatotoxicity and rescue: a mathematical model*. Theoretical biology and medical modelling, 2012. **9**(55).
293. Goldfine, A.B., et al., *A randomised trial of salsalate for insulin resistance and cardiovascular risk factors in persons with abnormal glucose tolerance*. Diabetologia, 2013. **56**(4): p. 714-723.
294. Krebs, H.A., *Chemical composition of blood plasma and serum*. Annual Review of Biochemistry, 1950. **19**: p. 409-430.
295. Frontiers, in, and Bioscience. *Whole blood, serum and plasma chemistry*. 2012 [cited 2012 14.06.12]; Available from: <http://www.bioscience.org/atlasses/clinical/chemist/a-z.htm>

296. Tasca, F., et al., *A third generation glucose biosensor based on cellobiose dehydrogenase from *Corynascus thermophilus* and single-walled carbon nanotubes*. *Analyst*, 2011. **136**(10): p. 2033-2036.
297. Stocker, M.E. and J.E. Montgomery, *Serum paracetamol concentrations in adult volunteers following rectal administration*. *British Journal of Anaesthesia*, 2001. **87**(4): p. 638-640.
298. Medications, and, and Drugs. *New Medications and Drugs*. 2012 [cited 2012 14.06.12]; Available from: <http://nursingmedications.blogspot.co.uk/2007/09/monitoring-blood-levels.html>.
299. Putnam, F.W., *The Plasma Proteins: Structure, Function and Genetic Control*. 2 ed. Vol. 1. 1975: Academic Press New York.
300. Hirayama, K., et al., *Rapid confirmation and revision of the primary structure of bovine serum albumin by ESIMS and frit-FAB LC/MS*. *Biochemical and Biophysical Research Communications*, 1990. **173**(2): p. 639-646.
301. Goodsell, D. *Serum Albumin*. 2012 [cited 2012 19/07/12]; Available from: <http://www.rcsb.org/pdb/101/motm.do?momID=37>.
302. Goodman, D.S., *The Interaction of Human Serum Albumin with Long-chain Fatty Acid Anions*. *Journal of the American Chemical Society*, 1958. **80**(15): p. 3892-3898.
303. Spector, A.A., K. John, and J.E. Fletcher, *Binding of long-chain fatty acids to bovine serum albumin*. *Journal of Lipid Research*, 1969. **10**(1): p. 56-67.
304. Zhao, Y., et al., *Simultaneous Electrochemical Determination of Uric Acid and Ascorbic Acid Using (L)-Cysteine Self-Assembled Gold Electrode*. *International Journal of Electrochemical Science*, 2006. **1**(7): p. 363-371.
305. Nassef, H.M., et al., *Amperometric sensing of ascorbic acid using a disposable screen-printed electrode modified with electrografted o-aminophenol film*. *Analyst*, 2008. **133**(12): p. 1736-1741.
306. Hidouri, S., et al., *Structural and functional characterisation of a biohybrid material based on acetylcholinesterase and layered double hydroxides*. *Talanta*, 2011. **85**(4): p. 1882-1887.
307. Firdoz, S., et al., *A novel amperometric biosensor based on single walled carbon nanotubes with acetylcholine esterase for the detection of carbaryl pesticide in water*. *Talanta*, 2010. **83**(1): p. 269-273.
308. Nugent, J.M., et al., *Fast Electron Transfer Kinetics on Multiwalled Carbon Nanotube Microbundle Electrodes*. *Nano Letters*, 2001. **1**(2): p. 87 - 91.
309. Zhang, L.P., et al., *Fabrication of Multilayer-Film-Modified Gold Electrode Composed of Myoglobin, Chitosan, and Polyelectrolyte-Wrapped Multi-Wall Carbon Nanotubes by Layer-by-Layer Assembled Technique and Electrochemical Catalysis for Hydrogen Peroxide and Trichloroacetic Acid*. *Russian Journal of Electrochemistry*, 2008. **44**(11): p. 1271-1279.
310. Hu, Z., et al., *Layer-by-layer assembly of poly(sodium 4-styrenesulfonate) wrapped multiwalled carbon nanotubes with polyaniline nanofibers and its electrochemistry*. *Carbon*, 2010. **48**(13): p. 3729-3736.
311. Liu, G.D. and Y.H. Lin, *Amperometric glucose biosensor based on self-assembling glucose oxidase on carbon nanotubes*. *Electrochemistry Communications*, 2006. **8**(2): p. 251-256.

312. Campàs, M., B. Prieto-Simón, and J.L. Marty, *A review of the use of genetically engineered enzymes in electrochemical biosensors*. *Seminars in Cell & Developmental Biology*, 2009. **20**(1): p. 3-9.
313. Florescu, M. and C.M. A. Brett, *Development and evaluation of electrochemical glucose enzyme biosensors based on carbon film electrodes*. *Talanta*, 2005. **65**(2): p. 306-312.
314. Decher, G., *Fuzzy Nanoassemblies: Toward Layered Polymeric Multicomposites*. *Science*, 1997. **277**(5330): p. 1232-1237.
315. Deng, C., et al., *A sensitive and stable biosensor based on the direct electrochemistry of glucose oxidase assembled layer-by-layer at the multiwall carbon nanotube-modified electrode*. *Biosensors and Bioelectronics*, 2010. **26**(1): p. 213-219.
316. Lupu, S. and A. Ficai, *Layer by layer deposition of redox polymers/enzyme assemblies onto electrodes surfaces for nitrate electrochemical sensing*. *Revue Roumaine de Chimie*, 2007. **52**(12): p. 1137-1143.
317. Ferreira, M., et al., *Enzyme-mediated amperometric biosensors prepared with the Layer-by-Layer (LbL) adsorption technique*. *Biosensors and Bioelectronics*, 2004. **19**(12): p. 1611-1615.
318. Mutlu, S., M. Mutlu, and E. Pişkin, *A kinetic approach to oxidase based enzyme electrodes: the effect of enzyme layer formation on the response time*. *Biochemical Engineering Journal*, 1998. **1**(1): p. 39-43.
319. Dubas, S.T. and J.B. Schlenoff, *Swelling and Smoothing of Polyelectrolyte Multilayers by Salt*. *Langmuir*, 2001. **17**(25): p. 7725-7727.
320. Yang, M., et al., *Layer-by-layer self-assembled multilayer films of carbon nanotubes and platinum nanoparticles with polyelectrolyte for the fabrication of biosensors*. *Biomaterials*, 2006. **27**(2): p. 246-255.
321. Goldstein, L., *Kinetic behavior of immobilized enzyme systems*. *Methods in enzymology*, 1976. **44**: p. 397-443.
322. Kamin, R.A. and G.S. Wilson, *Rotating ring-disk enzyme electrode for biocatalysis kinetic studies and characterization of the immobilized enzyme layer*. *Analytical Chemistry*, 1980. **52**(8): p. 1198-1205.
323. Cai, X., et al., *A layer-by-layer assembled and carbon nanotubes/gold nanoparticles-based bienzyme biosensor for cholesterol detection*. *Sensors and Actuators B: Chemical*, 2013. **181**(0): p. 575-583.
324. Guo, M., et al., *Carbon Nanotubes-Based Amperometric Cholesterol Biosensor Fabricated Through Layer-by-Layer Technique*. *Electroanalysis*, 2004. **16**(23): p. 1992-1998.
325. Chen, H., et al., *Bienzyme bionanomultilayer electrode for glucose biosensing based on functional carbon nanotubes and sugar-lectin biospecific interaction*. *Analytical Biochemistry*, 2010. **403**(1-2): p. 36-42.
326. Zhao, H.T. and H.X. Ju, *Multilayer membranes for glucose biosensing via layer-by-layer assembly of multiwall carbon nanotubes and glucose oxidase*. *Analytical Biochemistry*, 2006. **350**(1): p. 138-144.
327. Kobayashi, Y. and J.-i. Anzai, *Preparation and optimization of bienzyme multilayer films using lectin and glyco-enzymes for biosensor applications*. *Journal of Electroanalytical Chemistry*, 2001. **507**(1-2): p. 250-255.
328. Hou, S., et al., *Amperometric acetylcholine biosensor based on self-assembly of gold nanoparticles and acetylcholinesterase on the sol-gel/multi-walled carbon*

- nanotubes/choline oxidase composite-modified platinum electrode*. *Biosensors and Bioelectronics*, 2012. **33**(1): p. 44-49.
329. Chen, Q., et al., *Avidin-Biotin System-Based Enzyme Multilayer Membranes for Biosensor Applications: Optimization of Loading of Choline Esterase and Choline Oxidase in the Bienzyme Membrane for Acetylcholine Biosensors*. *Electroanalysis*, 1998. **10**(2): p. 94-97.
330. Li, W., et al., *Fabrication of multilayer films containing horseradish peroxidase and polycation-bearing Os complex by means of electrostatic layer-by-layer adsorption and its application as a hydrogen peroxide sensor*. *Analytica Chimica Acta*, 2000. **418**(2): p. 225-232.
331. Jie Liu, et al., *Fullerene Pipes*. *Science*, 1998. **280**: p. 1253-1256.
332. Luong, A., et al., *Molecular characterization of human acetyl-CoA synthetase, an enzyme regulated by sterol regulatory element-binding proteins*. *J Biol Chem*, 2000. **275**(34): p. 26458-66.
333. Yu, A. and F. Caruso, *Thin films of polyelectrolyte-encapsulated catalase microcrystals for biosensing* *Analytical Chemistry*, 2003. **75**(13): p. 3031-3037
334. Salazar, P., et al., *Improvement and characterization of surfactant-modified Prussian blue screen-printed carbon electrodes for selective H₂O₂ detection at low applied potentials*. *Journal of Electroanalytical Chemistry*, 2012. **674**(0): p. 48-56.
335. Lata, S., et al., *An amperometric H₂O₂ biosensor based on cytochrome c immobilized onto nickel oxide nanoparticles/carboxylated multiwalled carbon nanotubes/polyaniline modified gold electrode*. *Process Biochemistry*, 2012. **47**(6): p. 992-998.
336. Roche. https://e-labdoc.roche.com/LFR_PublicDocs/ras/11383175001_en_09.pdf. 18/07/11].
337. Chen, P.-Y., et al., *Detection of uric acid based on multi-walled carbon nanotubes polymerized with a layer of molecularly imprinted PMAA*. *Sensors and Actuators B: Chemical*, 2010. **146**(2): p. 466-471.
338. Ritesh Tipnis, et al., *Layer-by-Layer Assembled Semipermeable Membrane for Amperometric Glucose Sensors*. *J Diabetes Sci Technol*, 2007. **1**(2): p. 193-200.
339. Schleicher, E., *The clinical chemistry laboratory: current status, problems and diagnostic prospects*. *Analytical and Bioanalytical Chemistry*, 2006. **384**(1): p. 124-131.
340. Konno, T., J. Watanabe, and K. Ishihara, *Conjugation of Enzymes on Polymer Nanoparticles Covered with Phosphorylcholine Groups*. *Biomacromolecules*, 2004. **5**(2): p. 342-347.
341. Guder, W.G. *The quality of diagnostic samples*. 2001. **2013**, 1-7.
342. Brandenburg, K., et al., *Biophysical investigations into the interaction of lipopolysaccharide with polymyxins*. *Thermochimica Acta*, 2002. **382**(1-2): p. 189-198.
343. Yu, E.H., et al., *Feasibility study of introducing redox property by modification of PMBN polymer for biofuel cell applications*. *Appl Biochem Biotechnol*, 2010. **160**(4): p. 1094-101.
344. Park, J., et al., *Antibody immobilization to phospholipid polymer layer on gold substrate of quartz crystal microbalance immunosensor*. *Colloids and Surfaces B: Biointerfaces*, 2007. **55**(2): p. 164-172.
345. Tsubery, H., et al., *Structure-function studies of polymyxin B nonapeptide: implications to sensitization of gram-negative bacteria*. *J Med Chem*, 2000. **43**(16): p. 3085-92.

346. Shimada, T., et al., *Development of targeted therapy with paclitaxel incorporated into EGF-conjugated nanoparticles*. *Anticancer Res*, 2009. **29**(4): p. 1009-14.
347. Xiao, C.Q., et al., *Interaction between a cationic porphyrin and bovine serum albumin studied by surface plasmon resonance, fluorescence spectroscopy and cyclic voltammetry*. *Photochemical & Photobiological Sciences*, 2011. **10**(7): p. 1110-1117.
348. Reed, R.G., F.W. Putnam, and T. Peters, *Sequence of residues 400-403 of bovine serum-albumin*. *Biochemical Journal*, 1980. **191**(3): p. 867-868.
349. Ignat, T., et al., *Electrochemical characterization of BSA/11-mercaptoundecanoic acid on Au electrode*. *Materials Science and Engineering B-Advanced Functional Solid-State Materials*, 2010. **169**(1-3): p. 55-61.
350. Scott, T. and M. Eagleson, *Concise Encyclopedia: Biochemistry*. 1988, Walter de Gruyter, New York. p. 19-22.
351. Chen, C.-C. and Y. Gu, *Enhancing the sensitivity and stability of HRP/PANI/Pt electrode by implanted bovine serum albumin*. *Biosensors & Bioelectronics*, 2008. **23**(6): p. 765-770.
352. Spector, A.A., *Fatty acid binding to plasma albumin*. *Journal of Lipid Research*, 1975. **16**(3): p. 165-179.
353. Guo, W. and N. Hu, *Interaction of myoglobin with poly(methacrylic acid) at different pH in their layer-by-layer assembly films: An electrochemical study*. *Biophysical Chemistry*, 2007. **129**: p. 163-171.
354. Mori, H. and A.H.E. Muller, *New polymeric architectures with (meth)acrylic acid segments*. *Progress in Polymer Science*, 2003. **28**(10): p. 1403-1439.
355. Widjaja, A., et al., *Within- and Between-Subject Variation in Commonly Measured Anthropometric and Biochemical Variables*. *Clinical Chemistry*, 1999. **45**(4): p. 561-566.
356. Regouw, B.J.M., et al., *Specific determination of free fatty acid in plasma*. *Clinica Chimica Acta*, 1971. **31**(1): p. 187-195.
357. Hales, C.N. and P.J. Randle, *Effects of low-carbohydrate diet and diabetes mellitus on plasma concentrations of glucose, non-esterified fatty acid and insulin during oral glucose-tolerance tests* *The Lancet*, 1963. **281**(7285): p. 790-794.
358. Rogiers, V., *Stability of the long chain non-esterified fatty acid pattern in plasma and blood during different storage conditions*. *Clinica Chimica Acta*, 1978. **84**(1&2): p. 49-54.
359. Gabr, Y., F. Mansour, and N. Amin, *Calcium, phosphorus and fatty acids in plasma stored at room temperature*. *The Lancet*, 1966. **288**(7456): p. 196-198.
360. Mulder, C., J.A. Schouten, and C. Poppsnijders, *Determination of Free Fatty Acids: A Comparative Study of the Enzymatic Versus the Gas Chromatographic and the Colorimetric Method*. *Journal of Clinical Chemistry and Clinical Biochemistry*, 1983. **21**(12): p. 823-827.
361. Rogiers, V., *The application of an improved gas liquid chromatographic method for the determination of the long chain non esterified fatty acid pattern of blood plasma in children*. *Clinica Chimica Acta*, 1977. **78**(2): p. 227-233.
362. Dole, V.P., *A relation between non-esterified fatty acids in plasma and the metabolism of glucose*. *Journal of Clinical Investigations*, 1956. **35**(2): p. 150-154.
363. Forbes, A.L. and J.A. Camlin, *Effects of storage on serum nonesterified fatty acid concentrations*. *Proceedings of the Society for Experimental Biology and Medicine*.

- Society for Experimental Biology and Medicine (New York, N.Y.), 1959. **102**: p. 709-710.
364. Howorth, P.J.N., S. Gibbard, and V. Marks, *Evaluation of a colorimetric method (Duncombe) of determination of plasma non-esterified fatty acids*. Clinica Chimica Acta, 1966. **14**(1): p. 69-73.
365. Drury, J.L.S.a.P.E., *A titration method for blood fat*. Journal of Biological Chemistry, 1929. **84**: p. 741-748.
366. Davis, B.D., *The estimation of small amounts of fatty acid in the presence of polyoxyethylene sorbitan partial fatty acid esters (tween) and of serum proteins*. Archives of biochemistry, 1947. **15**(3): p. 351-358.
367. Fairweather, D.V.I. and R. Layton, *Observations on the collection and handling of blood samples for N.E.F.A. estimation*. Journal of Clinical Pathology, 1967. **20**(4): p. 665-667.
368. Miles, J., et al., *A micro-fluorometric method for the determination of free fatty-acids in plasma*. Journal of Lipid Research, 1983. **24**(1): p. 96-99.
369. Krebs, M., et al., *Prevention of in Vitro Lipolysis by Tetrahydrolipstatin*. Clinical Chemistry, 2000. **46**(7): p. 950-954.
370. Frayn, K.N., *The glucose-fatty acid cycle: a physiological perspective*. Biochemical Society Transactions, 2003. **31**: p. 1115-1119.
371. Hadvary, P., H. Lengsfeld, and H. Wolfer, *Inhibition of pancreatic lipase in vitro by the covalent inhibitor tetrahydrolipstatin*. Biochemical Journal, 1988. **256**(2): p. 357-361.
372. Gurd, F.R.N., *Lipide Chemistry*, ed. D.J. Hanahan. 1960: Wiley: New York.
373. Vogel, W.C. and L. Zieve, *Conversion of lecithin to lysolecithin as a source of fatty acids in incubated plasma or serum*. Proceedings of the Society for Experimental Biology and Medicine. Society for Experimental Biology and Medicine (New York, N.Y.), 1962. **111**: p. 538-540.
374. Carr, R.E., S.M. Humphreys, and K.N. Frayn, *Catecholamine Interference with Enzymatic Determination of Nonesterified Fatty Acids in Two Commercially Available Test Kits*. Clinical Chemistry, 1995. **41**(3): p. 445-457.
375. Ballard, F.B., et al., *Myocardial metabolism of fatty acids*. The Journal of clinical investigation, 1960. **39**: p. 717-723.
376. Rothlin, M.E. and R.J. Bing, *Extraction and release of individual free fatty acids by the heart and fat depots*. The Journal of clinical investigation, 1961. **40**: p. 1380-1386.
377. Choi, S.H., et al., *Amperometric biosensors employing an insoluble oxidant as an interference-removing agent*. Analytica Chimica Acta, 2002. **461**(2): p. 251-260.
378. Matsumoto, T., et al., *A long-term lifetime amperometric glucose sensor with a perfluorocarbon polymer coating*. Biosensors & Bioelectronics, 2001. **16**(4-5): p. 271-276.
379. Jia, W.-Z., K. Wang, and X.-H. Xia, *Elimination of electrochemical interferences in glucose biosensors*. Trac-Trends in Analytical Chemistry, 2010. **29**(4): p. 306-318.
380. Roberts, J.G., K.L. Hamilton, and L.A. Sombers, *Comparison of electrode materials for the detection of rapid hydrogen peroxide fluctuations using background-subtracted fast scan cyclic voltammetry*. Analyst, 2011. **136**(17): p. 3550-3556.
381. Zhang, Y.N., et al., *Elimination of the Acetaminophen Interference in an Implantable Glucose Sensor*. Analytical Chemistry, 1994. **66**(7): p. 1183-1188.
382. Zhao, Y.D., et al., *The interface behavior of hemoglobin at carbon nanotube and the detection for H₂O₂*. Talanta, 2005. **65**(2): p. 489-494.

383. Vaidya, R. and E. Wilkins, *Effect of interference on amperometric glucose biosensors with cellulose-acetate membranes*. *Electroanalysis*, 1994. **6**(8): p. 677-682.
384. Palmisano, F., et al., *Simultaneous monitoring of glucose and lactate by an interference and cross-talk free dual electrode amperometric biosensor based on electropolymerized thin films*. *Biosensors & Bioelectronics*, 2000. **15**(9-10): p. 531-539.
385. Frayn, K.N., *Cardiovascular disease : Diet, Nutrition and Emerging Risk Factors*. 2005: Blackwell Publishing.
386. Amin-ul-Haq, et al., *Association of serum uric acid with blood urea and serum creatinine*. *Pakistan Journal of Physiology*, 2010. **6**(2): p. 46-49.
387. Dehghan, A., et al., *High serum uric acid as a novel risk factor for type 2 diabetes*. *Diabetes Care*, 2008. **31**(2): p. 361-362.
388. Kelley. *Kelley's Textbook of Rheumatology 8th edition*. 2008 [cited 2012 06/07/12]; Available from: <http://www.mdconsult.com/books/page.do?eid=4-u1.0-B978-1-4160-3285-4..10087-7--s0150&isbn=978-1-4160-3285-4&type=bookPage&from=content&uniqId=344080340-212>.
389. Goyal, R.N., A. Brajter-Toth, and G. Dryhurst, *Futher insights into the electrochemical oxidation of uric acid*. *Journal of Electroanalytical Chemistry and Interfacial Electrochemistry*, 1982. **131**(0): p. 181-202.
390. Zidan, M., et al., *Electrochemical Oxidation of Paracetamol Mediated by Nanoparticles Bismuth Oxide Modified Glassy Carbon Electrode*. *International Journal of Electrochemical Science*, 2011. **6**(2): p. 279-288.
391. Ishihara, K., et al., *Hemocompatibility of human whole blood on polymers with a phospholipid polar group and its mechanism*. *J Biomed Mater Res*, 1992. **26**(12): p. 1543-52.